

Outdoor microalgae production

Jeroen H. de Vree

Thesis committee

Promotor

Prof. Dr R. H. Wijffels
Professor of Bioprocess Engineering Group
Wageningen University

Co-promotors

Dr R. Bosma
AlgaePARC operational manager, Bioprocess Engineering Group
Wageningen University

Dr M. J. Barbosa
Associate Professor, Bioprocess Engineering Group
Wageningen University

Other members

Prof. Dr. F.G. Acien Fernandez, Almeria University, Spain

Dr. B.G. Temmink, Wageningen University

Dr. L. Rodolfi, Florence University, Italy

Prof. Dr. E.J. van Henten, Wageningen University

This research was conducted under the auspices of the Graduate School VLAG

(Advanced studies in Food Technology, Agrobiotechnology, Nutrition and Health Sciences).

Outdoor production of microalgae

Jeroen Hendrik de Vree

Thesis

submitted in fulfilment of the requirements for the degree of doctor

at Wageningen University

by the authority of the Rector Magnificus

Prof. Dr A.P.J. Mol

in the presence of the

Thesis Committee appointed by the Academic Board

to be defended in public

on Friday 14 October 2016

at 4 p.m. in the Aula.

Jeroen H. de Vree

Outdoor production of microalgae,

177 pages.

PhD thesis, Wageningen University, Wageningen, NL (2016)

With references, with summary in English

ISBN 978-94-6257-878-4

DOI 10.18174/387236

Table of Contents

Chapter 1

Introduction 9

Chapter 2.....

Design and construction of the microalgal pilot facility AlgaePARC 15

Chapter 3.....

Comparison of four pilot-scale outdoor photobioreactors 47

Chapter 4.....

Turbidostat operation of outdoor pilot-scale photobioreactors 67

Chapter 5.....

Parameter estimation for *Neochloris oleoabundans* and *Nannochloropsis* sp. for modelling microalgal growth. 91

Chapter 6.....

Towards industrial products from microalgae 115

Chapter 7.....

General discussion: 145

References 159

Summary 167

Chapter 1

Introduction

1.1 Current status of microalgae production

Microalgae are unicellular microorganisms that are able to convert sunlight into biochemical energy via the process of photosynthesis. Microalgae are a promising feedstock for bulk commodities like chemicals, food and feed constituents, and biofuels [1-3]. However, the current application of microalgae lies in specialties, or high value products. Examples of high value products currently produced with microalgae are polyunsaturated fatty acids, such as EPA and DHA, and pigments such as astaxanthin, β -carotene, and phycobiliproteins (phycocyanins and phycoerythrins) [1].

High production costs hinder the implementation of algal biomass as a feedstock for bulk commodities. For commodities, production costs should decrease to less than 1 €/kg dry weight [4, 5] while current cost price is estimated to be 6.4 €/kg for a 100 ha facility [6]. A crucial parameter influencing biomass production costs is photosynthetic efficiency; the efficiency at which solar light energy is captured as chemical energy in biomass. Under identical climatological conditions, a higher photosynthetic efficiency results in a higher ground areal productivity and a better use of production capacity and thus a decrease in biomass production costs [3, 4]. Photosynthetic efficiencies obtained under outdoor conditions are lower than the values obtained under laboratory conditions, under laboratory conditions values of 6% are obtained while for outdoor production values of around 3-5% are maximally predicted [5]. Under outdoor conditions photo saturation occurs [7] and essential cultivation parameters, such as temperature, cannot be controlled to the same extend as under laboratory conditions [8].

1.2 State-of-the-art microalgae production systems

A multidisciplinary approach is needed in order to solve the issues currently preventing commercial large scale production of microalgae [4]. One of the key factors within this approach is the design of a suitable reactor system for large scale commercial production of microalgae. Reactor designs that are often used and that have a proven track record at a semi-industrial scale are the open raceway pond, horizontal and vertical tubular photobioreactors, and flat panel photobioreactors. Each of the reactor designs has its own advantages and disadvantages, which are discussed below.

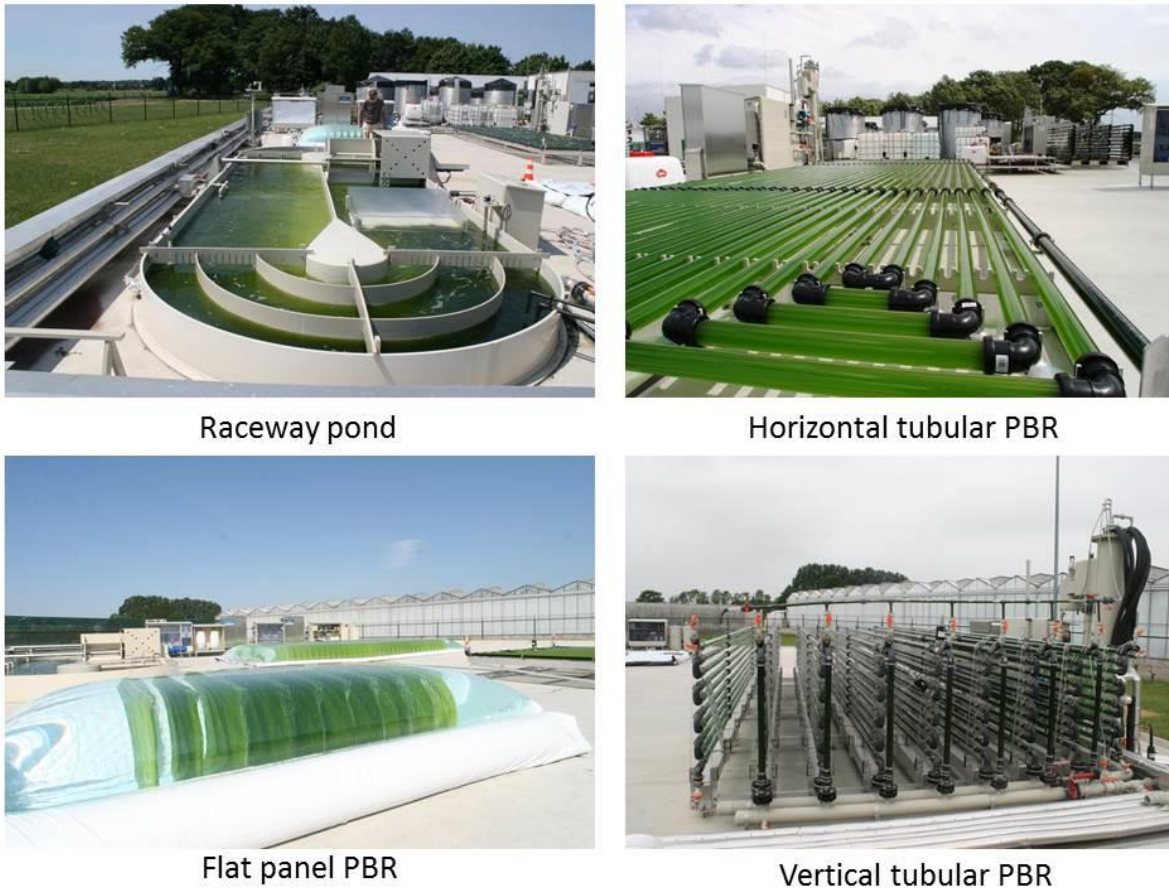


Figure 1.1 Overview of cultivation systems installed at the AlgaePARC pilot facility. PBR; photobioreactor.

1.2.1 Open raceway pond

The open raceway pond is a system in which the culture is not physically separated from the environment and ambient conditions. Open raceway ponds typically have a culture depth of 10-30 centimetre and the culture is mixed via a paddle wheel through long channels. As a result of the relatively long optical path lower biomass concentrations are found for open raceway ponds in comparison to other systems [9]. Open raceway ponds are commonly operated at liquid velocities around 0.25 m s^{-1} [9]. Raceway ponds are much longer than their width, a ratio of 10:1 is considered as optimal [10]. As raceway ponds are open, the system is more vulnerable to contaminations. Therefore, only a limited number of species, which can be grown under specific and very often extreme conditions that hinder contamination, can be cultivated. Raceway ponds require low investment costs, however, the low biomass concentrations result in significant costs for harvesting the microalgal biomass [2, 5].

1.2.2 Tubular systems

In tubular photobioreactors the culture is circulated through transparent tubes, and is in this way exposed to sunlight. Tubular systems can be found in different orientations; tubes arranged in a single horizontal plane, or arranged in multiple vertical planes (fence-like systems) Figure 1.1 [8].

Typically, the liquid velocity in tubular systems is $0.3\text{-}0.6\text{ m s}^{-1}$, while higher values ($0.6\text{-}0.9\text{ m s}^{-1}$) are used to prevent fouling. The use of higher liquid velocities results in higher production costs. Tube diameter varies from 0.02 to 0.15 m , with shorter diameters resulting in higher biomass densities. As a result of photosynthesis, dissolved oxygen accumulates in the algae suspension which is pumped through the tube. The extension of accumulation depends on the photosynthetic rate, length of the tubes, and culture velocity in the tubes. High dissolved oxygen concentrations are known to negatively affect growth [11]. Therefore, the oxygen needs to be removed and for this purpose a degasser is part of any tubular photobioreactor. Such a degasser can be a vertical bubble column where air, or an air/carbon dioxide mixture is injected [12]. The bubble column results in a dark volume where no net growth takes place. Moreover, the alternation between light (tubes) and darkness (degasser) could negatively affect growth [13]. The dark volume should therefore, be minimized in tubular photobioreactors.

1.2.3 Flat panel photobioreactors

Flat panel photobioreactors are narrow rectangular vertical vessels where the microalgal culture is mixed by aeration [8]. Flat panel photobioreactors are made from transparent materials: glass or plastic plates, or plastic films. As the culture is mixed by aeration ($\leq 1\text{ L}^{-1}\text{ L}^{-1}\text{ min}^{-1}$ or 1 vvm), the dissolved oxygen is removed where it is produced, therefore this system does not require a separate degasser. The culture depth (i.e. shortest optical path) is often short, ranging from 0.01 to 0.1 m [14]. A problem encountered with flat panels lies in their scale-up, which is usually done by increasing the number of units and not by increasing the volume of each unit. Due to their design mixing mainly takes place on the vertical axis, thus having a limited mixing over the horizontal axis of the reactor. This results in a maximal width for a unit, which is smaller than that of tubular reactors and raceway ponds. As a result of this, more infrastructure and especially labour is required to construct and operate a commercial plant with flat panels in comparison to tubular systems. Flat panels designs that have solved these issues are the ProviAPT system designed by Proviron (Figure 1.1), The Green wall panel developed at the University of Florence, and the Solix biofuels flat panels [15, 16].

1.3 Thesis aim and outline

The different reactor concepts; open raceway pond, tubular and flat panel photobioreactors are usually operated at the facility where the reactor concept was designed, thus at different locations and under different climatological conditions. These reactor concepts are often operated with different microalgae species. Furthermore, measurements done to evaluate the performance of a system are not uniform among the different research groups and companies. All these factors limit a proper comparison of different photobioreactor concepts. For this reason the AlgaePARC pilot facility was constructed, where the four most used reactor concepts can be compared [9]. The reactor concepts installed at AlgaePARC are an open raceway pond, a horizontal tubular photobioreactor, a vertically stacked horizontal tubular photobioreactor and a flat panel photobioreactor (Figure 1.1). During the work carried out for this thesis all reactor designs were operated with the same microalgae species; *Nannochloropsis* sp., the same cultivation media, the same pH and temperature, which was controlled between 20 and 35°C .

In **Chapter 2** the design and construction of the microalgae pilot plant facility AlgaePARC is reported; the **Algae Production And Research Centre**. This pilot facility was constructed in order to bridge the gap between laboratory research and commercial scale production facilities. This chapter

describes the development of the pilot facility, decisions made during the construction, and reports on the technical specifications on each of the cultivation systems used in this thesis.

In **Chapter 3** the effect of dilution rate on the productivity and photosynthetic efficiency of the four different photobioreactor designs was studied, which were operated as chemostat. High dilution rates will result in low biomass density and photo saturation of the culture will take place. Too high dilution rates can result in a washout of the culture. At decreasing dilution rates the biomass concentration will increase. At too low dilution rates biomass concentrations will become too high and photo limitation will hamper the performance of the culture. All these phenomena can result in a suboptimal operation of outdoor photobioreactors. For this reason, the optimal dilution rate (resulting in maximal production) was determined for each cultivation system.

In **Chapter 4**, the effect of biomass concentration on the productivity and photosynthetic efficiency was studied for three of the outdoor pilot scale photobioreactors (raceway pond, horizontal and vertical tubular PBR). In order to accomplish this these reactors were operated as a turbidostat. By means of turbidostat, biomass concentration is kept constant, while the dilution rate varies unlike in **Chapter 3**. Dilution is only activated during growth and culture washout is prevented. Similar to the study in **Chapter 3**, the optimal biomass concentration resulting in maximal areal productivity was determined for each reactor design.

In **Chapter 5**, model parameters for a growth model were determined for *Neochloris oleoabundans* and *Nannochloropsis* sp. The growth model includes both the influence of light and temperature on microalgal growth. The model and associated parameters allow predictions to be made on the productivity of large scale microalgae production plants. In this study such production predictions were made for scenarios with different regimes for irradiance, temperature. In addition, the impact of biomass concentration and microalgal specific light absorption coefficient were included in these predictions.

In **Chapter 6**, a techno-economic model is presented used to make projections on the biomass production costs for a 100 hectare scale facility for six geographical locations. For each of the locations the production costs were determined for four commonly used reactor designs on the basis of the experimental results in **Chapter 3**. In addition, a sensitivity analysis was done to determine the effect of improvements in different process parameters that can be expected in the near future. The results of the sensitivity analysis can be used as a guideline for future research.

In **Chapter 7**, the insights obtained in this thesis were combined with the techno-economic evaluation. In this general discussion projections are presented on the biomass production costs for a 100 hectare facility located in the Netherlands using vertically stacked horizontal tubular photobioreactors. The vertically stacked tubular photobioreactors were operated as chemostat at a daily dilution rate of 0.27 d^{-1} . Projections were made on reductions in biomass production costs when currently encountered challenges are resolved.

Chapter 2

Design and construction of the microalgal pilot facility AlgaePARC

This chapter has been published as:

R Bosma, **J.H. de Vree***, P.M. Slegers, M. Janssen, R.H. Wijffels, M.J. Barbosa (2014), **Design and construction of the microalgal pilot facility AlgaePARC**, Algal Research, 6 Part B, 160-169.

*J.H. de Vree, contributed significantly to the development of the pilot plant, executed all test runs and made improvements to the plant and co-authored the chapter.

2.1 Abstract

Microalgae gained much interest from industry as promising sustainable feedstock for the production of food, feed, bulk chemicals, and biofuels. Pilot scale research on microalgae is needed to bridge the gap between laboratory scale research and commercial applications. The AlgaePARC (Algae Production And Research Centre) pilot facility was constructed to bridge this gap. Objective of this pilot centre is to compare and improve photobioreactors and operational strategies under outdoor conditions. The pilot plant facility consists of four production systems (raceway pond, horizontal tubular reactor, vertically stacked tubular reactor and flat panels) and allows comparison of performance of these systems under identical climatological conditions. This paper describes the development of this pilot facility, decisions made during the building process and discusses the production systems including technical specifications, measurements and supporting facilities.

Highlights

- Description of an outdoor microalgal pilot facility
- Description of robust measurement and control system for continuous outdoor algal cultivation
- Description of upstream and harvesting process for algal production

Key words

Microalgae; pilot plant; photobioreactor; design

2.2 Introduction

Microalgal biomass is a promising biobased feedstock for industry. However, commercial microalgal production is still in its infancy and the market is still limited to high-value algal products [3, 17-19]. For commercial production of algae for commodities, production costs should decrease tenfold and scale of production should increase to industrial scale [5]. In the last five years, fundamental research on microalgae increased; publications on microalgae doubled and publications on photobioreactors tripled (search webofknowledge.com, 26-01-14). Most of this research is carried out on laboratory scale with artificial light under constant conditions. However, the translation of results from laboratory research to outdoor production for industrial applications needs to be done as well. Under outdoor conditions, photosynthetic efficiencies achieved are 3% in tubular systems [17, 20, 21] and even lower (1%) for raceway ponds [22]. Under controlled conditions in lab-scale flat panel reactors, photosynthetic efficiencies up to 6.5 % on solar energy are already achieved [23], being the theoretical efficiency of 7% when accounting for nightly biomass loss, light reflection and maintenance [19]. Norsker et al. [5] showed that an increase in photosynthetic efficiency from 3 to 5% leads to a reduction in costs of production of 35%. It is presently a challenge to reach high photosynthetic efficiencies (> 5%) on sunlight in a production system outdoors and maintain these throughout one growing season.

It is still not clear which production system is the best for commercial applications. Often it is assumed that production in raceway ponds is cheapest. Norsker et al. [5], however, showed that per kg of biomass produced this is not the case and that the possibilities to improve technology are much better for closed photobioreactors than for raceway ponds. It is essential that these improvements are made because a tenfold reduction in costs of production is necessary for commercial production of bulk commodities. Before improving existing technology we wanted to have practical data to obtain insight in the factors that determine the cost of production in different systems. Comparing the performance of different outdoor systems based on literature is impossible today as different species are cultivated, the reactors are placed at different locations, measurements often differ and the mode of operation is different. The AlgaePARC pilot facility was built to perform research to understand the cost factors in the different systems and to develop strategies to improve photobioreactor design and operational procedures. The uniqueness of AlgaePARC is that four different pilot scale photobioreactors were constructed outdoors on the same location. Together with nineteen industrial partners from the food, oil, chemical and technology development sectors, a five year research program was started to compare and improve production of biomass and specific biomass components. This paper describes the design and construction of this pilot facility, discusses the different production systems including technical specifications, states the online and offline measurements and describes supportive equipment.

2.2.1 Success criteria

AlgaePARC will be a success if:

A comparison is made between the different production systems under outdoor conditions based on the following parameters: photosynthetic efficiency, areal productivity, energy, water and nutrient usage, robustness and manpower

A photosynthetic efficiency on sunlight of 5% has been achieved in a production system outdoors and maintained throughout one growing season

An improved reactor concept and/or process strategy has been developed based on the outdoor results, in which the production costs and energy requirements are decreased

Sufficient basic information is obtained to design a demonstration-scale production facility for production of commodities (lipids, proteins)

2.2.2 Short overview

At the AlgaePARC pilot plant facility (51° 59' N, 5° 39' E), the following photobioreactor designs are compared: raceway pond, horizontal tubular reactor, vertically stacked tubular reactor and flat panels. These designs were selected based on the available photobioreactor concepts that have been scaled up so far. Four large reactors were constructed on about the same ground surface area (25 m²). The performance of these systems will be compared on the basis of horizontal ground surface area under the same climatological conditions. In addition, three smaller systems of 2.5 m² ground surface were built (tubular reactors and flat panels) to test new strains and operational concepts. In all systems water, energy, and in the gas phase carbon dioxide and oxygen are measured online. The direct and indirect light intensity are measured online as well. Nutrient usage and man power are logged per system offline. The systems are controlled via a central computer system for automatic operation, online data collection and generation of alarms in cases of problems during operation. The cultivation systems can be operated batch wise, as chemostat (constant dilution rate) and turbidostat (constant biomass concentration).

The lay-out of the systems and the environmental permits are discussed first. Then, all systems are described in detail, followed by online and offline measurements done during cultivation. Finally, the supportive facilities are addressed.

2.3 Construction of the Pilot plant

2.3.1 Layout AlgaePARC facility

Figure 2.1 shows the layout of the AlgaePARC facility; Table 2.1 shows the major equipment installed.

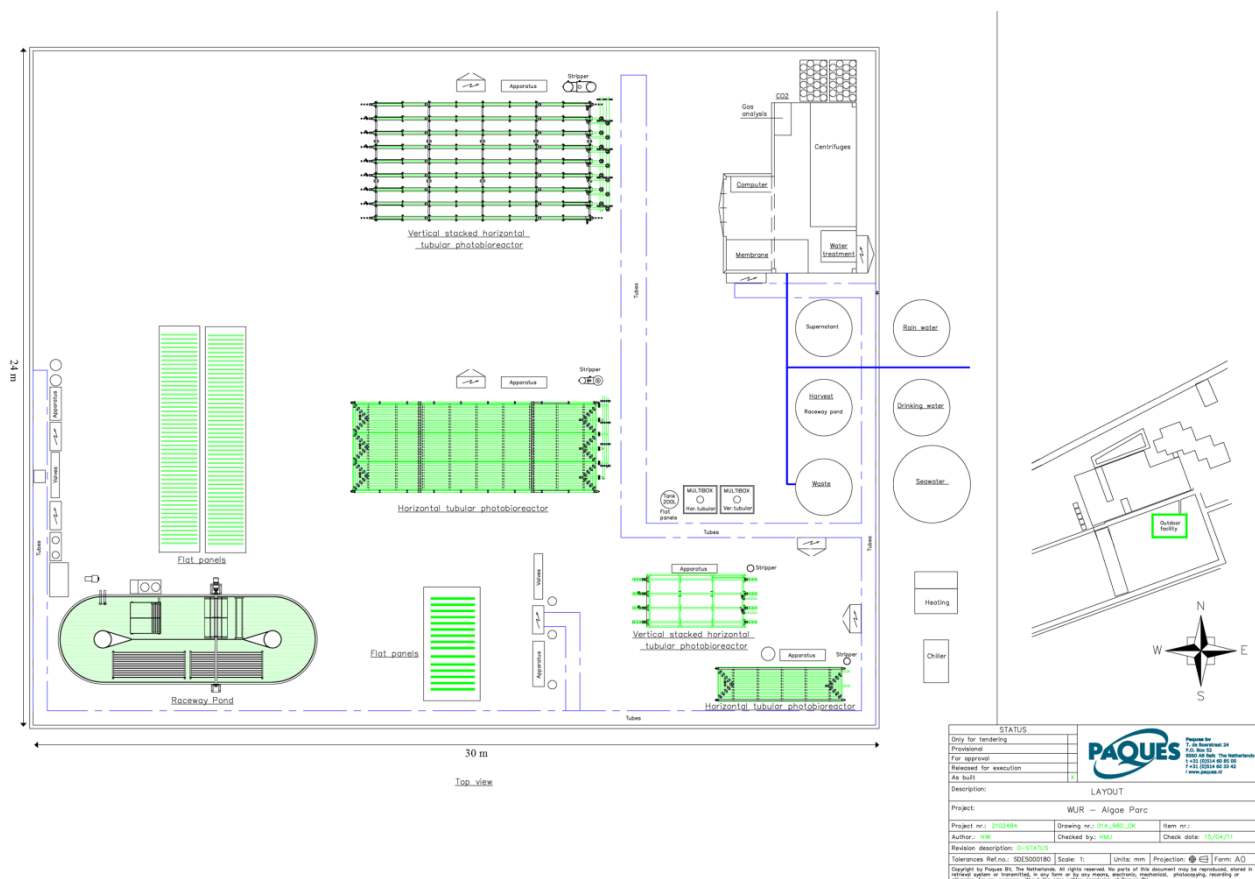


Figure 2.1. Layout AlgaePARC facility

Table 2.1. Specification of major equipment installed

Equipment	No.	Type	Remarks
Large reactors (25 m ² ground surface)	4	Design WageningenUR/Paques	ProviAPT bags by Proviron
Small reactors (2.5 m ² ground surface)	3	Design WUR/Paques	
Chiller	1	Rhoss TCAEY 238 T&P	Nominal cooling power 38.8 kW
Electrical heater	1	Welvy C82-45	Heating capacity 45 kW
Centrifuge	2	SSD 6	Max. cap 1 m ³ hr ⁻¹
Centrifuge	2	SSD 1	Max. cap 0.2 m ³ hr ⁻¹
Water sterilisation unit	1	Design van der Arend	Max. 2 bar water pressure
Ultrafiltration, 80 nm membrane	1	Design Bruine de Bruin	Max. cap 1.6 m ³ hr ⁻¹

2.3.2 Positioning of reactors

The reactor orientation (surface facing N-S or E-W) is not important for horizontal systems (raceway pond and horizontal tubular), because the received light intensity is independent of reactor orientation. However, in vertical systems (vertically stacked tubular reactors and flat panels) where shading takes place, reactor orientation affects productivity. Modelling studies by Slegers et al. [24] indicated that yearly areal biomass production in the Netherlands is improved up to 50% when the

walls of the reactor face N-S instead of E-W. Therefore, walls of all tubular reactors and flat panels in AlgaePARC face N-S. To prevent shading of the reactors by other reactors, the horizontal systems, being lowest, were built on the southern side of the facility. The necessary distance between reactor systems to prevent shading from the stripper was determined.

2.3.3 Permits

For the construction of the pilot facility, a construction and environmental permit were required from the municipality. To obtain the environmental permit strict measures were taken at AlgaePARC to prevent release of possibly harmful algae to the environment, because legislation is missing and authorities are unaware of the risks associated with algae. The reinforced concrete platform on which the plant was built was raised at the edges with 10 cm and all reactors are equipped with a level sensor that allows detection of reactor leakages. When a leakage occurs, the electronic sewer valve will be automatically closed, keeping the algae inside the platform, so the algae can be collected for inactivation before release to the sewage system. Bird protection (BirdXPeller PRO) was installed to prevent birds taking algae from the open pond, and a fence (dug 30 cm into the ground) was placed around the facility to prevent entrance of animals (cats/rats/rodents). The last two measures were also important to prevent damage of the systems. After centrifugation, the supernatant is pumped through an ultrafiltration membrane (80 nm) to remove remaining biomass. This biomass is collected and inactivated before discharge. Summarising, severe measures were taken at AlgaePARC pilot facilities to ensure that algae production takes place under containment because the authorities are unfamiliar with the environmental risks involved in algal cultivation. Little research has been done on these risks, but for commercial production it will be important to assess the risks and proof safety of the algae when released to the environment.

2.4 Overview of the photobioreactors installed at AlgaePARC pilot facilities

At AlgaePARC four large production systems and three small production systems were constructed, Figure 2.2 shows pictures of the large systems; their specifications are given in Table 2.2. The raceway pond is most voluminous due to its large optical path. Advantages of this system is that it is simple to construct and easy to operate. Therefore, most commercially available biomass is currently produced in raceway ponds [1, 25]. Because of its low illuminated area to volume ratio (A/V ratio), biomass concentrations in this system are low and expected photosynthetic efficiency on sunlight (PE) is low (generally 1-1.5%, [22], due to photo-inhibition at surface, darkness at the bottom and poor mixing between these two zones. Because it is an open system, it is prone to contamination, controllability of culture conditions (pH, temperature, salinity) is low and water evaporation is high [26, 27]. The other three (closed) production systems have higher A/V ratios, allowing higher biomass concentrations and better control of culture conditions.



Figure 2.2. Photobioreactors in operation

From the closed reactors, photosynthetic efficiency is expected to be lowest in the horizontal tubular reactor, because algae experience high incident light intensities and photo-inhibition can occur. Oxygen produced in tubular systems by the microalgae can exceed 300% oxygen saturation, which could lead to growth inhibition of the algae and a severe loss of productivity [11, 28]. Therefore, dissolved oxygen concentrations higher than 300% should be prevented by increasing stripper efficiency or increasing liquid velocity. Expected photosynthetic efficiencies on sunlight is about 3% [20, 21]. Due to the vertical orientation, light is diluted in vertical systems and incident light intensities experienced by the algae are lower and photo-inhibition is prevented. Therefore, the vertically stacked tubular reactor and flat panel reactor are expected to reach higher photosynthetic efficiencies close to the maximum of 7% efficiency on sunlight [19, 23, 24]. The advantage of the flat panels system over the tubular systems is that it has a smaller optical path, allowing higher biomass concentrations.

Table 2.2. Specifications of the large photobioreactors

Specifications	Raceway pond	Horizontal tubular reactor	Vertical stacked tubular reactor	Flat panels (ProviAPT)
Optical path (m)	0.20	0.046	0.046	0.02 ¹⁾
Volume (m ³)	4.73	0.56	1.06	0.390
Illuminated volume (%)	100	73	71	100
Ground area occupied (m ²)	25.4	27.0 ²⁾	31.0 ²⁾	26.9
Illum. surface A /V ratio (m ² /m ³)	5	63.7	.6	100
Expected. biomass conc. (g/L)	0.2 - 1	2 - 4	1 - 3	2 - 5

¹⁾ Average value, ²⁾ Including half of ground area occupied by the dummies at Northern and Southern side of the reactor

At AlgaePARC pilot facilities the main goal is to study principles of reactor design and scale up parameters, and compare the performances of the different designs. Robust systems were constructed allowing a long research time (> 10 yrs.) with the same systems and to focus on decreasing the

operational costs of these systems. As materials to build the production systems polyethylene, polypropylene, PMMA and RVS 316 were chosen, due to their resistance to sea water and long life time. PMMA, which is a transparent thermoplastic was used as material for the tubing (photoactive part) of the tubular reactors because it has a high transparency (98%), high light transmission (92.3%, 380-720 nm, technical properties Gevacril, D307), very good resistance to weather conditions and corrosion and good chemical resistance and resistance to breakage. Polyethylene and polypropylene were used because these materials can be welded, making connections strong and water tight. Polyethylene was used to build the reactors (non-photoactive part) and tubing because it is strong and highly resistant to UV light. Harvest and supply lines were constructed from polypropylene because this material is flexible and can withstand high pressures. RVS 316 was used as material for the heat exchangers because of its good heat and transfer coefficient and for bulk materials (screw, bolts etc.). On industrial scale, reactor material costs become important and cheaper and less energy intensive materials for the reactors should be chosen. In addition, the option of recycled material should be investigated. Improvement of materials for photobioreactors is a field that needs attention due to its impact in the production costs.

2.4.1 Detailed description of tubular reactors

Figure 2.3 shows the schematic set up of the large horizontal system. Tubes with an inner and outside diameter of 0.046 m and 0.05 m were chosen respectively.

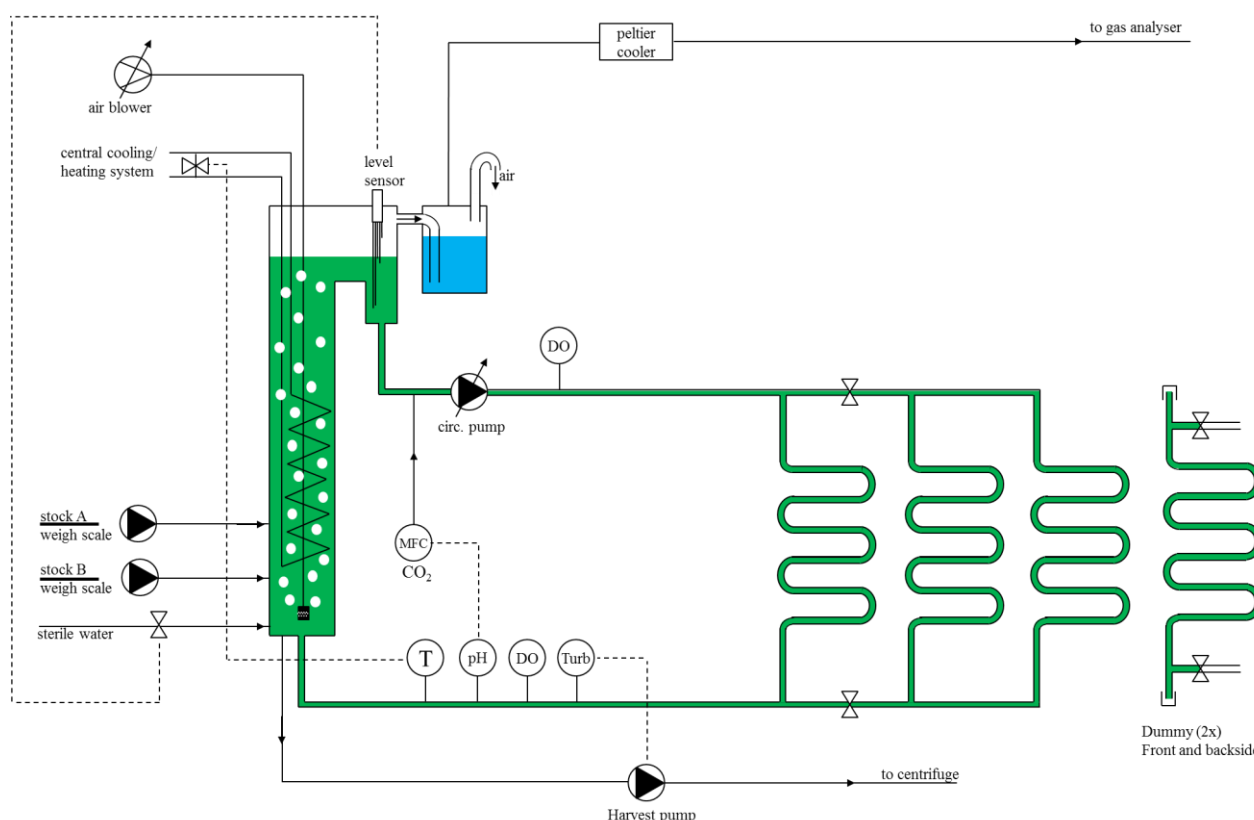


Figure 2.3. Schematic drawing of the large horizontal tubular system (HD). Dashed lines show control strategies.

Smaller diameters would implicate more pressure needed to circulate the liquid; higher diameters (> 0.1 m) are expected to lead to lower productivities [29] and are not desirable for harvesting because

more volume with lower biomass concentration need to be processed [27, 30, 31]. The tubes should be put close to each other based on modelling studies [29]. Due to the 180° bends needed in our system, a practical distance of 0.05 m between the tubes was chosen, implicating that only 50% ground area is covered in the horizontal system. A maximal loop length of 78 meter was calculated with a liquid flow rate of 0.6 m s⁻¹ to avoid dissolved oxygen concentrations higher than 300% (air saturation). The large horizontal system consists of 3 loops, of 80 m long (10 tubes of 8 m) each originating from and ending in central header tubes. The loops were placed 0.4 m above ground level to prevent dirt formation on the tubes by rainfall.

The vertical system consists of 7 similar loops placed vertically giving a loop height of 0.95 m. Also these vertically oriented loops were placed 0.4m above ground level (total loop height 1.35 m) to prevent dirt formation. The vertical distance between the tubes was kept at 0.05 m to allow fair comparison of both systems. Placing more tubes vertically is not beneficial because light intensity on the surface of the tubes at the bottom will become too low [29]. With the model of Slegers et al. [29] a distance of 0.50 m between the vertical loops was determined predicting good productivities in the Dutch weather conditions and also allowing to perform maintenance on the loops if needed (possibility to walk in between). In both large reactors, the first loop can be segmented from the other loops, allowing initial inoculation of the first loop with less inoculum, and after successful growth inoculation of the other loops.

Dummies were placed on the Northern and Southern side of the system (horizontal system: one tube; vertical system: one loop) filled with colorant to mimic shading effects. Without these dummies, the first tubes/loops at the Northern/Southern sides would receive more light from the side than the other loops and due to the size of the pilot plan this would have a relatively high effect on the overall productivity leading to an overestimation of industrial scale productivities when extrapolated.

Table 2.3. Specifications of major equipment in the large tubular systems HD: large horizontal tubular system, VD: large vertically stacked horizontal tubular system.

Equipment	No.	Type	Remarks
Circulation pump	1	ARBO KR-80-160	Close-coupled model 28 m ³ h ⁻¹
Harvest pump	1	Sigma 3 S3BA	Diaphragm metering pump, 0.55 kW
Nutrient pumps	2	Beta/4	Dosing pump
Air blower large systems	1	Elmo & Rietschle HD: G-BH7 VD: SAH 55	Single stage channel blower 0.55 kW 0.75 kW

Table 2.3 shows the major equipment of the large tubular systems. Low shear circulation pumps (low rotating velocity, large capacity) were chosen to circulate the culture because too high shear rates can damage algae [32]. Maximum liquid velocities were set at 0.6 m s⁻¹ for the tubular systems. High liquid velocities are required to prevent high oxygen concentrations, because it decreases algal residence time in the tubes [21] and prevents biofilm formation. However, high liquid velocities also imply high energy costs for pumping. Research is needed to determine the optimal liquid velocity at

which energy costs for pumping are decreases and performance of algal productivity of the system is not affected.

Temperature can be controlled between a low and high set point (e.g. 20 °C/30 °C). If temperature drops below the low set point, a three-way valve (Belimo LR24A-SR) opens (Proportional Integral Differential (PID) regulation) and hot water (max. 60 °C) flows through three heat exchange spirals in the stripper, heating up the system until the lower set point is reached. The same occurs for the high set point, but then chilled water (8 °C) flows through the heat exchange spirals, cooling the system until temperature drops below the higher set point.

The systems can be run continuously as turbidostat (biomass concentration is kept constant) and chemostat (dilution rate is kept constant). When the systems are harvested in either mode, algae are removed, and liquid level drops inside the stripper. This generates a “low level” signal by level sensors and automatically water and concentrated (100x) stock solutions are added on 1:100 ratio (flow proportional). Instead of flow proportional addition of nutrients, also a desired amount of stock solution can be added to the system over the day. Stock solutions are placed on balances, which are logged online, to monitor nutrients addition in the different systems.

Oxygen removal

To prevent high dissolved oxygen (DO) concentrations which could be growth inhibiting for the algae [11], oxygen produced by the algae has to be removed continuously. In the systems vertical strippers were installed in which air is sparged from the bottom through 1 mm holes by industrial air blowers. These blowers were equipped with an air filter (Induvac, MBH series cartridge, 1 µm) to prevent other algae and/or protozoa entering the reactor. Height for the stripper was set at 2.2 meter (to prevent shading) and the maximum stripper volume was set at 15% of total reactor volume. These settings led to a calculated diameter of 0.24 m (HD) and 0.37 m (VD). Total dark volume including piping was set to be 30% of total reactor volume. Maximum oxygen production was assumed to be 0.003 mol O₂ m⁻³s⁻¹ [21]. To remove this oxygen, airflows of 7 (HD) and 16 (VD) m³ h⁻¹ were calculated. During operation of the tubular systems in summer 2012, DO concentrations at the beginning of the loop were typically between 110-150% and DO concentrations at the end of the photoactive part never exceeded 300%, indicating sufficient oxygen removal.

Cleaning

To prevent biofilm forming or remove biofilm, presently two options are available: a pig that runs with the flow and cleans the systems (Microphyt, Montpellier) or granulate with higher and lower densities than culture medium (IGV GmbH, Germany, [27]). In a vertical system in which flow is distributed between several loops, using a pig is difficult, because when preferred flow of the pig to one loop occurs, only this loop is cleaned instead of all loops. Therefore, granulate was chosen to prevent biofilm formation in the tubular systems. Impellers of the circulation pumps were adapted to deal with the granulate (3-5 mm) of three different densities (Dowex polystyrene, 980 kg m⁻³; Pebax 7033 SP 01, 1020 kg m⁻³ and Arnitel® EL250, 1080 kg m⁻³) without damaging the pump and the balls. Initially Styron 678E (polystyrene resin) balls were tested, but due to the hardness of this material, it scratched the tube and therefore was replaced by elastomers.

De-aeration

In the tubular reactors, air pockets can be formed along the tubes and if not removed, circulation flow can completely stop due to pressure build up (especially in the vertically stacked horizontal tubular system). In total eight different types of mechanical de-aerators were installed at the end of each loop to release air from the system. These de-aerators worked fine with (sea)water, but during cultivation, the de-aerators were clogged by the algae and started to leak culture liquid. Therefore, as solution to remove the air and preventing pressure build up, a transparent tube at the end of the photoactive part was installed. This solution has as advantage that all gas leaves the system via the stripper (and not from other degassing points), making it possible to close carbon dioxide and oxygen balances, which is important for research purposes.

Measurement and control

Each system is controlled via a PLC (Programmable Logic Controller) and is connected to a central PLC which is connected to a computer with the supervisory control and data management system (SCADA). The SCADA is used to control the equipment and to log the online measurements.

2.4.2 Raceway pond

The raceway pond was designed with 9 m length, 3 m width, with centre pillars at the side which were connected with a plate to create a loop/raceway flow (Figure 2.4). Commercially, raceway ponds are designed with high length/diameter (L/D) ratios up to 150 [33]. However, we choose for a more compact system (L/D ratio of 3), based on the design from Weissman, because it is known that on pilot scale the high L/D ratios used in commercial systems are not optimal [34]. Due to the lower L/D ratio in our pilot plant system, mixing is more severe and productivities will probably be overestimated compared to larger commercial systems [35]. The raceway pond is operated with a liquid level of 20 cm resulting in a total volume of 4.7 m³. The liquid level is kept constant via a level sensor (Endress & Hauser, FTW31-B2A5CA0A, 5 pins); when liquid level decreases due to evaporation, automatically water is added and nutrients are added flow proportionally; at rainfall liquid culture is automatically harvested to keep the liquid level at 0.20 m.

A paddle wheel with six blades (L 0.145 m, W 0.235 m) was constructed, and the blades were installed 5 cm from the bottom. A frequency controlled motor (0.75 kW, see Table 2.4 for specifications) is used to drive the paddlewheel and power output of this motor can be varied between 0-100%. Carbon dioxide is supplied through membrane hoses (creating small bubbles) installed at the bottom of the pond which is covered by a Plexiglas hood to minimize CO₂ losses.

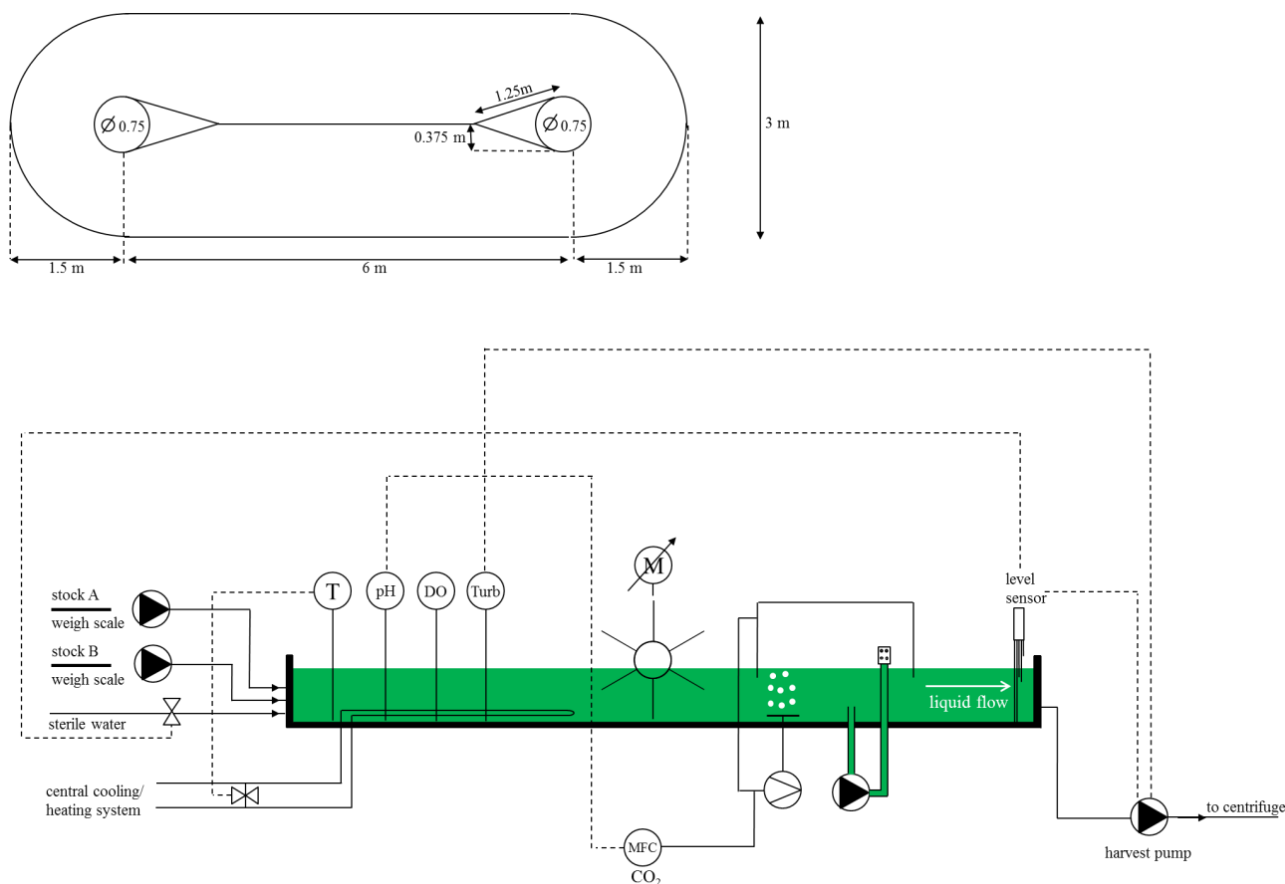


Figure 2.4. Schematic drawing of the raceway pond. Dashed lines show control strategies

Table 2.4. Specifications of major equipment in the open pond

Equipment	No.	Type	Remarks
Motor paddle wheel	1	SKH80B 4	0.75 kW
Air blower	1	Gardner & Denver G-BH1	0.20 kW
Harvest pump	1	Cent. Pump ARBO KR-32-95	4 m ³ /hr
Sprinkler pump	1	Gardena 3000/4	
Nutrient dosing	2	Dosmatic Minidos 12	Dosing at 1:100 ratio

The CO₂ enriched air is trapped by the hood and is recirculated by an industrial blower to prevent excessive losses of carbon dioxide. The CO₂ sparging led to foam formation under the hood; therefore a pump and two sprinklers were installed under the hood to mechanically break the foam. Temperature is measured and controlled by means of active heating via two heat exchangers installed on the bottom on the opposite side of the paddlewheel; cooling occurs via natural cooling by evaporation of water.

Flow distribution/dead zones

Microalgae settled especially in the corners of the raceway pond. To determine the flow distribution in the raceway pond, liquid velocities were measured at three locations over the width of the pond with a propeller current meter (Valeport “Braystroke” BFM002). It was found that especially in the corners, liquid velocities varied widely along the width of the pond, with being almost zero (dead zones) at the outside and up to 0.18 m s^{-1} close to the middle of the pond. At 40% output of the paddle wheel motor, without flow liners liquid velocities of 0.17 m s^{-1} were determined at a liquid level of 0.10 m (Figure 2.5). Higher motor outputs created waves in the open pond and could therefore not be used. To prevent dead zones, two flow liners were installed as proposed by Sompech et al. [33]. These flow liners resulted in a more uniform flow distribution over the width of the pond and additionally liquid velocities increased at all motor outputs by more than 50% (Figure 2.5).

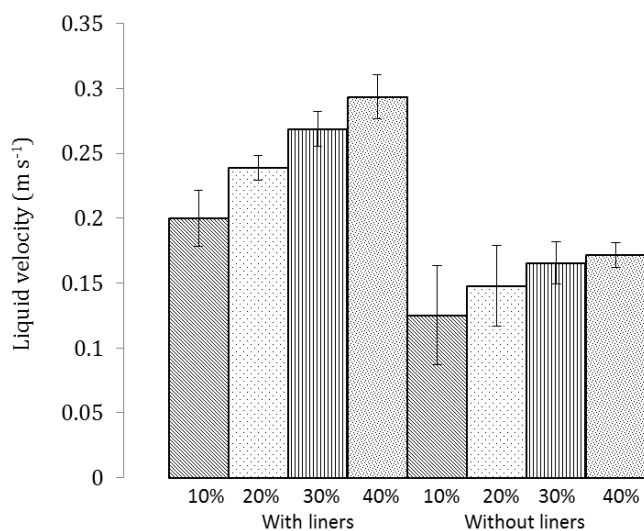


Figure 2.5. Average liquid velocities measured at a depth of 0.10 m over the width of the pond. Measurements were done at the opposite side of the paddlewheel with and without flow liners

2.4.3 Flat panels

Proviron developed a closed photobioreactor called ProviAPT (EP Patent 2,039,753, 2009, EP Patent 2,203,546, 2011). The photobioreactor is made completely from polyethylene of 180 μm thickness, therefore material requirements and costs are much lower. Two reactors were needed to cover a ground area of 25 m^2 . One reactor consists of 35 flat panels (Height 0.50 m, Width 1.25m, average diameter 0.02 m); the vertical panels are placed 0.25 m from each other. These flat panels are enclosed in a plastic bag that is filled with 6 m^3 water for structural support and temperature control (Figure 2.6). The air pressure over the cultivation chambers is kept higher (150 mbar) than the external air pressure to keep the panels inflated, with two industrial air blowers (Table 2.5). Medium is prepared in a separate vessel by adding a maximum of two nutrient stocks to sterile water. Medium from this vessel is pumped to a central feeding line that is attached to the flat panels and distributes the medium to each panel via the bottom of each vessel. When medium is added via the panels bottom, algae overflow at the top of the panels. This overflow is assembled in a central harvest line at the other side of the panels and flows into a separation tank. In this separation tank algae and air are separated and by recirculation of the air, the air pressure can be kept constant. From this

separator tank, algae are harvested with a pump. This system can be run as chemostat and daily up to three harvesting cycles can be done.

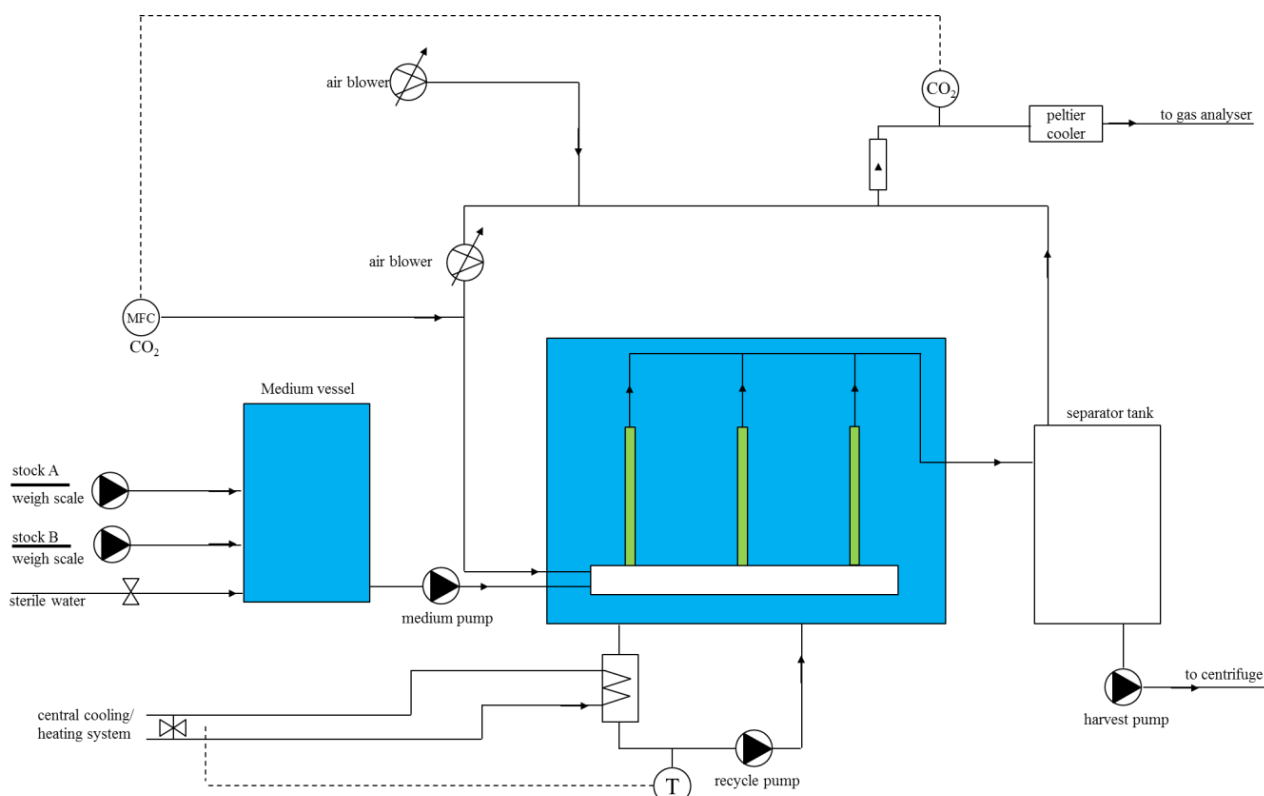


Figure 2.6. Schematic drawing of the flat panel system. Dashed lines show control strategies.

Table 2.5. Specifications of major equipment in the flat panel system

Equipment	No.	Type	Remarks
Air blower recirculation	1	Elmo & Rietschle G-BH7E	Single stage channel blower 1.5 kW
Air blower fresh air	1	KNF PM25432-838	
Medium pump	1	Verder V-MD-55H	centrifugal pump
Harvest pump	1	Jabsco 21560-9121	impeller pump, max. cap 0.9 m ³ /hr
Recirculation water pump	1	PSH Mini 2-33M	
Nutrient pumps	2	Beta/4	Dosing pump
Heat exchanger	1	PSA Heatline Heat 70	30 W at 60 °C

Temperature is controlled by heating/cooling the outer water buffer; the water is circulated with a pump over a heat exchanger; an electronic valve opens (like in the tubular systems) on demand. pH is automatically controlled by keeping the concentration of CO₂ in the recirculating gas phase constant by the addition of CO₂ on demand. To prevent too high oxygen concentrations, the oxygen concentration is measured in the gas phase and when it exceeds 30%, an automatic valve opens and the oxygen enriched air is released. Because pressure is kept constant, new air is automatically supplied to the system via the air blower and oxygen levels are reduced.

2.5 Measurements

The different systems will be compared on manpower and consumption of water, nutrient, carbon dioxide and energy. From biomass measurements, ground areal productivities will be determined and photosynthetic efficiencies will be calculated combining these productivities with online light measurements. To obtain data for comparing the systems, several online measurements are done (Table 2.6) every minute.

Table 2.6. Specifications of online measurements and equipment per system

Measurement/equipment	Sensor	Information
<i>All systems</i>		
Energy consumption	Saia-S AWD3D5W10	
Light measurement (PAR)	CaTec Li-Cor LI-190SA	PAR, $\mu\text{mol m}^{-2}\text{s}^{-1}$
Pyranometer	Delta-T devices Sunshine sensor BF5	Direct and indirect light
Gas analysis	Servomex 4100	0-100% O ₂ 0-2.5 % CO ₂
Temperature	Endress + Hauser TSM487-AFE	Easytemp
Nutrient addition	Sartorius Midrics MAPP	DC/FE
Water flow	Kobold MIK-5NA-20-A-E34R	MIK
Sample gas cooler	Buhler technologies PKE511	Peltier cooler
Water level	Endress & Hauser FTW31-B2A5CA0A	5 pins
<i>Tubular systems and open pond</i>		
pH/Temperature	Elscolab InPro3250/120/PT100	Stratos Pro
Dissolved oxygen	Mettler Toledo InPro6800/12/220	M300
Turbidity	Optek AS16-05	Control 4000
Carbon dioxide	Bronkhorst F201CV	EL-FLOW
Recirculation flow*	Endress + Hauser 50W40-UA0A1AA0AAAA	Promag 50
Airflow*	Kobold DOG-1101L-F25N-S-D	DOG
<i>Flat panels</i>		
CO ₂ sensor	Vaisala GMT221	
Airflow meter	DOG-1101LF25NSD	recirculation
Airflow meter	DOG-1102LF25NSD	new air
Pressure	Endress & Hauser PMC41	0-1000mbar

* Only tubular systems

In addition several offline measurements are done. All measurements will be discussed in detail in the following paragraphs; equations can be found in the supplementary material.

2.5.1 Online measurements

Temperature

In each system, temperature is measured and logged (example see appendix 2.I). Temperature is kept between a low and high set point by pumping hot/cold water of 60/8 °C from the central line via three-way valves to the systems on demand as explained earlier. The hot/cold water flows to the systems are logged via software (Priva Top Control 6.5 – TC vision) and from this data the energy consumed for heating/cooling the systems is determined.

Energy

In addition to the energy used for heating/cooling the systems, the energy consumption per production system is measured separately and logged.

Water

In each system the water flow (fresh/sea water) to the systems is measured and logged. In the harvesting vessels, level sensors (Endress Hauser Waterpilot FMX167) were installed and from these values, the volumes can be determined. As the ingoing and outgoing water flows are known, the water balances over each system can be closed.

On-line gas analysis

In all systems, a small fraction of the off gas is analysed on carbon dioxide and oxygen with two gas analysers. Off gas is first chilled down to 5°C with a Peltier cooler to remove water that could interfere with the gas analysis. Two gas analysers are present and electronic valves ensure that every 2 minutes each system is measured alternately. In addition, the outside air is measured. The gas analysers were installed in a temperature controlled room together with the water sterilization apparatus, centrifuges, ultrafiltration membrane and control computer. Each week gas analysers were recalibrated with pure nitrogen (zero), pure oxygen and 2.5% CO₂ with 20.0% O₂ in nitrogen. As control 20.0% O₂ was measured. Controls zero and full range values were reported. For oxygen, max. deviations for 27 weeks in 2014 were 0 ± 0.1 %, 20 ± 0.02 %, 100 ± 0.05 %. For carbon dioxide, max. deviations for the same period were 0 ± 0.01 %, 2.48 ± 0.06 %.

Nutrients

Two nutrient stock solutions are placed on separate nutrient balances and the weight of each nutrient vessel is measured and logged. In addition, nutrient concentration in the liquid culture are measured offline with a discrete analyser (Seal Analytics, Beun de Ronde, AQ2). By this, the nutrient consumption (nitrate, phosphate) by the algae can be determined per system.

Dissolved oxygen

In the large tubular systems, dissolved oxygen (DO) concentrations are measured before the culture enters the photoactive part and at the end of the loop before entering the degasser. By the difference in DO, it can be determined if the algae are photo synthetically active. In addition, the DO sensor can be installed at 24, 48 and 80 m from the beginning of the loop, via retractable ports and the oxygen build up along the tube length can be measured. In the raceway pond the dissolved oxygen concentration is measured before the paddlewheel. Once a week, all DO electrodes are recalibrated with outside air (100% air saturation).

Turbidity measurement

In all tubular systems and raceway pond, turbidity sensors were installed to measure biomass concentration online. The zero of the turbidity sensors is calibrated with seawater (when filling the systems for a new run), the slope by offline dry weight determinations. In all systems a linear relation of *Nannochloropsis sp.* (CCAP 211/78) dry weight concentrations and turbidity was found with high accuracy ($R^2 > 0.91$); this linear relation was found until 3.5 g L⁻¹ dry weight, higher biomass concentrations were not tested. With this online biomass concentration measurement the systems can be operated as turbidostat (constant biomass concentration, see Appendix 2.I for example). Advantage is that light and temperature are then the only variables outdoors and more algae are harvested when algal productivity is high. The turbidity sensor of the raceway pond is

cleaned daily, because otherwise biofilm would be formed on the sensor; the turbidity sensors of all tubular systems are cleaned each week, because flow in these systems are more turbulent and by weekly cleaning a stable signal was found.

2.5.2 Offline measurements

Biomass concentration

From the reactors samples are taken and optical densities at 680 and 750 nm (Hach Lange DR5000), pH (Mettler Toledo Education Line) and PAM (pulse modulated fluorometry, AquaPen-C AP-C 100) measurements are done on daily basis. In addition dry weight is measured three times a week and the correlation between OD₇₅₀ and dry weight is determined. With harvested volume, system volume and dry weight, productivities for each system can be calculated.

Manpower

Manpower is logged in an Excel file for each system separately. From these data, the amount of time required for cleaning, operation and start-up of each system can be calculated.

Microscope

Three times a week, culture is checked on contaminations microscopically (Leica Laborlux S).

Checklist

To make sure all calibrations are done and everything is regularly checked, a weekly checklist was made (Appendix 2.G)

2.6 Supportive equipment

Central cooling/heating system

To keep culture temperature between a certain range, for each system separately, a temperature set point for cooling and heating can be set. When temperature rises above the high temperature set point or decreases below the lower temperature set point, an automatic three-way valve connected to a central cooling/heating line opens and the reactor is cooled or heated. We chose for a central cooling/heating system, because otherwise each reactor should have its own heating/cooling system involving higher costs. A disadvantage of a central cooling/heating system is that the request for either heating or cooling is system dependent. Therefore, it could occur that one system needs heating while another system needs cooling; to prevent overheating of the culture, cooling is set dominant overheating. To calculate the required capacity of the chiller, a peak solar intensity of 1000 W m⁻² (peak solar intensity Netherlands June, Photovoltaic Geographical Information System, <http://re.jrc.ec.europa.eu/pvgis/apps4/pvest.php>) was used and multiplied by the total illuminated area for each system. For the horizontal systems it was assumed that 150% of the projected area of the horizontal tubes was exposed to sunlight (100% illuminated from the top, 50% reflected light), for the other reactors, the ground surface was taken. This resulted in a required chiller capacity of 45 kW. The central heating/cooling system was filled with a 30% glycol/water mixture to prevent freezing during winter.

Water sterilization

In AlgaePARC tap water, rain water and natural sea water can be supplied to the photobioreactors. Chemical sterilization was chosen over high UV sterilisation, as it was easier to realize and sealing

of UV sterilisation equipment is not resistant to salt water. At AlgaePARC sterilization is done by hypochlorite which is added to the silos containing the water. The chlorine is removed by active carbon filters before being pumped to the photobioreactors. In addition, sea water is filtrated through a cascade filter (10 μm , 5 μm , and 1 μm) to remove algae and/or protozoa left after chemical sterilization.

Harvesting

GEA Westfalia Separator supplied two continuous centrifuges (type SSD 6) with a maximum capacity of 1 $\text{m}^3 \text{hr}^{-1}$ and two smaller continuous centrifuges (SD 1) with a maximum capacity of 0.2 $\text{m}^3 \text{hr}^{-1}$. These centrifuges are cleaned automatically and can be used on industrial scale. The harvested pasta had an average final biomass concentration of 18% w/w dry weight/water with a maximum of 24% w/w. Separator efficiency was on average 96%. A growth test was performed with material from the feed to the centrifuge and the harvested algal paste. It was found that centrifugation has no negative effect on algal growth and it cleans to some extent the biomass by removing bacteria/protozoa. After centrifugation, the biomass paste is sealed with a vacuum machine (Youngsun, YS-DQ-420) and stored at $-20\text{ }^\circ\text{C}$.

Ultra-filtration Membrane

Discharge of microalgae in the sewage system, was only allowed if no algal cells were present. An ultrafiltration membrane (80 nm) was installed to remove and concentrate the remaining microalgae from the supernatant, after centrifugation. The concentrated microalgae are deactivated by active chlorine. In addition, the ultrafiltration unit will allow recycling of supernatant of the centrifuges to the photobioreactors (media recycling) to decrease water footprint and nutrient usage.

LCA

As mentioned earlier, man power and water, nutrient, carbon dioxide and energy consumption will be measured for each system and be compared between systems. This data will also be used as input for the Life Cycle Assessment (LCA) that will determine cumulative energy demand, global warming potential and water consumption per system. Cumulative energy demand accounts for the energy embodied in material inputs to the system and will therefore be a consideration for designs and plant layout. Fresh water consumption is critical to evaluate as it will become scarce in future. This will become more contentious if microalgae are cultivated at locations where drinking water supplies are scarce. Water recovery schemes and water sources will be highlighted in the assessment. As designs improve and systems change, LCA models will keep track of costs, resource utilization, and outputs to the environment.

2.7 Lessons learned

Minimum temperature control

Initially cooling was installed in each system and heating only for frost protection (keep temperature $> 4\text{ }^\circ\text{C}$). However, productivities were low or even negative in fall 2011, because temperatures were still too low in the morning while sunlight was already available, and therefore algae were probably photo inhibited. Additional heating was installed and culture temperature was always maintained a few degrees below the species optimal temperature. This solution led to increased photosynthetic

activity (measured by increased dissolved oxygen levels) immediately when sunlight was available, and therefore increased productivities.

Inoculum chain

In 2011, inoculum was produced in a 4.5 L flat panel system. This implicated that we had to start with the smallest system (94 L) and from this system larger systems were inoculated. To allow a fast start up after downtime, more inoculum capacity was required; four 25 L flat panel reactors were built and a new indoor tubular reactor (280 L) was installed in a greenhouse (see Appendix 2.G). From cultures grown in Erlenmeyer flasks, a 25 L reactor is started and this culture is used as inoculum for the indoor tubular reactor. PH and temperature of the indoor tubular system can be controlled and extra artificial light ($350 \mu\text{mol m}^{-2}\text{s}^{-1}$) can be supplied by six high pressure sodium lamps. The amount of inoculum produced in 3-4 weeks by this inoculum chain allows start-up of all systems outdoors in one week.

Dead corners/sharp edged corners

Dead corners in the pipe lines are difficult to clean and allow contaminants to grow; all dead corners have been removed. In addition in the tubular systems sharp bends ($> 90^\circ$) were installed giving a high back pressure. They have been replaced by smooth bends so flow is circulated at the same velocity with less energy requirements.

Segmentation of first loop

We segmented the first loop of both large tubular systems from the other loops by including valves. Advantage is that the systems can be inoculated with less inoculum and, if the algae grow well, the complete system can be inoculated from this first loop.

Level sensors

During the growth season we experienced that level sensors fouled during operation and high level alarms were reported, while water levels were low. Water tight connectors were ordered and installed, allowing us to clean the level sensors during operation of the photobioreactors once a week (Appendix 2.H: weekly checklist).

2.8 Supplementary data

Appendix 2.A. Calculation of required distance between the systems

Appendix 2.B. Biomass treatment

Appendix 2.C. Design note length and spargers large tubular systems

Appendix 2.D. Schematic design of de-aeration system

Appendix 2.E. Carbon dioxide addition in the raceway pond.

Appendix 2.F. Calculations from the measurements

Appendix 2.G. Inoculum chain

Appendix 2.H. Weekly checklist

Appendix 2.I. Trends of several online measurements

2.9 Acknowledgements

We would like to thank the Ministry of Economic Affairs and Province of Gelderland for financial support for the construction of AlgaePARC. The research program Biosolar Cells with financial contributions from BASF, BioOils, Cellulac, Drie Wilgen Development, DSM, Exxon Mobil, GEA Westfalia Separator, Heliae, Neste, Nijhuis Water Technology BV, Paques, Proviron, Roquette, SABIC, Simris Alg, Staatsolie Suriname, Synthetic Genomics, TOTAL and Unilever are acknowledged as well.

Appendix 2.A. Calculation of required distance between the systems

Height degasser	2.1	m
Empty space between reactors	4	m
Conversion factor ° to rad	3.1415/180	

Sun height angle when shadowing occurs: $\tanh\left(\frac{H}{E}\right) * 180/\pi = 27.6^\circ$

Eq. (2.A.1). Calculation with 6 m empty space gives a sun height angle of 19.3° .

For each 21th day of the month, sun heights were calculated per hour (Equations: Table 2.A.1). The 21th day was chosen because 21 December and 21 June are the shortest, longest day respectively. Figure 2.A.1 shows the hours when the stripper of the Southern reactor shades the more Northern reactor. From, March to September, with 4 m distance, about 3 hours shading occurs, at the start and end of the day when sun is inclining in the sky. The electricity closet, having a height of 1.2 m, shaded other reactors only for 2 hours. Chosen was for a distance of 4 m between the reactors.

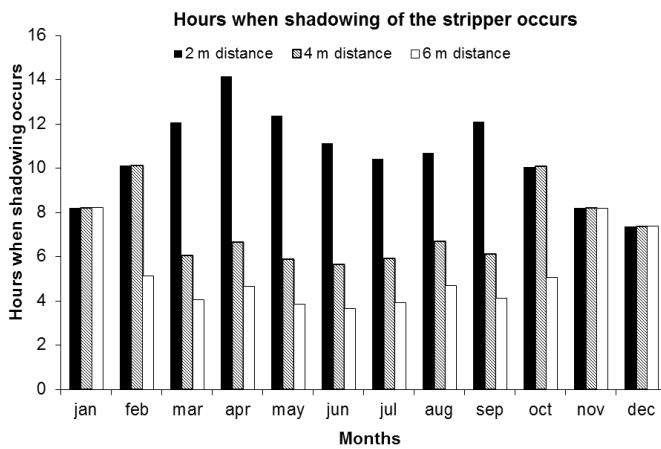


Figure 2.A.1 Hours of shading other photobioreactors by the stripper with 2, 4 and 6 m distance.

Table 2.A.1. Mathematic equations used to model the photobioreactor from [36].

$$\delta = 0.006918 - 0.399912 \cdot \cos \eta d - 0.006758 \cdot \cos 2\eta d - 0.002697 \cdot \cos 3\eta d + 0.070257 \cdot \sin \eta d +$$

$$0.000907 \cdot \sin 2\eta d + 0.00148 \cdot \sin 3\eta d \text{ with: } \eta = 2\pi/365 \text{ (rad)}$$

$$e = 0.0072 \cdot \cos \eta d - 0.0528 \cdot \cos 2\eta d - 0.0012 \cdot \cos 3\eta d - 0.1229 \cdot \sin \eta d - 0.1565 \cdot \sin 2\eta d - 0.0041 \cdot \sin 3\eta d$$

$$\text{with: } \eta = 2\pi/366 \text{ (rad)}$$

$$\text{WT(a)} = \text{time(a)} + \text{timezone} + \text{summertime} + \text{longitude}/15 + e$$

with: time(a) (hr), summertime (-1 hr), time zone(-1 hr), longitude photobioreactor (°)

$\omega(a) = (WT(a) - 12) \cdot 15^\circ$ and if $\omega(a) < -\pi$, $\omega(a) = -\omega(a) + 2\pi$

$\gamma(a) = a \sin(\sin \delta \cdot \sin \phi + \cos \delta \cdot \cos \phi \cos \omega(a))$ and $\gamma = 0^\circ$ if $\gamma < 0$

Daylength = $2/15 \cdot a \cos(-\tan(\phi) \cdot \tan(\delta)) \cdot 180/\pi$

Sunrise = $(12 - e - Daylength / 2 + 2 - longitude / 15)hr$

Sunrise = $(12 - e + Daylength / 2 + 2 - longitude / 15)hr$

Appendix 2.B. Biomass treatment

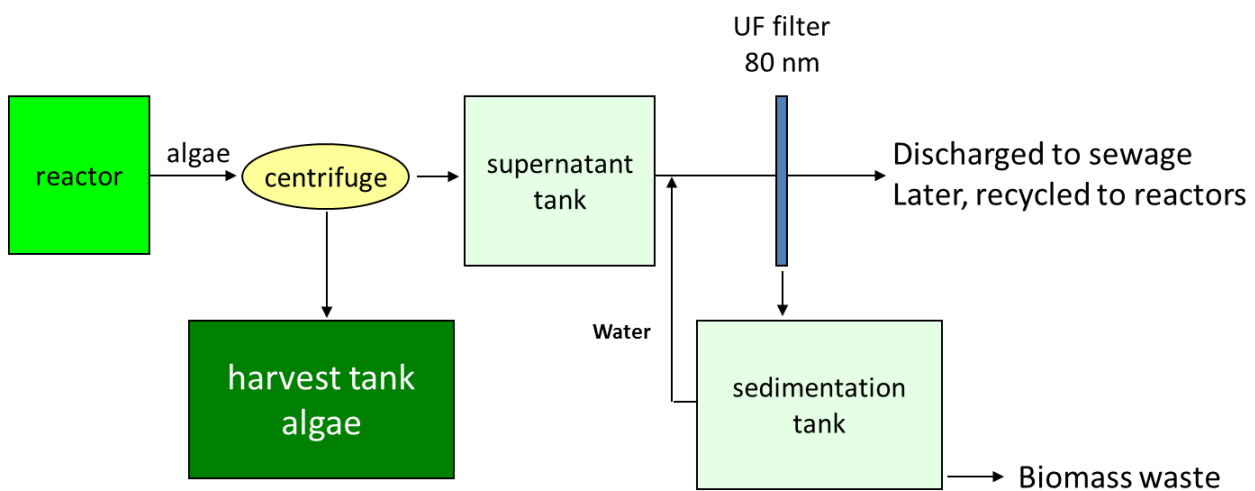


Figure 2.B.1 Separation of biomass

Appendix 2.C. Design note length and spargers large tubular systems

Length of the tubular reactor

Example calculation for horizontal system, sea water.

Estimated oxygen to be removed (RO₂): 0.003 mol m⁻³s⁻¹ [21]

Dissolved oxygen concentrations can be calculated via Henry's Law:

$$P_A = H \cdot C_A^*$$

HO₂ is 108.2 kPa m³mol⁻¹ for sea water, 35 ppt, 25 °C [37].

For water in equilibrium with air with an oxygen concentration of 100% (partial pressure of oxygen 0.2095 atm), a dissolved oxygen concentration of 0.19 mol m⁻³ can be calculated.

With $L = U_L \cdot ([O_2]_{out} - [O_2]_{in}) / R_{O_2}$ and outgoing oxygen concentration of 300% (0.58 mol m^{-3}), ingoing of 100% (0.19 mol m^{-3}) and liquid velocity of 0.6 m s^{-1} , a maximum tube length of 78 meter can be calculated.

Sparger horizontal tubular reactor

Volume of this reactor is 0.54 m^3 , implicating that with RO₂ of $0.003 \text{ mol m}^{-3} \text{ s}^{-1}$, 5.8 mol h^{-1} O₂ should be removed.

k_La_L can be estimated by the equations given by [38]:

$$k_L a_L = a / (U g^b - 1) \text{ with: a, b: } 0.874 \text{ and } -0.979 \text{ for tap water; } 2.222 \text{ and } -1.171 \text{ for sea water}$$

With an (assumed pressure less) superficial gas velocity (U_g) of 0.043 m s^{-1} calculated by dividing gas flow ($7 \text{ m}^3 \text{ h}^{-1}$) by area aerated (0.045 m^2), a k_La_L of 0.057 s^{-1} can be calculated for sea water.

The OTR (oxygen transfer rate) can be calculated via:

$$OTR = k_L a_L \cdot (C_{O_2, out} - C_{O_2, in}), \text{ giving } 0.022 \text{ O}_2 \text{ mol m}^{-3} \text{ stripper s}^{-1}$$

Reactor volume was 0.54 m^3 , max. stripper volume set was 15% or 0.081 m^3 .

This gives an oxygen removal rate of $0.022 \cdot 0.081 \cdot 3600 = 6.5 \text{ mol h}^{-1}$

Below the data is given for the both systems with tap and seawater.

Table 2.C.1. Rates of HD/VD for tap and sea water at 25 °C

	Horizontal system (HD)		Vertical tubular stacked system (VD)	
O ₂ produced (mol h ⁻¹)	5.83		13.2	
	tap water	sea water	tap water	sea water
K _L a _L (s ⁻¹)	0.042	0.057	0.042	0.056
OTR (mol O ₂ h ⁻¹)	5.87	6.54	13.1	14.6

Appendix 2.D. Schematic design of de-aeration system

Overview of the adaptations made to the de-aeration system in the vertically stacked horizontal tubular photobioreactor.

Sideview vertical demo

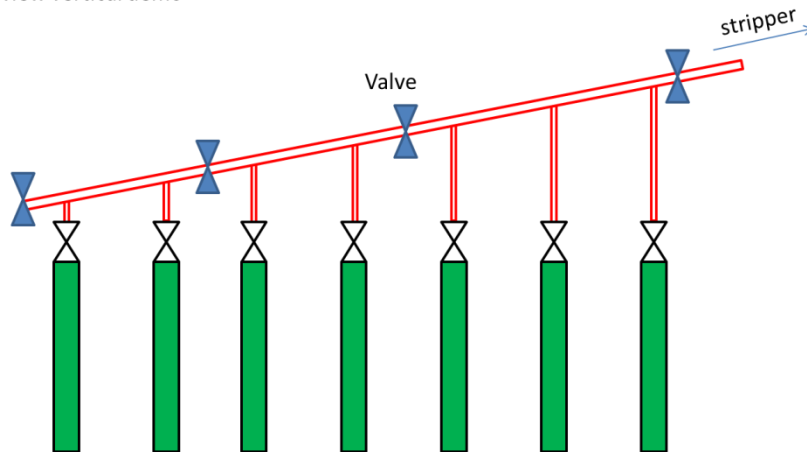


Figure 2.D.1. Schematic design of the de-aeration system of the vertical stacked horizontal tubular reactor. The aeration tube (red tube) is made of transparent plastic and from left to right increases in height to make sure that air bubbles go up. Connection to the stripper is made with silicon tube, to the top of the stripper.



Figure 2.D.2. De-aerator system in the large vertically stacked horizontal tubular system

Appendix 2.E. Carbon dioxide addition in the raceway pond.

Overview of the point of carbon dioxide addition in the open raceway pond.

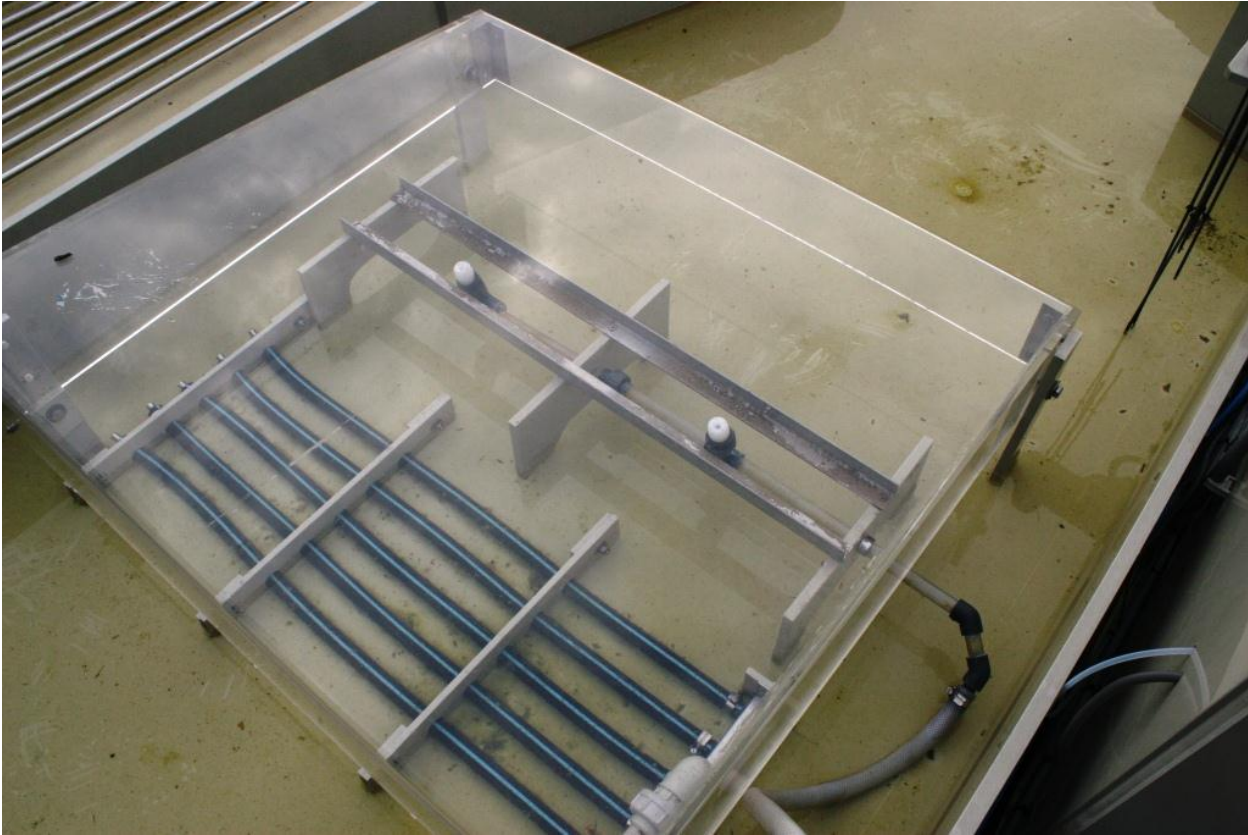


Figure 2.E.1. Carbon dioxide addition in the raceway pond

Appendix 2.F. Calculations from the measurements*Energy consumption cooling/heating*

Because the cooling/heating is shared, the energy consumption is approached by:

$$E_{system} = \frac{\phi_{system}}{\phi_{total}} \cdot E_{chiller/heater}$$

With ϕ_{system} : water flow to heat exchanger ($m^3 \text{ hr}^{-1}$); ϕ_{total} : total water flow of all systems ($m^3 \text{ hr}^{-1}$); $E_{chiller/heater}$: energy consumption of the chiller or heater (kW).

Water

Water balances can be calculated via:

$$\phi_{in} = \phi_{harvest} + \phi_{evaporation}$$

With ϕ_{in} : ingoing water flow (m^3); $\phi_{harvest}$: harvested volume (m^3); $\phi_{evaporation}$: water evaporated (m^3)

Gas balances

Oxygen balances (assuming equilibrium with the culture liquid) can be calculated via:

$$\phi_{stripper} \cdot [O_{2,air}] = \phi_{stripper} \cdot [O_{2,out}] + OPR$$

With $\phi_{stripper}$: gas flow stripper (mol h⁻¹); $[O_{2,air}]$: molar fraction of oxygen in the outside air (-); $[O_{2,out}]$: molar fraction of oxygen leaving the stripper (-); OPR: oxygen algal production rate (mol h⁻¹) [39].

Carbon dioxide balances (assuming equilibrium with the culture liquid) can be calculated via:

$$\phi_{in} = \phi_{stripper} \cdot [CO_{2,out}] + CUR$$

With ϕ_{in} : flow CO₂ (mol h⁻¹); $\phi_{stripper}$: gas flow stripper (mol h⁻¹); $[CO_{2,out}]$: molar fraction of carbon dioxide in the outflowing gas (-); CUR: carbon dioxide uptake rate by the algae (mol h⁻¹).

Productivity

Productivity per day can be calculated by:

$$P_{system} = \phi_{harvest} \cdot C_x + V_{system} \cdot (Cx_t - Cx_{t-1})$$

With: P_{system} : algal productivity (g d⁻¹); $\phi_{harvest}$: harvested volume (m³ d⁻¹); C_x : dry weight algal concentration (g m⁻³); V_{system} : system volume (m³); Cx_t , Cx_{t-1} : dry weight algal concentration in the photobioreactor (g m⁻³) at start and end of 24 hour period, respectively.

Nutrients

Nutrient consumption by the algae in the photobioreactor per day can be calculated via:

$$P_N = \phi_N \cdot C_N + V_{system} \cdot (C_{N_t} - C_{N_{t-1}}) + V_{harv} \cdot \frac{C_{N_t} - C_{N_{t-1}}}{2}$$

With P_N : nutrient consumption rate (mol h⁻¹); ϕ_N : nutrient flow (m³ d⁻¹); C_N : nutrient concentration (mol); V_{system} : system volume (m³); $C_{N,t}$, $C_{N,t-1}$: nutrient concentration (g m⁻³) at start and end of 24 hour period; V_{harv} : harvested volume (m³).

Appendix 2.G. Inoculum chain

Algal cultures are grown in 250 Erlenmeyer flasks placed on an orbital shaker incubator (Multitron, Infors HT, The Netherlands) at 120 rpm under 2% CO₂-enriched headspace, 70% humidity and 50 $\mu\text{mol m}^{-2} \text{s}^{-1}$ continuous light supply. These cultures were used as inoculum for the 25 L flat panels system (Figure 2.G.1), made by Wageningen UR workshop. Fluorescent lights could supply maximally 250 $\mu\text{mol m}^{-2} \text{s}^{-1}$ to the cultures. When the biomass density was about 3 g L⁻¹, the culture was used to inoculate an indoor tubular horizontal reactor (280 L, Figure 2.G.2). The photoactive part of this reactor was made of eight transparent flexible plastic LDPE tubes (8 m long, ϕ 94 mm;

Oerlemans Plastics, The Netherlands). The tubes were connected to a manifold, a recirculation pump and a reactor vessel. In the vessel, dissolved oxygen and pH sensors were placed, as well as cooling and heating coil. The pH was set at 7.5 and controlled by means of on demand CO₂ addition. Since the tubular reactor was located in a greenhouse, it was exposed to natural day/night cycles. To achieve higher biomass productivities, continuous light or light with a day/night rhythm (light intensity of 350 $\mu\text{mol m}^{-2}\text{s}^{-1}$) could be supplied by six high pressure sodium lamps (Hortilux, Schröder, the Netherlands) placed above the tubes.

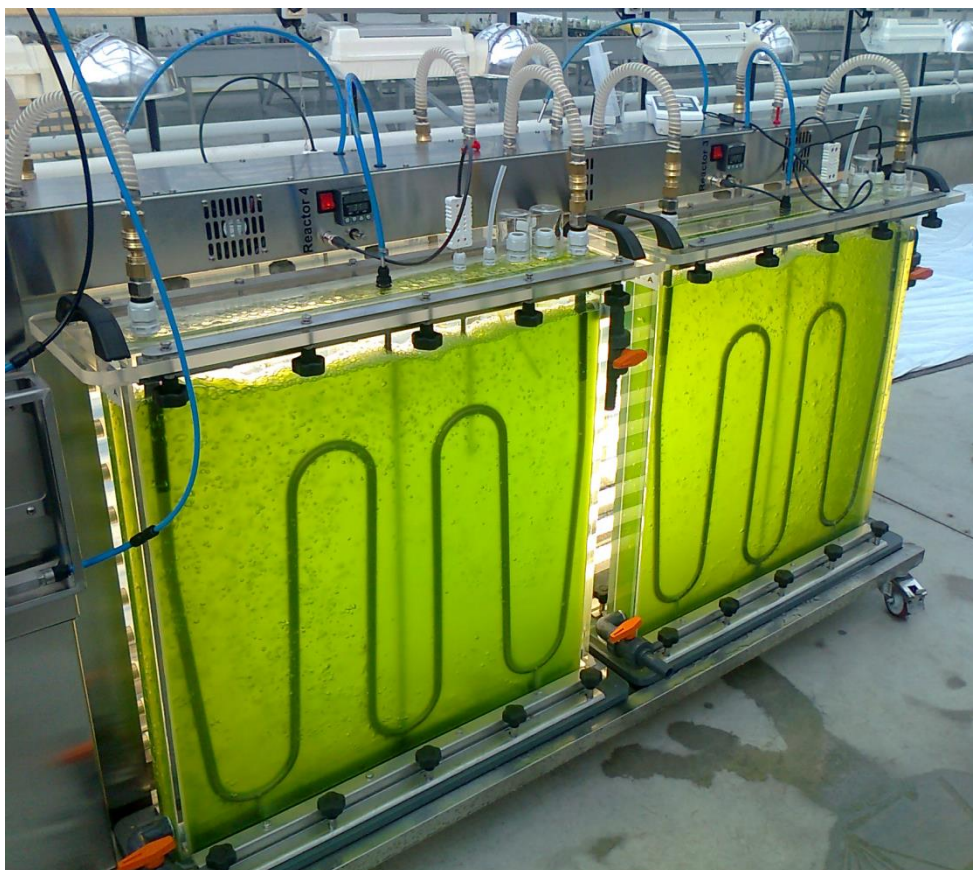


Figure 2.G.1. Four 25 L flat panel reactors



Figure 2.G.2. Indoor tubular reactor (280 L)

Appendix 2.H. Weekly checklist of AlgaePARC*Table 2.H.1. Weekly Checklist AlgaePARC pilot facility*

Week ... from ... to

	Mon	Tue	Wed	Thur	Fri	Sat	Sun
CO ₂ pressure > 20 bars							
Clean filters before harvest pumps							
Flush filters in harvest pipe with sea water							
Supernatant silo level <70%							
Restart computers to receive updates							
Calibrate gas analysers (CO ₂ and O ₂)							
Heating cooling system pressure >1.0 bar							
Sufficient gas flow to gas analysers							
Sufficient nutrients in all systems							
Nutrients cold room > 20L							
Level harvest silo, raceway pond < 60%							
Seawater level > 30%							
Sufficient antifoam in bottles of tubular systems							
Clean metal filter + hood pond							
Clean water locks of tubular systems							
Clean level sensors of all systems							
De-aerate heating/cooling system							
Make pictures of biofilm if present							
Clean turbidity sensor raceway pond							
Calibrate DO sensors with ambient air							
Clean turbidity sensors tubular systems							

Appendix 2.I. Trends of several online measurements.

Turbidity

Figure 2.I.1 shows trends of turbidity and light intensity for several days of the vertical large system that was operated as turbidostat. During the night, when no light is available, biomass concentration (measured as turbidity) decreased because the algae respire. After sunrise, turbidity increased and when turbidity reached 1700 NTU (1.01 g L^{-1}), the system was automatically diluted till it reached 1650 NTU (0.98 g L^{-1}). Harvesting occurred several times (dilution about 3% reactor volume per step) during the day.

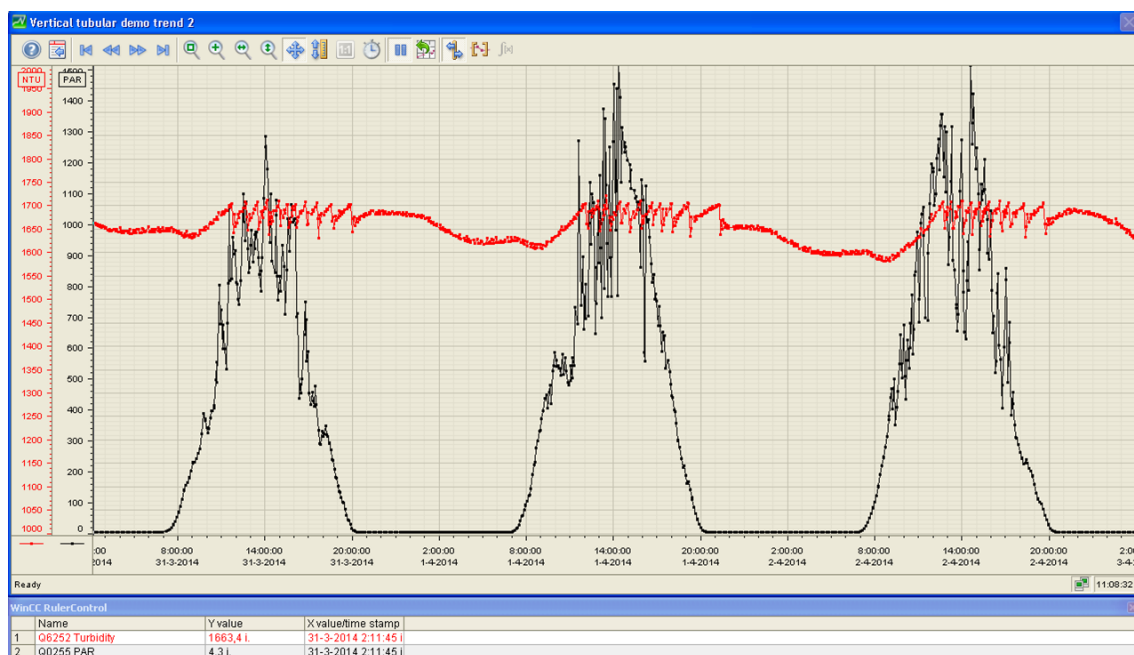


Figure 2.I.1. Trends of turbidity and light intensity in the large vertical system

Temperature control

Figure 2.I.2. shows culture temperature and light intensity for several days of the vertical large system. During the night, when culture temperature dropped below $20 \text{ }^{\circ}\text{C}$, heating occurred, keeping a minimal temperature of $19 \text{ }^{\circ}\text{C}$. When light increased, culture temperature also increased until it reached $30 \text{ }^{\circ}\text{C}$; then cooling occurred until temperature dropped again below $30 \text{ }^{\circ}\text{C}$. Maximum culture temperature reached during the day was $32 \text{ }^{\circ}\text{C}$.

pH control

Figure 2.I.3. shows trends of pH, carbon dioxide and light intensity for several days of the large vertical system. pH was controlled at pH 7.5 by adding carbon dioxide on demand. During the night a small carbon dioxide flow was needed because carbon dioxide was removed in the stripper by the air supplied. During the day, carbon dioxide flow increased when more light was available; pH was controlled between 7.3 and 7.7.

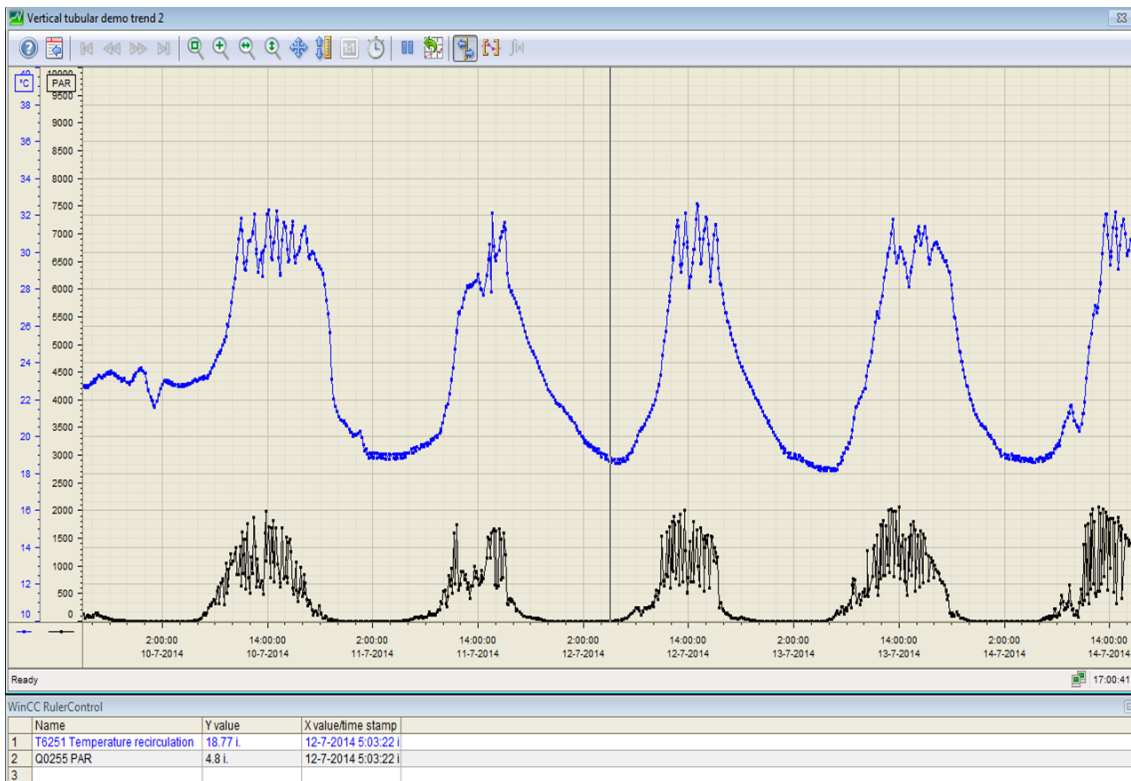


Figure 2.I.2. Trends of culture temperature and light intensity in the large vertical system

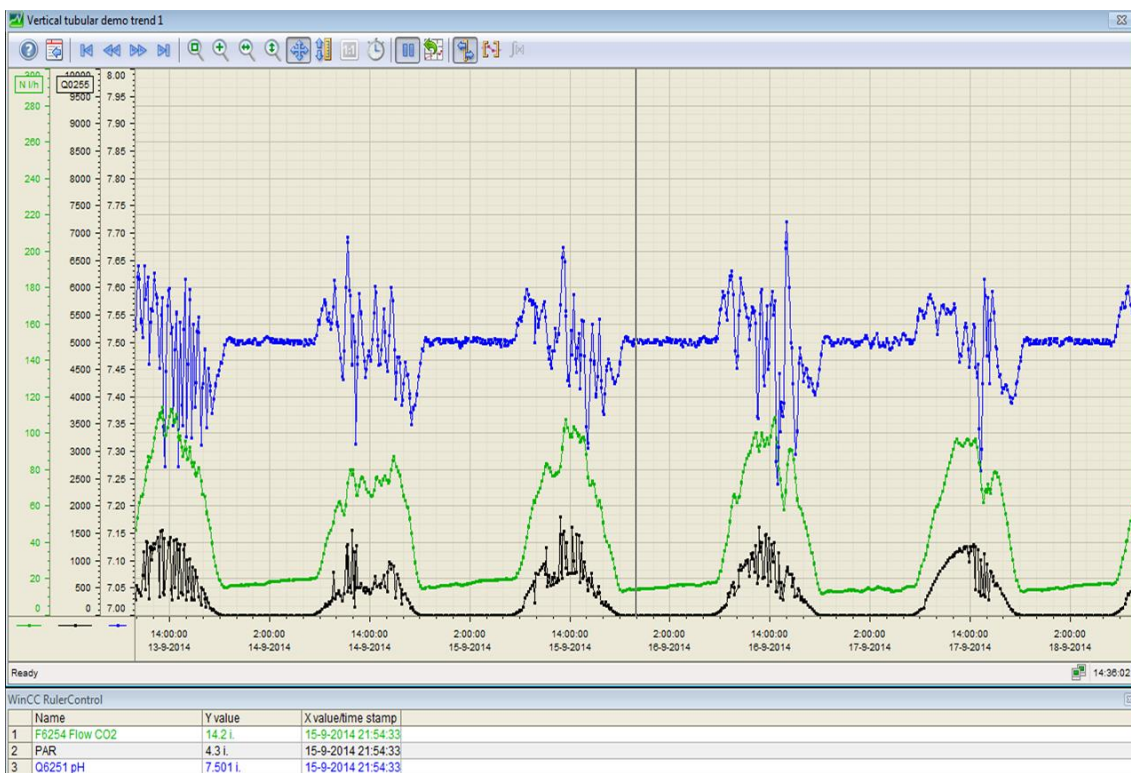


Figure 2.I.3. Trends of pH control, CO₂ addition and light intensity in the large vertical system

Chapter 3

Comparison of four pilot-scale outdoor photobioreactors

This chapter has been published as:

J. H. de Vree, R Bosma, M. Janssen, M.J. Barbosa, R.H. Wijffels (2015), **Comparison of four pilot-scale outdoor photobioreactors**, *Biotechnology for biofuels*, 8:215.

3.1 Abstract

Microalgae are a potential source of sustainable commodities of fuels, chemicals and food and feed additives. The current high production costs, as a result of the low areal productivities, limit the application of microalgae in industry. A first step is determining how the different production system designs relate to each other under identical climate conditions. The productivity and photosynthetic efficiency of *Nannochloropsis* sp. CCAP 211/78 cultivated in four different outdoor continuously operated pilot-scale photobioreactors under the same climatological conditions were compared. The optimal dilution rate was determined for each photobioreactor by operation of the different photobioreactors at different dilution rates.

In vertical photobioreactors, higher areal productivities and photosynthetic efficiencies, 19-24 g m⁻² d⁻¹ and 2.4-4.2%, respectively, were found in comparison to the horizontal systems; 12-15 g m⁻² d⁻¹ and 1.5-1.8%. The higher ground areal productivity in the vertical systems could be explained by light dilution in combination with a higher light capture. In the raceway pond low productivities were obtained, due to the long optical path in this system. Areal productivities in all systems increased with increasing photon flux densities up to a photon flux density of 30 mol m⁻² d⁻¹. Photosynthetic efficiencies remained constant in all systems with increasing photon flux densities. The highest photosynthetic efficiencies obtained were; 4.2% for the vertical tubular photobioreactor, 3.8% for the flat panel reactor, 1.8% for the horizontal tubular reactor, and 1.5% for the open raceway pond.

Vertical photobioreactors resulted in higher areal productivities than horizontal photobioreactors because of the lower incident photon flux densities on the reactor surface. The flat panel photobioreactor resulted, among the vertical photobioreactors studied, in the highest average photosynthetic efficiency, areal and volumetric productivities due to the short optical path. Photobioreactor light interception should be further optimized to maximize ground areal productivity and photosynthetic efficiency.

Keywords

Microalgae; outdoor, pilot-scale, photobioreactors, areal productivity, photosynthetic efficiency, *Nannochloropsis* sp.

List abbreviations

Symbol	Description	Units
PE_{sunlight}	Sunlight to biomass conversion efficiency	%
$P_{x,\text{ground}}$	Ground areal biomass productivity	$\text{g m}^{-2} \text{d}^{-1}$
V_{harvest}	Harvested volume	L
C_x	Biomass concentration	g L^{-1}
V_r	Volume of photobioreactor	L
A_{ground}	Ground area occupied by photobioreactor	m^2
$P_{x,\text{vol}}$	Volumetric biomass productivity	$\text{g L}^{-1} \text{d}^{-1}$
$I_{\text{ground,daily}}$	Daily ground areal photon flux density	$\text{mol m}^{-2} \text{d}^{-1}$
I_{ground}	Ground areal photon flux density	$\mu\text{mol m}^{-2} \text{s}^{-1}$
ΔH_c°	Standard enthalpy of combustion	kJ g^{-1}
E_{PAR}	Conversion factor PAR photons to joule	J mol^{-1}
D	Dilution rate	d^{-1}
OP	Optical path	cm
PFD	Photon flux density	$\text{mol m}^{-2} \text{d}^{-1}$
v_{gs}	Superficial gas velocity	m s^{-1}
Abbreviation	Description	
ORP	Open raceway pond	
HT	Horizontal tubular	
VT	Vertical tubular	
FP	Flat panel	

3.2 Introduction

Microalgae are a promising feedstock for bulk commodities like chemicals, food, feed and fuels. High production costs hinder the current implementation of algal biomass as a feedstock for bulk commodities; production costs should decrease to less than 1 €/kg dry weight [4]. A crucial parameter influencing biomass production costs is photosynthetic efficiency; the efficiency at which solar light energy is captured as chemical energy in biomass. Under identical conditions, a higher photosynthetic efficiency means a higher ground areal productivity and thus a decrease in biomass production costs [3, 4].

Microalgae are produced in a wide variety of cultivation systems including open raceway ponds, tubular, and flat panel photobioreactors. Open raceway ponds are ring-channel systems, with a typical depth of 0.2 meter. The culture is typically mixed at 0.25 m s^{-1} by a paddle wheel. Open raceway ponds are characterized by low cell densities up to 0.3 g L^{-1} [5]. The open raceway pond is currently the mostly used and cheapest cultivation system for commercial production of microalgae [40]. Norsker et al. estimated an investment cost of 0.37 M€/ha for a 100 ha scale open raceway pond plant [5].

Tubular photobioreactors are made of transparent tubing through which the culture is circulated at liquid velocities of typically 0.5 m s^{-1} [5]. To prevent high oxygen concentrations the transparent tubes are connected to a degasser or stripper vessel, where oxygen is removed by air injection. Tubular systems can be found in different orientations; horizontal tubes arranged in a single plane and multiple planes of vertically stacked horizontal tubes (fence-like systems). Diameters of the tubes vary with system orientation, diameters larger than 3 cm and smaller than 10 cm are typically used [40]. Tubular photobioreactors are more expensive to construct than open raceway ponds, especially vertically oriented tubular photobioreactors. Investment costs for a 100 ha horizontal tubular plant were estimated to be 0.51 M€/ha by Norsker et al. [5].

Flat panel photobioreactors are transparent flat vessels, where the culture is mixed by aeration ($\leq 1 \text{ L}^{-1} \text{ min}^{-1}$ or 1 vvm). The culture depth or optical path in flat panel systems varies from 1 cm to 20 cm and, consequently, biomass concentrations in these systems vary greatly [14]. For a 100 ha production plant using flat panel photobioreactors (optical path 3 cm), investment costs were estimated to be 0.8 M€/ha [5].

For the selection of a photobioreactor for large scale production, knowledge on the actual productivity and photosynthetic efficiency of different photobioreactor designs is required. Norsker et al. reported an overview of photosynthetic efficiencies obtained with different reactors, locations and microalgal species; 1.5% for open raceway pond, 3% for horizontal tubular photobioreactors and 5% for flat panel photobioreactors [5]. However, for a better comparison of photobioreactor designs data should be gathered at a single location with the same microalgal species. In this study, we simultaneously compared the performance of four pilot-scale outdoor photobioreactors with *Nannochloropsis* sp. under identical climatological conditions in The Netherlands. Four photobioreactors were installed at the AlgaePARC pilot facility; an open raceway pond (OPR), a horizontal tubular photobioreactor (HT), a vertical tubular photobioreactor (VT), and a flat panel photobioreactor (FP) [9]. The effect of daily dilution rates and photon flux densities on areal productivity and photosynthetic efficiency was evaluated for each cultivation system.

3.3 Methods

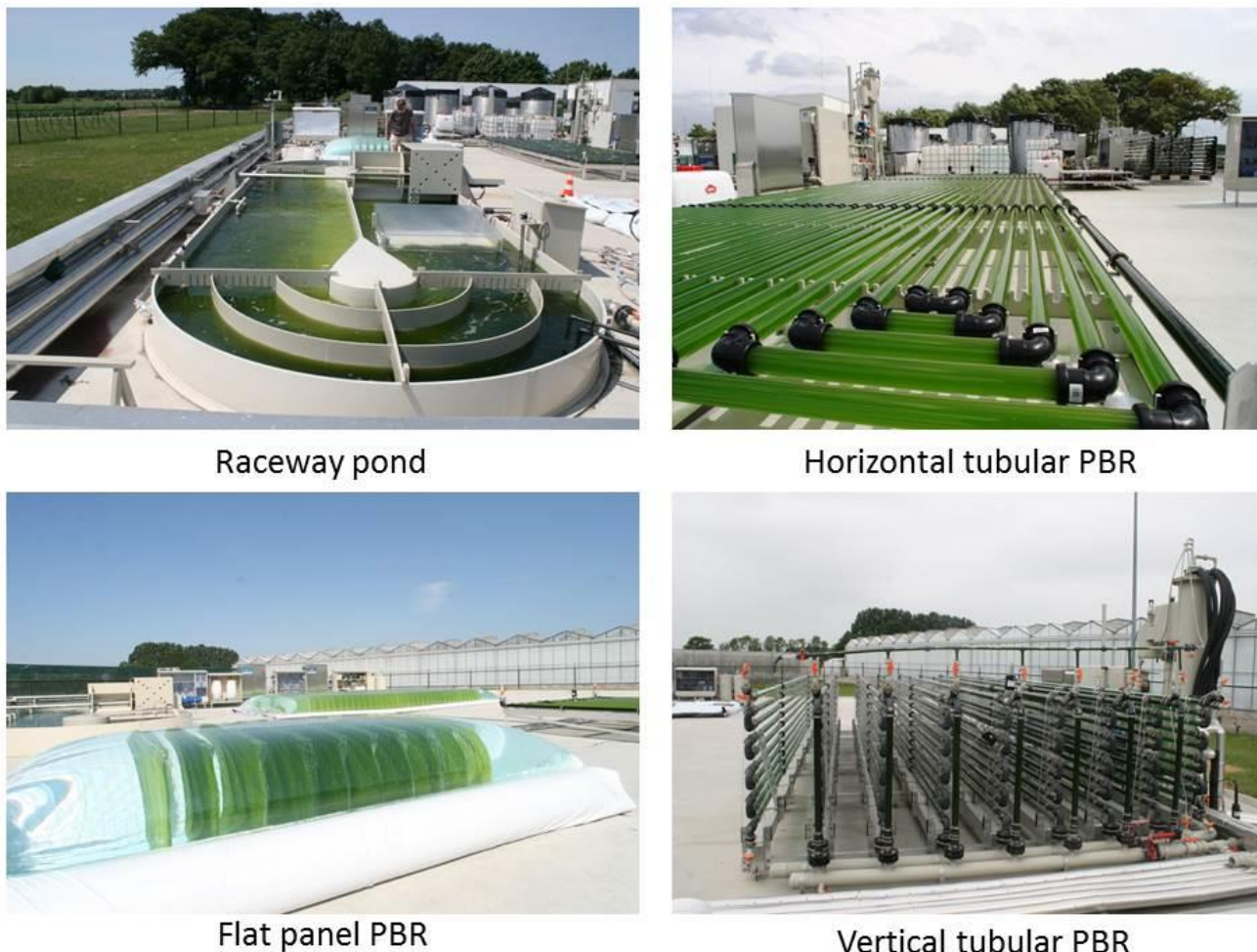
Inoculum production

Nannochloropsis sp. CCAP 211/78 was cultivated in enriched natural seawater (Oosterschelde, The Netherlands) with the following concentrations (in mM); NaNO₃, 25; KH₂PO₄, 1.7; Na₂EDTA, 0.56; Fe₂SO₄·7H₂O, 0.11; MnCl₂·2H₂O, 0.01; ZnSO₄·7H₂O, 2.3·10⁻³; Co(NO₃)₂·6H₂O, 0.24·10⁻³; CuSO₄·5H₂O, 0.1·10⁻³; Na₂MoO₄·2H₂O, 1.1·10⁻³. For the pre-cultures (250 mL Erlenmeyer flasks) and cultivation in the 4.5L flat panel reactor, HEPES (20mM) and Na₂EDTA (5mM) were added to the seawater. The pH was adjusted to 7.5 followed by sterilization (121 °C, 20 min); after sterilization, nutrients were added to the sterilized seawater through a sterile filter (0.45 µm). For all other cultivations (including outdoor cultivations), seawater was chemically sterilized (sodium hypochlorite), active chlorite was deactivated by filtration over active carbon, followed by filtration (1 µm).

The pre-cultures were placed in an orbital shaker incubator (Multitron, Infors HT, the Netherlands). Cultures were shaken at 120 rpm, illuminated with 50 µmolm⁻²s⁻¹, at a temperature of 25°C and headspace was enriched with 2% CO₂. The Erlenmeyer flasks were used as inoculum for cultivation in a 4.5L flat panel photobioreactor (optical path 2.5 cm); pH was controlled at 7.5 by on demand CO₂ addition, temperature was controlled at 25°C and mixing by aeration at 1.5 L⁻¹L⁻¹min⁻¹. The harvest of this 4.5L reactor was used to inoculate a 280L horizontal tubular photobioreactor placed in a greenhouse. Temperature was maintained at 25°C, pH was controlled at 7.5 by on demand CO₂ addition. This photobioreactor was operated at a liquid velocity of 0.3 m s⁻¹. To increase production, six 600 W high-pressure sodium lamps (Master SON-T PIA Green Power, Philips Eindhoven, the Netherlands) were placed above the transparent tubular section of the reactor, which in addition to sunlight delivered a photon flux density of 350 µmol m⁻²s⁻¹. All outdoor photobioreactors were inoculated within one week with the harvest from this system.

3.3.1 Outdoor pilot-scale photobioreactors

A short description of each photobioreactor (Figure 3.1) is given in this section; a more detailed description of the outdoor systems is given by Bosma et al. [9]. All cultivation systems were operated at a pH of ±7.5 by on demand CO₂ addition and culture temperatures were maintained between 20-30°C. Specifications of the different photobioreactors studied are given in Table 3.1.



Raceway pond

Horizontal tubular PBR

Flat panel PBR

Vertical tubular PBR

Figure 3.1. Photobioreactors in operation at AlgaePARC pilot facilities, Wageningen UR, the Netherlands.

Open raceway pond

The raceway pond has an optical path of 0.2 m and water was circulated in the pond by using a paddle wheel (L 1.45 m, W 0.235 m). The liquid velocity in the OPR was 0.25 m s^{-1} . Carbon dioxide was injected on-demand for pH control. At the point of injection a transparent cover was built above culture level in order to recirculate the gas phase and prevent excessive carbon dioxide losses. There was no need for active oxygen removal in the open raceway pond, as dissolved oxygen concentrations never reached values above 160%.

Horizontal tubular photobioreactor

The horizontal tubular photobioreactor consists of three loops of 80 meters each (Figure 3.1) connected via a manifold to a bubble column used for oxygen removal, temperature control, nutrient and antifoam addition (Silicone RE20 Snapsil, BRB international, the Netherlands). The horizontal photobioreactor was operated at a liquid velocity of 0.45 m s^{-1} . To prevent high concentrations of dissolved oxygen, a superficial gas velocity (v_{gs}) of 0.04 m s^{-1} was used in the bubble column (volume of 0.15 m^3 , 27 % of total reactor volume). High dissolved oxygen concentrations above 300% hamper the growth of *Nannochloropsis* sp. under dynamic oxygen concentrations (23). Similar dissolved oxygen concentrations were found inhibiting for *Neochloris oleoabundans* [11]. The

airflow in the bubble column was increased when dissolved oxygen concentration exceeded 300% to prevent inhibiting oxygen concentrations.

Table 3.1 Specifications of outdoor pilot-scale photobioreactors; ORP; open raceway pond, HT; horizontal tubular, VT; vertical tubular, FP; flat panel photobioreactor. ^a Average optical path of single panels. ^b Including half of ground area occupied by dummy panels/tube installed at northern and southern side of reactors. ^c Data from Norsker et al., 2011 [5]

Specifications	ORP	HT	VT	FP
Optical path (m)	0.2	0.046	0.046	0.02 ^a
Volume (m ³)	4.73	0.56	1.06	0.06
Illuminated volume (%)	100	73	71	100
Ground area occupied (m ²)	25.4	27.0 ^b	31.0 ^b	2.4
Illuminated volume/ground area (m ³ m ⁻²)	0.186	0.021	0.034	0.023
Expected PE _{sunlight} (%) ^c	1.5	3	n.a.	5

Vertical tubular photobioreactor

The vertical tubular photobioreactor consists of seven vertical loops of 80 meters each connected by a manifold to a bubble column used for oxygen removal, temperature control, nutrient and antifoam addition. The liquid velocity in the tubes was 0.45 m s⁻¹. To prevent high concentrations of dissolved oxygen a superficial gas velocity of (v_{gs}) 0.04 m s⁻¹ air was used in the bubble column (volume 0.31 m³, 29 % of total reactor volume). As in the horizontal system, the superficial gas velocity was increased when dissolved oxygen concentration exceeded 300% in order to decrease the dissolved oxygen concentration in the culture. On the northern and southern side of the reactor a dummy panel, filled with a green dye, was placed to prevent that the first and last panel receive a lot of direct light.

Flat panel photobioreactor

The flat panel system consists of 10 vertical panels (width 1.25 m, height 0.5 m, depth 0.02 m), with 0.25 m distance between the panels. The total occupied ground surface was 2.4 m² and thus 10 times smaller than that of the other photobioreactors (Table 3.1) studied. In contrast to the other systems, the culture was not mixed over the entire reactor; passive mixing takes place over a panel. In addition, the culture moves in a plug flow manner through each panel; fresh media is added at one side of the panel and simultaneously harvesting is done at the other side by overflow. The culture in the flat panels was mixed by gassing the culture at a rate of 1 L⁻¹ L⁻¹ min⁻¹ (v_{gs} 0.01 m s⁻¹). The gas phase was continuously recycled and the carbon dioxide and oxygen concentration in this gas phase were continuously monitored. pH control was achieved by addition of pure carbon dioxide whenever the concentration decreased below 1% v/v. High dissolved oxygen concentrations were prevented by bleeding a part of the recirculated gas flow as soon as the oxygen concentration in the gas phase exceeded 30% v/v. The large water volume surrounding the panels acts as a temperature buffer and can be cooled or heated via a heat exchanger (Figure 3.1).

3.3.2 Harvesting regime

The photobioreactors were diluted with a fixed daily dilution rate for 7 days. After seven days, dilution rate was changed to the next dilution rate (Table 3.2). The range of dilution rates for each photobioreactor was set based on growth rates determined in these systems in 2013 (unpublished

data). In the tubular and flat panel photobioreactors dilution rates were applied for each experimental run in the following order; medium, low, medium, high, medium. In the raceway pond the short operational timeframe did not allow the repetition of the intermediate dilution rate. The culture in tubular systems and raceway pond were diluted by harvesting several small volumes distributed over the day from the reactor (every hour for 15 minutes between 10:00-15:00) and adding sterilized natural seawater during daytime and nutrients. In the raceway pond, nutrients were added flow proportionally to the flow of seawater with a Dosmatic Minidos 12 system. The flat panel was harvested once at 9:00 a.m. and diluted with complete medium (nutrient stock enriched seawater) that was prepared in a separate vessel.

Table 3.2. Overview of the four dilution rates (d^{-1}) applied to each photobioreactor

Photobioreactor /Dilution rate	D1	D2	D3	D4
Open raceway pond	0.08	0.16	0.24	
Horizontal tubular	0.15	0.30	0.45	
Vertical tubular	0.10	0.20	0.30	
Flat panel reactor	0.10	0.20	0.30	0.40

3.3.3 Measurements and analysis

The photobioreactors were sampled daily between 9:00 and 10:00 a.m. for optical density measurement (680nm and 750nm) on a DR5000 spectrophotometer (Hach Lange, Germany). From the same samples, three times a week dry weight determinations were done in triplicate as described by Zhu et al. [41]. The dry weight concentration was correlated to the optical density measured at 750 nm (OD_{750}). The harvested volume was determined daily for each photobioreactor and the harvest was mixed by a pump and then sampled for optical density measurement at 680 nm (OD_{680}) and at 750 nm (OD_{750}). The OD_{750} measurements of the harvest and of sample taken from the reactors were used to calculate the productivity of each photobioreactor. Nitrate concentrations in the harvest were maintained above 1 mM to ensure nutrient replete conditions. For this, the nitrate content of a sample from the harvest vessel was measured; 2 mL was centrifuged and the supernatant was analysed for nitrate content with an AQ-2 nutrient analyser, (Seal Analytic, USA) as described by Benvenuti et al. [42] (HMSO, 1981; APHA/AWWA/WEF, 4500; USEPA, 19932).

3.3.4 Calculations

All values were calculated over a period between two consecutive sampling points with Equations 1-3.

Ground areal biomass productivity

Daily ground areal biomass productivities were calculated with Equation 1. In equation 1 the accumulation of biomass in the reactor and the harvested biomass were taken in account.

$$P_{x,ground} = \left(\frac{(V_{harvest} \cdot C_{x,harvest}) + (V_R * C_x(t) - C_x(t-1))}{A_{ground}} \right) \quad \text{g m}^{-2} \text{d}^{-1} \quad \text{Eq. 1}$$

With: $P_{x,ground}$: ground areal biomass productivity ($\text{g m}^{-2} \text{d}^{-1}$); $V_{harvest}$: harvested volume (L); $C_{x,harvest}$: dry weight algal concentration in the harvest (g L^{-1}); V_R : photobioreactor volume (L); A_{ground} : occupied ground area photobioreactor (m^2); $C_x(t)$, $C_x(0)$: dry weight algal concentration in

photobioreactor (g L^{-1}), on consecutive sampling points; t : time between consecutive sampling points; ± 24 hours. For the calculation of the ground area, the area used is indicated in Figure 3.2.

In the tubular systems a dummy tube in HT and in VT a dummy panel was placed on the northern and southern side. The dummy tubes and dummy panels were filled with green dye to exclude the side panels/tube of receiving more direct light. The installation of dummy panels in the flat panel PBR was not possible. For the calculation of the ground area in the flat panel, the area taken up by the panels was considered and not the area of the entire bag as this area would be smaller in a larger version of the photobioreactor.

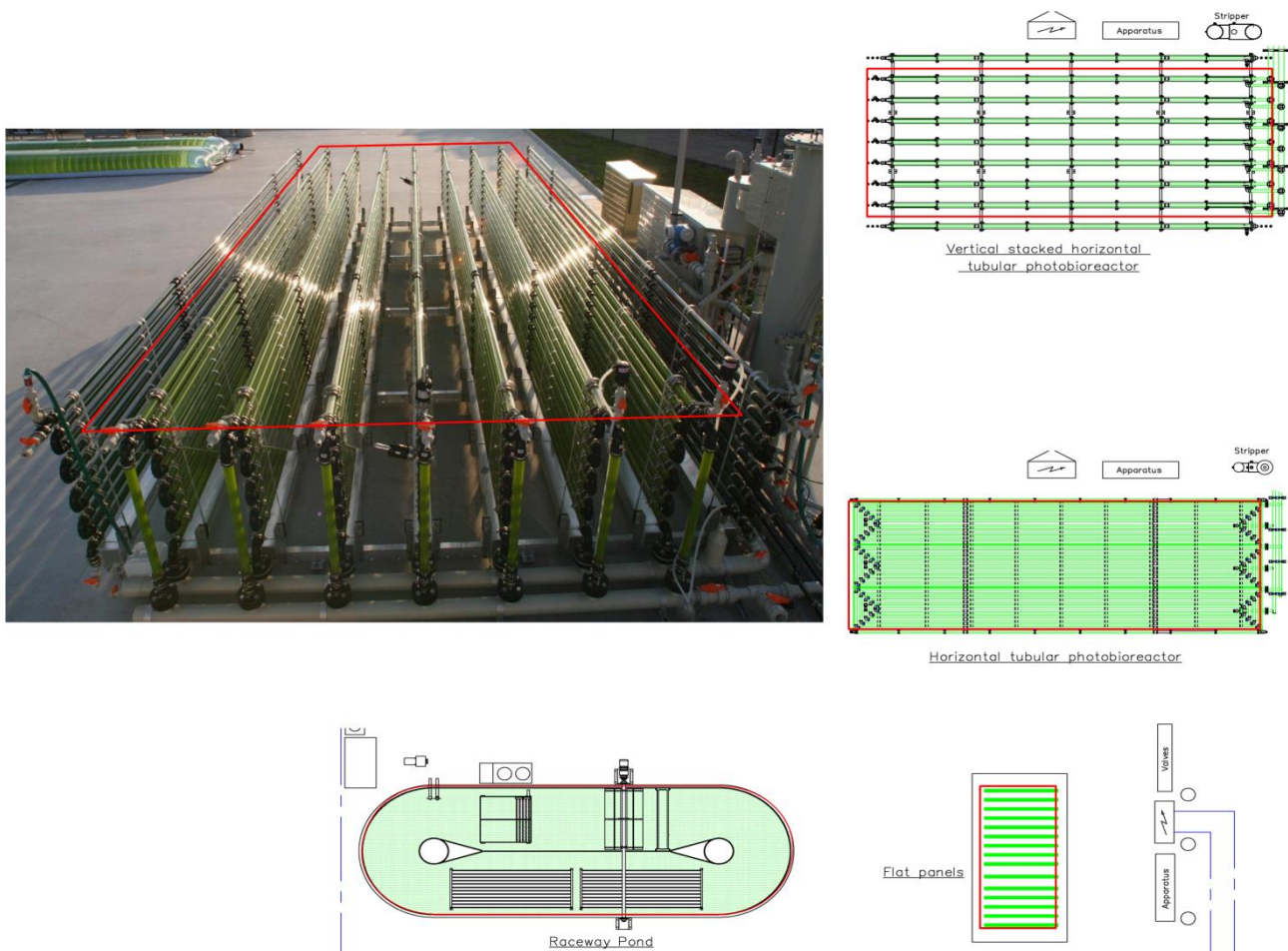


Figure 3.2 Ground area considered for calculation of areal productivity and photosynthetic efficiency for each photobioreactors. Top left; photograph of vertical tubular photobioreactor with area considered as ground area indicated by red lines.

Volumetric biomass productivity

The volumetric biomass productivity was calculated from the ground areal productivity with Equation 2.

$$P_{x,vol} = P_{x,ground} * \frac{A_{ground}}{V_R} \quad \text{g L}^{-1} \text{ d}^{-1} \quad \text{Eq. 2.}$$

With: $P_{x,vol}$: volumetric productivity ($\text{g L}^{-1} \text{d}^{-1}$); $P_{x,ground}$: ground areal biomass productivity ($\text{g m}^{-2} \text{d}^{-1}$); V_R : photobioreactor volume (L); A_{ground} : ground area photobioreactor (m^2)

Photon flux density

$$I_{grounddaily} = \sum_{t=1}^{t=1440} I_{ground}(t) * 60 * 10^{-6} \quad \text{Eq. 3.}$$

The daily ground areal photon flux density ($I_{ground,daily}$ $\text{mol m}^{-2} \text{d}^{-1}$) was calculated with Equation 3. Ground areal photon flux densities (I_{ground} ; $\mu\text{mol m}^{-2} \text{s}^{-1}$) were measured on a horizontal plane every minute with a Li-Cor-190SA 2π PAR quantum sensor (LiCOR, USA) present at the AlgaePARC pilot facility. The photon flux densities measured every minute, between two consecutive reactor sampling points (± 24 hours), were summed and multiplied by 60 (i.e. conversion from seconds to minutes).

Photosynthetic efficiency on sunlight

The photosynthetic efficiency was calculated with Equation 4.

$$PE_{sunlight} = \frac{(P_{x,ground} * \Delta H_c^o)}{((I_{grounddaily} * (0.43 * E_{PAR}))/10^3)} \quad \text{Eq. 4.}$$

With: $PE_{sunlight}$: photosynthetic efficiency (% sunlight); $P_{x,ground}$: average ground areal productivity ($\text{g m}^{-2} \text{d}^{-1}$); ΔH_c^o : standard enthalpy of combustion (22.5 KJ g^{-1}); $I_{ground,daily}$: average daily areal photon flux density, equation 3 ($\text{mol m}^{-2} \text{d}^{-1}$ (PAR, photosynthetic active radiation)); E_{PAR} : energetic content of the PAR fraction of sunlight (4.76 J mol^{-1}), ASTM G173-03 [43]; and 0.43 the conversion factor from sunlight to PAR light on an energy basis (J J^{-1}).

3.4 Results and discussion

Areal productivity and photosynthetic efficiency of four different outdoor photobioreactors operated at different dilution rates were determined. The effect of the photon flux density on the areal productivity for each dilution rate is evaluated. Furthermore, the effect of photon flux density on photosynthetic efficiency is evaluated for all systems studied. The horizontal tubular photobioreactor, vertical tubular photobioreactor, open raceway pond and flat panel were in operation for 111, 102, 42 and 77 days, respectively. During these periods, all four systems were restarted three times due to different reasons. In the tubular photobioreactors this was due to fouling, in the OPR this was due to contamination and growth limiting temperatures ($< 20 \text{ }^\circ\text{C}$). The flat panel was restarted because of clogging of aeration holes, resulting in suboptimal operation.

3.4.1 Effect of photon flux density on productivity

In Figure 3.3, areal productivities versus photon flux densities are shown for all cultivation systems operated. For all systems, areal productivities increased with higher photon flux densities, indicating cultures could experience light limitation at low photon flux densities. For HT, VT and ORP areal productivities appear to increase linearly with PFD up to $30 \text{ mol m}^{-2} \text{d}^{-1}$, this has been reported

previously by [44-47]. For the flat panel photobioreactor this trend could not be observed, a possible explanation could come from the limited mixing of the culture over the entire reactor. Maximal areal productivities for all systems were obtained above $30 \text{ mol m}^{-2} \text{ d}^{-1}$. Highest areal productivities were obtained with the flat panel photobioreactor. In the vertical tubular system similar areal productivities as in the flat panel photobioreactor were obtained, followed by the horizontal tubular photobioreactor and the raceway pond. The areal productivities in the ORP were low in comparison to the other systems. The large optical path (0.2 m) and long light dark cycles as a result of poor mixing in this system contribute to lower areal productivity [48-50].

In vertical photobioreactors, microalgal cells dissipate less of the absorbed light energy as a result of lower photon flux densities because of light dilution on the reactor surface in comparison to the horizontal systems. Therefore, higher areal productivities were found in vertical systems. The higher photon flux density on the exposed reactor surface of the horizontally oriented cultivation systems results thus in lower areal productivity and photosynthetic efficiency.

The short optical path of the flat panel photobioreactor results in a small dark zone in the culture; respiration takes place in a small part of the culture. The long optical path in the open raceway pond results in a large dark zone in the culture [48-50]. In the dark zone microalgae respire energy that otherwise could be used for growth. The presence of a dark zone in a cultivation system will reduce the net productivity of the culture, as part of the culture in the dark has negative growth. A long optical path results in lower productivities (Figure 3.3) [49, 51]. Higher photon flux densities will penetrate deeper in the culture and will decrease the size of the dark zone present in the culture.

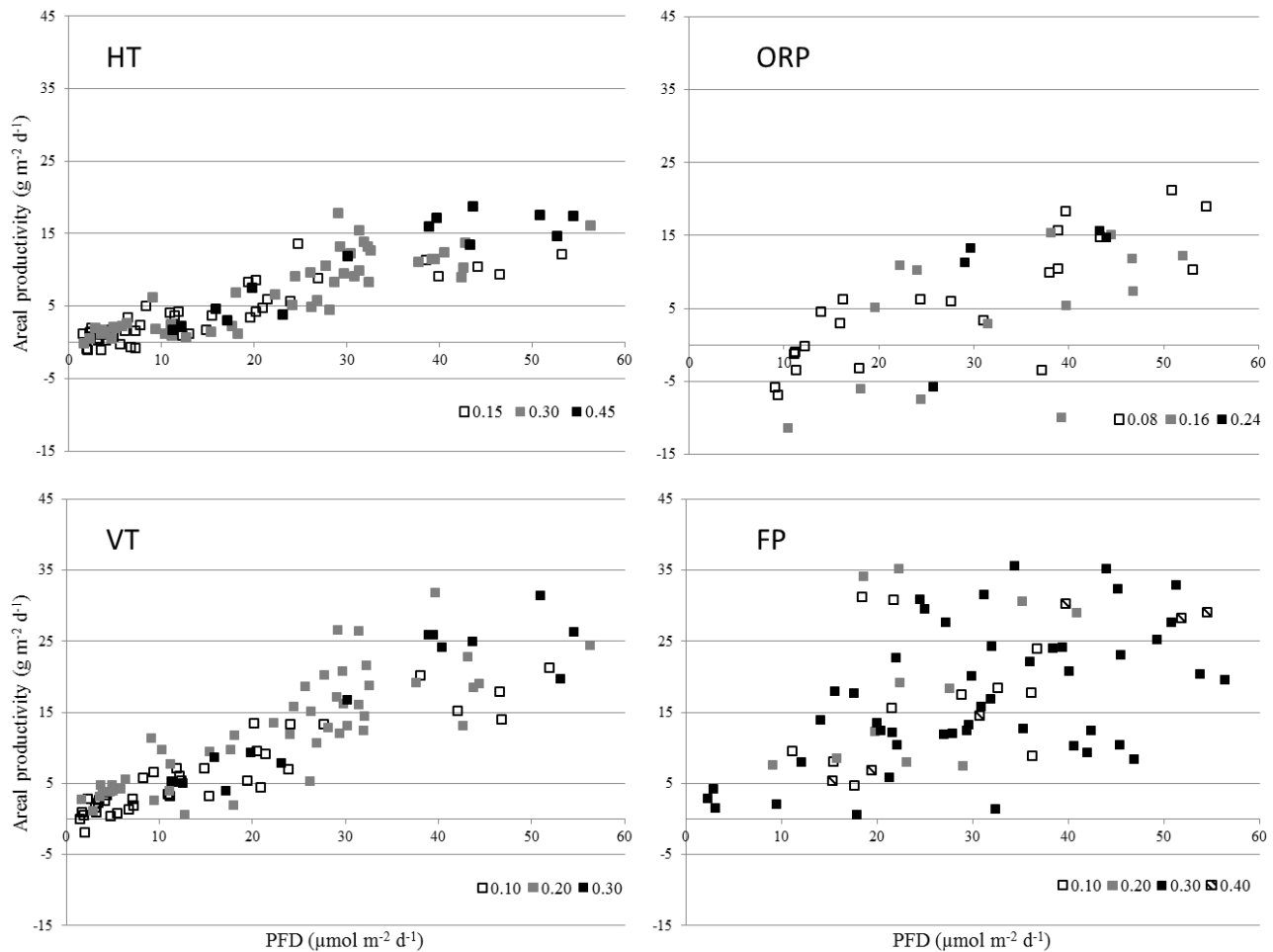


Figure 3.3 Influence of daily photon flux density and dilution rate on areal productivity. For the horizontal tubular (HT), open raceway pond (ORP), vertical tubular (VT) and flat panel (FP). The different colours of markers indicate the different dilution daily rates

Variations in areal productivity were larger for all photon flux densities and dilution rates in the flat panel photobioreactor and the open raceway pond than in the tubular systems. The large variations in the flat panel photobioreactor are a result of the plug flow regime moving the culture through each panel. The culture is not mixed well over all panels, while in the other systems the entire culture volume is mixed resulting in less variation in areal productivity.

In the open raceway pond the large variation in areal productivity is the result of low culture temperatures and automated level control. The low culture temperatures resulted in suboptimal conditions during a large part of the day, for many days throughout the experimental period. The automated level control in the open raceway pond resulted in negative areal productivity; for days with heavy rainfall, dilution rates were higher than intended because of the automated level control.

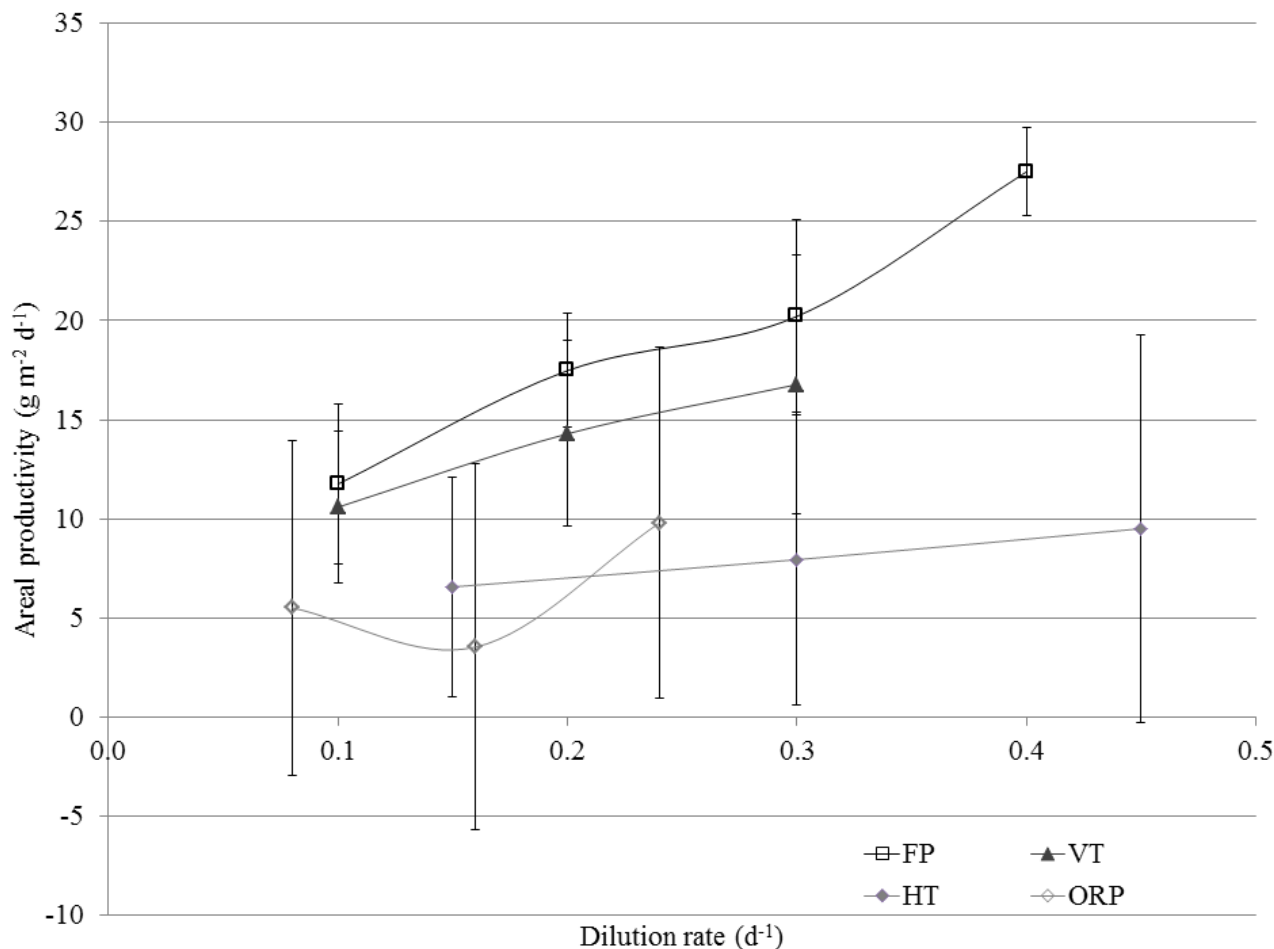


Figure 3.4 Average areal productivity versus dilution rate for each photobioreactor. Flat panel (FP), Vertical tubular (VT), horizontal tubular (HT) and open raceway pond (ORP). Average areal productivity was calculated over a number of days for each dilution rate; FP; 6, 3, 40, 4, VT; 18, 39 and 14, HT; 19, 38 and 11, ORP; 22, 13 and 5.

The variations in areal productivities within the different photobioreactors are a result of variations in biomass concentrations. The biomass concentrations in the different cultivation systems varied as a result of applied dilution rates and photon flux densities. The highest dilution rates in the flat panel photobioreactor (0.4 d^{-1}) and open raceway pond (0.24 d^{-1}) were only applied for a short period of time, 6 days and 11 days respectively, as these resulted in a strong decrease in biomass concentration. For each cultivation system the average areal productivity was calculated for each dilution rate. This average values was calculated over the summer period to ensure similar values for photon flux density (Figure 3.4).

The system with the shortest optical path (0.02 m), the flat panel photobioreactor, resulted in the overall highest average areal productivity. The overall lowest average areal productivity was obtained with the open raceway pond, because of the long optical path (0.2 m). The vertical tubular photobioreactor resulted in higher average areal productivity compared to the horizontal tubular. The vertical tubular photobioreactor has a lower photon flux density on the surface of the reactor that

penetrates less far in the culture. The horizontal tubular photobioreactor resulted in a higher biomass concentration, as this system receives higher photon flux density. No significant difference in average areal productivity at different dilution rates was found among all cultivation systems with the exception of the flat panel.

3.4.2 Effect of photon flux density on photosynthetic efficiency

Photosynthetic efficiency (PE_{sunlight}) is an important parameter for the evaluation of photobioreactor performance. Photosynthetic efficiency is the efficiency at which solar light energy is captured as stored chemical energy in biomass and it allows the estimation of the productivity for other locations if the photon flux density is known. Photosynthetic efficiency was calculated based on the ground areal productivity and ground areal irradiance. At the same ground areal photon flux density, vertical photobioreactors have lower photon flux densities on the surface of the cultivation system than horizontal systems. Lower photon flux densities result in less energy dissipation by microalgal cells in the form of heat, resulting in a higher photosynthetic efficiency.

In Figure 3.5, photosynthetic efficiencies versus photon flux densities are shown for all cultivation systems operated. For all systems, photosynthetic efficiencies varied over the range of photon flux densities. Maximal photosynthetic efficiencies were obtained for the three closed photobioreactors below $20 \text{ mol m}^{-2} \text{ d}^{-1}$. Furthermore, the more stable culture temperatures in the closed photobioreactors could have contributed to the higher photosynthetic efficiencies. Highest photosynthetic efficiencies were obtained with the vertical photobioreactors with intermediate dilution rates; 0.2 d^{-1} for VT and 0.3 d^{-1} for FP. Lower photosynthetic efficiencies were obtained with the horizontal tubular photobioreactor and the raceway pond. The photosynthetic efficiency is low in the horizontal tubular compared to the other closed systems. Variations in photosynthetic efficiencies were the result of the variations in areal productivities that were discussed before.

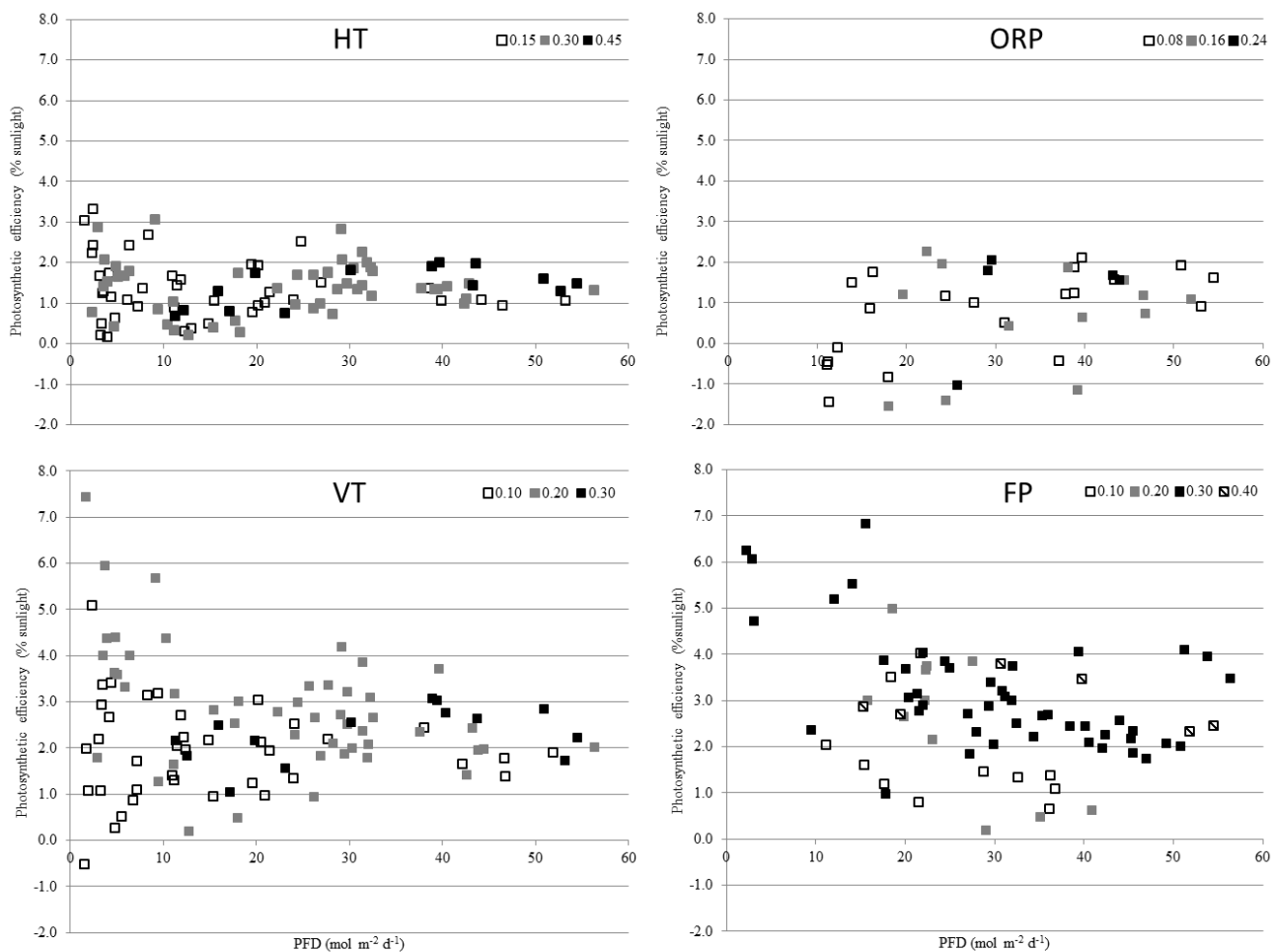


Figure 3.5 Influence of daily photon flux density on photosynthetic efficiencies on sunlight for the different photobioreactors. For the horizontal tubular photobioreactor (HT), open raceway pond (ORP), vertical tubular photobioreactor (VT) and flat panel photobioreactor (FP). The different colours of the squares indicate different dilution rates applied to each different photobioreactor.

3.4.3 Evaluation of performance

For a comparison of the performance of the cultivation systems among each other and with literature average and maximal values, for areal productivity and photosynthetic efficiency, were calculated over summer (Table 3.3). Volumetric productivities were calculated as these are often reported in literature.

Table 3.3. Overview of average and maximal areal and volumetric productivities and average and maximal photosynthetic efficiencies obtained in summer 2013 (July-August). Dilution rates are measured values. Maximal areal and volumetric productivities were obtained in a single week in July with a high average photon flux density; $44 \text{ mol m}^{-2} \text{ d}^{-1}$.

Photobioreactor	ORP		HT		VT		FP	
	Avg.	Max	Avg.	Max	Avg.	Max	Avg.	Max
$P_{x,\text{ground}}$ ($\text{g m}^{-2} \text{ d}^{-1}$)	9.7	14.0	12.1	15.7	19.4	24.4	20.5	27.5
$P_{x,\text{vol}}$ ($\text{g L}^{-1} \text{ d}^{-1}$)	0.03	0.08	0.65	0.85	0.57	0.71	0.90	1.20
Dilution rate (d^{-1})	0.14	0.12	0.25	0.34	0.27	0.40	0.27	0.36
Number of days	24	8	36	8	36	8	36	4
Photosynthetic efficiency (% sunlight)	1.1	1.5	1.5	1.8	2.4	4.2	2.7	3.8
Dilution rate (d^{-1})	0.16	0.12	0.25	0.28	0.27	0.24	0.27	0.18
Number of days	24	8	36	6	36	9	36	3

The highest average areal productivity was found in the flat panel photobioreactor, followed by the vertical tubular, the horizontal tubular photobioreactor and open raceway pond. Maximal areal productivities for each photobioreactor were obtained in a single week in July with a high average daily photon flux density of $44 \text{ mol m}^{-2} \text{ d}^{-1}$. The highest average photosynthetic efficiency was found for the flat panel (FP) photobioreactor followed by the vertical tubular (VT) photobioreactor, horizontal tubular (HT) photobioreactor and the open raceway pond (ORP). The highest maximal photosynthetic efficiency was found for the VT; followed by the FP, HT and ORP.

In the flat panel photobioreactor the highest areal and volumetric productivities and photosynthetic efficiencies were obtained. The highest volumetric productivity obtained for the FP ($1.20 \text{ g L}^{-1} \text{ d}^{-1}$) is higher than values reported in literature, with the exception of data reported by Zou et al, of $1.7 \text{ g L}^{-1} \text{ d}^{-1}$ [14]. However, this higher volumetric productivity was obtained in a flat panel photobioreactor with a shorter optical path of 1.3 cm, resulting in a higher light supply per volume of culture [14]. The photosynthetic efficiency obtained in this study for the flat panel photobioreactor is almost double of the values reported by Camacho-Rodriguez et al. for *Nannochloropsis gaditana* (1.7-0.3%) and Rodolfi et al. for *Nannochloropsis* sp. F&M-M24 (0.96%) [52, 53].

In the vertical tubular photobioreactor similar photosynthetic efficiencies (2-3.5%) were obtained as for a modular flat panel system illuminated with artificial light as reported by Zittelli et al., [54]. In our study a lower volumetric productivity ($0.3\text{-}0.7 \text{ g L}^{-1} \text{ d}^{-1}$) was obtained than values reported by Zittelli et al. [54] because of a larger optical path; 0.05 m versus 0.012 m. The larger optical path could result in the formation of a dark zone in our system; resulting in a lower volumetric productivity. In our study a higher areal productivity ($24 \text{ g m}^{-2} \text{ d}^{-1}$) was obtained than the areal productivity reported by Zittelli et al ($10 \text{ g m}^{-2} \text{ d}^{-1}$). Higher photon flux density than the photon flux density used by Zittelli et al., were measured outdoors, which contributed to the higher areal productivity obtained in our study. San Pedro et al., reported a maximal areal productivity of $15 \text{ g m}^{-2} \text{ d}^{-1}$ or $0.59 \text{ g L}^{-1} \text{ d}^{-1}$ for *Nannochloropsis gaditana* at a dilution rate of 0.3 per day [55]. These values are in the range of the values obtained in this study.

Table 3.4 Overview of volumetric and areal productivities and photosynthetic efficiencies (PE_{sunlight}) for different photobioreactors outdoors reported in literature. The values for the raceway pond and FP for this study were collected in summer 2013. For both tubular photobioreactors average productivities and photosynthetic efficiencies were used to indicate the range of productivities and photosynthetic efficiencies; average data was obtained over the period from July to December 2013. *Calculated based on the illuminated area, not considering the ground area occupied by the photobioreactor

Photobioreactor	Optical path (cm)	Algal species	$P_{x,\text{vol}}$ ($\text{g L}^{-1} \text{d}^{-1}$)	$P_{x,\text{ground}}$ ($\text{g m}^{-2} \text{d}^{-1}$)	PE_{sunlight} (%)	Author	Location
Horizontal tubular	4.3	<i>Nannochloropsis</i> sp.	0.51-0.76	13-19.5*	2.3-3.5*	[56]	Italy
Horizontal tubular	9.0	<i>Nannochloropsis gaditana</i>	0.12-0.20	10.8-18.0	0.7-1.04*	[52]	Almeria Spain
Horizontal tubular	4.6	<i>Nannochloropsis</i> sp.	0.30-0.85	5.8-15.7	1.2-1.8	This study	The Netherlands
Vertical panel	1.2	<i>Nannochloropsis</i> sp.	0.61-1.45	5.8-10.2	2.0-3.5*	[54]	Artificial light
Vertical tubular	10.4	<i>Scenedesmus obliquus</i>	?	21.76	2.5*	[57]	South Spain
Vertical tubular	5	<i>Nannochloropsis gaditana</i>	0.59	15.4	-	[55]	Almeria Spain
Vertical tubular	4.6	<i>Nannochloropsis</i> sp.	0.31-0.71	10.6-24.4	2.4-4.2	This study	The Netherlands
Raceway pond	30	<i>Scenedesmus obliquus</i>	0.03	8.26	0.95*	[57]	South Spain
Raceway pond	30	<i>Muriellopsis</i> sp.	0.04	8-20	0.97-0.69*	[58]	South Spain
Raceway pond	12	<i>Nannochloropsis salina</i>	0.2	24.5	-	[59]	Israel
Raceway pond	11	<i>Nannochloropsis gaditana</i>	0.09-0.19	22.4	-	[60]	Almeria Spain
Raceway pond	20	<i>Nannochloropsis</i> sp.	0.03-0.08	6.2-14.0	0.5-1.5	This study	The Netherlands
Flat panel	1.3-17	<i>Nannochloropsis</i> sp.	1.7-0.25	11-22	-	[14]	Israel
Flat panel	10	<i>Nannochloropsis</i> sp.	0.27	14.2	-	[61]	Israel
Flat panel	5	<i>Nannochloropsis gaditana</i>	0.16-0.36	8-18	1.74-0.31*	[52]	Almeria Spain
Flat panel	4.5	<i>Nannochloropsis</i> sp.	0.36	15.8	0.96*	[16]	Italy
Flat panel	5	<i>Nannochloropsis oculata</i>	0.15-0.37		-	[15]	Colorado, U.S.
Flat panel	2	<i>Nannochloropsis</i> sp.	0.9-1.2	20.5-27.5	2.7-3.8	This study	The Netherlands

Volumetric productivities (0.3 to $0.85 \text{ g L}^{-1} \text{ d}^{-1}$) for the horizontal tubular photobioreactor obtained in this study are similar to the volumetric productivities (0.5 - $0.7 \text{ g L}^{-1} \text{ d}^{-1}$) reported by Zittelli et al., [56]. Lower volumetric productivities (0.12 - $0.2 \text{ g L}^{-1} \text{ d}^{-1}$) were reported by Camacho-Rodriguez et al., probably due to the larger tube diameter (9 cm). In our design, distance between tubes equals the diameter of the tube (external diameter 5 cm), this results in a lower culture volume per ground area, resulting in lower areal productivities than values reported by Zittelli et al. [56]. Camacho-Rodriguez et al. found similar areal productivities (10 - $18 \text{ g m}^{-2} \text{ d}^{-1}$) as in this study for *Nannochloropsis gaditana* cultivated in a horizontal tubular photobioreactor [52].

Areal productivities obtained for the open raceway pond in this study, 6 - $14 \text{ g m}^{-2} \text{ d}^{-1}$, were lower than the areal productivities reported by Arbib et al. and Blanco et al. (8 - $20 \text{ g m}^{-2} \text{ d}^{-1}$), due to the higher photon flux densities at the locations of the studies of Arbib et al. and Blanco et al. [57, 58]. Higher photon flux densities penetrate further and reduce the dark zone in a culture. Furthermore, in the south of Spain higher ambient temperatures are present, avoiding low culture temperatures down to 15°C at night as experienced in our study. San Pedro et al. found maximal volumetric and areal productivity ($0.19 \text{ g L}^{-1} \text{ d}^{-1}$ and $22.4 \text{ g m}^{-2} \text{ d}^{-1}$) for shallow (11 cm deep) raceway ponds [60]; the lower depth results in a smaller dark zone. In the study of San Pedro, higher productivities were obtained at higher photon flux densities and at temperatures close to optimum for growth [60]. Boussiba et al. reported higher areal productivity ($24.5 \text{ g m}^{-2} \text{ d}^{-1}$) as well for *Nannochloropsis salina* cultivated in a shallow pond [59], this indicates that lower culture depth or more light per culture volume results in higher productivity.

3.5 Conclusions

The performance of different pilot-scale photobioreactor designs under identical conditions was evaluated. Flat panel photobioreactors resulted in high ground areal productivities ($\geq 24 \text{ g m}^{-2} \text{ d}^{-1}$) and high ground areal photosynthetic efficiencies ($\geq 2.7\%$) over 36 days. Average photosynthetic efficiencies for the other systems were: VT; 2.4% , HT; 1.5% and ORP; 1.2% .

Vertical photobioreactors resulted in higher areal productivities than horizontal photobioreactors because of the higher light interception and the resulting lower incident photon flux densities on the reactor surface. Among the vertical photobioreactors studied, the flat panel photobioreactor showed the highest average photosynthetic efficiency, areal and volumetric productivities due to its short optical path.

Concluding, photobioreactor light interception should be optimized to maximize ground areal productivity and photosynthetic efficiency. This makes vertical photobioreactors promising for large scale production. However, an economical analysis should be made to assess if the higher photosynthetic efficiency and higher areal productivity compensate for the higher investment costs generally associated with vertical photobioreactors.

3.5 Acknowledgements

The authors would like to thank the Dutch Ministry of Economic Affairs, Agriculture and Innovation, the Province of Gelderland and BioSolar Cells, BASF, BioOils, Cellulac, Drie Wilgen Development, DSM, Exxon Mobil, GEA Westfalia Separator, Heliae, Neste, Nijhuis, Paques,

Proviron, Roquette, SABIC, Simris Alg, Staatsolie Suriname, Synthetic Genomics, TOTAL and Unilever for the financial support of the AlgaePARC research program.

Chapter 4

Turbidostat operation of outdoor pilot-scale photobioreactors

This chapter has been published as:

J. H. de Vree, R Bosma, M. Janssen, M.J. Barbosa, R.H. Wijffels (2016), **Turbidostat operation of outdoor pilot-scale photobioreactors**, *Algal Research*, 18, 198-208.

4.1 Abstract

The effect of biomass concentration on areal productivity and photosynthetic efficiency of *Nannochloropsis* sp. CCAP211/78 was studied in three outdoor pilot-scale photobioreactors: an open raceway pond (OPR), a horizontal tubular (HT) photobioreactor and a vertically stacked horizontal tubular (VT) photobioreactor. The reactors were operated continuously as turbidostat at different biomass concentrations. For all systems highest areal productivities were obtained on days with a high light intensity, while the highest photosynthetic efficiencies were obtained on days with a low light intensity. Ground areal biomass concentration exceeding 51 g m^{-2} had a negative effect on the areal productivity and photosynthetic efficiency. No significant effect of biomass concentration on the productivity was found for the HT at ground areal biomass concentration lower than 51 g m^{-2} . Also for the VT, no significant effect of biomass concentration was found with the exception of the highest biomass concentration of 2.0 g L^{-1} (68 g m^{-2}) resulting in decreased productivity. For the open raceway pond the highest biomass concentration (0.5 g L^{-1} or 94 g m^{-2}) resulted in significantly lower areal productivity, compared to the lower biomass concentration (0.25 g L^{-1} or 47 g m^{-2}). Highest areal productivities were obtained for OPR and VT, most likely due to more efficient light interception. In this study we observed that night biomass loss was coupled to net growth. At lower biomass concentrations and concomitant higher growth rates the specific biomass loss rate was higher. Microalgal specific light absorption coefficient was correlated to biomass concentration; higher biomass concentrations resulted in higher specific absorption coefficients, resulting in a steeper light gradient in the microalgal cultures.

Keywords

Microalgae; outdoor pilot-scale photobioreactors, areal productivity, photosynthetic efficiency, *Nannochloropsis* sp., biomass concentration.

List of symbols and abbreviations used

Symbol	Description	Units
PE_{sunlight}	Efficiency of sunlight conversion into biomass	%
$P_{x,\text{ground}}$	Ground areal biomass productivity	$\text{g m}^{-2} \text{d}^{-1}$
F_{harvest}	Harvested volume	L/24 hr
C_x	Biomass concentration	g L^{-1}
V_r	Volume of photobioreactor	L
A_{ground}	Ground area occupied by photobioreactor	m^2
$P_{x,\text{vol}}$	Volumetric biomass productivity	$\text{g L}^{-1} \text{d}^{-1}$
$I_{\text{ground,daily}}$	Daily ground areal photon flux density	$\text{mol m}^{-2} \text{d}^{-1}$
I_{ground}	Ground areal photon flux density	$\mu\text{mol m}^{-2} \text{s}^{-1}$
ΔH_c^o	Standard enthalpy of combustion	kJ g^{-1}
E_{PAR}	Conversion factor PAR photons to joule	J mol^{-1}
D	Dilution rate	d^{-1}
OP	Optical path	m
v_{gs}	Superficial gas velocity	m s^{-1}
Abbreviation	Description	
PBR	Photobioreactor	
ORP	Open raceway pond	
HT	Horizontal tubular	
VT	Vertically stacked horizontal tubular	
FP	Flat panel	

4.2 Introduction

High biomass production costs prevent the current implementation of microalgae in bulk applications; production costs should decrease below 1 €/kg DW. The high production costs are a result of low photosynthetic efficiencies and high energy costs for operation of cultivation systems and harvesting [62]. Currently, efforts are being made to achieve higher photosynthetic efficiencies under outdoor conditions.

Photosynthetic efficiencies obtained under outdoor conditions are still lower than the values obtained under laboratory conditions [31]. Under outdoor conditions lower photosynthetic efficiencies are obtained because of photo saturation [7] and because essential parameters for growth, such as temperature, cannot be controlled to the same extent as under laboratory conditions. Photo saturation could be reduced by reactor design [23, 63], but is practically complicated because light intensity and light direction vary over the day and over the seasons. The light regime within microalgal cultures can be manipulated by means of controlling the biomass concentration and culture mixing. Too high or too low biomass concentrations can result in suboptimal operation [7]. Too low biomass concentration will result in an incomplete light absorption and possibly photo inhibition, and too high biomass concentrations will result in dark zones where biomass is lost due to cellular maintenance (i.e. endogenous respiration).

In most studies done at outdoor conditions, a fixed daily dilution rate is used as operational strategy [55, 64–66]. However, the application of a fixed dilution rate results in varying biomass concentrations during the day and year, because of day/night cycles and seasonal variations. If the dilution rate is too high the biomass concentration is low and photo inhibition could occur. If the dilution rate is too low the biomass concentration can become so high that the dark zone in the reactor is so large that a significant amount of biomass production is lost due to endogenous respiration [31, 48, 57]. Operation of photobioreactors with a fixed biomass concentration (turbidostat mode) can prevent culture washouts as dilution of the culture only takes place when growth occurs. Operation at the optimal biomass concentration should theoretically result in the highest productivity as light interception is maximized, photo inhibition is minimized, and at the same time excessive dark zones are prevented [62, 64, 67].

In laboratory experiments the use of a fixed biomass concentration or a constant light intensity (a fixed amount of light per cell) was shown to positively influence productivity of *Neochloris oleoabundans* [68]. Cuaresma et al., showed that a fixed light absorption by the culture could result in high biomass yields on light [69]. The effect of biomass concentrations on the productivity of different outdoor photobioreactors was shown in model simulations by different authors [24, 29, 70] [71, 72]. However, applying a fixed biomass concentration under outdoor production conditions has only been investigated by a limited number of authors [51, 73]. Michels et al., investigated the effect of biomass concentration on the productivity of *Tetraselmis suecica*; a biomass concentration of 0.7 g L⁻¹ resulted in the highest productivity and biomass yield. Grima et al., investigated the effect of biomass concentration on productivity in tubular photobioreactors with different optical paths for *Tetraselmis suecica* and showed that smaller optical path systems resulted in higher volumetric productivity while higher areal productivities were found for longer optical path systems.

In order to maximize productivity and photosynthetic efficiency in outdoor photobioreactors, the optimal biomass concentration needs to be determined for each type of photobioreactor. Therefore, we compared the performance of three different pilot-scale outdoor photobioreactors under identical climatological conditions. These reactors were operated in turbidostat mode with different biomass concentrations of *Nannochloropsis* sp.. The photobioreactors investigated in this study were an open raceway pond (OPR), a horizontal tubular photobioreactor (HT), and a vertically stacked horizontal tubular photobioreactor (VT).

4.3 Materials and Methods

4.3.1 Inoculum production

Inoculum production was done as described by [66]. *Nannochloropsis* sp. CCAP211/78 was cultivated in 250 mL Erlenmeyer flasks, followed by cultivation in a flat panel photobioreactor and a horizontal tubular photobioreactor located in a greenhouse. The flat panel photobioreactor was a 25L flat panel photobioreactor having an optical path of 40 mm, pH was controlled at 7.5 ± 0.5 by blending CO₂ in the airflow, and temperature was controlled at 25°C. The indoor horizontal tubular photobioreactor (280L) was operated at a liquid velocity in the tubes of 0.3 m s^{-1} , a temperature of 25°C, and pH was controlled at 7.5 by on demand addition of carbon dioxide.

Nannochloropsis sp. CCAP 211/78 was cultivated in seawater (Eastern Scheldt, the Netherlands) enriched with a stock solution resulting in the following concentrations (in mM); NaNO₃, 25; KH₂PO₄, 1.7; Na₂EDTA, 0.56; Fe₂SO₄·7H₂O, 0.11; MnCl₂·2H₂O, 0.01; ZnSO₄·7H₂O, $2.3 \cdot 10^{-3}$; Co(NO₃)₂·6H₂O, $0.24 \cdot 10^{-3}$; CuSO₄·5H₂O, $0.1 \cdot 10^{-3}$; Na₂MoO₄·2H₂O, $1.1 \cdot 10^{-3}$. For pre-cultures (100 mL culture, 250 mL Erlenmeyer flasks) HEPES (20mM) and Na₂EDTA (5mM) were added to the seawater, and pH was adjusted to 7.5 followed by heat sterilization (121 °C, 20 min). The nutrient stock solution was added to the heat sterilized seawater through a sterile filter (0.2 μm).

4.3.2 Outdoor pilot-scale photobioreactors

A short description of each photobioreactor (Figure 4.1) is given in this section; a more detailed description of the used outdoor systems is given by Bosma et al.[9]. All outdoor photobioreactors were operated at a pH of 7.5 by on-demand CO₂ addition and culture temperatures were maintained between 20-30°C. Volumes of the systems were: HT; 560L, VT; 1060L and ORP; 4713L. Optical path length in the tubular systems was 0.046 m and depth of the open raceway pond was 0.2 m. Each system covers a ground area of $\pm 25 \text{ m}^2$. High dissolved oxygen concentrations in the tubular photobioreactors by increasing the airflow in the bubble column, when concentrations of 300% were reached. In the open raceway pond dissolved oxygen concentrations reached a maximum of 160%.



Figure 4.1 Outdoor cultivation systems in operation at AlgaePARC facility, Wageningen University and Research centre, the Netherlands.

Turbidostat operation

All cultivation systems were operated in turbidostat mode to study the effect of biomass concentration on the productivity. During turbidostat operation harvesting starts automatically when the biomass concentration set point is reached. Biomass concentration (turbidity) was measured by a single channel NIR absorption probe (AS56-N, Optek, Elscolab, the Netherlands) and harvesting via a pump was initiated via a programmable logic controller (PLC) and supervisory control and data management system (SCADA). Harvesting was done at a flow rate of 12.5 L min^{-1} , water addition took place at a flow rate of 10 L min^{-1} . The stability of turbidostat operation was visualized in supplementary data a previous publication on the construction of the pilot plant where experiments were executed [9]. The biomass concentrations studied under turbidostat operation are given in Table 4.1. Operational setpoints for turbidostat operation are given in the supplementary data A. The corresponding biomass densities when expressed in gram per m^2 of occupied ground area are included in Table 4.1. The research started with biomass concentrations comparable to the biomass concentrations encountered during chemostat operation in a previous study [66]: ORP; 0.5 g L^{-1} , HT; 1.5 g L^{-1} and VT; 1.0 g L^{-1} . In a next step biomass concentration was set to lower and higher values in order to determine the effect on photobioreactor productivity.

Table 4.1 Overview of the biomass concentrations (g L^{-1}) and ground areal biomass concentration (g m^{-2}) for each photobioreactor. Ground areal biomass concentrations were obtained by division of total biomass in system by occupied ground area of the photobioreactor.

PBR/runs	1		2		3		4	
	g L^{-1}	g m^{-2}						
Open raceway pond	0.25	47	0.50	94				
Horizontal tubular	0.38	7.8	0.75	16	1.50	31	2.50	51
Vertically stacked hor. tubular	0.25	8.6	0.50	17	1.00	34	2.00	68

Natural seawater was added on demand when a lower liquid level in the system was detected as a result of harvesting, or evaporation (in the case of the ORP). Simultaneously, the stock solution used to enrich the natural seawater was automatically added to the culture flow proportional to the addition of seawater. An increase in culture depth as a result of precipitation, in the ORP pond was prevented by automated harvesting.

4.3.3 Measurements and analyses

The photobioreactors were daily sampled between 9:00 and 10:00 a.m. for optical density measurement (680nm and 750nm) on a DR5000 spectrophotometer (Hach Lange, Germany). Three times a week dry weight determinations [66] and absorption coefficients were measured [11]. Nitrate was daily measured to check that there was no nitrogen limitation; 2 mL of culture was centrifuged and the supernatant was analysed for nitrate content with an AQ-2 nutrient analyser, (Seal Analytic, USA) as described by [42] (HMSO, 1981; APHA/AWWA/WEF, 4500; USEPA, 19932). In the tubular photobioreactors the harvested volume was determined by the measurement of the natural seawater addition over 24 hours. For the open raceway pond, the harvested volume was calculated from the level increase in the harvest vessel.

4.3.4 Definitions and calculations

Ground areal biomass productivity

Daily ground areal biomass productivity was calculated with Equation 1:

$$P_{x,ground} = \left(\frac{(F_{harvest} \cdot C_{x,reactor})}{A_{ground}} \right) \quad \text{g m}^{-2} \text{ d}^{-1} \quad \text{Eq. 1}$$

With: $P_{x,ground}$: ground areal biomass productivity ($\text{g m}^{-2} \text{ d}^{-1}$); $F_{harvest}$: harvested volume (L/24hr); $C_{x,reactor}$: dry weight biomass concentration in the reactor (g L^{-1}); A_{ground} : occupied ground area photobioreactor (m^2).

Volumetric biomass productivity

Daily volumetric biomass productivity was calculated with Equation 2:

$$P_{x,vol} = P_{x,ground} * \frac{A_{ground}}{V_R} \quad \text{g L}^{-1} \text{ d}^{-1} \quad \text{Eq. 2}$$

With: $P_{x,vol}$: volumetric productivity ($\text{g L}^{-1} \text{ d}^{-1}$); $P_{x,ground}$: areal biomass productivity ($\text{g m}^{-2} \text{ d}^{-1}$); V_R : volume of photobioreactor (L); A_{ground} : occupied ground area photobioreactor (m^2).

Photon flux density of PAR (PFD)

$$I_{ground,daily} = \left(\sum (I_{ground}(t_0 : t) * 60) \right) / 10^6 \quad \text{mol m}^{-2} \text{ d}^{-1} \quad \text{Eq. 3}$$

The daily ground areal photon flux density ($I_{ground,24}$, $\text{mol m}^{-2} \text{ d}^{-1}$) was calculated with Equation 3. Ground areal photon flux densities (I_{ground} ; $\mu\text{mol m}^{-2} \text{ s}^{-1}$) were measured every minute with a Li-Cor-190SA 2π PAR quantum sensor on a horizontal plane. All the measured photon flux densities between two consecutive reactor sampling points (24 hours) were summed up and multiplied by 60 (conversion from seconds to minutes).

Photosynthetic efficiency on sunlight

The photosynthetic efficiency is calculated with Equation 4:

$$PE_{sunlight} = \frac{(P_{x,ground} * \Delta H_c^o)}{((I_{ground,daily} * (E_{PAR} / 0.43)) / 10^3)} \quad \text{Eq. 4.}$$

With: $PE_{sunlight}$: photosynthetic efficiency (% sunlight); $P_{x,ground}$ average ground areal productivity ($\text{g m}^{-2} \text{d}^{-1}$); ΔH_c^o : standard enthalpy of biomass combustion (22.5 KJ g^{-1}); $I_{ground,daily}$: average daily areal photon flux density equation 3 ($\text{mol m}^{-2} \text{d}^{-1}$ (PAR, photosynthetic active radiation)); E_{PAR} : energetic content of the PAR fraction of sunlight (J mol^{-1}) 4.76, ASTM G173-03 [43]; and 0.43 the conversion ratio from sunlight to PAR light.

Specific night biomass loss rate

Specific biomass loss rates during the night were calculated with equation 5 as previously described by [51].

$$\frac{LN(C_{X(t)}) - LN(C_{X(t-0)})}{C_{x,setpoint}} \quad \text{Eq. 5.}$$

Specific biomass loss rate was calculated by the difference in biomass concentration one hour before sunrise ($C_{X(t)}$) and one hour after sunset ($C_{X(0)}$), divided by the biomass concentration used as set point for turbidostat operation ($C_{x,setpoint}$). The online measured turbidity (NTU) was converted to biomass concentration (g L^{-1}) using the linear relationship present between these.

4.3.5 Statistical analysis

An analysis of covariance (ANCOVA) was done to evaluate the effect of biomass concentration on the biomass productivity while compensating for values for daily ground areal photon flux density (the covariate). The ANCOVA was done with a significance level of 5% ($\alpha=0.05$) and the posterior pair-wise comparison test of Bonferroni was used to identify intra-groups differences. Two of the assumptions of the analyses of variance were tested: normality (using the test of Kolmogorov-Smirnov, $\alpha=0.05$) and homoscedasticity (Levene's test, $\alpha=0.05$). For some cases the assumptions were not guaranteed, suggesting data transformation was required. After data transformation (both LogN and ranking) some cases still did not meet the requirements of ANCOVA (p-values <0.05). For that, ANCOVA with simple bootstrapping was done (1000 simulations) at a confidence interval of 95% (in percentiles). Bootstrapping is a random sampling method used to estimate variables with increased accuracy and for data that do not meet the requirements of statistical after data transformation [74].

4.4 Results and Discussion

For this research multiple cultivations outdoors were started; the horizontal tubular photobioreactor was inoculated 11 times over the experimental period of in total 211 measurement days. The vertically stacked horizontal tubular photobioreactor was restarted 8 times over 190 measurement days and the open raceway pond was restarted 6 times over 166 measurement days. Data collection for the open raceway pond was limited to the period between late spring to early fall due to limited heating capacity.

4.4.1 Effect of photon flux density on areal productivity and photosynthetic efficiency

To visualize trends, raw data (supplementary materials) was condensed by calculating mean values over four ranges of daily photon flux densities (PFD); 0-15, 15-30, 30-45 and 45-60 mol/m²/d. The mean areal productivities and mean photosynthetic efficiencies are presented in Figure 2. As expected, for all systems, the mean areal productivities increased with increasing daily PFD illustrating that microalgae production is light limited. Furthermore, for all systems, mean photosynthetic efficiencies decreased with increasing daily photon flux densities most likely caused by increased photo saturation in the photic zones of the microalgal culture. Similar trends were previously reported by [46, 48, 55, 66]. Highest mean areal productivities were obtained for the open raceway pond, at the lowest biomass concentration (0.25 g L⁻¹) and for the vertically stacked horizontal tubular photobioreactor (0.5 and 1.0 g L⁻¹). The lowest mean areal productivities and photosynthetic efficiencies were obtained for the horizontal tubular photobioreactor. A possible explanation lies in the distance between the horizontal tubes, which equals tube diameter. This results in a less efficient capture of the light falling on the ground surface occupied by the horizontal tubular photobioreactor. The tubes must be placed close to each other to achieve maximal areal productivity for a horizontal system, placing the tubes closer results in an efficient light capture [75]. Light capture by the vertical tubular system was higher and that of the raceway pond was maximal (all light enters the culture). A similar trend was observed in a previous study on the same systems while operating under chemostat conditions [66].

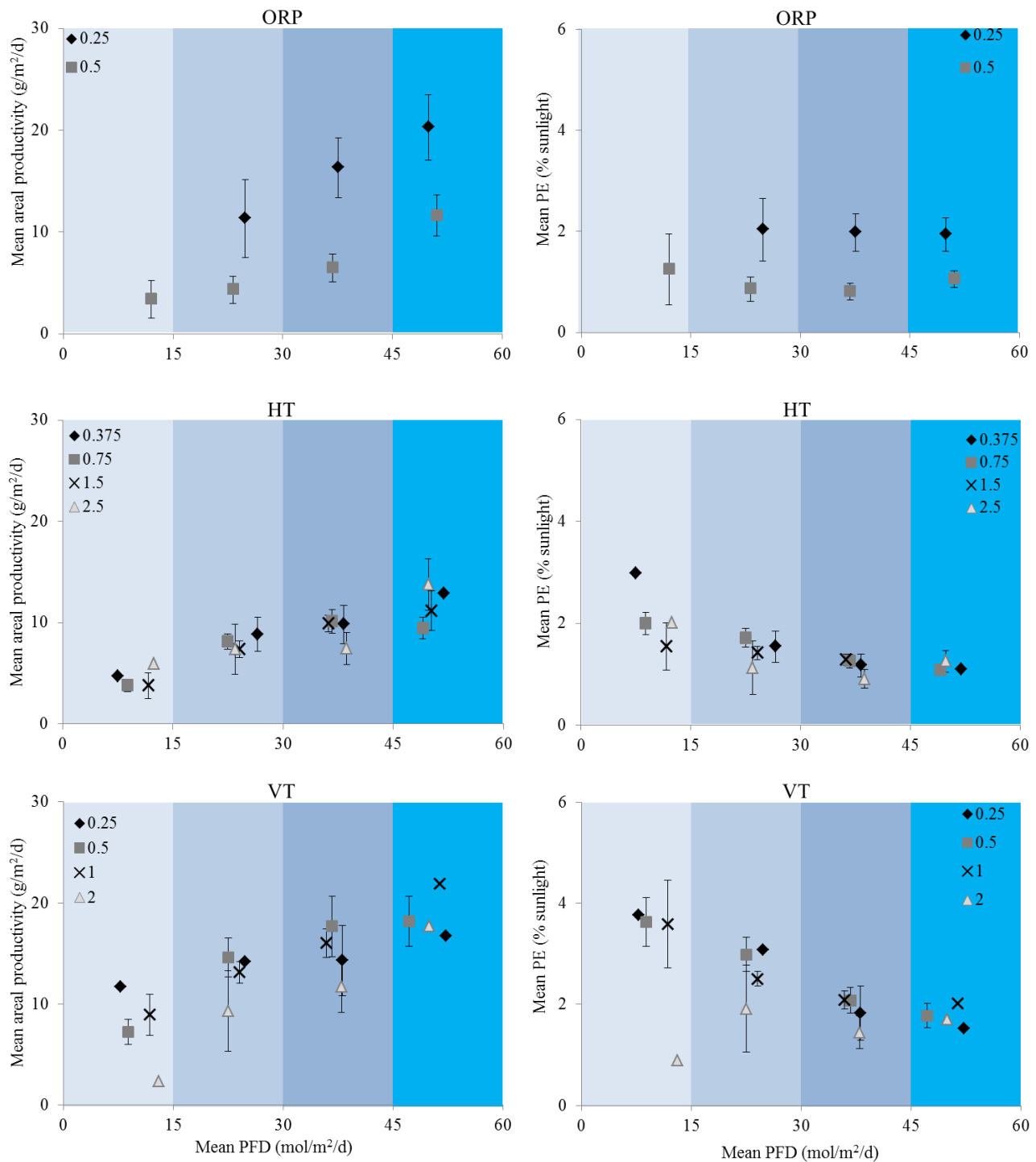


Figure 4.2 Mean areal productivities and mean photosynthetic efficiencies vs mean daily ground areal photon flux densities. Results were averaged and grouped over four light ranges: 0-15, 15-30, 30-45 and 45-60 mol/m²/d. With ORP; open raceway pond, HT; horizontal tubular photobioreactor and VT; vertically stacked horizontal tubular photobioreactor. Legend indicates biomass concentrations tested for each cultivation system. Error bars indicate 95% confidence intervals, data points with no error bars represent data points with a population size smaller than 3. For 0.25 g L⁻¹ for ORP no data was obtained in the low range of PFD (0-15 mol m⁻² d⁻¹). Original data can be found in Appendix 4.B.

4.4.2 Effect of biomass concentration on areal productivity

The photon flux density (PFD) has a major influence on areal productivities but the PFD cannot be manipulated in outdoor photobioreactors. The light regime can only be influenced by the biomass concentration. In this study biomass concentration was directly controlled by turbidostat cultivation. The productivity therefore is influenced by two variables, PFD and biomass concentration. An analysis of covariance allows for the separation of the effects of different variables. The results of the ANCOVA with bootstrapping are represented in Figure 4.3.

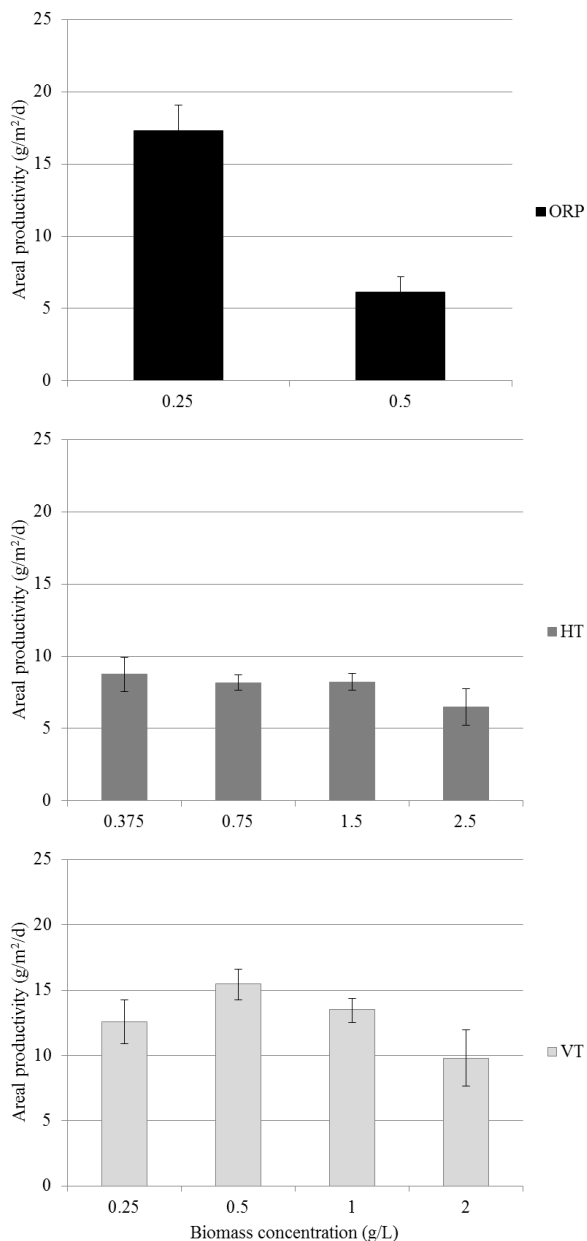


Figure 4.3 Results of the ANCOVA (with bootstrapping); areal productivity vs. biomass concentration for the HT, VT, ORP while statistically correcting for the effect of photon flux density (PFD). In our analyses a simple bootstrapping was done using 1000 simulations at the confidence interval of 95% (percentiles)

In Figure 4.3 similar trends are observed as in Figure 4.2; for ORP a significant difference is observed in the average areal productivities obtained with the two different biomass concentrations studied. The strong increase in areal productivity by decreasing biomass concentration from 0.5 to 0.25 g L⁻¹ for the ORP shows that 0.5 g L⁻¹ is above the optimal biomass concentration for maximal areal productivity, as reported also by [57]. The biomass concentration of 0.5 g L⁻¹, corresponds to the highest ground areal biomass loading of 94 g m⁻², resulting in the lowest light supply per unit of biomass. At 0.5 g L⁻¹ a larger dark zone is therefore present in the culture, possibly resulting in unfavourable light/dark dynamics and increased requirement for cellular endogenous respiration. This possible negative effect of light/dark cycling on productivity has been observed in dedicated laboratory-scale studies. Specifically; long light/dark cycles in the order of tens of seconds have a negative effect on productivity and such long cycles are likely to occur in the optically deep raceway pond [13, 49, 50, 76]. The higher biomass loading was not able to compensate for the lower average growth rate obtained for the ORP, as visualized in Appendix 4.D.

For the vertically stacked horizontal stacked tubular photobioreactor no significant differences were observed for the three lowest biomass concentrations tested (0.25, 0.5 and 1.0 g L⁻¹). However, the mean areal productivity obtained for the highest biomass concentration of 2.0 g L⁻¹ (68 g m⁻²) was significantly lower than the areal productivities obtained for 0.5 and 1.0 g L⁻¹. The decrease in areal productivity found at 2 g L⁻¹ or 68 g m⁻² shows that this biomass concentration is above the optimal biomass concentration for the VT, leading to a larger dark zone and by that increased energy required for cellular maintenance. Also, for this system, similar to the ORP, an effect of unfavourable light dark cycling cannot be excluded. For the horizontal tubular photobioreactor, the horizontal orientation together with the short optical path results in relatively large exposure of the culture to mainly high light intensities. Therefore, much higher biomass concentrations, in comparison to the VT, are needed before a significant dark zone forms in the culture. For HT, biomass concentration had no significant effect on average areal productivities.

Our study shows that biomass concentration only had an effect when the areal biomass density was more than 51 g m⁻². Increased areal biomass concentrations reflect the increase in the relative volume of the microalgal culture which is in darkness due to self-shading. Apparently, beyond a value of 51 g m⁻² the size of this dark volume results in a measureable and negative effect on areal productivity and photosynthetic efficiency. This decrease in both areal productivity and photosynthetic efficiency can be related to two biological mechanisms. First, higher areal biomass concentrations, and consequent dark volume, will result in an increased requirement for endogenous respiration energy reducing the amount of light energy available for growth [77]. Second, an increased dark volume will affect the light/dark cycling the microalgae are exposed to when they are moving through the light gradients present in the photobioreactor. Long light/dark cycles in the orders of tens of seconds have demonstrated to result in lower photosynthetic efficiencies [13, 49, 50]. This could be explained by unfavourable acclimation responses, or increased pigmentation leading to even more photo saturation and in the high-light exposed surface layers of the culture. Increased pigmentation at higher biomass concentration was observed and will be discussed later. In addition, it was hypothesised by others that the effect of photo inhibition and light/dark fluctuations in microalgal cultures are tightly coupled, and that photo inhibition becomes more dominant in slowly mixed systems with relatively long exposure times to high light in the surface layers of the culture [78].

When comparing the different systems it is important to note that configuration and mixing are completely different [57, 79, 80]. Slower mixing along the light gradient in the ORP therefore could explain the bigger impact of high biomass concentration on productivity in comparison to the VT and HT.

4.4.3 Turbidostat versus chemostat

For the ORP turbidostat operation at low biomass concentration resulted in higher areal productivities and photosynthetic efficiency compared to operation with fixed daily dilution rates for chemostat operation in 2013 (Table 4.2). During chemostat operation, biomass concentrations were generally higher (0.32-0.53 g L⁻¹ overall data from chemostat operation) and this resulted in a larger dark zone as present during turbidostat operation at 0.5 g L⁻¹. The presence of a larger dark zone resulted in reduced performance due to increased respiration losses and/or unfavourable light/dark cycling as discussed above. The values obtained in this study for the open raceway pond are similar to values reported in literature, which were obtained on locations with higher PFD or in shallower systems [57-60].

Table 4.2 Overview of areal productivities and photosynthetic efficiencies obtained under chemostat operation (Chem) vs turbidostat operation (Turb) in the outdoor systems under high PFD conditions (45-60 mol m⁻² d⁻¹) [66]. ORP; open raceway pond, HT; horizontal tubular photobioreactor and VT; vertically stacked horizontal tubular photobioreactor. ^a High photosynthetic efficiencies for chemostat were obtained over a short period of time under low PFD conditions with less photo saturation (November 2013). Grey shaded cells are a result of the set values.

Photobioreactor	ORP		HT		VT	
	Chem	Turb	Chem	Turb	Chem	Turb
Areal productivity (g m ⁻² d ⁻¹)	14.0	20.3	15.7	10.1	24.4	18.2
Dilution rate (d ⁻¹)	0.12	0.44	0.34	0.60	0.40	1.02
Biomass concentration (g L ⁻¹)	0.65	0.25	2.40	0.75+1.5	1.73	0.5
Number of days	8	15	8	15	8	7
Photosynthetic efficiency (% sunlight)	1.5	2.0	1.8 ^a	1.9	4.2 ^a	3.6
Dilution rate (d ⁻¹)	0.12	0.23	0.28	0.22	0.24	0.36
Biomass concentration (g L ⁻¹)	0.65	0.25	2.32	0.75+1.5	0.49	0.5+1.0
Number of days	8	15	6	37	9	38

Areal productivities for the HT during turbidostat operation were lower than areal productivities obtained during chemostat operation in a previous study. However, these higher values for chemostat operation were obtained over a short period of time (8 days), during which a downwards trend in biomass concentration was observed, indicating that these high productivities might not be obtained for long periods of time. The same argumentation holds for the higher productivity values reported for the vertically stacked horizontal tubular photobioreactor.

For the HT we did not observe an effect of biomass concentration on the areal productivity, which is not completely in agreement with what has been reported for *Tetraselmis suecica* [51]. However, these experiments were carried out over a narrower range of PFD conditions and with a different microalga. The higher growth rate of *Tetraselmis suecica* in comparison to *Nannochloropsis* sp. used in this study influences productivity, as productivity is the result of growth rate and biomass

concentration. Camacho-Rodríguez et al., reported similar values for areal productivity for a horizontal tubular photobioreactor, with a tubular reactor with a long optical path (0.09 m) at higher PFD (south Spain)[52]. For the vertically stacked horizontal tubular system, a higher photosynthetic efficiency was obtained during chemostat operation compared to turbidostat operation.

In general, productivity under turbidostat and chemostat was comparable but turbidostat operation resulted in more stable operation. This was most prevalent for the tubular photobioreactors at medium biomass concentrations. In addition, for the open raceway pond turbidostat operation allowed for a more accurate assessment and control of the biomass concentration resulting in increased performance.

4.4.4 Algal pigmentation in outdoor photobioreactors

The specific absorption coefficient, representing cellular pigmentation, was used as indicator for light limitation or saturation [62]. Under outdoor conditions, cultures adapt pigmentation to the light regime [46, 52]. The light regime depends on the incident light intensity but also on system design (i.e. optical path and mixing rate), and biomass concentration. In laboratory experiments under continuous (24/7) light, absorption coefficients were found to decrease with increasing daily photon flux densities [81-83]. In this study, we observed no influence of PFD on the absorption coefficients (Supplementary data). However, we did observe a correlation between absorption coefficients and biomass concentration (Figure 4.4). We found an increase in absorption coefficients with increasing biomass concentration, this could indicate that the culture experiences light limitation at higher biomass concentrations. The reason for apparent insensitivity of specific absorption coefficients to the daily PFD under outdoor conditions is not clear at this moment and requires an in-depth study.

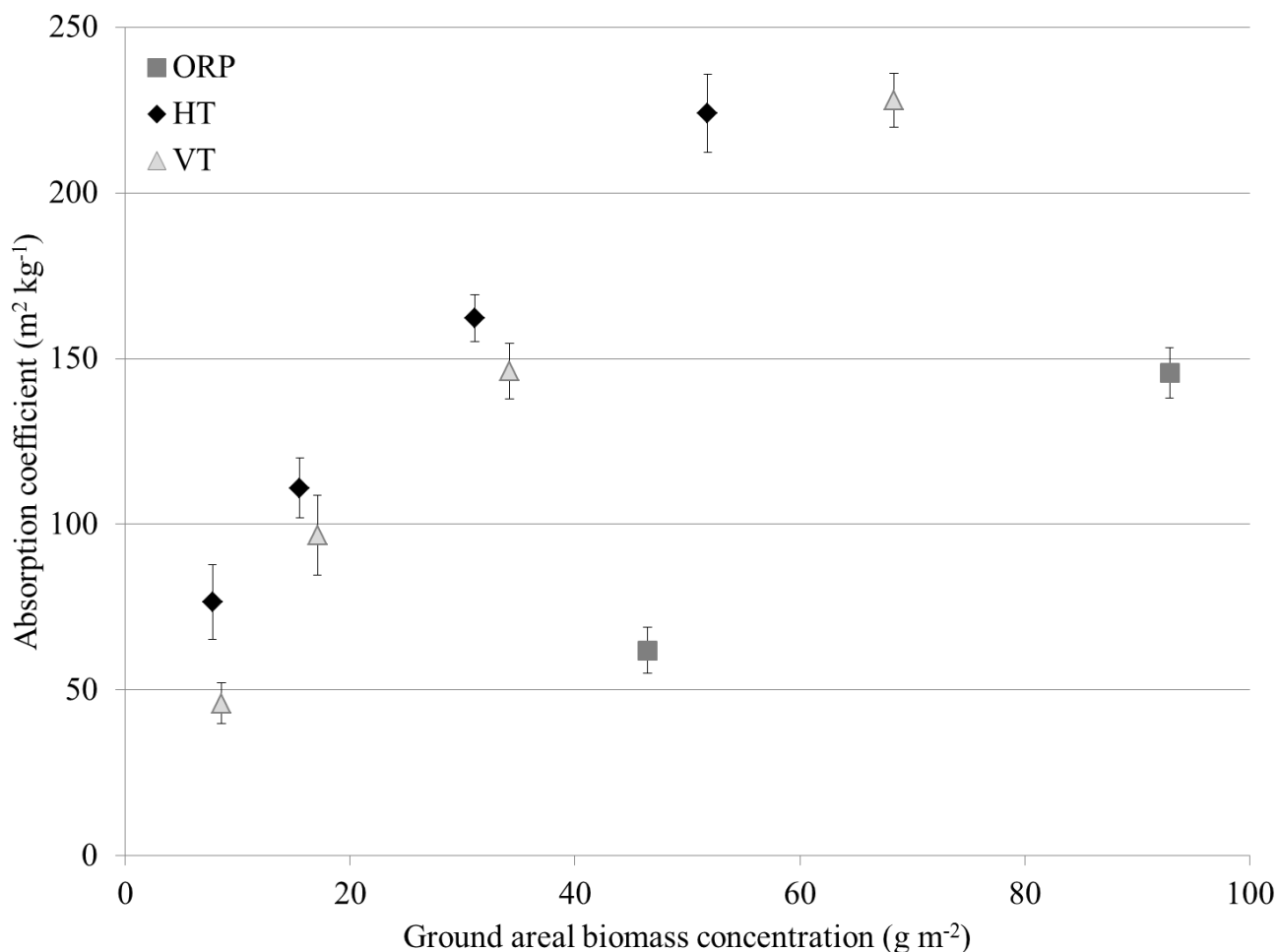


Figure 4.4 Specific light absorption coefficient versus ground areal biomass concentration during the operation of the ORP, HT, and VT. Error bars indicate 95% confidence intervals.

In Figure 4.4 the specific absorption coefficient is plotted versus the areal biomass density as this is a better indication of the average light exposure of the culture than the volumetric biomass concentration. The change in the specific absorption coefficients follows a similar trend for the two tubular photobioreactors. At equal areal biomass concentration the specific light absorption coefficient appears to be higher in the HT in comparison to the VT.

This difference can be explained by the more efficient sunlight capture in the VT; due to the differences in design; an equal ground areal biomass concentration results in a larger exposure in the VT in comparison to the HT. Furthermore, the effect of differences in mixing induced light dark cycles cannot be excluded. Specific absorption coefficients for the ORP deviate from the trend observed for the tubular reactors. The specific light absorption coefficient was lower in the ORP in comparison to the tubular photobioreactors although an considerable increase was observed when comparing the lower biomass concentration with the higher value (Figure 4.4). A explanation for this observation is still lacking.

The differences in absorption coefficients observed in our study at different biomass concentrations reflect the acclimation to the different light conditions experienced by the culture. However, this

acclimation did not result in changes in areal productivity for the tubular photobioreactors as was presented before. Based on a theoretical considerations an increase of the specific light absorption leads to more light saturation of individual microalgal cells at the light exposed tube surface [67, 84]. Therefore, a lower photosynthetic efficiency and lower biomass productivity would be expected. Such a decrease was only observed for the highest biomass concentration tested in the VT and not for the other 3 biomass concentrations (Figure 4.4). For the ORP the increase in specific absorption coefficient might have played a role in the low productivity observed at the highest biomass concentration tested.

4.4.5 Specific night biomass loss rate

The specific night biomass loss rates were determined for the two tubular photobioreactors operated at different biomass concentrations. For the ORP the relative night biomass loss could not be determined because of the low turbidity values compared to the background noise of the turbidity sensor used. During the night a decrease in biomass was observed for the tubular PBRs (Figure 4.5). Most likely cellular compounds like carbohydrates are consumed (respiration) to supply energy for cellular processes such as cell division [82, 85]. For both tubular photobioreactors the lowest specific night biomass losses were found for the highest biomass concentrations (VT 2.0 g L⁻¹ and HT 2.5 g L⁻¹), expressing the lowest specific growth rates. For both tubular photobioreactors the specific night biomass loss rate increased with decreasing biomass concentrations while expressing increasing specific growth rates.

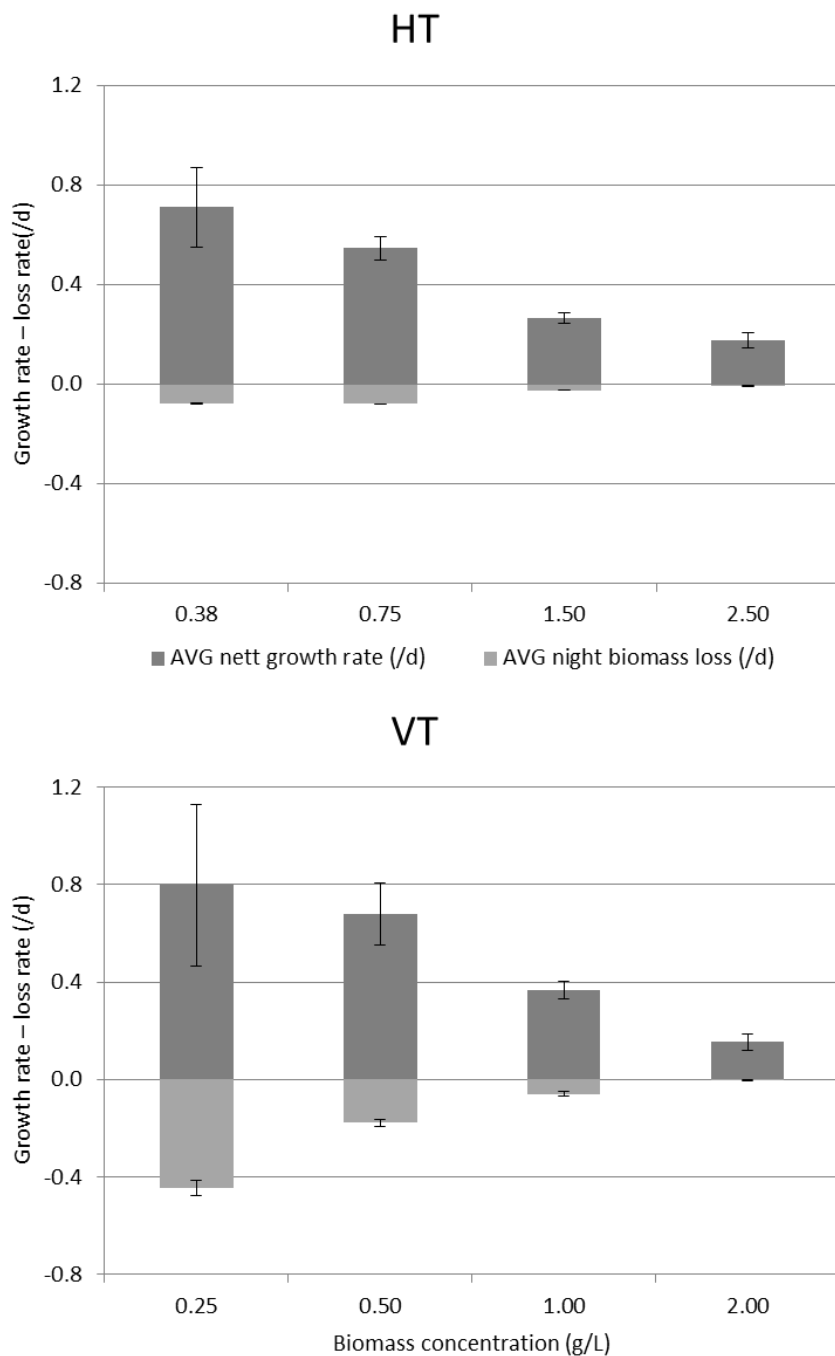


Figure 4.5 Average specific growth rate and average specific night biomass loss rate for the tubular photobioreactors for each biomass concentration. For HT, horizontal tubular PBR and VT, vertically stacked horizontal tubular PBR. Error bars represent 95% confidence interval.

Higher specific biomass loss rates were observed for the vertically stacked horizontal tubular photobioreactor compared to the horizontal tubular system. At lower biomass concentration more variation was observed in the specific growth rates hence the larger variation in the specific night biomass loss rates. We observed a direct relation between the net specific growth rate and the

specific night biomass loss rates. These findings are in line with previous data reported for *Tetraselmis suecica* [51] cultivated in a similar horizontal tubular photobioreactor operated in Vlissingen, the Netherlands. Clearly, a large part of night biomass loss is coupled to net growth as recently also shown in laboratory experiments for *Scenedesmus obliquus* by Sforza [86]. Even more so, a direct relation between net microalgal growth and respiration has already been reflected upon by Geider and Osborne [87] who concluded that the largest part of respiration is directly coupled to growth and that the remaining part is required for endogenous respiration.

4.5 Conclusions

Highest average areal productivities were found for the vertically stacked horizontal tubular photobioreactor and open raceway pond on days with high PFD; 20.3 and 18.2 g m⁻² d⁻¹, respectively. Highest average photosynthetic efficiencies were obtained with the vertically stacked horizontal photobioreactor at low photon flux densities; 3.6%.

Ground areal biomass concentrations of above 51 g m⁻² negatively affect the areal productivity and photosynthetic efficiency of outdoor photobioreactors. Biomass concentration had the largest influence on the areal productivity and photosynthetic efficiency of the ORP, probably due to the long optical path (20 cm) of this system. For the ORP a lower ground areal biomass concentration of 47 g m⁻² resulted in higher productivities and photosynthetic efficiencies compared to the higher ground areal biomass concentration (94 g m⁻²). Ground areal biomass concentrations did not have this strong influence on areal productivity in the tubular photobioreactors where areal biomass concentration in general were below 51 g m⁻². For maximal productivity ground areal biomass concentrations should be lower than 51 g m⁻² in outdoor photobioreactor.

Absorption coefficients were found to be biomass concentration specific; higher biomass concentrations resulted in higher values. In this study we observed that night biomass loss was coupled to net growth; at lower biomass concentrations and thus higher growth rates higher specific biomass loss rates were observed.

Appendix 4.A Specifications of outdoor pilot scale photobioreactors. ORP open raceway pond, HT, horizontal tubular PBR and VT, vertically stacked horizontal tubular PBR.

An overview of system specifications is given and an overview of the operational setpoints for turbidostat operation are given.

Table 4.A.1 with specifications of outdoor pilot-scale photobioreactors

Specifications	ORP	HT	VT
Optical path (m)	0.2	0.046	0.046
Volume (m ³)	4.73	0.56	1.06
Illuminated volume (%)	100	73	71
Ground area occupied (m ²)	25.4	27.0 ^a	31.0 ^a
Illuminated volume/ground area (m ³ m ⁻²)	0.186	0.021	0.034

^a Including half of ground area occupied by dummy panels installed at northern and southern side of reactor

^b Data from Norsker et al., 2013 [5]

Table 4.A.2 with operational setpoints for turbidostat operation, for each system, biomass concentration start and stop setpoints for turbidostat control are given. Furthermore the percentage in biomass variation during turbidostat operation is given.

System	ORP		HT				VT			
Cx setpoint (g L ⁻¹)	0.25	0.5	0.375	0.75	1.5	2.5	0.25	0.5	1	2
Start harvest	400	845	600	1100	2370	2910	300	800	1700	2547
Stop harvest	385	830	580	1080	2350	2890	280	780	1680	2527
%	3.8	1.7	3.3	1.8	0.8	0.7	6.7	2.5	1.1	0.7

Appendix 4.B overview of raw data obtained during turbidostat operation in the different cultivation systems.

Raw data for areal productivities and photosynthetic efficiencies obtained for each biomass concentration for each system are presented.

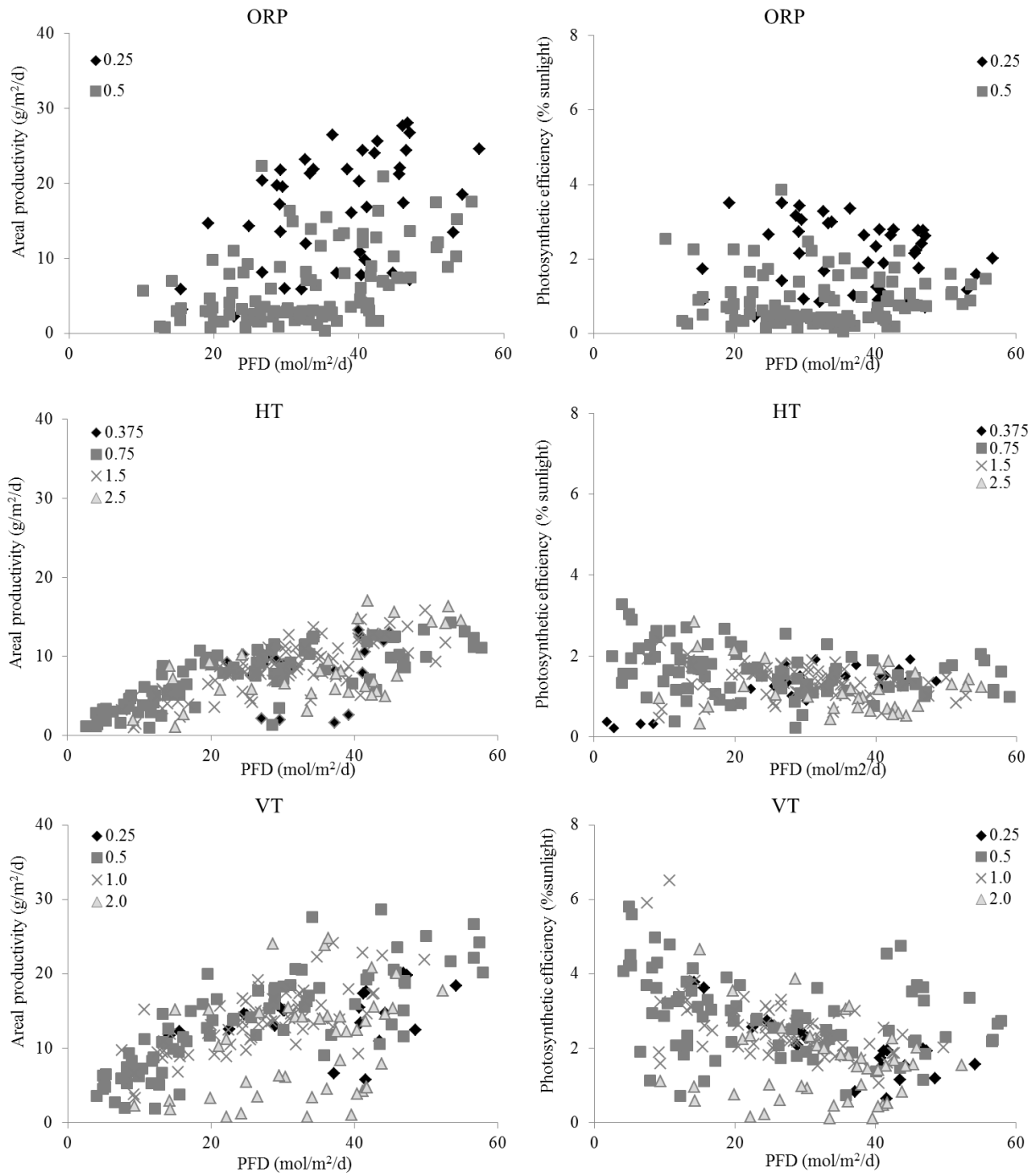


Figure 4.B.1 Overview of areal productivities and photosynthetic efficiencies vs the daily photon flux density obtained during operation at different biomass concentrations in the cultivation systems. With ORP; open raceway pond, HT; horizontal tubular photobioreactor and VT; vertically stacked horizontal tubular photobioreactor.

Appendix 4.C Absorption coefficients versus the daily photon flux density for the different systems.

An overview of the values for the absorption coefficients obtained for each biomass concentration in each system.

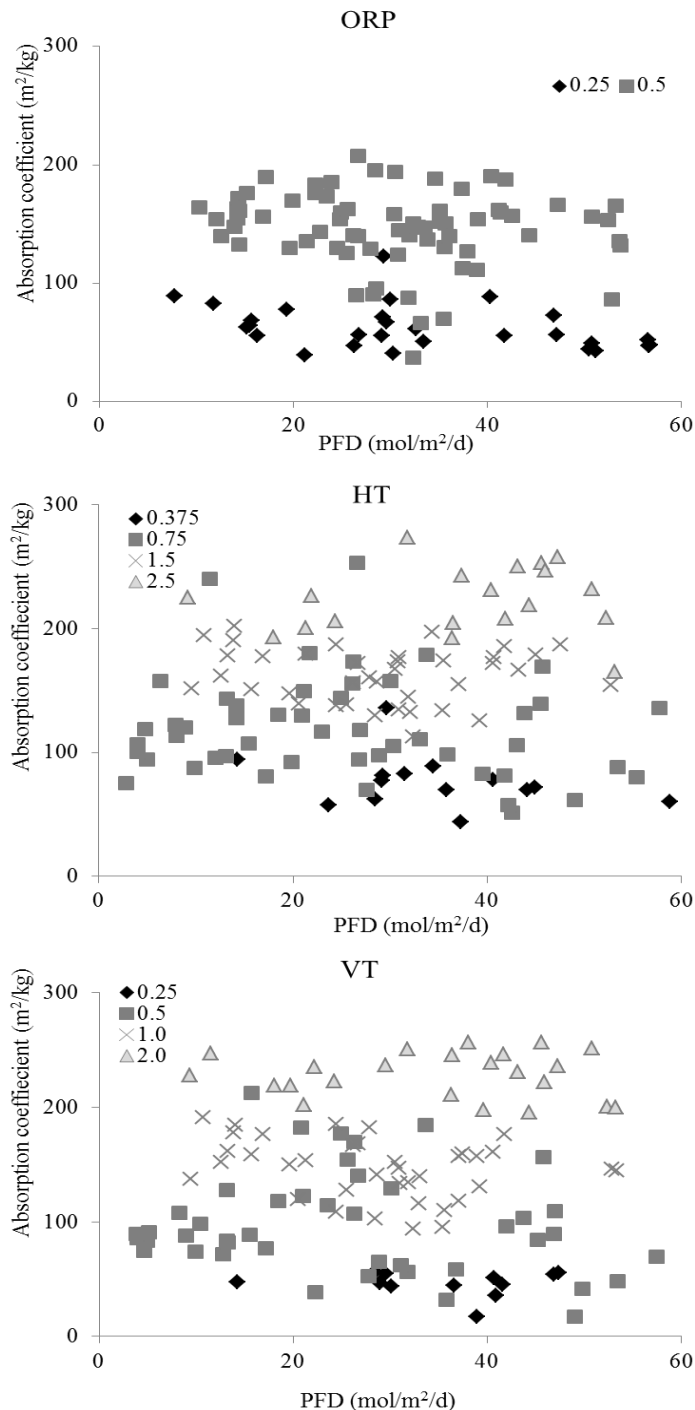


Figure 4.C.1 Overview of specific absorption coefficients vs the daily photon flux density obtained during operation at different biomass concentrations in the cultivation systems. With ORP; open raceway pond, HT; horizontal tubular photobioreactor and VT; vertically stacked horizontal tubular photobioreactor.

Appendix 4.D Average growth rate for each biomass concentration in each photobioreactor.

Overview of the average growth rate calculated for each biomass concentration in the different cultivation systems

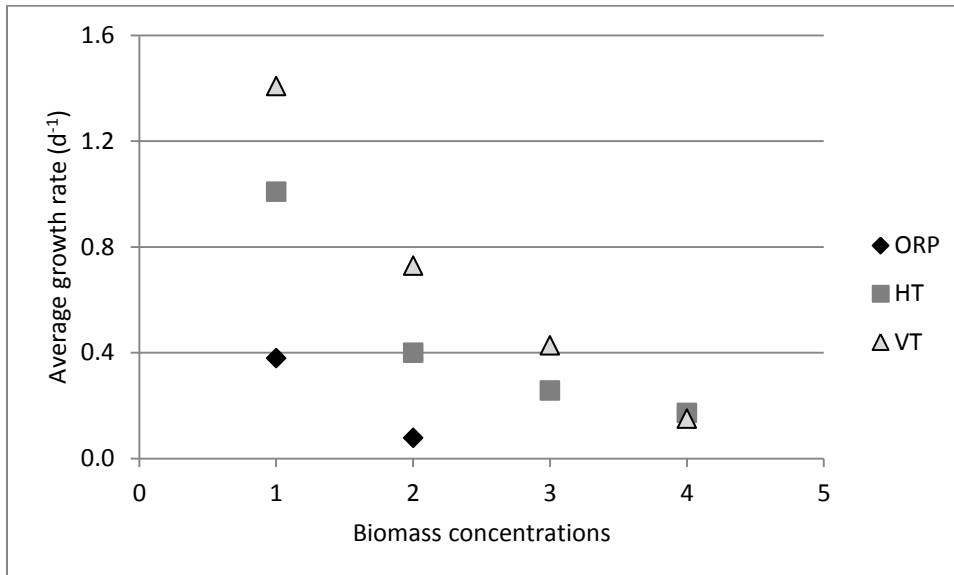


Figure 4.D.1 Overview of average growth rates versus different biomass concentrations in the cultivation systems. with the following biomass concentrations; ORP 1; 0.25 g L⁻¹, 2; 0.5 g L⁻¹. HT; 1; 0.375 g L⁻¹, 2; 0.75 g L⁻¹, 3; 1.5 g L⁻¹, 4; 2.5 g L⁻¹. VT; 1, 0.25 g L⁻¹, 2; 0.5 g L⁻¹, 3; 1.0 g L⁻¹, 4; 2.0 g L⁻¹. With ORP; open raceway pond, HT; horizontal tubular photobioreactor and VT; vertically stacked horizontal tubular photobioreactor.

Chapter 5

Parameter estimation for *Neochloris oleoabundans* and *Nannochloropsis* sp. for modelling microalgal growth.

This chapter is being prepared for submission

J. H. de Vree, P.M. Slegers, R Bosma, M. Janssen, M.J. Barbosa, R.H. Wijffels

5.1 Abstract

A reliable estimation of the economic potential and environmental footprint of large scale microalgae production is essential to guide future development of this new production process of biomass. An important aspect of such estimations is the productivity of algae cultivation systems. Mathematical models are able to predict algal growth under varying light and temperature. These models require strain specific parameters, which are often not available. In this study parameters for a growth model were obtained for two potential production strains rich in lipids; *Neochloris oleoabundans* and *Nannochloropsis* sp. These parameters were obtained based on bench-scale photobioreactor experiments in combination with a statistical parameter estimation routine. The obtained parameter values were used to predict the effect of process conditions on the productivity of microalgae cultivation systems. These simulations showed that biomass productivity only decreases slowly when exceeding the optimal biomass concentration, which explains previous observations in outdoor photobioreactors. In addition, a less tight temperature control (20 – 35 °C) was shown to result in a 20-30% reduction in productivity in comparison to a more tight temperature control (24-28 °C). The specific growth rate and specific absorption coefficient showed to have a big impact on the prediction and it is hypothesized that the maximal specific growth rate of *Nannochloropsis* sp. differs considerably among strains.

Keywords

Microalgae; *Neochloris*, *Nannochloropsis*, growth model, light, temperature, parameter estimation.

List of symbols and abbreviations used

Symbol	Description	Units
α	Specific absorption coefficient	$\text{m}^2 \text{g}^{-1}$
ρ	Density	g L^{-1}
μ	Specific growth rate	d^{-1}
μ_m	Maximal specific growth rate	d^{-1}
μ_{local}	Local specific growth rate (z)	d^{-1}
$\mu_{m,opt}$	Maximal specific growth rate at optimal temperature	d^{-1}
ABS_λ	Absorbance at wavelength λ	-
A_R	light-exposed reactor area	m^2
f_T	Temperature factor based on cardinal temperature model	-
C_x	Biomass concentration	g L^{-1}
D	Dilution rate	d^{-1}
PFD_{abs}	Absorbed photon flux density	$\text{mol}_{ph} \text{m}^{-2} \text{s}^{-1}$
PFD_{avg}	Average photon flux density	$\text{mol}_{ph} \text{m}^{-2} \text{s}^{-1}$
PFD_{in}	Incident photon flux density	$\text{mol}_{ph} \text{m}^{-2} \text{s}^{-1}$
PFD_{local}	Local photon flux density	$\text{mol}_{ph} \text{m}^{-2} \text{s}^{-1}$
PFD_{out}	Outgoing photon flux density	$\text{mol}_{ph} \text{m}^{-2} \text{s}^{-1}$
P_{areal}	Areal biomass productivity	$\text{g m}^{-2} \text{d}^{-1}$
q_{ph}	Specific photon supply rate	$\text{mol}_{ph} \text{g}^{-1} \text{s}^{-1}$
r_{ph}	Maintenance requirement on light	$\text{mol}_{ph} \text{g}^{-1} \text{s}^{-1}$
r_m	Maintenance rate	d^{-1}
T_{max}	Maximal temperature for microalgae growth	$^{\circ}\text{C}$
T_{min}	Minimal temperature for algae growth	$^{\circ}\text{C}$
T_{opt}	Optimal temperature for algae growth	$^{\circ}\text{C}$
V_h	Effluent volume	L
V_r	Reactor volume	L
$Y_{x/ph,m}$	Maximal biomass yield on light	g mol_{ph}^{-1}
z	Light path	M
d	Culture depth	M
Abbreviations		
EXP	Experimentally determined	-
LED	Light emitting diode	-
rpm	Rotations per minute	-

5.2 Introduction

Microalgae are a potential resource for the sustainable production of commodities for food and non-food applications [4, 40]. In several studies the economic feasibility and environmental impact of large-scale microalgae production is evaluated [88-90]. Areal productivity, or the related photosynthetic efficiency, is often used as an input for these studies. However, measured values for areal productivity for large scale production are currently not available. Instead, mathematical models can be used to predict the productivity at large-scale [29, 70, 91]. The accuracy of these depends on the accurate experimental determination of model parameters [91, 92]. Temperature and light are key parameters influencing the rate of photosynthesis and therefore the productivity of a photobioreactor [66, 92-94]. In large scale production systems temperatures will be controlled within bandwidth as wide as possible to reduce production costs [6]. Therefore, in models used to predict the productivity at a commercial scale the effect of variations in both light and temperature on the productivity should be considered.

In this study *Nannochloropsis* sp. and *Neochloris oleoabundans* were investigated. For both species no reliable estimations were available for their maximal photosynthetic efficiency (i.e. biomass yield on light) and their maintenance rate, and therefore these were determined. The effect of temperature and light on the specific growth rate of *Nannochloropsis* sp. was reported by Sukenik et al., [95]. For *Neochloris oleoabundans* the effect of both light and temperature on growth has not been reported in a single study. Data available for *Neochloris oleoabundans* were obtained employing different reactor geometries and light sources [11, 96-98]. These different experimental set-ups prevent the determination of required model parameters. The effect of light and temperature on the specific growth rate of *Neochloris oleoabundans* was therefore determined in laboratory experiments. The data were used for a statistical estimation to obtain the parameter values resulting in the best model fit. The microalgal growth model was combined with a simplified light model of a photobioreactor in order to make projections of its productivity under outdoor conditions. Specifically the impact of biomass concentration and temperature control was evaluated.

5.2.1 Model description

The model developed is based on the exponential model first used by Webb and Burley [99] and later successfully employed by Dubinsky and co-workers [100] and Geider and co-workers [101]. The model describes the relation between microalgal specific growth rate μ (unit: d^{-1}) and light intensity PFD , i.e. the photon flux density (unit: $\text{mol}_{\text{ph}} \text{m}^{-2} \text{s}^{-1}$).

$$\mu = (\mu_m + r_m) \cdot \left(1 - e^{-\frac{\alpha \cdot Y_{x/ph,m} \cdot PFD \cdot 3600 \cdot 24}{(\mu_m + r_m)}} \right) - r_m \quad \text{Eq. 1.}$$

Where parameter μ_m represents the maximal specific growth rate (unit d^{-1}); α is the specific absorption coefficient (unit: $\text{m}^2 \text{g}^{-1}$); $Y_{x/ph,m}$ is the maximal biomass yield on light (unit: $\text{g mol}_{\text{ph}}^{-1}$); PFD is the light intensity (unit: $\text{mol}_{\text{ph}} \text{m}^{-2} \text{s}^{-1}$); r_m represents the maintenance rate (unit: d^{-1}). The product of α and PFD within the exponential term is equal to the biomass

specific photon supply rate: q_{ph} (unit: $\text{mol}_{ph} \text{g}^{-1} \text{d}^{-1}$). At sub-saturating light conditions, the model follows a linear relationship between the specific growth rate and the light supply rate.

Taking the limit value of Eq.1 for the *PF*D approaching zero the following relation is derived:

$$\mu = \alpha \cdot Y_{x/ph,m} \cdot PFD - r_m \quad \text{Eq. 2.}$$

Which is equivalent to:
$$\mu = Y_{x/ph,m} \cdot q_{ph} - r_m \quad \text{Eq. 3.}$$

Or:
$$q_{ph} = \frac{\mu}{Y_{x/ph,m}} - r_{ph} \quad \text{with: } r_{ph} = \frac{r_m}{Y_{x/ph,m}} \quad \text{Eq. 4.}$$

The latter relation is comparable to the Pirt relation [102] and is particularly useful for the practical assessment of the maximal yield of biomass on photons ($Y_{x/ph,m}$) and the maintenance requirement for photons (r_{ph}). The maintenance requirement for photons then can be interconverted into a maintenance rate (r_m) by multiplication with the maximal yield of biomass on photons. Equation 4 shows that both parameters can be determined over chemostat experiments under sub-saturating light conditions at different dilution rates (equal to μ) while measuring the specific photon supply rate (q_{ph}). The exact procedure is explained in the materials and methods sections and has been validated in other studies [39, 86, 103].

Cultivation temperature affects enzymatic cellular processes and therefore reduces the maximum growth rate at sub-optimal temperatures. This decrease can be described by correcting the maximal growth rate at optimal temperature ($\mu_{m,opt}$) with a temperature factor (f_t), having a value between 0 and 1.
$$\mu_m = \mu_{m,opt} \cdot f_t \quad \text{Eq. 5}$$

This temperature factor is calculated with the cardinal temperature model developed by Rosso et al., [104].

$$f_T = \frac{(T-T_{max}) \cdot (T-T_{min})^2}{(T_{opt}-T_{min})[(T_{opt}-T_{min})(T-T_{opt}) - (T_{opt}-T_{max})(T_{opt}+T_{min}-2T)]} \quad \text{Eq. 6}$$

With T_{min} (unit: °C) the temperature below which no growth is observed; T_{max} (unit: °C) the temperature above which no growth is observed; and, T_{opt} (unit: °C) the temperature at which the maximal specific growth rate (d^{-1}) is obtained.

5.2.2 Scenario studies

In this study projections to outdoor productivity were made under, different scenarios that can be expected outdoors. More specifically, different regimes for temperature control and daily irradiance, and different values for the specific absorption coefficient were used for simulations (details given in M&M, Figure 5.). The reactor for which simulations were made is horizontal, flat, and has a depth of 0.2 m (for example raceway pond). The microalgal culture is ideally mixed and light is assumed to hit reactor surface perpendicularly and thus not taking into account solar elevation. Reflection of light on the culture surface as well as

light scattering within the culture were neglected. As such, the local light intensity could be calculated with Lambert-Beer law:

$$PFD_{local} = PFD_{in} * e^{-\alpha * C_x * z} \quad \text{Eq. 7}$$

With PFD_{in} incident light intensity (unit: $*10^{-6} \text{ mol}_{ph} \text{ m}^{-2} \text{ s}^{-1}$), α , specific absorption coefficient (unit: $\text{m}^2 \text{ kg}^{-1}$), C_x biomass concentration (unit: g L^{-1}) and z reactor depth (unit: m).

The local specific growth rate (μ_{local} unit: d^{-1}) was then calculated for each position z employing equation 8, with local light intensities calculated via equation 7. The temperature correction factor was included and calculated with equation 5, and equation 6. The assumption was made that the microalgal photosynthetic rate immediately responds to changes in the local light intensity as a result of mixing-induced movement of the microalgae through the light gradient.

$$\mu_{local} = (\mu_{m,opt} \cdot f_t + r_m) \cdot \left(1 - e^{-\frac{-\alpha \cdot Y_{x/ph,m} \cdot 3600 \cdot 24 \cdot PFD_{local}}{(\mu_{m,opt} \cdot f_t + r_m)}} \right) - r_m \quad \text{Eq. 8}$$

The average specific growth rate (μ_{avg} : unit d^{-1}) of the microalgal culture now can be calculated by integrating the local specific growth rate over the culture depth.

$$\mu_{avg} = \int_{z=0}^{z=d} \mu_{local} \cdot dz \quad \text{Eq. 9}$$

Where d (unit m) is the maximal light path, equivalent to the culture depth in case of perpendicular light. The areal productivity (P_{areal} , unit: $\text{g m}^{-2} \text{ d}^{-1}$) was calculated with equation 10:

$$P_{areal} = \mu_{AVG} * C_x * 3600 * 24 * C_x * \frac{V}{A} \quad \text{Eq. 10}$$

The multiplication with 3600 and 24 is done to convert from per second to per day. With $C_x * \frac{V}{A}$ being equal to the ground areal biomass loading in g m^{-2} , a useful parameter for the comparison of outdoor photobioreactors [105].

5.3 Materials and Methods

The work flow in this work is visualized in Figure 5.1. First experiments were carried out to determine the maximal biomass yield on light ($Y_{x/ph,m}$) and the maintenance rate (r_m) for both *Nannochloropsis* sp. and *Neochloris oleoabundans*. In addition, for *Neochloris oleoabundans* also the effect of temperature and light on the specific growth rate was experimentally determined.

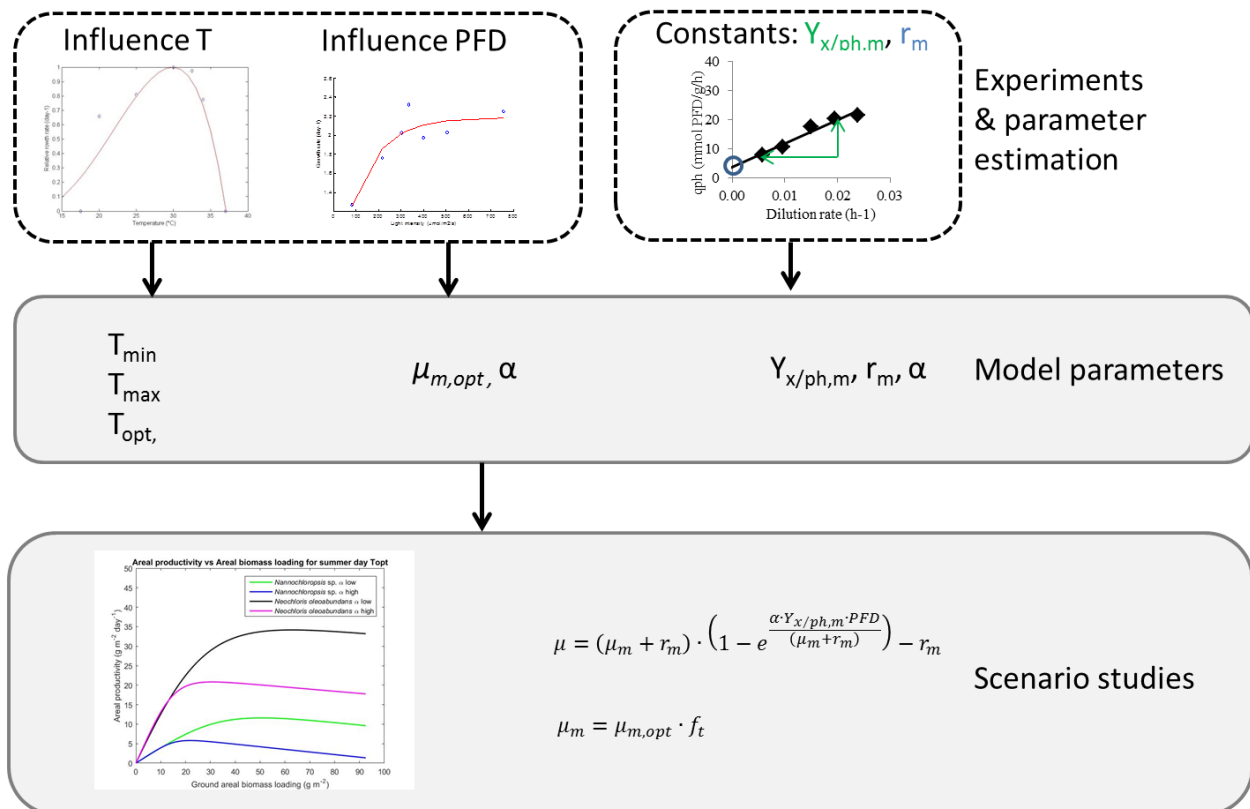


Figure 5.1 workflow followed in this study. Experiments were done to determine the relation between specific growth rate and temperature and light intensity. In addition, experiments were performed under light limiting conditions to determine the relation between specific growth rate and the specific light supply rate. Based on these experimental data all parameters of the microalgal growth model were estimated by statistical regression tools.. Scenario studies were done to evaluate the effect of biomass concentration and temperature control strategy on the predicted productivity for an outdoor photobioreactor. For the scenario studies measured extreme values (low and high) for the specific absorption coefficient (α) were used.

5.3.1 Inoculum production

Neochloris oleoabundans UTEX1185 and *Nannochloropsis* sp. CCAP 211/78 pre-cultures were cultivated in an orbital shaker incubator (Multitron, Infors HT) at 120 rpm, and illuminated with $50 \cdot 10^{-6} \text{ mol}_{ph} \text{ m}^{-2} \text{ s}^{-1}$, at a temperature of 25°C , while the headspace was enriched with 2% CO_2 . *Neochloris oleoabundans* and *Nannochloropsis* sp. were cultivated on natural seawater (Oosterschelde, The Netherlands) enriched with the following nutrients (in mM); Urea, 25; KH_2PO_4 , 1.7; Na_2EDTA , 0.56; $\text{Fe}_2\text{SO}_4 \cdot 7\text{H}_2\text{O}$, 0.11; $\text{MnCl}_2 \cdot 2\text{H}_2\text{O}$, 0.01; $\text{ZnSO}_4 \cdot 7\text{H}_2\text{O}$, $2.3 \cdot 10^{-3}$; $\text{Co}(\text{NO}_3)_2 \cdot 6\text{H}_2\text{O}$, $0.24 \cdot 10^{-3}$; $\text{CuSO}_4 \cdot 5\text{H}_2\text{O}$, $0.1 \cdot 10^{-3}$; $\text{Na}_2\text{MoO}_4 \cdot 2\text{H}_2\text{O}$, $1.1 \cdot 10^{-3}$. HEPES (20mM) and Na_2EDTA (5mM) were added to the seawater; pH was adjusted to 7.5 followed by heat sterilization (20 minutes at 121°C). After autoclaving, the nutrients were added through a sterile filter ($0.20 \mu\text{m}$). For the cultivation of *Nannochloropsis* sp. CCAP 211/78 sodium nitrate was used as nitrogen source in the media, with a final concentration of 25mM.

5.3.2 Labscale photobioreactor (AlgaeMIST)

Labscale flat panel air-lift photobioreactors, as described by Breuer et al., [106] were used for the different experiments. This lab-scale PBR has a working volume of 380 ml and an optical path of 14 mm, continuous illumination (24/24) was used via warm white LED lamps (Bridgelux, BXRA W1200). On-demand CO₂ addition was used to control the pH at 7.5, and an airflow of 800 ml min⁻¹ was used to mix the cultures. All experiments were performed aseptically. The dilution rate was calculated by measuring the weight of the collected effluent daily at 11:00. Both the effluent and the growth medium vessel were stored in the dark and at 4 °C. The growth medium vessel was sterilized, and was periodically refilled with fresh media through a 0.20 µm sterile filter.

Chemostat experiments; determination maximal biomass yield on light and maintenance rate. The maintenance rate (r_m) and maximal biomass yield on light ($Y_{x/ph,m}$) were determined in a series of chemostat experiments under light limited conditions as discussed in the theory section for *Neochloris oleoabundans* and *Nannochloropsis* sp. To achieve light limited conditions an incident light intensity of $100 * 10^{-6} \text{ mol}_{ph} \text{ m}^{-2} \text{ s}^{-1}$ [39] was used. The set dilution rates for the chemostat experiments were lower than the specific growth rates reported in literature. This was done to obtain dense cultures and light limited conditions [39]. Nutrients were present in excess and the estimated optimal temperatures for growth were used: 30 °C for *Neochloris oleoabundans* [98] and 25 °C for *Nannochloropsis* sp. [95]. Applied experimental conditions are given in Table 5.. During chemostat operation the specific growth rate (μ) is equal to the dilution rate. The calculation of the specific photon supply rate (q_{ph}) is covered later in equation 14. For the chemostat experiments steady state was defined as stable operation for 9 days or more with a maximal deviation of 15% in dilution rate, optical densities, and outgoing light intensity. Average values and standard deviations for different parameters were calculated.

Table 5.1 Experimental settings used for determination of the maximal biomass yield on light and the maintenance rate for *Nannochloropsis* sp. and *Neochloris oleoabundans*.

<i>Microalgal species</i>	<i>Nannochloropsis</i> sp.	<i>Neochloris oleoabundans</i>
Applied dilution rates (d ⁻¹)	0.1, 0.2, 0.4, 0.5 & 0.6	0.4, 0.5, 0.6, 0.7, 0.8, 0.9 & 1.2
Incident light intensity (* 10 ⁻⁶ mol _{ph} m ⁻² s ⁻¹)	100	100
Temperature (°C)	25	30

Turbidostat experiments; effect of temperature and light on growth of Neochloris oleoabundans

Turbidostat experiments were done to determine the effect of light and temperature on the specific growth rate of *Neochloris oleoabundans*. Table 5. shows the used experimental conditions. To achieve the same biomass concentration throughout the turbidostat experiments, the ratio between incident and outgoing light intensity was maintained at 33% (for more details on the used light settings see supplementary data, appendix 5.A). For turbidostat operation steady state was defined as stable operation for at least 10 reactor

volumes or more and the specific growth rate was calculated in the same way as for chemostat operation.

Table 5.2 Experimental conditions to determine the specific growth rate of *Neochloris oleoabundans* under the influence of light and temperature.

	<i>Temperature</i>			<i>Incident light intensity</i>
$PFD_{in} (* 10^{-6} mol_{ph} m^{-2} s^{-1})$	100	200	300	100, 200, 300, 400, 500, 750
<i>Temperature (°C)</i>	17.5		17.5	30
	20	20	20	
	25	25	25	
	30	30	30	
	32.5		32.5	
	34		34	
	37		37	

5.3.3 Sample analysis

For the daily offline measurements of optical density (680nm and 750nm, Hach Lange DR5000), pH (Mettler Toledo education line) a sample was directly taken from the lab-scale photobioreactors at 11:00 a.m.. At the same time the effluent bottles were replaced by an empty pre-weighed bottle for the calculation of the dilution rate. After reaching stable optical densities (750 and 680 nm) and dilution rates for 5 days, we assumed steady state had been reached. Until a steady state was maintained for 10 reactor volumes (turbidostat) or 9 days (chemostat) dry weight determinations and absorption coefficient measurements were done as described by [107].

5.3.4 Definitions and calculations

The specific growth rate (dilution rate for chemostat) during turbidostat experiments were calculated according to equation 11.

$$\mu = D = \frac{V_h}{V_r * \rho} \tag{Eq. 11}$$

With μ as specific growth rate (unit: d^{-1}), D as dilution rate (unit: d^{-1}), V_h the effluent weight (unit: g), V_r the reactor volume (0.38 L), and ρ the density of the culture here equal to seawater (1030 g L^{-1}).

The absorbed light intensity (PFD_{abs}) was calculated according to equation 12.

$$PFD_{abs} = (PFD_{in} - PFD_{out}) \tag{Eq. 12}$$

With incident light intensity (PFD_{in}) and outgoing light intensity (PFD_{out}), the unit for both is: $mol_{ph} m^{-2} s^{-1}$. The outgoing light intensity is the average value calculated over 27 equally distributed measurement points over the backside of the reactor.

The average light intensity (PFD_{avg}) was calculated according to equation 13.

$$PFD_{avg} = \frac{PFD_{abs}}{LN(PFD_{in}/PFD_{out})} \tag{Eq. 13}$$

The specific photon supply rate q_{ph} (unit: $\text{mol}_{ph} \text{g}^{-1} \text{s}^{-1}$) required for the determination of the biomass yield on light and the maintenance rate was calculated using a light balance over the whole reactor volume:

$$q_{ph} = \frac{PFD_{abs} * 3600 * A_R}{C_x * V_R} \quad \text{Eq. 14}$$

With PFD_{abs} absorbed photons (unit: $\text{mol}_{ph} \text{m}^{-2} \text{s}^{-1}$), 3600 for the conversion of per second to per hour, A_R specific reactor area (0.0285 m^2), C_x , biomass concentration (unit: g L^{-1}) and V_r , reactor volume (0.38 L^{-1}).

5.3.5 Statistical parameter estimation

Additional model parameters of the biological growth model were estimated using a statistical parameter estimation. For this we used a non-linear regression. The MATLAB function *nlinfit* was applied for this purpose. Additionally the 95% confidence intervals were calculated to indicate the validity of the estimation. For both species the parameter estimation was applied in order to obtain model parameter values resulting in the best model fit. This was done separately for the temperature parameters T_{opt} , T_{min} , and T_{max} using equation 6, and for the maximal specific growth rate μ_m using equations 1 (at T_{opt}) and 7.

Seven data points for different temperature conditions at two incident light intensities were used for the estimation of parameter values for the temperature model for *Neochloris oleoabundans* (100 and $300 * 10^{-6} \text{ mol}_{ph} \text{m}^{-2} \text{s}^{-1}$). The experimental settings are given in Table 5.2 experimental data was reported in Figure and Appendix 5.B. For the parameter estimation of the maximal growth rate at optimal temperature ($\mu_{m,opt}$) of *Neochloris oleoabundans* eight experimental data points collected at different light intensities were used (all at 30°C). During the parameter estimation the following values were fixed for the remaining model parameters: for r_m ; 0.067 d^{-1} , QY; $1.78 \text{ g mol}_{ph}^{-1}$, C_x ; 0.82 g L^{-1} and α ; $76 \text{ m}^2 \text{ kg}^{-1}$. The data are given in Appendix 5.D table 5.D1.

For *Nannochloropsis* sp. the data set reported by Sukenik [95] was used, which contained 7 data points at different light intensities (50 to $600 * 10^{-6} \text{ mol}_{ph} \text{m}^{-2} \text{s}^{-1}$) at a temperature of 25°C . The effect of temperature on the specific growth rate *Nannochloropsis* sp. was also determined by Sukenik at 5 temperatures; 10 , 18 , 25 , 32 and 38°C . No growth for *Nannochloropsis* sp. was reported for 10 and 38°C . The data are given in Appendix 5.D table 5.D.2. The following values were fixed for the remaining model parameters; r_m ; 0.055 d^{-1} , QY; $1.23 \text{ g mol}_{ph}^{-1}$, C_x ; 0.1 g L^{-1} and α ; $132 \text{ m}^2/\text{kg}$.

5.3.6 Scenario studies

In the scenario studies the estimated parameter values were used in the growth model which was combined with a light model (see theory). In the scenario studies two regimes for temperature control were used; a narrow bandwidth ($T_{min} 24^\circ \text{C}$ and $T_{max} 28^\circ \text{C}$) and a broad bandwidth ($T_{min} 20^\circ \text{C}$ and $T_{max} 35^\circ \text{C}$) (Figure 5.). For ease of simulation the temperature evolution over the day was described with a sine function. For the irradiance two scenarios were used; a typical spring day (PFD max; $1060 * 10^{-6} \text{ mol}_{ph} \text{m}^{-2} \text{s}^{-1}$, day length 12 hrs, PFD total $\pm 30 \text{ mol}_{ph} \text{m}^{-2} \text{d}^{-1}$), and a typical summer day (PFD max $1500 * 10^{-6} \text{ mol}_{ph} \text{m}^{-2} \text{s}^{-1}$, day

length 16 hrs, PFD total $\pm 52 \text{ mol}_{ph} \text{ m}^{-2} \text{ d}^{-1}$). The irradiance on a horizontal plane was modelled with a sine curve (Figure 5.). For the specific absorption coefficients minimum and maximum values were used, which were measured in this work, or reported in literature by the same authors [105].

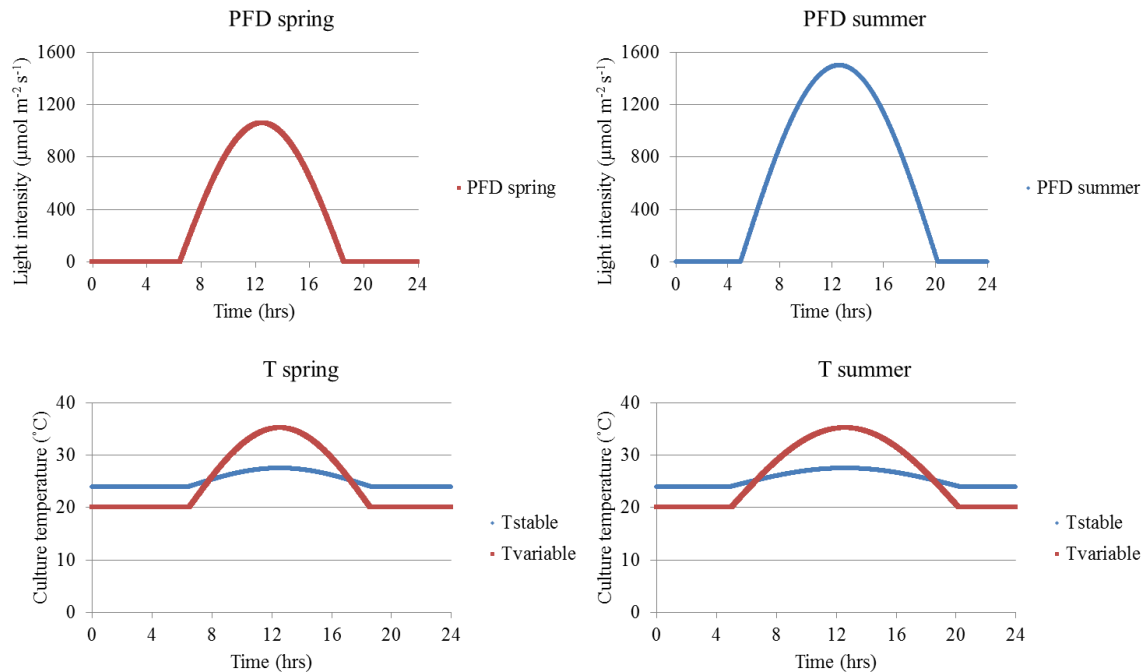


Figure 5.2 Overview of the different irradiance and temperature scenarios used for predicting the areal productivity of an outdoor photobioreactor. The scenarios studied were: A spring day, 12 hour day length and a light intensity of $1060 * 10^{-6} \text{ mol}_{ph} \text{ m}^{-2} \text{ s}^{-1}$ at solar noon; a summer day, 15 hour day length and a light intensity of $1500 * 10^{-6} \text{ mol}_{ph} \text{ m}^{-2} \text{ s}^{-1}$ at solar noon. T_{stable} refers to a daily temperature fluctuation from 24-28°C, while $T_{variable}$ refers to a daily temperature fluctuation from 20-35°C.

5.4 Results and discussion

5.4.1 Determination of biomass yield and maintenance requirement

Chemostat experiments under light limited conditions were done to determine the biomass yield on light and the maintenance rate of *Neochloris oleoabundans* and *Nannochloropsis* sp.. The specific photon supply rate (q_{ph}) is plotted in Figure 5.3 as a function of the measured specific growth rate (μ). A linear relation is observed as expected (See equation 2). This linear trend confirms that the microalgae were growing under light limited conditions. The inverse of the slope of this trend line represents the maximal biomass yield on light ($Y_{x/ph,m}$).

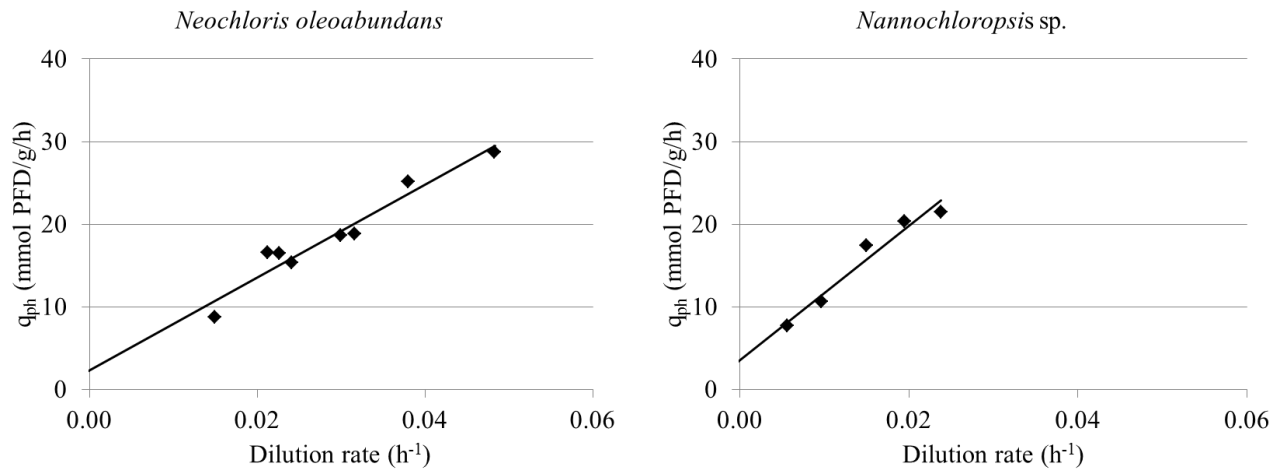


Figure 5.3 Determination of the maximal biomass yield on light and the maintenance requirement for light. The specific light supply rate (q_{ph}) vs the specific growth rate (μ) for *Neochloris oleoabundans* ($q_{ph} = 561.8 \mu + 2.31$, with $R^2 0.94$) and *Nannochloropsis* sp. ($q_{ph} = 812.58 \mu + 3.53$, with $R^2 0.96$).

For *Neochloris oleoabundans* a maximal biomass yield of 1.78 g of biomass per mol of photons was found, and for *Nannochloropsis* sp. a maximal biomass yield of 1.23 g of biomass per mol of photons was obtained. Our values are in line with Janssen et al., [7] who estimated minimal and maximal values of 1.20-2.10 g mol_{ph}⁻¹ for the theoretical maximal biomass yield of a microalgal species [108]. In the current study the biomass yield on light obtained for *Neochloris oleoabundans* was considerably higher than that observed for *Nannochloropsis* sp.. This could be explained by the used nitrogen source because *Nannochloropsis* sp. was grown on nitrate and *Neochloris oleoabundans* was grown on urea. Our values are in line with the value reported by Kliphuis et al [39]. Furthermore, it cannot be excluded that *Nannochloropsis* sp. simply dissipates more of the absorbed light energy, or uses the metabolic energy generated (NADPH and ATP) less efficiently.

The offset of the trend line in Figure , represents the maintenance requirement for light (r_{ph}). The maintenance requirement was re-calculated to a maintenance rate (r_m) according to equation 3. As such, a maintenance rate of 0.055 d⁻¹ was calculated for *Neochloris oleoabundans* and 0.067 d⁻¹ for *Nannochloropsis* sp.. The maintenance rate for *Nannochloropsis* sp. is a bit higher than for *Neochloris oleoabundans*. However, this difference is small and is within the uncertainty of these values. The maintenance requirement for light determined in this study are in line with values reported in literature [39].

5.4.2 The effect of temperature and light on the growth rate of *Neochloris oleoabundans*

The effect of temperature on the specific growth rate of *Neochloris oleoabundans* was studied in turbidostat experiments at three light intensities (Figure). The measured specific growth rates are shown in Figure . Growth rates increase with increasing light intensities, as expected. The highest specific growth rate (2.32 d⁻¹ ± 0.10) was found at an incident light intensity of 300 * 10⁻⁶ mol_{ph} m² s⁻¹ at a temperature of 30°C. At 20 and 25 °C no significant difference was observed in the growth rates for the three light intensities studied. Temperatures higher

than 30°C resulted in a decrease in growth rate in comparison to the maximal specific growth rate observed at 30°C. The obtained results are in line with the findings of other authors [11, 96-98]. In this study no growth was obtained at 17.5 and 37°C. A reduction in enzyme activity for enzymes that play a role in cellular processes explains the obtained lower growth rates for temperatures deviating from the optimal temperature [109].

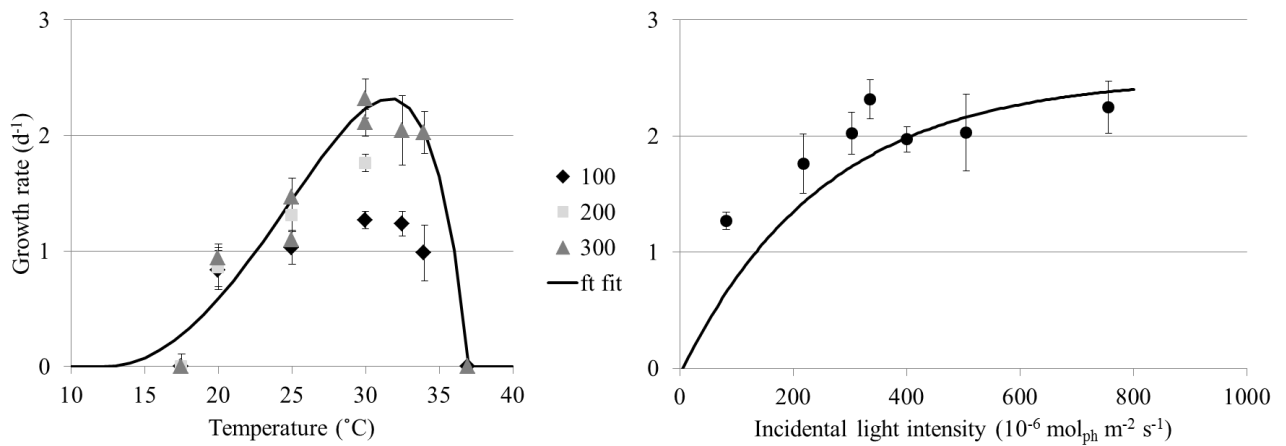


Figure 5.4 The effect of temperature (left) and average light (right) on the specific growth rate of *Neochloris oleoabundans*. For the effect of temperature three incident light intensities ($\times 10^{-6} \text{ mol}_{\text{ph}} \text{ m}^{-2} \text{ s}^{-1}$) were used, for the effect of the average light intensities a temperature of 30°C was used. Error bars indicate standard deviation over steady state period.

Additional experiments were done to determine whether incidental light intensities above $300 \times 10^{-6} \text{ mol}_{\text{ph}} \text{ m}^{-2} \text{ s}^{-1}$ resulted in higher specific growth rates for *Neochloris oleoabundans* (Figure). For these experiments different turbidostat experiments were carried out at the following incident light intensities; 400, 500 and $750 \times 10^{-6} \text{ mol}_{\text{ph}} \text{ m}^{-2} \text{ s}^{-1}$ (Appendix 5.B). Higher light intensities did not result in higher specific growth rates (Figure 5.B.2). The observations made in this work are in line with values reported in literature [97]. For *Neochloris oleoabundans* photosynthesis becomes saturated at an incident light intensity of $300 \times 10^{-6} \text{ mol}_{\text{ph}} \text{ m}^{-2} \text{ s}^{-1}$.

5.4.3 Determination maximal specific growth rate and temperature parameters

The remaining parameters of the growth model were estimated using non-linear regression. This estimation is based on the relation between the specific growth rate, temperature and light intensity. For *Neochloris oleoabundans* the required experimental data were determined in this study and these are reported in Figure 5.4. For *Nannochloropsis* sp. the effect of light and temperature on the specific growth rate was already reported by Sukenik et al. [95], and those data were used as detailed in the materials and methods. A representation of the model fit during parameter estimation is given in Figure 5.5.

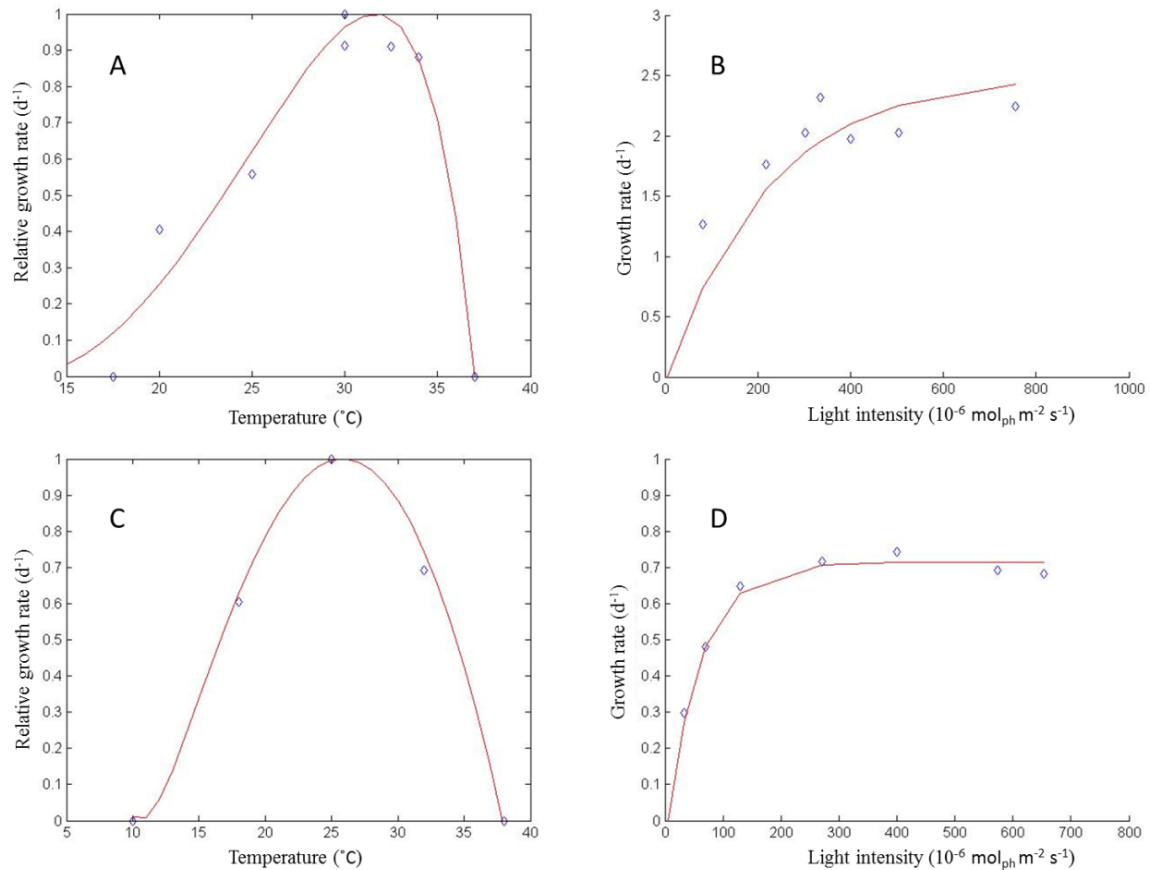


Figure 5.5 Model fit of temperature model (left) and growth model (right). A (high light $300 \cdot 10^{-6} \text{ mol}_{\text{ph}} \text{ m}^{-2} \text{ s}^{-1}$) & B for *Neochloris oleoabundans* and C & D for *Nannochloropsis* sp..

For *Neochloris oleoabundans* the temperature model does not fit the measured data very well at lower temperatures (Figure .A). for the higher temperatures ($> 25^{\circ}\text{C}$) the predicted values align better with the measured values. The cardinal temperature model is not able to accurately describe the steep decline of the specific growth rate of *Neochloris oleoabundans* below 20°C . The estimated parameter values (Table 3.3) for the minimal temperatures for growth is relatively low especially for *Neochloris oleoabundans* (12.4°C), while in the experimental work no data could be obtained for in experiments carried out at 17.5°C . For *Nannochloropsis* sp. the model describes the influence of temperature on the growth rate better (Figure C). For *Nannochloropsis* sp. the minimal temperature for growth is also close to the value of 10°C , which was reported by [95]. The model parameter values estimated for the optimal temperature for both species are close to the experimental observations. Also, the maximum temperature estimated for both species are close to the experimentally obtained values: 37°C for *Neochloris oleoabundans* and 38°C for *Nannochloropsis* sp..

The growth model predicts the growth rate under the influence of light for *Nannochloropsis* sp. more accurate in comparison with *Neochloris oleoabundans*. For *Neochloris oleoabundans* predicted growth rates appear to increase beyond the highest specific growth rate measured. For the maximal growth rate, the estimated value for *Neochloris oleoabundans* is higher than the experimentally determined value of 2.32 d^{-1} . For *Nannochloropsis* sp. the

estimated maximal growth rate is similar to the value of 0.71 d^{-1} reported in literature [95]. The underestimation of the growth at lower light intensities and underestimation of the growth by the model could be the result of not considering photoacclimation in this model. In our experiments photoacclimation was observed especially at light intensities below $50 * 10^{-6} \text{ mol}_{\text{ph}} \text{ m}^{-2} \text{ s}^{-1}$ (Appendix 5.B figure 5.B.1). The effect of the light intensity on the absorption coefficient, or photo acclimation, is not taken in to account in the currently used model. Photoacclimation will result in increased light absorption and thus growth under light limiting conditions [110]. If more data points would have been obtained in the higher light range a better prediction could have been obtained. The estimated parameter values and their confidence intervals are given in Table 3.3.

Table 3.3 Estimated values for the maximal specific growth rate and the temperature parameters obtained via nonlinear regression for each microalgae species

<i>Microalgae</i>	<i>Neochloris oleoabundans</i>	<i>Nannochloropsis sp.</i>	<i>Units</i>
$\mu_{\text{m,opt}}$	2.51 ± 0.48	0.71 ± 0.03	d^{-1}
T_{min}	12.37 ± 6.4	10.53 ± 3.5	$^{\circ}\text{C}$
T_{opt}	31.62 ± 2.0	25.84 ± 1.7	$^{\circ}\text{C}$
T_{max}	36.99 ± 0.5	37.89 ± 1.0	$^{\circ}\text{C}$

5.4.4 Projections to outdoor productivity

The estimated parameter values were used in scenario studies to predict the productivity for an open raceway pond under the influence of light and temperature. The effect of using different scenarios for the daily variation in temperature and light on the predicted productivity is visualized in Figure . For all scenarios, predicted areal productivity increases for lower ground areal biomass loading until a plateau is reached followed by a more gradual decrease observed for higher ground areal biomass loadings. This decrease starts later for both species when low specific absorption coefficients are used. Higher values for the absorption coefficient result in a stronger light gradient and a more rapid onset of a dark zone where maintenance leads to biomass loss. During the outdoor cultivation of *Nannochloropsis* sp. in various pilot-scale photobioreactors a broad optimum for biomass concentrations was obtained [105] Predicted areal productivities for a higher specific absorption coefficients increase steeper compared to the values predicted for the lower specific absorption coefficient. In all scenarios higher productivities are predicted using a lower specific absorption coefficient. This is the result of a better distribution of the light throughout the culture, as a result of the smaller antenna size [111].

For both species more stable culture temperatures (narrow bandwidth temperature control) resulted in the prediction of higher productivities. The narrow bandwidth range of temperatures can be found for systems where the reactor volume is large in relation to the sunlight exposed reactor area. Examples of such systems are raceway ponds, or photobioreactors where a large water buffer is included (ProviAPT system, or Solix biofuels system) [9, 15, 66]. An example of a system having a broader range of temperatures during the day are tubular systems, either horizontal or vertical, as previously discussed by De Vree et al., [66]. The highest productivities are predicted for the scenario simulating a summer day in the Netherlands.

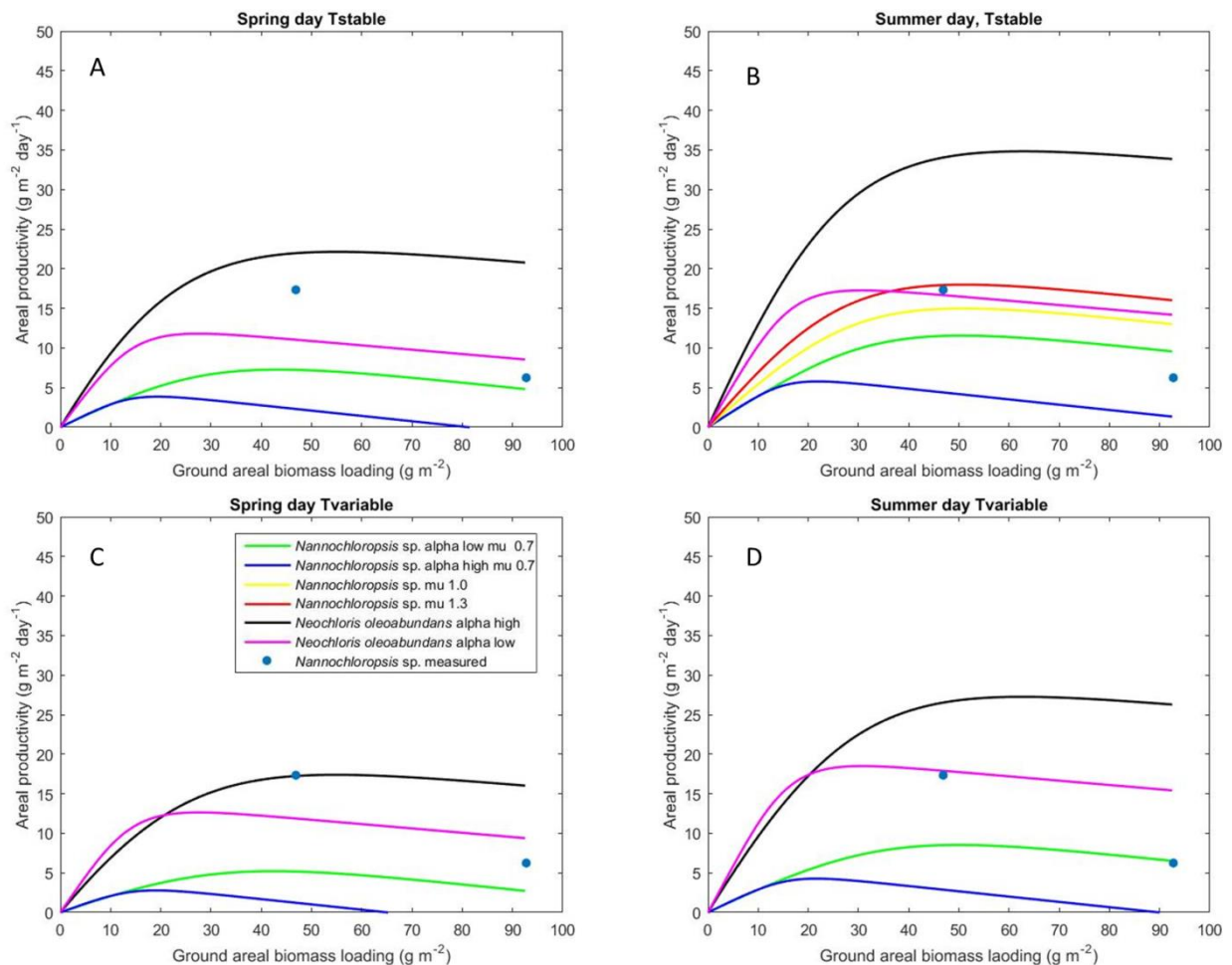


Figure 5.6 Predicted areal productivity versus ground areal biomass loading for the different scenarios. For each scenario low and high values were used for the absorption coefficient for each microalgae species: 77 and $170 \text{ m}^2 \text{ kg}^{-1}$ for *Neochloris oleoabundans* and 70 and $224 \text{ m}^2 \text{ kg}^{-1}$ for *Nannochloropsis* sp.. The spring day refers to a shorter day length with a lower maximal solar noon (12 hours, $1060 * 10^{-6} \text{ mol}_{\text{ph}} \text{ m}^{-2} \text{ s}^{-1}$). The summer day refers to a longer day length and higher maximal solar noon (15 hours, $1500 * 10^{-6} \text{ mol}_{\text{ph}} \text{ m}^{-2} \text{ s}^{-1}$). Tstable refers to a temperature fluctuating from 24 °C to 28 °C following a sine, while Tvariable refers to a daily temperature fluctuation from 20 °C to 35 °C following a sine. For the summer day with stable temperatures, the effect of different maximal specific growth rates ($\mu_{m,opt}$) on the prediction was studied for *Nannochloropsis* sp. (B). Blue circles indicate values obtained in open raceway pond at AlgaePARC with *Nannochloropsis* sp. [105].

Higher productivities are predicted for both species when a more stable temperature range is used; 20% for *Neochloris oleoabundans* and 30% for *Nannochloropsis* sp.. Higher predicted areal productivities for *Neochloris oleoabundans* are a result of the higher maximal growth rate and higher maximal biomass yield on light in comparison to *Nannochloropsis* sp.. The specific maximal growth rate of a strain influences the maximal areal productivity that can be expected under outdoor conditions.

The predicted areal productivity for *Nannochloropsis* sp. is low in comparison to the value of $17.3 \text{ g m}^{-2} \text{ d}^{-1}$ which was measured for an open raceway pond operated with *Nannochloropsis* sp. CCAP 211/78. (Figure A-D). The highest predicted areal productivity of $12 \text{ g m}^{-2} \text{ d}^{-1}$ was predicted for a summer day with a stable temperature regime. A possible explanation could come from the fact that the maximum specific growth rate was obtained for a different species of *Nannochloropsis* sp. than the one used in this previous study. Sukenik [95] used an unspecified species of *Nannochloropsis* sp. obtained from an aquaculture company, while in the current work *Nannochloropsis* sp. CCAP211/78 was used. The latter could very well be a different species with different characteristics. Literature suggests a maximal specific growth rate of 1.0 d^{-1} for the species used in this study [112]. In another study done by the authors a daily averaged net growth rate of 0.8 d^{-1} was obtained during the cultivation of *Nannochloropsis* sp. CCAP 211/78 in an outdoor vertical tubular photobioreactor [105]. This net average growth rate was determined over 13 days with an average day length of 15.5 hours. We corrected the growth rate of 0.8 d^{-1} to a 24 hour day and with the maintenance rate resulted in a maximal specific growth rate of 1.3 d^{-1} . The effect of the three discussed growth rates; 0.71 , 1.0 and 1.3 d^{-1} was studied in the model simulations. Simulations done with a maximal specific growth rate of 1.3 d^{-1} are in accordance with highest measured areal productivity compared to the predictions for the lower growth rates.

5.5 Conclusions

In this study we determined the specific growth rate of *Neochloris oleoabundans* under the influence of light and temperature. We found a maximal growth rate for *Neochloris oleoabundans* of 2.32 d^{-1} at a temperature of 30°C and an average light intensity of $180 * 10^{-6} \text{ mol}_{\text{ph}} \text{ m}^{-2} \text{ s}^{-1}$. Furthermore, we determined the maximum biomass yield on light and maintenance requirement for *Neochloris oleoabundans* ($1.68 \text{ g mol}_{\text{ph}}^{-1}$ and of 0.055 d^{-1}) and *Nannochloropsis* sp. ($1.23 \text{ g mol}_{\text{ph}}^{-1}$ and 0.067 d^{-1}). The resulting set of parameter values allowed predicting the areal productivity for both species with a model, while simulating conditions that can be expected during mass cultivation. Further, a more stable culture temperature regime ($24\text{-}28^\circ\text{C}$) resulted in the prediction 20-30% higher areal productivities compared to more variable culture temperatures ($20\text{-}35^\circ\text{C}$). The highest prediction for areal productivity was obtained when a low value for the specific absorption coefficient was used. The specific maximal growth rate and specific absorption coefficient have a large effect on the predicted areal productivity

Acknowledgements

The authors would like to thank the Dutch Ministry of Economic Affairs, Agriculture and Innovation, the Province of Gelderland and Biosolar Cells, BASF, BioOils, Drie Wilgen Development, DSM, Exxon Mobil, GEA Westfalia Separator, Heliae, Neste, Nijhuis, Paques,

Cellulac, Proviron, Roquette, SABIC, Simris Alg, Staatsolie Suriname, Synthetic Genomics, TOTAL and Unilever for the financial support of the AlgaePARC research program. In addition, the authors would like to thanks the people who contributed to the practical work for this publication; Mark van den Braak, Gerard 't Lam, Erik Bolder, Nick Kosterink and Lisanne van Dam.

Appendix 5.A Ratios set between PFD_{in} , PFD_{out} and expected PFD_{avg}

The selected ratio between the ingoing light intensity and outgoing light intensity resulted in a biomass concentration of approximately 1 g L^{-1} .

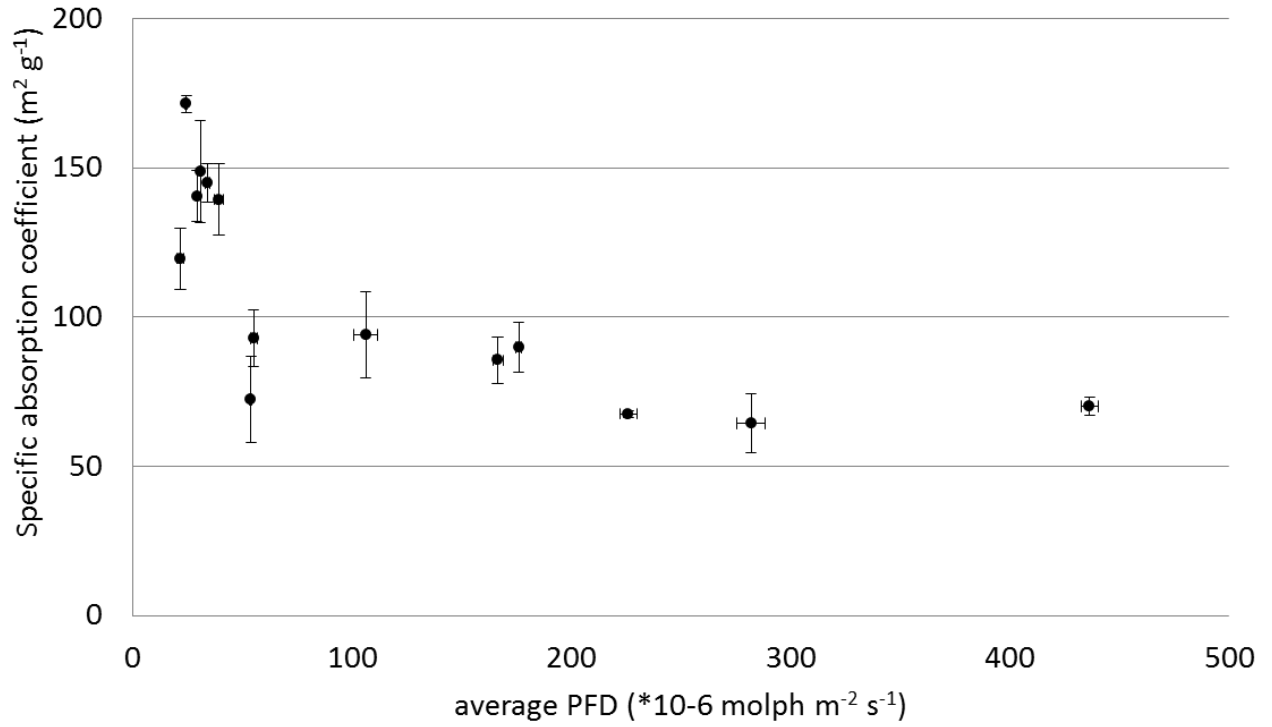
Table 5.A.1: Overview of set incident & outgoing and corresponding calculated average light intensities used to study the effect of light on the growth rate of Neochloris oleoabundans.

Incident PFD	Outgoing PFD	Average PFD
<i>(*$10^{-6} \text{ mol}_{ph} \text{ m}^{-2} \text{ s}^{-1}$)</i>		
<i>100</i>	<i>30</i>	<i>60</i>
<i>200</i>	<i>60</i>	<i>120</i>
<i>300</i>	<i>90</i>	<i>180</i>
<i>400</i>	<i>120</i>	<i>240</i>
<i>500</i>	<i>150</i>	<i>300</i>
<i>750</i>	<i>220</i>	<i>480</i>

Appendix 5.B Effect of PFD_{avg} on specific absorption coefficient and growth rate for *Neochloris oleoabundans*

An overview of the values obtained for the specific absorption coefficient at different average light intensities for *Neochloris oleoabundans*.

Figure 5.B.1 effect of average PFD on the specific absorption coefficient for *Neochloris oleoabundans*.



Appendix 5.C Model fit during parameter estimation of temperature model

Overview of the experimental data used for the parameter estimation for the temperature model for *Neochloris oleoabundans* for high and low light intensity and for *Nannochloropsis* sp. for an intermediate light intensity.

Table 5.C.1 experimental data used for parameter estimation of T_{opt} , T_{min} and T_{max} for *Neochloris oleoabundans* for high light intensity.

PFD_{in} (* 10^{-6} mol _{ph} m ⁻² s ⁻¹)	Growth rate (day ⁻¹)	Rel growth rate (day ⁻¹)	α (m ² /kg)	Temperature (°C)
244.66	0	0	0	17.5
296.31	0.94	1.11	46.38	20
244.66	2.11	0.36	77.63	32.50
244.66	2.04	0.36	77.63	34
244.66	0	0	0	37
296.31	1.47	1.03	47.69	25
309.24	1.31	1.34	57.73	25
311.67	1.10	0.69	60.79	25
335.21	2.32	0.81	77.63	30

Figure 5.C.2 Model fit for parameter estimation of cardinal temperature model for *Neochloris oleoabundans*, for low incident PFD ($100 * 10^{-6}$ mol_{ph} m⁻² s⁻¹)

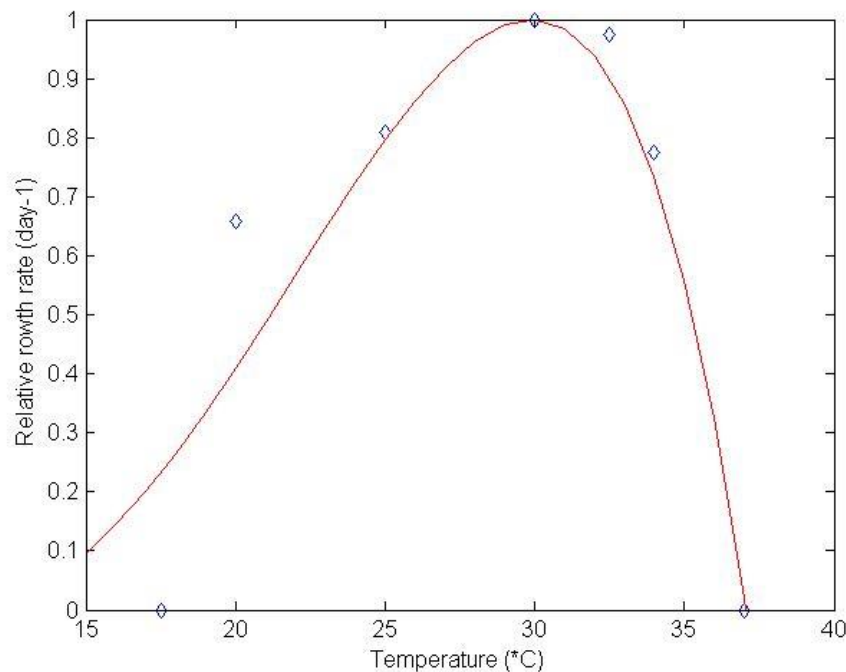


Table 5.C.2 Experimental data used for the parameter estimation of T_{opt} , T_{min} , T_{max} at low light intensity for *Neochloris oleoabundans*.

PFD_{in} ($\cdot 10^{-6} \text{ mol}_{ph} \text{ m}^{-2} \text{ s}^{-1}$)	Growth rate (day^{-1})	Relative growth rate (day^{-1})	α (m^2/kg)	Temperature ($^{\circ}\text{C}$)
77.80	0	0	0	17.5
77.80	0.84	0.94	58.54	20
131.46	1.03	0.76	54.42	25
81.65	1.27	0.64	82.48	30
81.65	1.24	0.32	82.48	32.50
81.65	0.98	0.32	82.48	34
81.65	0	0	0	37

Table 5.C.3 Experimental input values used for parameter estimation for T_{opt} , T_{min} , T_{max} for *Nannochloropsis* sp. at $150 \cdot 10^{-6} \text{ mol}_{ph} \text{ m}^{-2} \text{ s}^{-1}$.

PFD_{in} ($\cdot 10^{-6} \text{ mol}_{ph} \text{ m}^{-2} \text{ s}^{-1}$)	Growth rate (day^{-1})	Relative growth rate (day^{-1})	Temperature ($^{\circ}\text{C}$)
150	0	0	10
150	0.49	0.60	18
150	0.81	1.00	25
150	0.56	0.69	32
150	0	0	38

Appendix 5.D Model fit during parameter estimation of maximal specific growth rate.

Overview of the experimental data use for the parameter estimation for the growth model for *Neochloris oleoabundans* and *Nannochloropsis* sp..

Table 5.D.1 used experimental data for parameter estimation using equation 1 for *Neochloris oleoabundans*; while using a fixed value for r_m (0.067) and QY (1.78) Cx 0.82 L^{-1} . α 76 m^2/kg .

PFD_{in} ($*10^{-6}$ mol_{ph} m^{-2} s^{-1})	Growth rate (d^{-1})	Relative growth rate (d^{-1})
0	-0.055	-0.023
81.65	1.27	0.55
217.23	1.76	0.76
302.60	2.02	0.87
302.60	2.02	0.87
335.21	2.32	0.81
400.23	1.97	0.85
504.74	2.03	0.87
755.60	2.25	0.97

Table 5.D.2 Experimental data used for *Nannochloropsis* sp.; while using a fixed value for r_m (0.055) and QY (1.23) Cx 0.1 $g L^{-1}$. α 132 m^2/kg . Data is from [95].

PFD_{in} ($*10^{-6}$ mol_{ph} m^{-2} s^{-1})	Growth rate (d^{-1})	Relative growth rate (d^{-1})
0	-0.067	-0.082
32.43	0.30	0.37
70.27	0.48	0.59
129.72	0.65	0.80
270.25	0.72	0.88
399.97	0.74	0.91
572.93	0.69	0.85
654.01	0.68	0.84

Chapter 6

Towards industrial products from microalgae

An adapted version of this chapter has been published as:

J. Ruiz, G. Olivieri, **J. H. de Vree***, R Bosma, P. Willems J. H. Reith, M.H.M. Eppink, D.M.M. Kleinegris, R.H. Wijffels, M.J. Barbosa, *Towards industrial products from microalgae*. Energy and Environmental Science, 2016, DOI: 10.1039/c6ee01493c.

*J.H. de Vree, was responsible for the input data in the model and was involved in the decision making process and the writing of the manuscript

6.1 Abstract:

Microalgae show an enormous potential as sustainable feedstock for numerous bioproducts. The current work analyses the feasibility the commercial production of microalgae. We perform a techno-economic evaluation of a process chain on the cultivation for a 100 hectares facility in six locations. Our projections show a current cost per unit of dry biomass of $3.4 \text{ €} \cdot \text{kg}^{-1}$ for microalgae cultivation in Spain, with an expected reduction to $0.5 \text{ €} \cdot \text{kg}^{-1}$ in ten years. A sensitivity analysis reveals the roadmap to achieve this.

6.2 Introduction

Microalgae are considered a promising sustainable feedstock for food and feed products, materials, chemicals, fuels and various high-value products [113, 114]. Algae do not require arable land or freshwater supply and can be harvested nearly all-year-round [115], which makes them attractive for commercial exploitation. Thus microalgae can be an alternative to current unsustainable overexploitation of natural resources, with options to become a solution to the environmental dilemma of food and energy. However, the reality is not so categorical and in practice there are some hurdles limiting their expansion and establishment. Commercialization of different functional components requires selective biorefining of biomass with a cascade approach that still remains a challenge [116]. Besides, technology readiness on cultivation and development of commercialization have been debated recently [4]. Currently, microalgae production aims for niche markets with almost absent competition, which results in inflated product prices. Once the industry expands, competition will force prices to adjust to markets and strategies to adapt accordingly.

Limited knowledge about costs on microalgal cultivation and processing at commercial scale is available, particularly concerning closed photobioreactors. Model-based simulations, combined with pilot-plant production data, can fill this gap. This study revisits economics, and thereby feasibility, by combining techno-economic models for microalgae production. The projections include six locations (The Netherlands, Canary Islands, Turkey, Curaçao, Saudi Arabia and south of Spain), but discussion is focused on south of Spain, an attractive location within Europe.

6.3 Methods

A techno-economic model was developed for biomass production processing. The model is based on available empirical information and literature, allowing to project scenarios from different assumptions and to perform sensitivity analysis on the processes. Projections are done for a 1 hectare and 100 hectares production scales in different cultivation systems. It should be noted that the assumptions used in the models involve an inherent uncertainty, like scalability of the results or extrapolation to different locations.

6.3.1 Locations and climatology:

Six different locations are included in this study: The Netherlands ($52^{\circ}17' \text{ N } 4^{\circ}46' \text{ E}$), Canary Islands ($27^{\circ}55' \text{ N } 15^{\circ}22' \text{ W}$), South of Spain ($37^{\circ}15' \text{ N } 6^{\circ}56' \text{ W}$), Turkey ($38^{\circ}30' \text{ N } 27^{\circ}01' \text{ E}$), Saudi Arabia ($24^{\circ}42' \text{ N } 46^{\circ}47' \text{ E}$) and Curaçao ($12^{\circ}7' \text{ N } 68^{\circ}56' \text{ W}$). Parameters that change

with location are included in this study; i.e. climatic conditions, energy cost, cost of labour, employer's contribution to labour costs and standard workweek hours (Table 6.1). In case of Curaçao climatic data from the Coast of Venezuela (10°36′ N 66°58′ W; ~200 km away) was used.

6.3.2 Labour:

Manpower cost derives from the estimated number of workers (assuming a standard workweek of 40 hours), qualification and cost of working hour (from salary and number of hours per workweek) (Table 6.1). Salaries are based on minimum wages per location, being assigned salaries of a plant manager, supervisor and operator 6.7, 4.3 and 3 times minimum wage respectively (from [117], assuming the occupation titles “Industrial production managers”, “First-Line Supervisors of Mechanics, Installers, and Repairers” and “Installation, Maintenance, and Repair Occupations” from the study for plant manager, supervisor and operator respectively). The employer's contribution is added to the manpower cost to cover for the liability of work-related accidents and occupational illness (Table 6.1). Labour cost is finally increased by 20% for labour supervision activities.

6.3.3 Electricity supply and wastewater:

Industrial prices for electricity supply at the location of production are considered (Table 6.1). Treatment of wastewater performed at a cost of $0.43 \text{ €}\cdot\text{m}^{-3}$ [118], by an external party is assumed (the energy to perform it is excluded from the study).

Table 4.1: Specific parameters affecting the economic analysis for different locations

Location	Energy Cost (€·kWh ⁻¹)	Minimum wages (€·Yr ⁻¹)	Employer's contributions (% of labour cost)	Standard workweek (hours)
Canary Islands	0.122 ^a	9,080 ^d	23.6 ^g	40 ^d
The Netherlands	0.096 ^a	18,021 ^d	18.8 ^h	40 ^d
Saudi Arabia	0.029 ^b	6,936 ^c	11 ⁱ	48 ^d
Curaçao	0.307 ^c	7,608 ^f	10.9 ^j	45 ^l
Turkey	0.093 ^a	5,091 ^d	22.5 ^k	45 ^d
South of Spain	0.122 ^a	9,080 ^d	23.6 ^g	40 ^d

^a [119]

^b Source: Saudi Electricity Company. For a currency conversion 1 € = 5.19 Saudi Arabian Riyal

^c [120] For a currency conversion 1 € = 1.89 Netherlands Antillean Guilder

^d Source: EUROSTAT

^e Source: U.S. Department of State

^f [121]

^g Source: Ministerio de Empleo y Seguridad Social

^h Source: Netherlands Foreign Investment Agency

ⁱ Source: HSBC Expat

^j Source: [122]

^k Source: Expat Guide Turkey

^l Source: Curaçao chronicle

6.3.4 Capital costs:

Major equipment is depreciated over 15 years with an 8% interest rate. Major equipment costs (MEC) are not location dependent. Lang factors are used for estimation of capital investment, by multiplying the major equipment cost by specific Lang factors to obtain the weight of the different items in this cost (Table 6.2). This technique is used frequently to obtain cost estimates of a process plant, varying these factors upon the type of product or process.

In the model for algae cultivation, Lang factors used for the breakdown of the capital investment are similar as used in [17] for a microalgae production plant, with the exception of instrumentation and control, land cost, construction expenses, contingency, contractor's fee and purchase tax (Table 6.2). In our experience, the cost of instrumentation and control is higher for closed cultivation systems than considered in the previous study [17] and, consequently is increased by a factor ten (150% of major equipment cost). In addition, construction expenses and

contingencies are also increased; the former changes to the average for ordinary chemical process plants (10% of the total direct costs) [123] and the latter to the highest value commonly used due to the novelty of the process, i.e. 15% of the direct and indirect plant costs [123]. Contractor's fee is estimated as 5% of the direct plant cost, average number given by [123].

Table 6.2: Procedures for estimating CAPEX and OPEX

		Cultivation	
FIXED CAPITAL INVESTMENT	Direct Cost (DC)	Major equipment	MEC
		Installation costs	20% MEC
		Instrumentation and control	15 ^a - 150% ^b MEC
		Piping ^c	20% MEC
		Insulation	0% MEC
		Electrical	10% MEC
		Buildings	23% MEC
		Land improvements	12% MEC
		Service facilities	20% MEC
	Indirect Cost (IC)	Construction expenses	10% DC
	Engineering and supervision	30% MEC	
Other Cost (OC)	Contractor's fee	5% (DC)	
	Contingency (Major equipment)	15% (DC+IC)	
	Working capital	OPEX first three months of operation	
CAPEX	Depreciation	(DC+IC+OC)/15 years	
	Interest	8% of depreciation	
	Property tax	1% of depreciation+interest	
	Insurance	0.6% of depreciation+interest	
	Purchase tax	Excluded	
	Land	1.100 €·Ha ⁻¹ ·Yr ⁻¹	
OPEX	Energy	Calculated from MEC consumption	
	Labour	Salaries + Employer's contribution +Supervision	
	Raw materials	Calculated from mass balances	
	Utilities	Calculated from MEC consumption and mass balances	
	Wastewater treatment	Calculated from mass balances	
	Consumables	Calculated from MEC design	
	Others	Maintenance	4% MEC
	Operating supplies	0.4% (Electricity + Raw materials + Utilities)	
	Contingencies	15% (Raw materials + Utilities)	
	Overheads	55% (Labour + Maintenance)	

^a Raceway pond ^b Closed systems ^c Piping used to channel cooling water from the sea is considered major equipment and calculated as part of MEC (see below)

Purchase tax is neglected; since this is recoverable (a profitable company would get tax return). Land is rented at a not location-specific cost established as 1.100 €·Ha⁻¹·Yr⁻¹ (data based on price

of rented agricultural land in The Netherlands). The extra land required, such as space to place major equipment, buildings or roads, was considered as 20% of the total photobioreactor area (1 or 100 hectares), the total land for the facility being 1.2 or 120 hectares. With the method of Lang factors, total capital investment for the biomass production facility becomes 501% the major equipment cost for closed systems and 324% for raceway ponds.

6.4 MICROALGAL CULTIVATION:

6.4.1 Basis:

Four types of microalgae cultivation systems are analysed: horizontal tubular photobioreactor, vertically stacked horizontal tubular photobioreactor, flat panel photobioreactor and raceway pond. Each projection is based on one of these four systems. The algal production chain starts with natural seawater, which is pumped and enriched in nutrients in a mixing unit. This seawater based medium is sterilized by filtration and added to the selected cultivation system. Medium addition to the systems takes place only during daylight hours, while the broth leaves the reactors continuously. Carbon dioxide supply units add inorganic carbon to the culture. The culture is mixed via a pump, blower or paddle wheel depending on the system. The harvest is continuously pumped from the culture systems to centrifuges, obtaining algal slurry (15 % w/w) as end product of cultivation. The slurry at this concentration can be pumped and used in a biorefinery process. In the projection for the optimized case a microfiltration unit pre-concentrates the culture prior to dewatering by centrifuges. A combination of heat exchangers, pipes and pumps is installed to control temperature in closed systems. Deep sea water is directly used as cooling water and then discharged back to the sea. The use of a hypothetical cooling tower as alternative source of cooling water is also studied as an option.

The facility produces microalgal biomass as slurry with 15% solids (dry weight). The amount of biomass produced per year is calculated from the total annual irradiation for the selected location with the photosynthetic efficiencies obtained outdoors at AlgaePARC pilot facility in The Netherlands (fraction of total light energy converted into chemical energy during photosynthesis) and the chemical energy stored in the biomass (biomass combustion enthalpy, considered constant for non-stressed biomass at a value of 22.5 kJ·g⁻¹ [62, 124, 125]). AlgaePARC (www.algaeparc.com) is a pilot facility in The Netherlands aiming to fill the gap between fundamental research on algae and full-scale production facilities.

The following formula is used to calculate the biomass productivity:

$$\text{Annual Productivity} = \frac{\text{Light intensity} \times \text{Photosynthetic efficiency}}{\text{Biomass combustion enthalpy}} \times \frac{\text{Days of operation}}{365 \text{ days}}$$

For The Netherlands, 270 days of operation per year are considered, while for other locations with more favourable climatic conditions the simulation is done for 300 operational days per year. Downtime is required for maintenance, starting new cultures, possible contingencies or because the weather does not allow production. For cleaning and maintenance selective unit operations will be out of order without affecting the overall operation. An exception will be The

Netherlands as frost limits the operational timeframe, hence a longer downtime. The number of operational days affects annual plant productivity, volumes processed and energy consumption. Input data for projections are experimental results from the pilot plant facility AlgaePARC, climatological database (<http://www.energy.gov/>; <http://www.soda-is.com/eng/index.html>; <http://www.windguru.cz>), suppliers of equipment, suppliers of raw materials and literature, as shown in more detail in other sections. Climatologic information used in this study is based on average hourly data. Irradiation values influence biological parameters such as productivity and oxygen production, which combined with day length and dilution rate determine the major equipment needed. Data on temperature, irradiation, relative humidity, wet bulb temperature, dew point temperature and wind speed are used to estimate the requirements for temperature control of the culture.

6.4.2 Cost analysis:

Total annual costs divided by total dry biomass annual production yields the biomass cost ($\text{€} \cdot \text{kg}^{-1}$). Since the biomass is produced as slurry with water, the unit production cost is based on the dry weight of the biomass in the slurry and not the volume of the entire slurry. Total annual costs are calculated by summing annual capital expenditures (CAPEX) and operating expenses (OPEX). Cost of major equipment, consumables and materials is obtained directly from suppliers when possible; otherwise prices are derived from standard engineering estimates or literature. In case the retrieved cost for a certain component is not from the current year, the price is then updated to the base year using the Harmonized Indices of Consumer Prices (HICP) for the European Union (Source of Data: Eurostat). These costs are listed in Tables 6.3 and 6.4.

Table 6.3: Details about the major equipment considered in the study. * 30 seconds retention time [126]

Numbers in FIG 6.1	SCALE (Ha)	MAJOR EQUIPMENT	Capacity	€·unit ⁻¹	Power
1, 12	1	Pumps	2 m ³ ·h ⁻¹	455	0.18 kW
1, 12	1	Pumps	4 m ³ ·h ⁻¹	1,035	0.40 kW
1, 12	100	Pumps	200 m ³ ·h ⁻¹	13,544	5.9 kW
3	1	Sterilization	5.99 m ³ ·h ⁻¹	16,665	-
3	100	Sterilization	59.9 m ³ ·h ⁻¹	117,979	-
2	1	Mixing unit*	0.1 m ³	14,000	0.05 kW
2	100	Mixing unit*	4 m ³	220,000	2.07 kW
2	100	Mixing unit*	8 m ³	243,000	4.15 kW
2	100	Mixing unit*	25 m ³	291,000	12.96 kW
4	1	Culture circulation pump	700 m ³ ·h ⁻¹	28,105	See “liquid circulation”
4, 10	100	Culture circulation pump and temperature control	28,000 m ³ ·h ⁻¹	595,600	See “liquid circulation”
5	1	Air blower	1,000 m ³ ·h ⁻¹	5,653	3.96 kW
5, 7	100	Air blower	2,499 m ³ ·h ⁻¹	11,182	11.15 kW
6	1 and 100	Paddle wheel	1 Ha of ponds	13,679	0.36 W·m ⁻² (Flow 0.25 m·s ⁻¹)
7	1	Air blower	200 m ³ ·h ⁻¹	3,027	0.99 kW
7	1	Degasser	0.66 m ³	1,214	-
7	100	Degasser	6.6 m ³	2,503	-
8	1 and 100	CO ₂ supply unit	1 Ha	4,717	Insignificant
9	1 and 100	Piping (cooling)	1 m	350	-
11	1 and 100	Heat exchanger	-	-	See “Temperature control”
10	1 and 100	Cooling tower	-	-	See “Temperature control”
13	1 and	Microfiltration unit	32 L·m ⁻¹	71 €·m ⁻¹	0.375 kW·m ⁻³

	100		$^2 \cdot h^{-1}$	2	
				membr	
14	1	Centrifuge	$0.13 \text{ m}^3 \cdot \text{h}^{-1}$	27,000	1.1 kW
14	1	Centrifuge	$2.1 \text{ m}^3 \cdot \text{h}^{-1}$	51,000	4.0 kW
14	1 and 100	Centrifuge	$16.3 \text{ m}^3 \cdot \text{h}^{-1}$	115,000	22 kW
14	100	Centrifuge	$65 \text{ m}^3 \cdot \text{h}^{-1}$	300,000	55 kW
-	1 and 100	Steel mesh casing (flat panel)	$0.875 \text{ kg} \cdot \text{m}^{-2}$	$650 \text{ €} \cdot \text{ton}^{-1}$	-
-	1 and 100	Metal poles (vertical tubular)	$3.8 \text{ kg} \cdot \text{m}^{-1}$	ton^{-1}	-

Table 6.4: Information about the raw materials and consumables used in the simulation. *20% installation cost is included

RAW MATERIALS AND CONSUMABLES	Price	Lifetime (Years)
Commercial CO ₂	$184 \text{ €} \cdot \text{ton}^{-1}$	-
CO ₂ from flue gas	$29 \text{ €} \cdot \text{ton}^{-1}$	-
Nitrogen from urea	$633 \text{ €} \cdot \text{ton}^{-1}$	-
Phosphorus from triple superphosphate	$1,155 \text{ €} \cdot \text{ton}^{-1}$	-
Polyethylene tubes (horizontal tubular)*	$0.20 \text{ €} \cdot \text{m}^{-1}$	1
Glass tubes (vertical tubular)*	$4.13 \text{ €} \cdot \text{m}^{-1}$	20
Plastic lining (raceway pond)*	$102,000 \text{ €} \cdot \text{Ha}^{-1}$	25
Polyethylene film (flat panel)*	$0.19 \text{ €} \cdot \text{m}^{-2}$	1
Microfiltration membranes	$26 \text{ €} \cdot \text{m}^{-2}$	3
Chemical cleaning	$668 \text{ €} \cdot \text{m}^{-3}$	-
Plastic granulates (cleaning in tubular systems)	$22.9 \text{ €} \cdot \text{kg}^{-1}$	3
Rental of cleaning device (cleaning in raceway ponds)	$409 \text{ €} \cdot \text{day}^{-1}$	-

The optimum equipment in terms of performance and capacity for the location, scale, system and operation is selected in each specific case among those in Table 6.3. Number of units of major equipment for each specific case is based on mass balances for the peak capacity, i.e. for the month with the highest irradiation. To achieve a conservative economic estimate the number of processing units is calculated considering operation at 90% of the maximum capacity of equipment. The number of units needed is rounded to the next larger integer.

CAPEX is derived from the capital investment, its depreciation and interest, while OPEX is the annual sum of raw materials, consumables, energy, utilities, labour, maintenance, operating supplies, overheads, contingencies and wastewater treatment cost. Maintenance, operating supplies and general plant overheads are calculated as factors of the purchased major equipment by following the same procedure as [17] (Table 6.2). Other contingencies related to raw materials and utilities are increased to 15% (Table 6.2) compared to 5% used previously [17] since this is not a mature process yet.

Tubes, polyethylene film and plastic liners for tubular systems, flat panels and raceway ponds respectively, as well as filtration membranes are considered as consumables. The annual cost of these consumables is obtained by multiplying the unit cost by the number of units, and then divided by the lifetime. Nutrients (nitrogen, phosphorus and carbon dioxide) and cost of cleaning are considered as raw materials, with quantities obtained from mass balances and prices from suppliers (Table 6.4). For the base cases, all natural seawater used in the process is treated afterwards as wastewater; recycling of culture medium is not done for the base case scenarios. Energy cost is estimated as the product of the total power consumption and the location specific electricity supply cost (Table 6.1).

Number of employees, standard workweek hours, employer's contribution, rank, assigned salary and cost of supervision are the factors used to estimate labour cost at each location (Table 6.1). 10 workers for the operation of a 1 hectare production facility has been considered a logical value, breaking down in 1 plant manager, 1 supervisor and 8 operators of different skill levels. The relationship between labour requirements and size is not linear, therefore, according to the 0.25 power of the capacity ratio often used to scale up labour [123] 32 workers are needed in the 100 hectares facility (1 plant manager, 3 supervisors and 28 operators).

6.4.3 Technical description and operation parameters of culture systems in the study:

Design and operation of culture systems are based on AlgaePARC pilot facility, however systems in this study are meant for industrial scale and therefore the design is adapted accordingly when needed. More details about AlgaePARC pilot facility can be found in [9, 66]. An overview of a hypothetical plant is given in Appendix 6.A Figure 6.1.

Horizontal tubular photobioreactor:

This closed system is a serpentine tubular photobioreactor where a pump circulates the culture at a liquid velocity of $0.45 \text{ m}\cdot\text{s}^{-1}$. The reactor is built up from standard units consisting of two straight transparent tubes connected to form a loop, which are placed on the ground. At the end of the loop, excess oxygen is removed from the culture by sparging ambient air in a separate vessel (degasser). Then, the broth returns to the transparent tube and carbon dioxide is added.

Disposable tubes of low density polyethylene with 0.057 m diameter are considered for the serpentine reactor. A horizontal distance of 0.05 m between tubes is selected for the design (volume:ground area ratio $23.8 \text{ L}\cdot\text{m}^{-2}$); similar to the system installed at AlgaePARC. Maximum

length of units is limited by oxygen build up and depends on different factors that change with scenario. These factors are irradiation, flow velocity, dissolved oxygen concentration before the degasser and maximum photosynthetic rate value [127]. The maximum volumetric photosynthesis rate ($\text{mol O}_2 \cdot \text{m}^{-3} \cdot \text{s}^{-1}$) is calculated from the productivity for the maximum hourly irradiation ($\text{kg biomass} \cdot \text{m}^{-3} \cdot \text{h}^{-1}$) and photosynthetic quotient for the urea ($1.11 \text{ mol O}_2 \cdot \text{mol assimilated CO}_2^{-1}$, calculated from the empirical formula for microalgae of $\text{C}_{106}\text{H}_{181}\text{O}_{45}\text{N}_{16}\text{P}$ [128]). Length of the two tubes constituting each standard unit is this maximum in order to minimize corners and elbows. Photo-inhibition is not considered in this estimation due to the existing limits to predict its effect on culture performance. High partial oxygen pressure reduces algal growth, hence the required degassing. Maximum dissolved oxygen concentration before the degasser is set to 300% of oxygen saturation; higher concentrations are avoided at AlgaePARC. The gas exchange unit, where dissolved oxygen is released can be connected to several standard units. The volumetric gas-liquid mass transfer coefficient (kLa) in the degassers is 0.08 s^{-1} for 1.52 volume of air per degasser volume and time [38]. These values are fulfilled for both scales, i.e. 1 and 100 hectares.

Vertical stacked horizontal tubular photobioreactor:

Similar to the aforementioned tubular system, this system also consists of straight transparent tubes containing the algae suspension. The tubes are made from rigid borosilicate glass stacked parallel to the ground in a vertical structure. A pump is circulating the culture liquid (liquid velocity 0.45 m s^{-1}) from the tubes to the degasser at the end of the loop and back to the tubes.

Units of tubes with 0.065 m diameter are connected to form the standard unit (one loop of two tubes in opposite directions). Mimicking the design at AlgaePARC, the distance between vertical stacks is set to 0.50 m, the height being 0.95 m, while the vertical distance between tubes is 0.05 m (volume:ground area ratio $47 \text{ L} \cdot \text{m}^{-2}$). One loop consists therefore of 8 vertically stacked horizontal tubes. The estimation of the maximum length for the standard unit is analogous to the horizontal tubular system. The degasser design and maximum oxygen concentration at the end of the standard unit are also identical to the previous system. Metal poles of hot-dip galvanized steel are used as structure for the tubes (Table 6.3). Steel angles with equal leg buried 0.95 m in the ground and reaching the same height as the system (0.95 m) are placed at a distance of 10 meters (equal to the length of the connection between tubes). The metal price from the stock exchange is used as reference to calculate cost of poles and is increased with a 50% as profit margin for the supplier.

Flat panel photobioreactor:

This closed flat panel photobioreactor is mixed by air bubbling from the bottom, which prevents build-up of dissolved oxygen and provides mixing. The culture grows in a bag of polyethylene film enclosed in steel mesh casing (Table 6.3). The dimensions of the panels are identical to those from AlgaePARC, being the light path in the panel 0.02 m, the height 0.50 m and the panels placed 0.25 m apart (volume:ground area ratio $37 \text{ L} \cdot \text{m}^{-2}$). The entire surface area is illuminated; the front surface is exposed to direct radiation, while diffuse and reflected light

reach the back surface, improving the efficiency of light conversion. The aeration flow was set to 0.32 volume of air per culture volume and time, used by some authors [129] and within the range used at AlgaePARC (Table 6.5).

Raceway pond:

The raceway ponds in the study are open, ring-channel systems in the form of a single loop with a depth of 0.20 m (volume:ground area ratio $200 \text{ L}\cdot\text{m}^{-2}$), where the culture is circulated at a liquid velocity of $0.25 \text{ m}\cdot\text{s}^{-1}$; similar values as for the raceway pond installed at AlgaePARC. Selected dimensions for hectare-scale ponds in the simulations are 510 m length and 28 m total width, identical to a real demonstration plant [130]. Similarly to the raceway pond at the AlgaePARC pilot, the flow is accomplished by one paddle wheel per pond; in practice at large scale it may result in a less turbulent regime in the broth than for the system present at AlgaePARC due to increased length. The bottom of the pond is lined with reinforced and thermo-sealed PVC. There is one carbonation sump per pond to promote the carbon transfer to the liquid phase and to ensure adequate carbon supply. The carbonation sump is 1 m deep and 0.65 m long with the same width as the channel; this design has been proven as appropriate for its purpose [131].

6.4.4 Empirical data:

Experimental data used for simulations were obtained in the pilot production systems (ground area $\sim 25 \text{ m}^2$) at the AlgaePARC pilot facility in Bennekom, The Netherlands [66]. For the flat panel photobioreactor data was obtained with a smaller production system (ground area 2.5 m^2). The pilots were operated in continuous mode as chemostat between April and August 2013; Table 6.5 shows the average photosynthetic efficiencies on sunlight (PE), associated dilution rates and amount of days that are used to calculate these values for the different systems.

Table 6.5: Experimental data used in the study; obtained outdoors at AlgaePARC in pilot plant production systems [66]

Reactor	Raceway pond	Horizontal tubular	Vertical stacked tubular	Flat panels ^a
Photosynthetic efficiency (% sunlight)	1.2	1.5	2.4	2.7
Daily dilution (%)	16	25	27	27
Days	24	36	36	36
Flow of culture ($\text{m}\cdot\text{s}^{-1}$)	0.25	0.45	0.45	-
Aeration (vvm)	-	-	-	0.3-0.6

^a 2.5 m^2 pilot plant production system

6.4.5 Culture medium and carbon dioxide source:

Nutrients considered for the cost analysis of the culture medium are nitrogen (as urea) phosphorus (as triple-superphosphate) and carbon dioxide, since these are main components of biomass and have most impact on the economics compared to other elements. Nutrient concentrations in the culture medium, and therefore the cost (Table 6.4), are calculated separately for each case, based on biomass concentration and biomass composition. Biomass composition used for the simulation is the empirical formula for microalgae of $C_{106}H_{181}O_{45}N_{16}P$ [128]. Commercial carbon dioxide is the source of carbon in this work. The amount of carbon dioxide needed for biomass production is directly calculated from the productivity, considering a CO_2 :biomass ratio of 1.87 derived from the considered elemental composition [128]. Carbon, nitrogen and phosphorus losses are neglected.

6.4.6 Temperature control:

Maximum culture temperature in closed systems is kept at 30°C, similar to the operational strategy at AlgaePARC. Temperature control for simulations is performed by a combination of heat exchangers and cooling water from the sea. In cases where temperature control is needed, the cooling water is pumped through the in-the-culture-submerged heat exchangers. The heat flow in the photobioreactors and the expected temperature of the culture are calculated on an hourly basis. The temperature control units are active during those periods with an expected value above the setpoint. Cooling water from the sea comes from a depth of 200 m for all locations, excepting The Netherlands where depth used is 20 m, as in this location surface water is colder. Temperature of water considered as given by the National Centers for Environmental Information, National Oceanic and Atmospheric Administration (www.nodc.noaa.gov). Heat flows are calculated according to [70, 132, 133]. Irradiance, radiation and convection are the factors considered in the analysis; in the open system the effect of evaporation and condensation are estimated in addition. Less influential heat flows generated from algae growth and conduction from the ground or evaporation and condensation in closed systems are neglected. For this analysis, the light falling on the ground surface is assumed to be completely absorbed in all systems. Rate of temperature change during a certain hour results from heat flow during the interval (in Watts) divided by the product of specific heat of water ($C_p = 4,186 \text{ J}\cdot\text{Kg}^{-1}\cdot\text{°C}^{-1}$), seawater density ($\rho = 1,027 \text{ kg}\cdot\text{m}^{-3}$) and total culture volume. This temperature change is added to culture temperature of the previous hour to determine the current temperature. Initial culture temperature at time zero equals dry bulb temperature of the surrounding air. Once the expected temperature is known, the energy to lower it to 30°C is calculated (in W):

$$\text{Energy to remove from the culture} = \frac{(\text{Expected temperature in } ^\circ\text{C} - 30^\circ\text{C}) \times C_p \times \rho \times \text{Culture volume}}{\text{Time}} \quad \text{Eq. 1}$$

The mass flow of cooling water needed to remove that energy from the culture in the heat exchanger comes from (in $\text{m}^3\cdot\text{h}^{-1}$):

$$\text{Mass flow of cooling water} = \frac{\text{Energy to remove from the culture}}{C_p \times \Delta T \times \rho} \quad \text{Eq. 2}$$

Where ΔT is the difference between *Temperature cooling water_{out}* and *Temperature cooling water_{in}*. *Temperature cooling water_{in}* is the temperature of the sea water. *Temperature cooling water_{out}* is the temperature of the cooling water leaving the heat exchanger and discharged again to the sea. It is calculated using the following equation and considering an efficiency of heat exchange of 75% [134]:

$$\text{Temp. cooling water}_{out} = \text{Temp. cooling water}_{in} + \text{Efficiency} \times \left(\frac{\text{Temp. of the culture}}{\text{Temp. cooling water}_{in}} \right) \quad \text{Eq. 3}$$

The rate of heat transfer in the heat exchangers is (in $\text{J} \cdot \text{h}^{-1}$):

$$\text{Rate of heat transfer} = \text{Mass flow of cooling water} \cdot \text{Specific heat of water} \cdot \Delta T \quad \text{Eq. 4}$$

The following equation gives the total area of heat exchangers (in m^2):

$$\text{Area of heat exchangers} = \frac{\text{Rate of heat transfer}}{\text{Heat transfer coefficient} \times \Delta T} \quad \text{Eq. 5}$$

Heat transfer coefficient in heat exchangers is estimated as $852 \text{ W} \cdot \text{m}^{-2} \cdot \text{°C}^{-1}$ [135].

Cooling involves CAPEX (from cost of pumps, heat exchangers and pipes) and OPEX (energy consumption, cost of chemical treatment of the water and maintenance). The cost for heat exchanger is derived from [135], for a shell and tube U-tube type heat exchanger, made of cs/316 stainless with a working pressure below 4 bars. When the required area of heat exchangers is above $1,115 \text{ m}^2$ the estimation may not be realistic according to the source. In that case several units of $1,115 \text{ m}^2$ are used. Area of heat exchangers and mass flow of cooling water are calculated per hour (from Eq. 2 and 5); maximum values for each case are used in the estimation of CAPEX, i.e. for summer. Energy consumption for temperature control is the energy used by pumps. Pumps number 5 from Table 6.3 are used here with a shaft power calculated assuming 3 m of water column pressure, using $1,027 \text{ kg} \cdot \text{m}^{-3}$ as seawater density and a pump efficiency of 75% [135]. Cost of chemically treating the water is $0.004 \text{ €} \cdot \text{m}^{-3}$ of cooling water [136]. As an alternative, use of wet cooling towers as source of cooling water is also studied. In this case cooling water passes on demand through the cooling tower and evaporation lowers its temperature. Surface water is used for this, which is continuously recirculated. This avoids catchment of deep waters and reduces the amount of seawater used. The water is also passed through the heat exchangers (using identical specifications as abovementioned for area and cost). The climatic conditions in Curaçao (high relative humidity and air temperature) make the use of cooling towers unfeasible to keep culture temperature below 30 °C . Therefore this option is not studied in Curaçao. In Eq. 2, *temperature cooling water_{in}* is the temperature of the cooling water leaving the cooling tower and entering the heat exchanger instead. It is 2.8 °C above the wet bulb temperature for the time and location. 2.8 °C is the approach of the cooling tower (difference in temperature between the cooled-water temperature and the entering-air wet bulb temperature) [136]. Similarly, when using towers, *temperature cooling water_{out}* in Eq. 2 is the temperature of the cooling water leaving the heat exchanger and entering the cooling tower. It is also calculated considering an efficiency of heat exchange of 75% [134]. If cooling towers are involved, cooling involves CAPEX (from cost of cooling tower, heat exchangers, pipes and additional equipment) and OPEX (energy consumption and cost of water, including chemical treatment and

replacement of lost water). The technology used in cooling towers for 1 and 100 hectares facility changes with scale: mechanical draft towers and hyperbolic natural draft towers are used respectively. Mass flow of cooling water for 1 hectare facility is within the range that allows the calculation of cost of the tower according to [135] for all the cases (between 4,542 and 341 m³·h⁻¹). Consequently this method is used for a tower made of redwood (a cost effective material and in abundant supply) and a factor “*f*” calculated in each particular case depending on the temperature difference of water entering and leaving the cooling tower. Non-installed price was obtained reducing the value a 20% according to the same source [135]. Mass flow of cooling water and temperature range for 100 hectares facility is within the scale of the cooling tower under study in [137], where 5,735,294 € is the total investment cost for a cooling tower with a flow of cooling water of 70,000 m³·h⁻¹. Based on this relation and using the mentioned tower as basic unit size, the cost of cooling towers is scaled up or down using the following exponential law [17]:

$$CostB = CostA \times \left(\frac{SizeB}{SizeA} \right)^{0.85} \quad \text{Eq. 6}$$

When using cooling towers, energy consumption for temperature control (equipment) and cost of water (chemical treatment and make-up of losses) are 0.40 kWh·m⁻³ and 0.004 €·m⁻³ of cooling water respectively [136]²⁸. Length of piping used to transport cooling water from the sea to the systems and back is assumed to be 600 m. If cooling towers are not used, water uptake requires 4,000 m extra of pipes to reach the required depth (400 m in case of The Netherlands). A pipe of precast concrete with a diameter of 2 m is required, at the cost indicated Table 6.3.

6.4.7 Cleaning:

Closed reactors operating for long times tend to accumulate an algae film in the inner surface, restricting sunlight supply. Open systems can accumulate external material as consequence of winds and animals. Besides, culture contamination with undesired species or pathogens occurs, especially in open systems. Therefore, cleaning is a necessary task to perform in a microalgae production facility. In the projections, three cleanings per year take place, similar way to operation at AlgaePARC. Chemical cleaning is used for closed reactors, where systems are filled with 3% of a cleaning solution composed of 35% H₂O₂ and 7.5% glycerin (Table 6.4). Small plastic granulates [9] are added in addition to tubular systems at a concentration of 0.5 Kg·m⁻³ (Table 6.4), which are recovered afterwards and can be reused for 3 years. These granulates are also used in the broth during cultivation in tubular systems to prevent biofilm formation [9]. Open ponds are cleaned using compact road sweepers (Table 6.4), which vacuum clean the bottom of the pond. They are rented at a price of 409 €·day⁻¹ and cover 10.8 hectare per day (based on general information available on websites from rental companies).

6.4.8 Inoculum production:

10% of area in the production facility is dedicated to inoculum production to supply biomass, free of contamination, to the systems. This area is considered identical to the rest of facility in terms of costs (OPEX and CAPEX). However, since this biomass is not continuously produced

and is not harvested, but transferred to the continuous systems, this area is assumed as non-productive. Consequently, average photosynthetic efficiencies or productivities for the whole facility (Table 6.5) are reduced with this percentage.

6.4.9 Power requirement for liquid circulation in tubular systems and raceway pond:

The power consumption to maintain the flow in tubular systems is calculated according to standard hydrodynamic principles. In tubular systems, the shaft power is calculated using $1,027 \text{ kg}\cdot\text{m}^{-3}$ as seawater density and a pump efficiency of 75% [135]. Energy dissipated due to major losses from friction and minor losses from bends is calculated and added to the total energy of the system [138, 139]. The Darcy Weisbach equation for energy loss in turbulent regime is used for friction, as well as the Swamee-Jain Equation for friction factor. The roughness of tubes, affecting friction, is $3\cdot 10^{-7} \text{ m}$ and each elbow leads to an equivalent length of 30 (information from providers). Other minor head losses are neglected. Energy required to mix the open ponds is estimated according to [138, 140]. The total electrical efficiency of paddle wheels in open ponds is assumed to be 15% [141]. Values of 3.2, 1.8 and 0.3 are used for bend loss coefficients, drag coefficients for paddles and slippage factors respectively. Manning's friction coefficient of $0.012 \text{ s}\cdot\text{m}^{-1/3}$ is selected for the lining (thermosealed PVC). Consequently energy needed to overcome head losses in bends, curves and friction are considered in the open system, on the other hand those head losses from carbonation sump, rising bubbles (carbonation) and effect caused by winds are neglected.

6.4.10 Optimization – Future scenarios:

Different parameters are changed, from the original case for 100 hectares facility, to values expected to be feasible in the future. Future projections are done for flat panel systems located in south of Spain considering the following assumptions (all of these assumptions need confirmation):

- An increase of the average photosynthetic efficiency by a factor 2.22, resulting in an efficiency of 6%. The 6% photosynthetic efficiency in flat panel has already been obtained at lab-scale [23] and is still below the theoretical maximum of 8 to 10% [142].
- Maximum temperature in the culture is kept at 45°C. Algae able to grow at 50°C have already been identified [143].
- Light path of the flat panel is reduced to 0.01 m.
- Flue gas is used as source of carbon dioxide. A price of $29 \text{ €}\cdot\text{ton}^{-1}$ is considered (Table 6.4), which accounts for all upstream operations to concentrate CO_2 from the flue gas stream and make it usable in the process [144]. Transportation cost for this gas is also included, based on a recent study [145]. This cost is calculated conservatively, using 180 km as supply distance; the largest from [145]. Therefore, transportation in pipelines involves an energy of 13.68 kWh/ton of CO_2 [145]. Energy cost for the studied location (Table 6.1) will then bring the transportation cost for flue gas.

- Aeration in is lowered during the night from 0.32 volume of air per liquid volume and time (vvm) to 0.05 vvm; a flow already used outdoors in a previous study [146]. Similarly, the flow is reduced during the day to 0.22 vvm, value used by [147].
- 310 operational days and only one cleaning performed per year.
- Number of employees is reduced to one person per 10 Ha (1 plant manager, 1 supervisor and 8 operators for 100 hectares); this number has already been mentioned in a previous study [17].
- The fraction of the facility used to prepare inoculum is reduced from 10 to 5% of the total area.
- Wastewater treatment is avoided. Pollutants, such as nitrogen and phosphorus, are below discharge limits in the wasted medium and can be discharged after harvesting.
- Harvesting is performed by microfiltration and subsequent centrifugation (Figure 6.1). This combination has shown to be more cost effective than a single-step centrifugation [148]. Both methods are conventional in industry, showing high reliability and robustness when changes in the culture appear compared to other methods such as coagulation-flocculation-decantation or dissolved air flotation. By using membrane filtration, the biomass is concentrated about 15 times. The concentrated fraction (retentate) is further processed by the more expensive and energy-intensive centrifugation, giving a slurry with a final concentration of 15% dry solid biomass [148]. $32 \text{ L}\cdot\text{m}^{-2}\cdot\text{h}^{-1}$ has been a proven flux in microalgae cultures that combines the advantages of reasonable filtration with low fouling [148] and was therefore selected.
- Polyethylene plastic films in flat panels can be used for 2 years.
- 30% of nutrients added to the culture are reclaimed, after biomass is refined.

6.5 Current status of autotrophic microalgae production: Culture systems

Biomass production is the starting point for commercialization of industrial products from algae; we have estimated costs for obtaining harvested biomass in an industrial cultivation facility of 100 hectares for different culture systems. The study includes four state-of-the-art production systems: horizontal tubular photobioreactor, vertically stacked tubular photobioreactor, flat panel photobioreactor and open raceway pond. The cost projections are supported by experimental results obtained at AlgaePARC pilot facility [17, 122], where non-GMO microalgae are used. AlgaePARC was designed to bridge the gap between fundamental research on algae and industrial production facilities, allowing us to extrapolate the empirical data from its operation to commercial-scale. Discussion on the best production system is an ongoing debate, due to the fact that none of the systems seems to completely surpass others. Raceway ponds are simple and imply about half of the initial investment than closed systems at the expense of also lower productivities ($27 \text{ ton}\cdot\text{ha}^{-1}\cdot\text{Yr}^{-1}$ for south of Spain, Figure 6.1), about one order of magnitude more diluted cultures and consequently greater volumes to process. Besides, the culture is more prone to contamination and heavy rain can interfere with proper operation. Although closed

systems need a greater investment, they offer higher productivities (between 34 and 61 $\text{ton}\cdot\text{ha}^{-1}\cdot\text{Yr}^{-1}$ for current projections in south of Spain; Figure 6.1) and more degrees of freedom in design, construction and operation (implying also more complexity); definitely closed systems have more potential for improvement. Our study shows that the flat panels reactor is the most convenient system in terms of costs (Figure 6.1), as also shown recently [149]. It is a finding regardless of location, with current biomass production costs that would reach $3.4 \text{ €}\cdot\text{kg}^{-1}$ in Spain at 100 ha scale.

Microalgae
production
cost ($\text{€}\cdot\text{kg}^{-1}$)

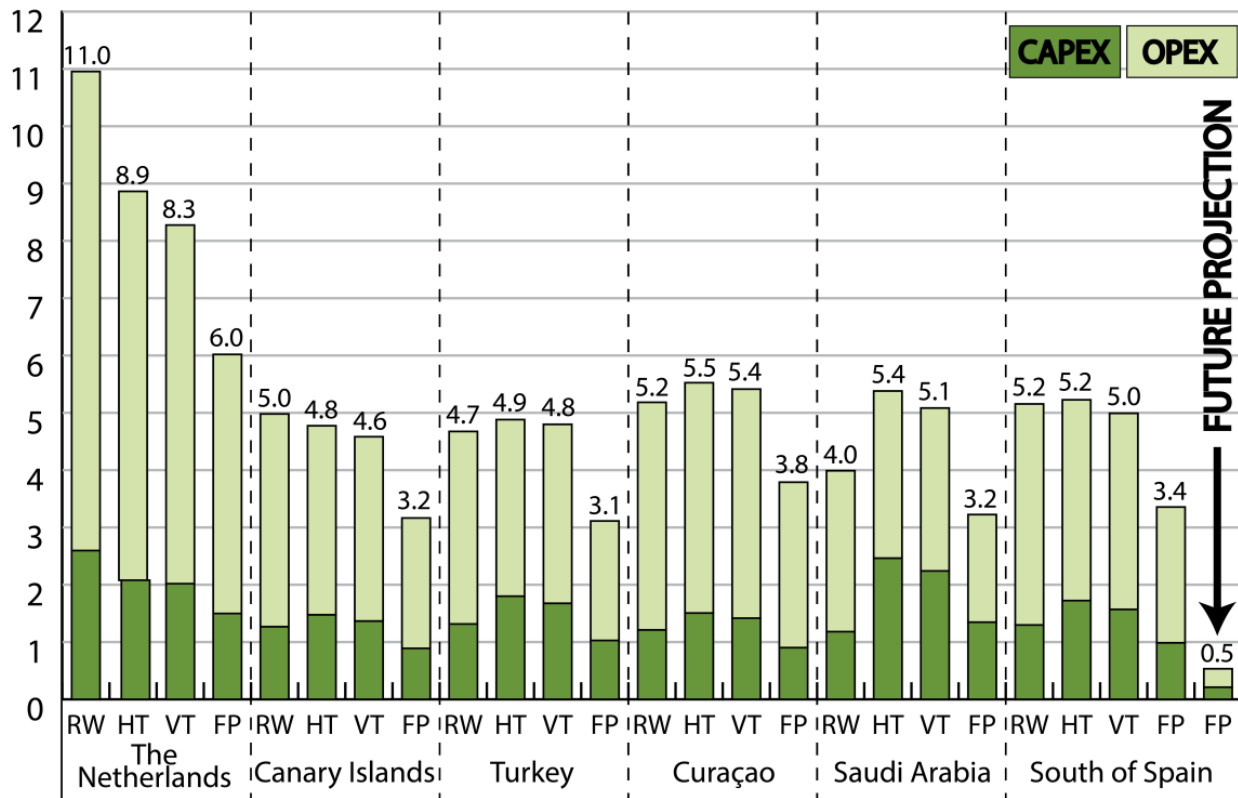


Figure 6.1: Projected biomass production costs (cultivation and harvesting) in the studied locations for current scenarios and the future projection for south of Spain. Costs as the sum of CAPEX and OPEX. RW: raceway pond; HT: horizontal tubular photobioreactor; VT: vertically stacked horizontal tubular photobioreactor; FP: flat panels photobioreactor. Values related to the presented results can be found in Appendix 6.B tables 6.1 and 6.2.

Large-scale cultivation in closed systems involves some constraints to consider. Overheating can be lethal to microalgae [150, 151] and temperature control in closed reactors is mandatory. This is solved in different ways; either immersing the systems in a body of water, spraying water on the surface of reactors or using heat exchangers. Build-up of oxygen must be controlled, since it could inhibit growth and cause the collapse of cultures. Oxygen control is a basic premise in the

design of closed systems. This can be done by limiting the tube length in tubular photobioreactors and by designing efficient degassers, increasing therefore complexity. Cleaning is required in both open and closed systems, but closed photobioreactors require chemicals to remove the biofouling from the inner surface, since it can restrain growth [57].

In open systems, water evaporation restrains excessive temperature raise. Our energy balances show that temperatures in the open ponds would not exceed 32°C for any of the studied locations. Therefore, forced cooling is absent in raceway ponds in this study. On the contrary, a non-cooled closed system can imply culture temperatures above 60°C, making temperature control indispensable to cultivate microalgae. This work is based on cooling using an external source of water, which implies a cost of 0.4, 0.5 and 0.8 €·kg⁻¹ for flat panels, vertical and horizontal tubular reactors respectively. Cooling towers could be used instead as source of cooling water if an external source, such as the sea, is not available. This option would result more expensive, increasing cooling cost to 2.0, 2.2 and 3.6 €·kg⁻¹ for the above-mentioned systems. Separation of the biomass from the culture medium is usually identified as one of the major bottlenecks in the process [152]. This is valid for raceways, where our projections show that harvesting contributes to about 23% of cultivation cost (1.2 €·kg⁻¹), whereas it is only between 5 and 7% of total costs in closed systems (0.2 to 0.3 €·kg⁻¹) due to higher biomass concentrations.

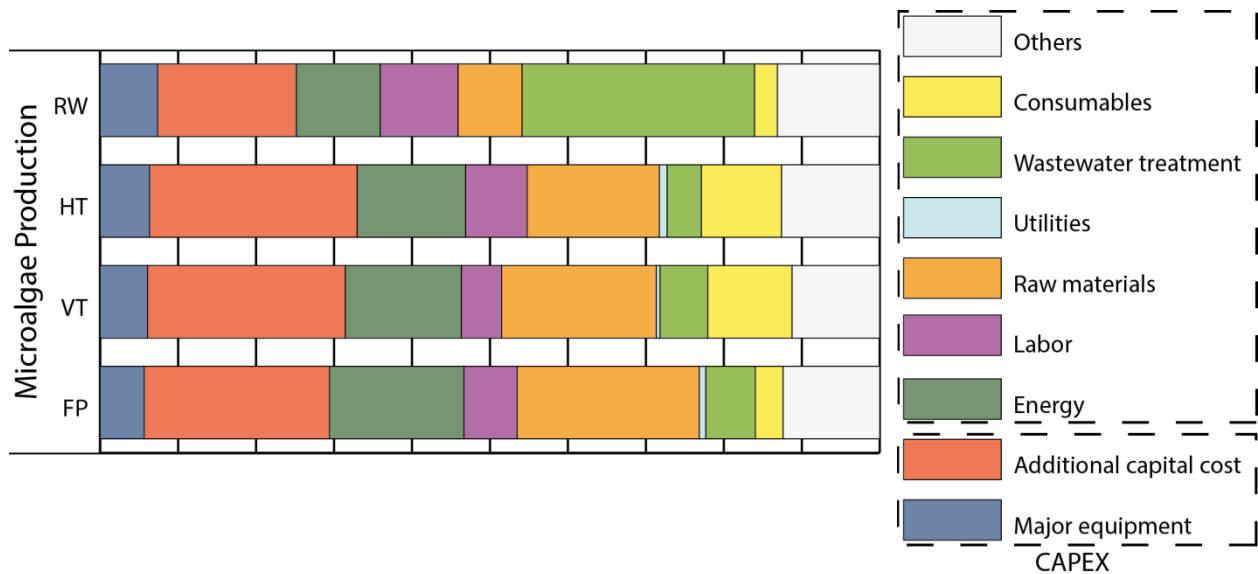


Figure 6.2: Cost breakdown analysis for projections on current microalgae production (cultivation and harvesting) in south of Spain. RW: raceway pond; HT: horizontal tubular photobioreactor; VT: vertically stacked horizontal tubular photobioreactor; FP: flat panels photobioreactor.

Figure 6.2 shows a detailed breakdown of costs, where *major equipment* and *additional capital cost* define capital costs in CAPEX, while the rest of contributors account for operational costs (OPEX). The most influential factors on the cost of microalgae production vary with production system, but our estimations identify different trends in open and closed systems (Figure 6.2). Cost of wastewater treatment plays an important role in the raceway pond, but has only limited influence in closed systems. It is a consequence of greater volumes processed in raceways due to a more diluted culture. On the other hand, costs of raw materials (17-23%; mainly due to cleaning) and energy consumption (14-17%) become relevant items in closed systems. A closer look to these systems would show that energy for mixing represents more than 80% of total energy consumption.

Photosynthetic efficiency (PE; percentage of the solar irradiation converted to biomass) is greater in vertical systems, with values of 2.7% and 2.4% for flat panels and vertical tubular photobioreactors respectively (Table 6.5). Due to the principle of light dilution, placing the reactors vertically increases the volume per ground area, thereby average light intensity impinging on reactor surface is decreased, leading to these enhanced productivities [4]. Thus building upright is a convenient strategy that cost-wise seems to compensate the extra costs involved in frames, materials and energy, by increased productivity. Consequently, there is a reduction in the final cost of produced biomass (Figure 6.1).

6.6 Industrial microalgae chains: Current status, future potential and roadmap

The commercial production costs of microalgal biomass production can be estimated: projected costs vary greatly depending on scale; cost of cultivation, harvesting would be $3.4 \text{ €} \cdot \text{kg}^{-1}$ of biomass⁻¹ for a facility of 100 hectares in south of Spain (Figure 6.1). Whereas, according to our projections, a facility of 1 hectare would imply costs of $28.4 \text{ €} \cdot \text{kg}^{-1}$ for cultivation. Parameters associated to scale effects such as labour demand, price and efficiency of equipment are responsible for this higher cost. Increasing scale even further (>100 hectares) should not result in a relevant reduction in costs; equipment and production systems in the cultivation are modular and more units with identical design would be used. Location is not trivial either, factors as productivity, temperature or cost of labour and energy makes choosing a suitable location essential (Figure. 6.1). In 2011, the costs of algal cultivation and harvesting in flat panels were estimated on $5.96 \text{ €} \cdot \text{kg}^{-1}$ [5]. There has been an important improvement in biomass production costs (Figure 6.1), due to better insight in the process and operation strategies.

Nevertheless, we are still facing immature technologies for production [2]. Accordingly, this field is continuously evolving and further reductions in costs can be expected in the coming years. The progress in cultivation is particularly important since improvements in productivity, quality and composition of the biomass are not only relevant to the upstream processing, but have pronounced effects on the downstream and market price as well. A sensitivity analysis (Figure 6.3) aids us to draw an interdisciplinary roadmap for long-term research on microalgae production, pinpointing the major obstacles towards market penetration. Establishing flat panels

systems in south of Spain as base case ($3.4 \text{ €}\cdot\text{kg}^{-1}$ as aforementioned), individual parameters are changed to the value expected for the future, which in combination lead to the mentioned $0.5 \text{ €}\cdot\text{kg}^{-1}$. It pinpoints PE as the most influential parameter on production cost, with a potential reduction of $1.6 \text{ €}\cdot\text{kg}^{-1}$ (47% reduction in cost from base case) (Figure 6.3). Greater industrial PE in outdoors conditions than our future projection have been achieved using engineered cyanobacteria and improved systems [153]. Both cases are still below the theoretical maximum PE of 8 to 10% [142]. It leads us to think that projected enhancements in PE are foreseeable. In this regard, strain improvement on performance (robustness, increased tolerance to photo inhibition, photo saturation, oxygen saturation and capture and conversion of CO_2) is essential for the achievement of higher year-round PE.

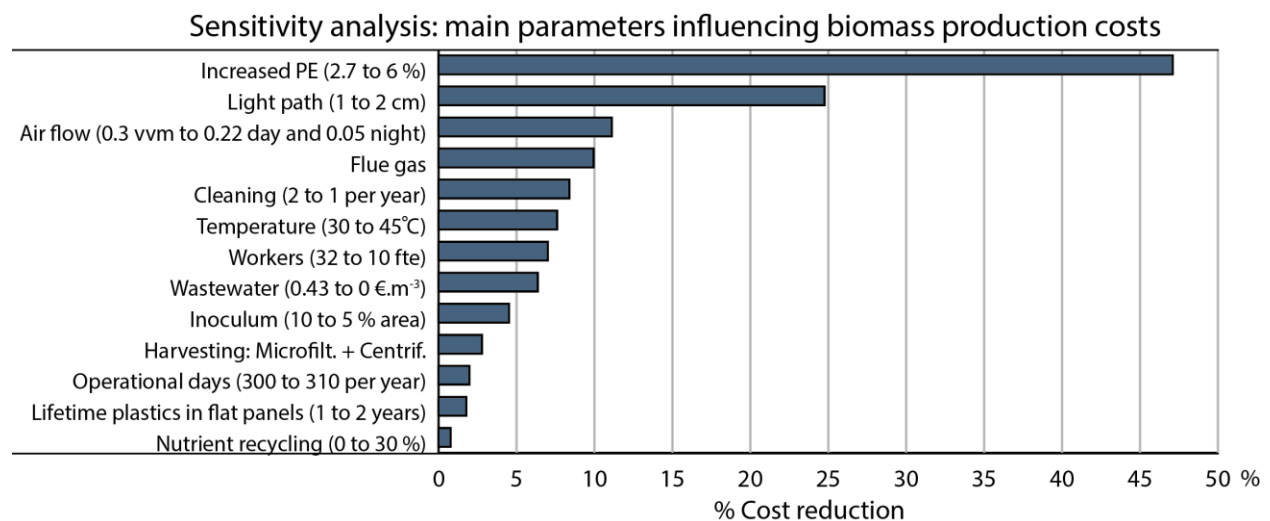


Figure 6.3: Sensitivity analysis on biomass production (cultivation and harvesting) using as base case flat panels in south of Spain. Effect of individual parameters on cost is shown in horizontal axis. Parameters are changed to the value used for the future projection.

The base for design of current available commercial photobioreactors is primarily empirical; nonetheless recent engineering tools, arisen from a deeper knowledge on microalgal biotechnology, enable step-change designs that will foster more effective technologies [154]. Efforts should not be spared on improvements in reactors; in fact there is an array of new patents, reactor designs and materials on photobioreactors [154-156]. Efficient thinner systems that could be operated at higher biomass concentration, less prone to fouling (cleaning) and more automated (labour) could drop costs by $1.3 \text{ €}\cdot\text{kg}^{-1}$ (Figure 6.3).

In general, high purity CO_2 gas is not essential; microalgae have demonstrated the ability to directly use flue gas to grow, using some combustion gasses as source of nutrients such as NO_x [157]. Use of flue gas should not be an issue even in those specific cultures requiring a purified gas, since the capture of CO_2 from these currents is a mature technology commercially available

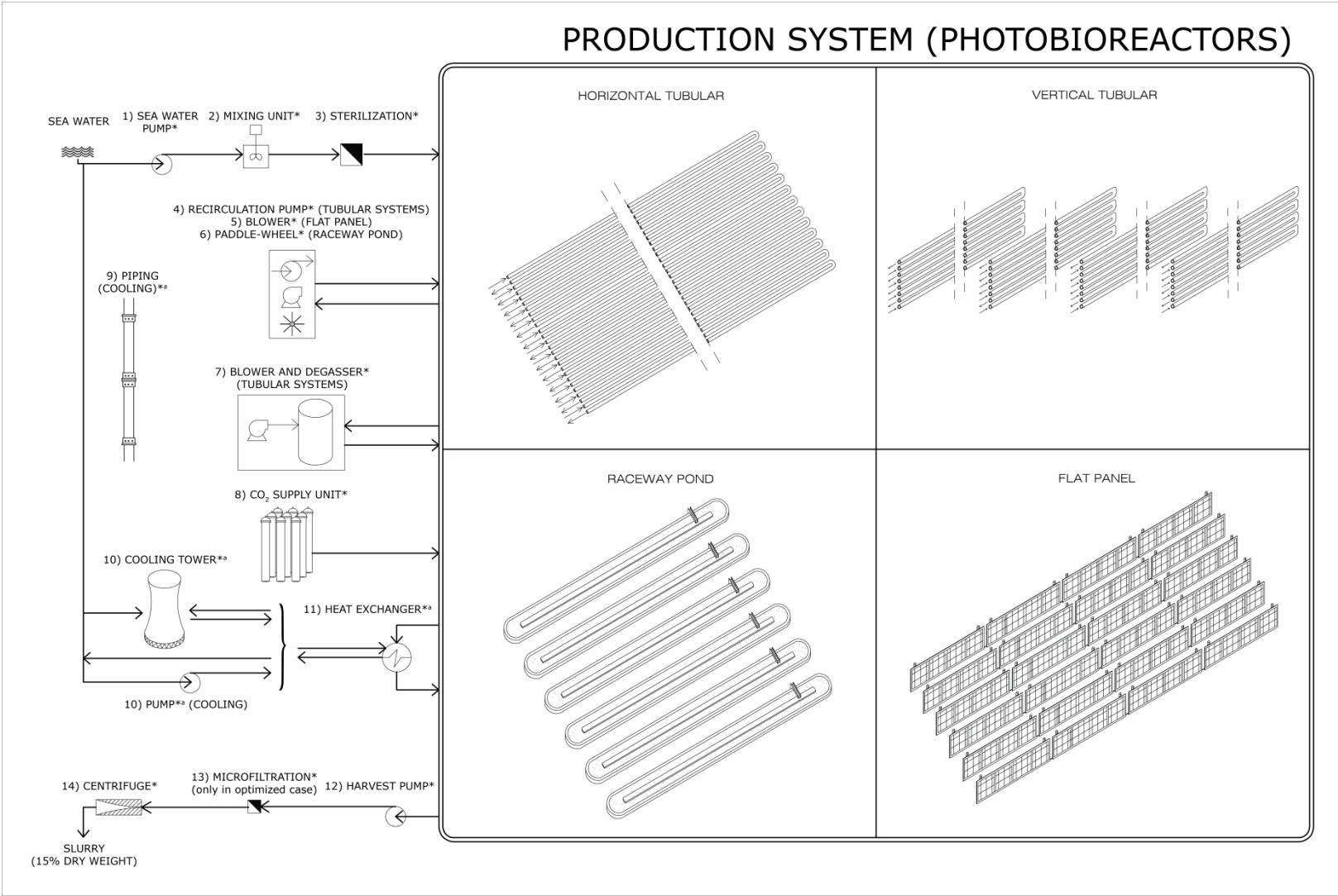
[158]. Therefore, a strategy directed to combining microalgae growth and carbon fixation from flue gas can be realistic. Nutrient recycling from the downstream is required for standalone operation and is likely a key factor in sustainability [159]. However, it still remains a relatively unknown topic, as a consequence of the limited experience on downstream processes and a wide range of options. Feasibility of nutrient recycling largely depends on the selected catalysts and operating conditions, being the accumulation of growth inhibitors the main barrier [160, 161]. Nevertheless, reuse of nutrient shows high potential [159-161]. The use of carbon dioxide from flue gas and recycling part of the nutrients from the downstream would make a hefty contribution, saving $0.4 \text{ €} \cdot \text{kg}^{-1}$.

There is not a consensus regarding standard operating procedures in microalgae production. On the contrary, process operation shows considerable divergences among authors and sources. Relevant parameters in operation are numerous; aeration is one of them and can illustrate the diversity in practices. The range of aeration per unit of volume in flat panels is very wide, being the difference as large as 1 order of magnitude for outdoors systems [8, 16]. Therefore, a “best practice” to operate microalgal facilities, used as a benchmark, could be a valuable tool to increase productivity, drop costs and energy consumption. Proper operation strategies are essential; reduced aeration and night “cutbacks” result in savings of $0.4 \text{ €} \cdot \text{kg}^{-1}$ and up to 51% reduction of energy use. Wastewater treatment is a burden, particularly in raceway ponds (Figure 6.2); this could be reduced or avoided with a complete recycling of the spent culture medium or keeping pollutants below discharge limits. Indeed researchers are studying the subject in considerable depth. While further studies are still essential to elucidate the challenges of water recycling on large scale, several authors point to its benefits, even enhancing the growth in some cases [162-164].

Temperature control deserves a special focus, since it has a substantial effect on cost, adds complexity to the process and needs a source of cooling water. Reactor design, floating cultivation systems, and strain improvement are the main approaches to reduce the costs involved with temperature control. Regarding reactor design, materials reflecting near-infrared light, known as “heat radiation”, will avoid part of the heat inflow to the culture without effects on productivity [4]. Offshore cultivation, like the OMEGA system from NASA [165], where surrounding water acts as temperature buffer, controlling reactor temperature could be a future alternative. From a biological perspective, temperature acclimation by a microalgal strain is complex and specific strategies are involved [166]. The biotechnology of microalgae has entered into a rapid developing phase [167]⁴⁶, and although genetic engineering remains a challenge, an increase of optimal temperature has already been proved with long term adaptation strategies [166]. Culture of strains adapted to temperatures of 45°C could reduce costs by $0.3 \text{ €} \cdot \text{kg}^{-1}$ (8%) (Figure 6.3).

In sum, we face a process that despite the long road ahead to reach maturity appears already to be lucrative. We know the existing shortcomings and how to approach them, let's keep on the right path; the benefits will justify the effort.

Appendix 6.A.1: Scheme of the microalgal production facility. *Major equipment. ^a Only in closed systems.



Appendix 6.B

Table 6.B.1: Set of projected results for microalgae production in 100 hectares (cultivation and harvesting). RW: raceway pond; HT: horizontal tubular photobioreactor; VT: vertically stacked horizontal tubular photobioreactor; FP: flat panels photobioreactor. CU: Curaçao; TN: The Netherlands; SP: Spain; CI: Canary Islands; TU: Turkey; SA: Saudi Arabia

SCENARIO	RESULTS FOR MICROALGAE CULTIVATION										
	System	Location	Biomass cost (€/kg)	Biomass Capacity (Ton/Yr)	Initial investment (M€)	Total cost (M€/Yr)	CAPEX (M€/Yr)	OPEX (M€/Yr)	CAPEX (€/kg)	OPEX (€/kg)	Biomass conc. (mg/L)
RW	TN	11.0	1296	47.7	14.2	3.4	10.8	2.6	8.4	0.15	0.73
RW	CI	5.0	2838	51.2	14.1	3.6	10.5	1.3	3.7	0.30	1.44
RW	TU	4.7	2672	49.9	12.5	3.5	9.0	1.3	3.4	0.28	1.35
RW	SP	5.2	2708	49.9	14.0	3.5	10.4	1.3	3.9	0.28	1.37
RW	SA	4.0	3049	51.2	12.2	3.6	8.6	1.2	2.8	0.32	1.55
HT	TN	8.9	1621	47.8	14.4	3.4	11.0	2.1	6.8	1.01	0.80
HT	CI	4.8	3548	75.3	16.9	5.2	11.7	1.5	3.3	1.98	1.15
HT	TU	4.9	3340	86.8	16.3	6.0	10.3	1.8	3.1	1.87	1.00
HT	SP	5.2	3385	84.1	17.7	5.8	11.9	1.7	3.5	1.89	1.05
HT	SA	5.4	3811	136.6	20.5	9.4	11.1	2.5	2.9	2.13	0.92
VT	TN	8.3	2593	75.3	21.5	5.2	16.2	2.0	6.3	0.76	0.77
VT	CI	4.6	5676	112.6	26.0	7.8	18.3	1.4	3.2	1.49	1.13
VT	TU	4.8	5344	130.3	25.6	9.0	16.7	1.7	3.1	1.40	0.98
VT	SP	5.0	5417	123.6	27.0	8.5	18.5	1.6	3.4	1.42	1.03
VT	SA	5.1	6097	199.7	31.0	13.7	17.3	2.2	2.8	1.60	0.93
FP	TN	6.0	2917	62.6	17.6	4.4	13.2	1.5	4.5	1.08	0.71
FP	CI	3.2	6386	82.0	20.2	5.7	14.5	0.9	2.3	2.13	1.38
FP	TU	3.1	6012	89.3	18.7	6.2	12.5	1.0	2.1	2.00	1.30
FP	SP	3.4	6094	86.9	20.5	6.0	14.4	1.0	2.4	2.03	1.32
FP	SA	3.2	6859	134.4	22.1	9.2	12.9	1.3	1.9	2.29	1.36

Towards industrial products from microalgae

FP	SP (Fut.)	0.5	14771	44.4	7.9	3.1	4.8	0.2	0.3	9.18	13.23
RW	CU	5.2	3089	53.3	16.0	3.7	12.3	1.2	4.0	0.32	1.57
HT	CU	5.5	3861	83.9	21.3	5.8	15.5	1.5	4.0	2.16	1.18
VT	CU	5.4	6178	127.3	33.4	8.8	24.7	1.4	4.0	1.62	1.17
FP	CU	3.8	6951	90.7	26.3	6.3	20.1	0.9	2.9	2.32	1.47

Appendix 6.B

Table 6.B.2: Summary of projected results for microalgae production in 100 hectares (cultivation and harvesting). RW: raceway pond; HT: horizontal tubular photobioreactor; VT: vertically stacked horizontal tubular photobioreactor; FP: flat panels photobioreactor. CU: Curaçao; TN: The Netherlands; SP: Spain; CI: Canary Islands; TU: Turkey; SA: Saudi Arabia

SCENARIO		COST BREAKDOWN FOR MICROALGAE CULTIVATION (as % of cost)								
System	Location	Major equipment	Additional capital cost	Raw materials	Consumables	Utilities	Energy	Labour	Wastewater treatment	Others
RW	TN	6.9	16.8	3.9	2.9	0.0	7.5	18.7	26.4	16.9
RW	CI	7.5	18.0	8.5	2.9	0.0	10.6	9.9	29.5	13.2
RW	TU	8.2	19.9	9.0	3.3	0.0	9.2	5.5	33.3	11.5
RW	SP	7.4	17.8	8.2	2.9	0.0	10.8	10.0	29.8	13.1
RW	SA	8.7	20.9	10.6	3.4	0.0	3.0	6.6	34.2	12.7
HT	TN	4.4	19.0	15.6	12.7	0.0	8.4	18.5	4.9	16.4
HT	CI	5.9	25.0	18.1	10.8	0.9	13.9	8.2	4.6	12.6
HT	TU	7.1	29.8	18.3	11.2	1.2	11.9	4.2	4.8	11.5
HT	SP	6.3	26.6	17.0	10.3	1.0	13.9	7.9	4.4	12.6
HT	SA	8.9	36.9	15.5	8.9	5.4	3.7	3.9	3.8	13.0
VT	TN	4.7	19.7	19.3	13.6	0.0	9.5	12.4	6.9	13.9
VT	CI	5.8	24.1	21.0	11.2	0.2	14.8	5.4	6.3	11.2
VT	TU	6.8	28.2	20.8	11.4	0.7	12.4	2.7	6.4	10.7
VT	SP	6.1	25.4	19.8	10.8	0.5	14.9	5.2	6.1	11.3
VT	SA	8.6	35.5	18.3	9.4	4.2	3.9	2.6	5.3	12.3
FP	TN	4.7	20.2	19.6	4.1	0.0	14.0	15.2	6.7	15.5
FP	CI	5.4	22.7	24.2	3.6	0.9	17.5	6.9	6.4	12.4
FP	TU	6.3	26.7	25.3	3.9	1.1	14.4	3.7	7.0	11.6
FP	SP	5.6	23.8	23.3	3.5	0.8	17.2	6.8	6.4	12.4
FP	SA	8.1	33.7	23.0	3.3	5.0	4.2	3.6	5.9	13.3

Towards industrial products from microalgae

FP	SP (Fut.)	7.5	32.3	24.9	5.5	0.1	10.2	6.0	0.0	13.6
RW	CU	6.9	16.5	8.1	2.5	0.0	23.7	5.8	26.0	10.5
HT	CU	5.2	22.0	15.0	8.5	2.0	29.5	4.4	3.6	9.6
VT	CU	5.1	21.1	17.0	8.7	1.2	30.4	2.8	4.9	8.8
FP	CU	4.6	19.2	19.5	2.8	1.6	34.6	3.5	4.9	9.3

Chapter 7

General discussion

Microalgae receive increased attention from both industry and academia, as microalgae are a sustainable source for a wide range of products [3, 4]. Commercial production of microalgae currently takes place at a relatively small scale. The production of microalgae at a larger scale for commodity products is currently hindered by high production costs [6].

The microalgal pilot facility AlgaePARC was constructed, as described in **Chapter 2**, to bridge the gap between fundamental lab research and industrial outdoor production. In different production systems the productivity of microalgae was compared under the same climatological conditions. Such a facility was unique as no comparison had been made between different reactor designs operated at the same location with the same strain. At the AlgaePARC facility an open raceway pond, a horizontal tubular photobioreactor, a vertically stacked horizontal tubular photobioreactor, and a flat panel photobioreactor were simultaneously operated. These systems occupied an equal ground area ($\pm 25 \text{ m}^2$) and were operated with *Nannochloropsis* sp. CCAP 211/78. Biomass concentration influences the performance of outdoor photobioreactors [35, 46]. The relation between biomass concentration and photobioreactor productivity has also been shown by the model evaluation described in Chapter 5. Therefore, the effect of two operational strategies on outdoor photobioreactor productivity was studied in this thesis; chemostat and turbidostat. A turbidostat provides direct control of biomass concentration whereas a chemostat provides indirect control by means of the reactor dilution rate.

In **Chapter 3**, we describe the study of the effect of different dilution rates on the productivity of four outdoor photobioreactors (chemostat operation). In the flat panel reactor and vertically stacked horizontal photobioreactor higher areal productivities and higher photosynthetic efficiencies were obtained compared to the raceway pond and horizontal tubular photobioreactor.

The effect of direct control of biomass concentration on the productivity was studied in three outdoor photobioreactors as described in **chapter 4**; open raceway pond, horizontal tubular and vertically stacked horizontal tubular photobioreactor. The reactors were operated as turbidostat; biomass was harvested continuously on the basis of an on-line turbidity measurement in the reactor. Also under turbidostat operation a higher productivity was obtained in the vertically stacked horizontal tubular photobioreactor in comparison to the horizontal tubular reactor (Figure 7.1). A high productivity was also obtained in the open raceway pond provided it is operated at sufficiently low biomass concentration (Figure 7.1).

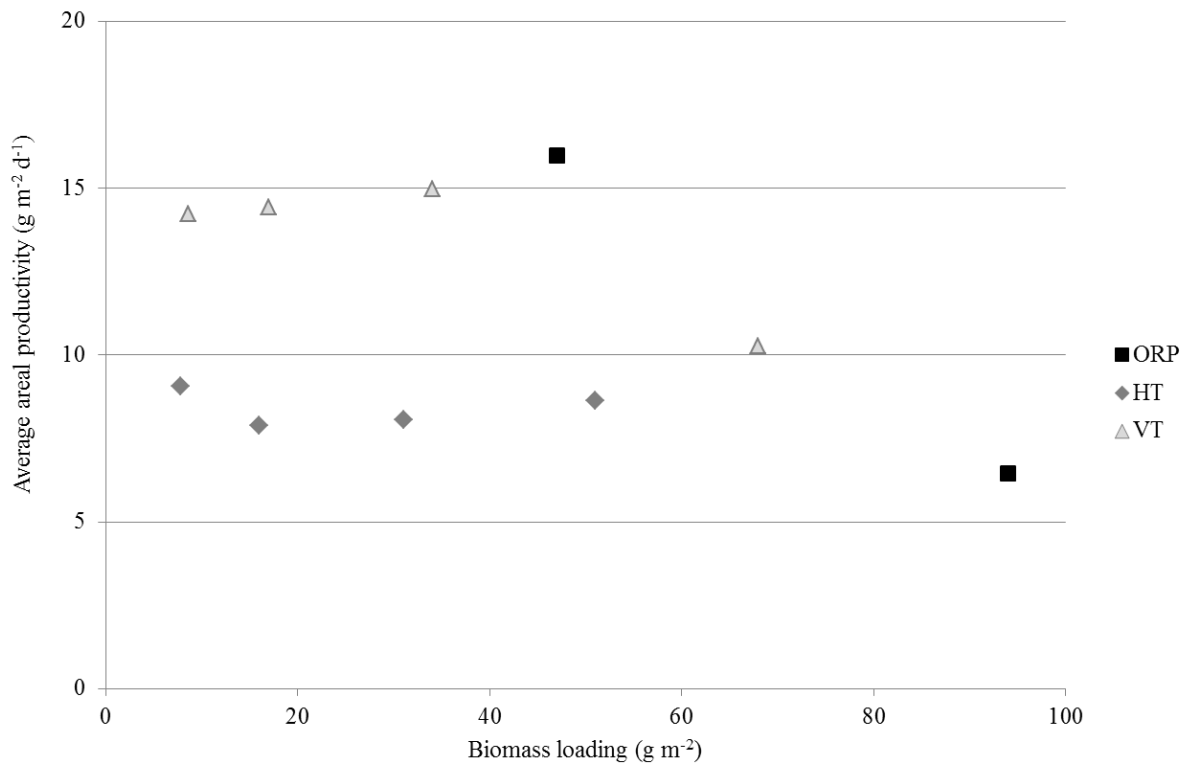


Figure 7.1 Effect of ground areal biomass loading on the areal productivity for three photobioreactors during turbidostat operation. ORP; open raceway pond, HT; horizontal tubular photobioreactor and VT; vertically stacked horizontal tubular photobioreactor.

The open raceway pond expressed a high productivity when using a lower biomass concentration (0.25 g/L). The productivity of the raceway pond was comparable to that of the vertically stacked horizontal tubular photobioreactor. At ground areal biomass loadings above 51 g. m⁻² the areal productivity dropped, for the open raceway pond and vertically stacked horizontal tubular photobioreactor (for horizontal tubular photobioreactor no data was obtained above this value). Both the vertically stacked horizontal tubular photobioreactor and the open raceway pond intercept the ground areal sunlight efficiently compared to the horizontal tubular photobioreactor. The tubes of the horizontal systems were spaced that far apart (0.05 m) that considerable sunlight could not be absorbed explaining its lower productivity. Besides biomass concentration light interception is thus a critical parameter to achieve high areal productivity. Efficient light interception is especially challenging when designing complex tubular geometries.

The biomass production costs were calculated using a techno-economic model for six locations in **Chapter 6**. The biomass production costs were calculated for a 1 and 100 hectare facility for each of the reactor concepts tested at AlgaePARC. Calculations were done on the basis of the results obtained in **Chapter 3**, which were extrapolated to other climatological conditions and larger scale. For all locations lowest biomass production costs were obtained with flat panel photobioreactors. The techno-economic model showed that the photosynthetic efficiency obtained in outdoor systems strongly influences the biomass production costs. Reduction in the estimated production costs have been obtained as a result of increased

insight in production technologies from 6 € kg⁻¹ in 2010 to 3 € kg⁻¹ for a flat panel photobioreactor in Southern Spain in our model calculations [5].

On the basis of the experience obtained at AlgaePARC in the period 2013-2015 further insights in operation of outdoor photobioreactors were acquired. The major factors to reduce production costs are pointed out and recommendations for further research are made. For this evaluation the techno-economic model was used.

7.1 How to reduce costs of algae production?

A number of technical challenges were encountered during operation of AlgaePARC. We will propose improvements and show its effect on the cost price of algae production. For this evaluation a hypothetical 100 ha production plant based in the Netherlands was used.

Base case scenario: Chemostat operation

Projections were done with the model described in **Chapter 6**. The base case was a vertically stacked horizontal tubular photobioreactor because its performance was the best. The horizontal tubular resulted in lower productivity and for the open raceway pond operation was limited by low culture temperatures. The values of several parameters (Table 7.1) were chosen based on the experience obtained during chemostat operation at pilot scale (AlgaePARC).

Table 7.5 Overview of values used for base case scenario for the techno-economic evaluation

Parameter	Value	Units
Scale	100	ha
Chemostat operation – dilution rate	0.27	d ⁻¹
Photosynthetic efficiency	2.4	% (sunlight)
Run time	5	Weeks
Cleaning time (per run)	1	Weeks
Winter period with no production	8.5	Weeks
Tube diameter	0.05	m
Liquid velocity in tubes	0.45	m s ⁻¹
Aeration rate (bubble column only)	1.03	VVM (L L ⁻¹ min ⁻¹)
Labour requirement	267	FTE (full time equivalent)
Area allocated to inoculum production	10	%

A dilution rate of 0.27 d⁻¹, was used as this dilution rate resulted in maximal productivity as described in **Chapter 3** and **Chapter 6**. The 5 week duration of a production run was based on the experience during chemostat operation described in **Chapter 3**. For cleaning and inoculation, a period of 1 week was taken into account. In winter low productivities were obtained in the chemostat study due to low light intensities in the Netherlands, and operation was therefore stopped for 8.5 week resulting in 305 operational days per year. A liquid velocity of 0.45 m s⁻¹ and an aeration rate of 1.03 vvm (L L⁻¹ min⁻¹) were used during operation; these values are similar to the settings used at AlgaePARC. Labour hours were

assumed to be equal to those in the Dutch horticulture industry resulting in 267 FTE for a 100 hectare facility; with 210 FTE for operators, 50 FTE for Supervisors and 7 FTE for plant managers [168]. For the base case of a production plant in the Netherlands employing vertically stacked horizontal tubular photobioreactors this results in a projected biomass production cost of 22.87 € kg⁻¹. Labour costs were the largest contributor with 42% of the total costs followed by the costs for others 26%. (Figure 7.2 and Appendix 7.A, table 7.A.1). The category others include costs for maintenance, supplies, general plant overheads and contingencies. Maintenance includes a fixed fee of 4% of the major equipment costs. Operating supplies includes raw materials and energy and is assumed to be 0.4% of the major equipment costs. The general plant overheads are the biggest contributor at 55% of the major equipment costs. While contingencies make up for 15% of the major equipment costs. (For further details see **Chapter 6**).

Biomass production costs for chemostat and turbidostat operation

The data obtained for the vertically stacked horizontal tubular photobioreactor during turbidostat operation at 1.0 g L⁻¹ were used to evaluate the economics of this mode of operation in comparison to the chemostat base case. The biomass concentration of 1.0 g/L was selected as it resulted in the highest areal productivity (**Chapter 4**). In **Chapter 4** a photosynthetic efficiency of 2.6% was obtained for the vertically stacked horizontal tubular photobioreactor during turbidostat operation, which was slightly higher than the 2.4 % obtained under chemostat operation (**Chapter 3**). All other parameters did not change and were thus the same as in Table 7.5. A small reduction in the production costs per kg of biomass was obtained from 22.87 € kg⁻¹ to a value of 21.93 € kg⁻¹, when the systems were operated as turbidostat (Appendix 7A, table 7.A.1).

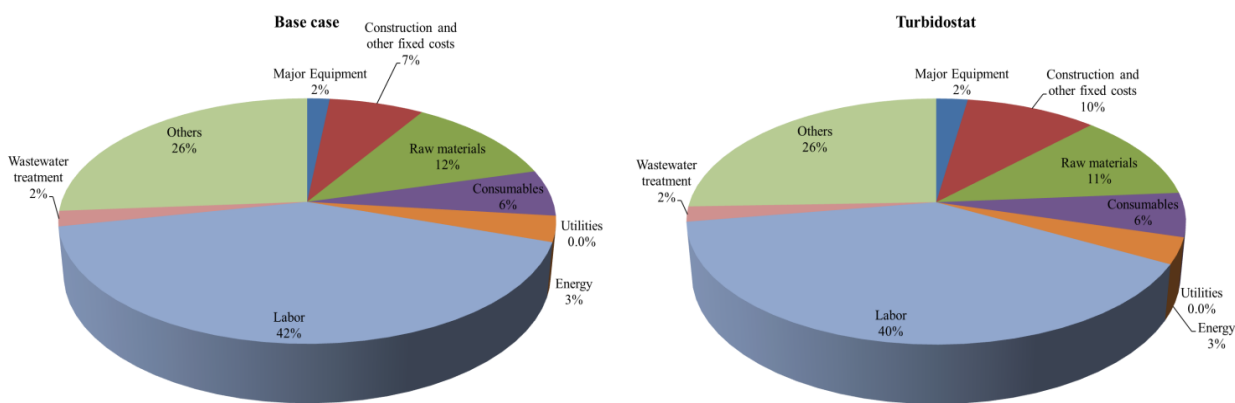


Figure 7.2 Overview of the contribution of different items to the total biomass production costs for chemostat (base case; left) and turbidostat operation (right).

Differences among the costs between the base case (Chemostat) and turbidostat are due to slightly increased photosynthetic efficiency and productivity, therefore the relative

contribution for labour costs to the costs per kilogram of biomass decreased for turbidostat operation (Figure 7.2 Appendix 7.A Table and Table 7.A.2). Further, an increase in the costs for major equipment and construction and other fixed costs were obtained, while costs for all other parameters decreased.

Towards improved production: Higher photosynthetic efficiency

The application of a microalgal growth model to predict the areal productivity of outdoor microalgae cultivation (**Chapter 5**) showed that strain characteristics can have a profound effect on productivity. Specifically, a high maximal specific growth rate and/or low specific absorption coefficient will result in improved areal productivity. Selection of novel strains with such characteristics could thus result in higher areal productivity. Also reactor design (light dilution) could result in improved photosynthetic efficiency. For example, when employing a rapidly growing mesophilic microalga, *Chlorella sorokiniana*, photosynthetic efficiencies of 3.9 – 5.9 % have been reached at lab-scale while simulating outdoor solar conditions [23]

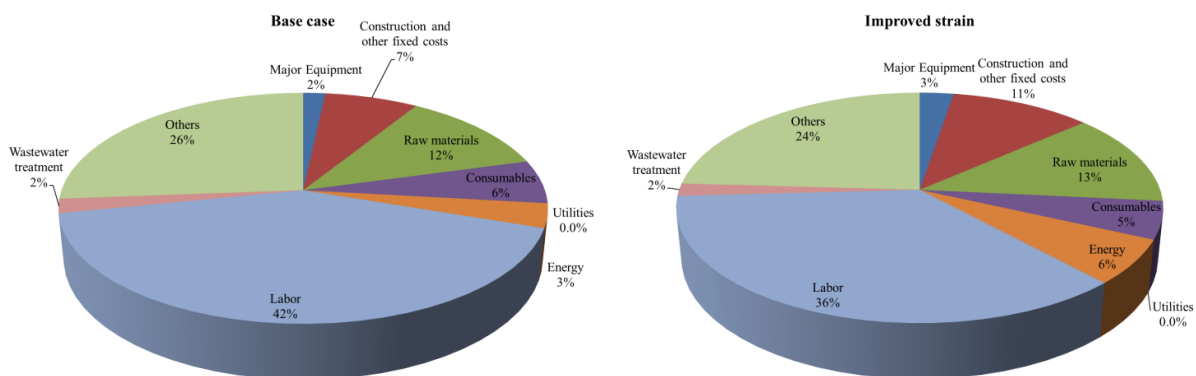


Figure 7.3 Comparison of the contribution of different parameters to the total biomass production costs for base case scenario (left) and improved strain having a higher photosynthetic efficiency (6% compared to 2.4%).

In the techno-economic model the photosynthetic efficiency of the production process can be increased representing the effect of a better strain and/or a novel way of diluting light. The effect of a high photosynthetic efficiency (6%) on the biomass production costs was therefore compared with the base case scenario (2.4%) [6, 23, 142] (Figure 7.3 Appendix 7.A, Table 7.A.1 and Table 7.A.3). Based on the model calculations the cost of production will reduce from 22.87 € kg⁻¹ for the base case scenario (chemostat, PE 2.4%) to 10.42 € kg⁻¹.

Towards stable production without fouling

One of the main issues that results in unstable production in time is the formation of fouling in closed photobioreactors. Length of a production run is limited by fouling as it needs to be

removed before light availability to the culture becomes too low. This results in reduction of the operational timeframe, and in a larger downtime because of cleaning procedures. One of the approaches to reduce fouling in tubular photobioreactors is to increase the flow rate in tubes. In this thesis, an effect of liquid velocity within the tubes on the formation rate of biofouling was observed for both tubular photobioreactors at AlgaePARC. In figure 7.4 the results of areal productivities at liquid flows of 0.45 m s^{-1} to 0.25 m s^{-1} are given. In this thesis, lower liquid velocities resulted in a higher biofilm formation rate, and thus lower areal productivities. The operational timeframe for a run in both tubular photobioreactors was reduced when adopting lower liquid velocities. In practice fouling is prevented or reduced by operation at higher liquid velocities of $0.6\text{-}0.9 \text{ m s}^{-1}$ (Personal communication IGV/Emilio Grima). The use of higher liquid velocities, however, will result in higher operational expenses [57, 169] and for this reason were not used in this thesis.

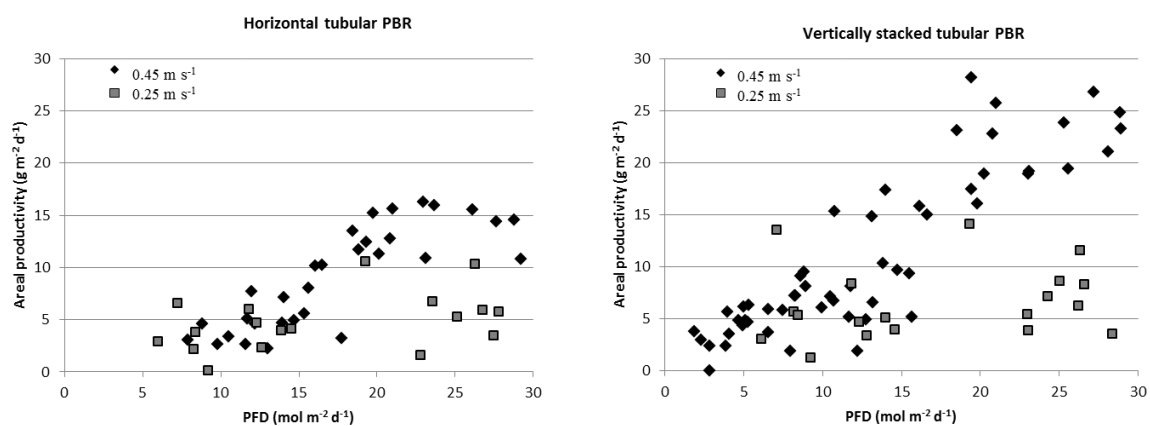
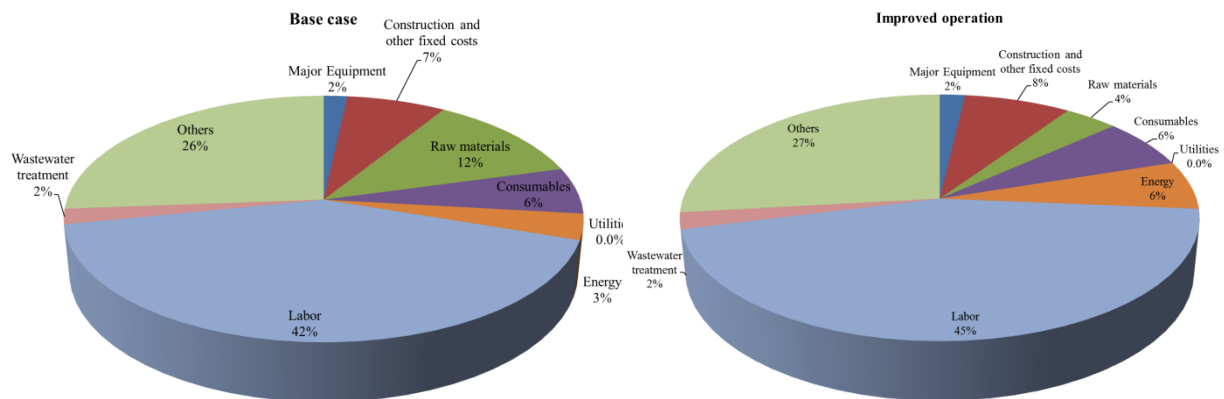


Figure 7.4 Comparison of areal productivities obtained in the tubular photobioreactors operated at AlgaePARC with liquid velocities of 0.25 and 0.45 m s^{-1} .

A deeper understanding in the mechanisms involved in the formation of fouling could help to find a solution for this problem. Strains characteristics in combination with material (tube) characteristics and operating conditions will all play a role. Engineering solutions might exist to combat fouling, such as using a so-called pig, which mechanically removes fouling. To simulate the potential of such advancements we used the techno-economic model. In the simulations we addressed the use of three different liquid velocities; 0.25 , 0.45 (base case) and 0.90 m s^{-1} . The reduction of the liquid velocity (0.25 m s^{-1}) resulted in a decrease of 0.07 € kg^{-1} , while the increased liquid velocity (0.90 m s^{-1}) resulted in a 0.58 € kg^{-1} increase in biomass production costs. The use of higher liquid velocities could reduce the amount of cleaning required per year. The effect of less cleaning cycles was simulated with the techno-economic model; 7 (base case), 3 and 1 cleaning per year. Lower number of cleanings per year result in lower biomass production costs: by 1.45 € kg^{-1} to 21.12 € kg^{-1} for 3 cleanings and even further for 1 cleaning per year to 20.40 € kg^{-1} . The number of cleanings per year has a stronger influence on the biomass production costs than the liquid velocity. The assumption was made that 10% of the production facility was reserved for preparation of inoculum. When less cleanings are needed also less inoculum needs to be produced, therefore, we assumed that a smaller area was required for inoculum preparation (5% instead of 10%). This results in a

reduction in the biomass costs of 1.15 € kg^{-1} . Overall, using a high liquid velocity (0.90 m s^{-1}), less cleaning cycles (only 1) and a smaller area for inoculum production (5%) result in a reduction of 2.67 € kg^{-1} . Resulting in a biomass production cost of 19.90 € kg^{-1} .

If all these improvements would be attained during production this results in a reduction in the biomass production costs from 22.57 € kg^{-1} to 19.90 € kg^{-1} (Appendix 7.A, Table 7.A.1 and Table 7.A.3). Largest reduction in the cost breakdown is observed for raw materials, as shown in Figure 7.5. As a result of the higher liquid velocities the energy costs increase by 75%.



*Figure 7.5 Comparison of contributors to the total biomass production costs for the base case scenario and the scenario having improved operation
Towards improved production: more automatization*

At AlgaePARC harvesting and operation of the cultivation systems was fully automated (**Chapter 2**). However, further automatization is required for microalgal production to take place at a large scale. Labour is the largest contributor to biomass production costs for the base case scenario. The amount of FTEs were based on the data from the Dutch horticulture sector [168]. For the production of microalgae, less labour is expected as less manual labour is involved compared to the production of vegetables in horticulture. This expectation comes from the difference in the production: microalgae have to be pumped around, while vegetables require manual harvesting, maintenance and weed control. Further, automatization of processes taking place in the production plant will result in a reduction in the labour requirements. Examples of technologies for further automatization can be obtained from the Dutch horticultural industry. Automatizing the preparation of cultivation medium using installations normally used in horticulture is a clear example. Further, centrifugation can be automatized by starting the feed at a high level signal in harvest tanks, and discharge of the slurry from the centrifuge can be controlled by a turbidity measurement in the liquid discharge stream. Further, cleaning and inoculation can be automated by the development of software protocols, used in different industries. All these together should result in an estimated reduction in man power by 75%, from 268 to 65 FTE [123]. This would result in

the following distribution among the different qualifications: 58 operators, 6 supervisors and 1 plant manager (Appendix 7.A, table 7.A.4).

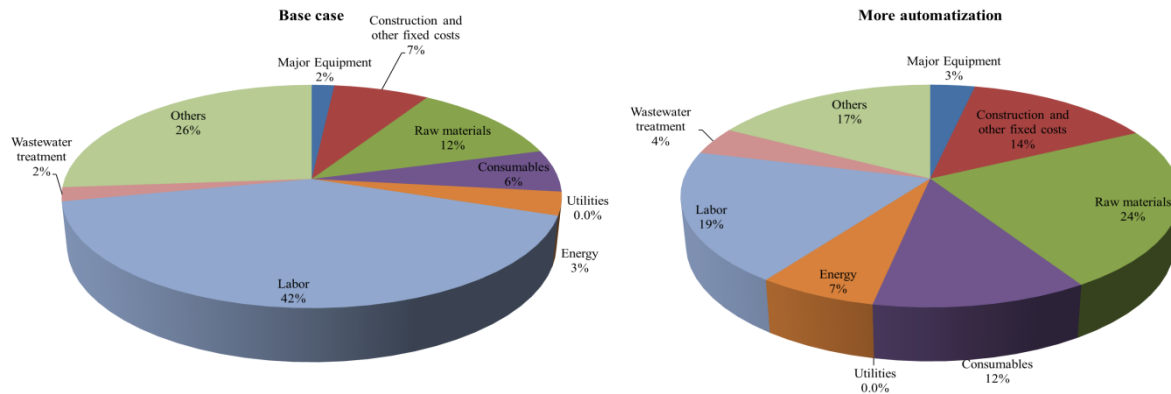


Figure 7.6 Comparison in contribution to the total biomass production cost for different parameters for base case (left) and a scenario considering reduced labour as a result of more automatization. The latter considers 68 FTE compared to 254 FTE in base case.

The reduction in the labour requirement for the base case (chemostat) results in a significant reduction in the cost price for a dry kilogram of biomass. The biomass production costs reduce from 22.57 € kg⁻¹ to 11.38 € kg⁻¹. The contribution of labour to the biomass cost price reduces from 40% to 19% as shown in Figure 7.6. The largest contributor now becomes the raw materials contributing for 24% to the biomass production costs.

7.2 Conclusions

All the discussed improvements have a positive effect on the biomass production costs at a commercial scale. An overview of the reduction in the biomass costs for the different improvements is given in figure 7.7.

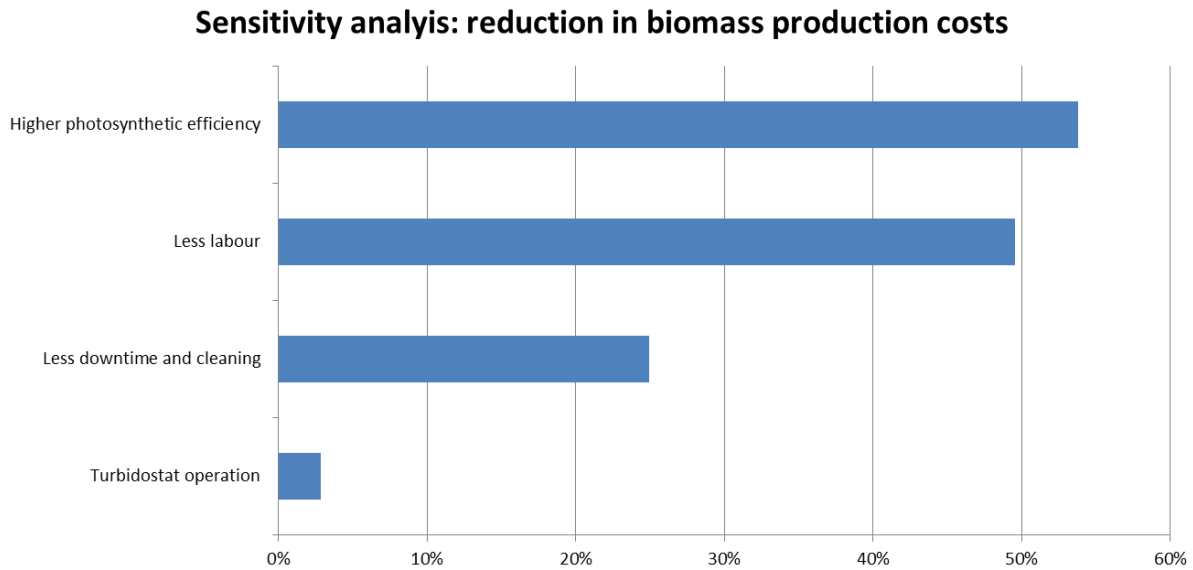


Figure 7.7 Sensitivity analysis on biomass production costs (cultivation and harvesting) using as a base case vertically stacked horizontal tubular photobioreactors in the Netherlands. Effect of individual parameters in cost reduction is shown in the horizontal axis. Scenarios represent the previously discussed changes.

The largest contributor to the reduction in costs price is obtained is the increase in photosynthetic efficiency from 2.4% to 6.0 %, resulting in a costs reduction of 53%. The second largest reduction in the biomass production costs was obtained when labour was reduced by more automatization. Followed by improved operation (Less downtime and less cleaning cycles) and the smallest improvement was obtained when the plant was operated as turbidostat instead of chemostat. The combined effect of the different scenarios results in the reduction of biomass production costs from 22.37 € kg⁻¹ for the base case scenario down to 5.62 € kg⁻¹ (Appendix 7, table 7.A.5). This means that a relative reduction of 75% in the biomass production costs can be obtained for vertical tubular photobioreactors.

The current high production costs hinder microalgae production to move from a relatively small scale to commercial production at a 100 hectares scale. Developments in automatization technologies, cultivation systems and strains will result in longer operational timeframes and more stable production. Projections on biomass production costs were made with a techno-economic model developed previously. For this a microalgal production facility using vertically stacked tubular photobioreactors operated as chemostat in the Netherlands was considered. Projections show that a reduction in the biomass production costs from 22.87 € kg⁻¹ to 5.62 € kg⁻¹ can be obtained in the Netherlands.

Appendix 7.A

Cost breakdown for the different scenarios evaluated in this chapter:

Table 7.A.1 Comparison in the biomass production for chemostat and turbidostat operation for each contributor

Breakdown of biomass production costs	Chemostat		Turbidostat	
Major equipment	0.38	€·kg ⁻¹	0.52	€·kg ⁻¹
Construction and other fixed costs	1.62	€·kg ⁻¹	2.18	€·kg ⁻¹
Raw materials	2.67	€·kg ⁻¹	2.51	€·kg ⁻¹
Consumables	1.37	€·kg ⁻¹	1.27	€·kg ⁻¹
Utilities	0.00	€·kg ⁻¹	0.00	€·kg ⁻¹
Energy	0.76	€·kg ⁻¹	0.75	€·kg ⁻¹
Labour	9.39	€·kg ⁻¹	8.67	€·kg ⁻¹
Wastewater treatment	0.45	€·kg ⁻¹	0.43	€·kg ⁻¹
Others	5.91	€·kg ⁻¹	5.61	€·kg ⁻¹
Total	22.57	€·kg ⁻¹	21.93	€·kg ⁻¹

Table 7.A.2 Cost breakdown for the base case having a photosynthetic efficiency of 2.4% with an improved strain resulting in a photosynthetic efficiency of 6%.

Breakdown of biomass production costs	Chemostat 2.4%		Chemostat 6%	
Major equipment	0.38	€·kg ⁻¹	0.27	€·kg ⁻¹
Construction and other fixed costs	1.62	€·kg ⁻¹	1.14	€·kg ⁻¹
Raw materials	2.67	€·kg ⁻¹	1.36	€·kg ⁻¹
Consumables	1.37	€·kg ⁻¹	0.55	€·kg ⁻¹
Utilities	0.00	€·kg ⁻¹	0.00	€·kg ⁻¹
Energy	0.76	€·kg ⁻¹	0.66	€·kg ⁻¹
Labour	9.39	€·kg ⁻¹	3.76	€·kg ⁻¹
Wastewater treatment	0.45	€·kg ⁻¹	0.18	€·kg ⁻¹
Others	5.91	€·kg ⁻¹	2.51	€·kg ⁻¹
Total	22.57	€·kg ⁻¹	10.42	€·kg ⁻¹

Table 7.A.3 Cost breakdown for the base case compared to improved operation: less cleaning cycles; from 7 to 1, less areal for inoculum production; from 10% to 5% and higher liquid velocity from 0.45 m s⁻¹ to 0.90 m s⁻¹.

Breakdown of biomass production costs	Chemostat 2.4%		Improved operation	
Major equipment	0.38	€·kg ⁻¹	0.36	€·kg ⁻¹
Construction and other fixed costs	1.62	€·kg ⁻¹	1.54	€·kg ⁻¹
Raw materials	2.67	€·kg ⁻¹	0.77	€·kg ⁻¹
Consumables	1.37	€·kg ⁻¹	1.30	€·kg ⁻¹
Utilities	0.00	€·kg ⁻¹	0.00	€·kg ⁻¹
Energy	0.76	€·kg ⁻¹	1.27	€·kg ⁻¹
Labour	9.39	€·kg ⁻¹	8.90	€·kg ⁻¹
Wastewater treatment	0.45	€·kg ⁻¹	0.43	€·kg ⁻¹
Others	5.91	€·kg ⁻¹	5.33	€·kg ⁻¹
Total	22.57	€·kg ⁻¹	19.90	€·kg ⁻¹

Table 7.A.4 comparison between the production costs for the base case and labour reduction as a result of automatization

Breakdown of biomass production costs	Chemostat		Automatization	
Major equipment	0.38	€·kg ⁻¹	0.38	€·kg ⁻¹
Construction and other fixed costs	1.62	€·kg ⁻¹	1.62	€·kg ⁻¹
Raw materials	2.67	€·kg ⁻¹	2.67	€·kg ⁻¹
Consumables	1.37	€·kg ⁻¹	1.37	€·kg ⁻¹
Utilities	0.00	€·kg ⁻¹	0.00	€·kg ⁻¹
Energy	0.76	€·kg ⁻¹	0.76	€·kg ⁻¹
Labour	9.39	€·kg ⁻¹	2.17	€·kg ⁻¹
Wastewater treatment	0.45	€·kg ⁻¹	0.45	€·kg ⁻¹
Others	5.91	€·kg ⁻¹	1.94	€·kg ⁻¹
Total	22.57	€·kg ⁻¹	11.38	€·kg ⁻¹

Table 7.A.5 Cost break down for overall improvements (all the above) on the cost break down

Breakdown of biomass production costs	Chemostat		Automatization	
Major equipment	0.38	€·kg ⁻¹	0.35	€·kg ⁻¹
Construction and other fixed costs	1.62	€·kg ⁻¹	1.46	€·kg ⁻¹
Raw materials	2.67	€·kg ⁻¹	0.54	€·kg ⁻¹
Consumables	1.37	€·kg ⁻¹	0.43	€·kg ⁻¹
Utilities	0.00	€·kg ⁻¹	0.00	€·kg ⁻¹
Energy	0.76	€·kg ⁻¹	0.92	€·kg ⁻¹
Labour	9.39	€·kg ⁻¹	0.70	€·kg ⁻¹
Wastewater treatment	0.45	€·kg ⁻¹	0.43	€·kg ⁻¹
Others	5.91	€·kg ⁻¹	0.78	€·kg ⁻¹
Total	22.57	€·kg ⁻¹	5.62	€·kg ⁻¹

References

References

1. Spolaore, P., et al., *Commercial Applications of Microalgae*. Journal Of Bioscience And Bioengineering, 2006. **101**: p. 87-96.
2. Draaisma, R.B., et al., *Food commodities from microalgae*. Current Opinion in Biotechnology, 2012(0).
3. Wijffels, R.H., M.J. Barbosa, and M.H.M. Eppink, *Microalgae for the production of bulk chemicals and biofuels*. Biofuels, Bioproducts and Biorefining, 2010. **4**: p. 287-295.
4. Wijffels, R.H. and M.J. Barbosa, *An outlook on microalgal biofuels*. Science, 2010. **329**: p. 796-799.
5. Norsker, N.-H., et al., *Microalgal production -- A close look at the economics*. Biotechnology Advances, 2011. **29**: p. 24-27.
6. Jesús Ruiz, G.O., Jeroen de Vree, Rouke Bosma, Philippe Willems, J. Hans Reith, Michel H.M. Eppink, Dorinde M.M. Kleinegris, René H. Wijffels, Maria J. Barbosa, *Towards industrial products from microalgae*. Energy and Environmental Science, 2016(submitted).
7. Janssen, M. and L. Jack, *Chapter Four - Microalgal Photosynthesis and Growth in Mass Culture*, in *Advances in Chemical Engineering*. 2016, Academic Press. p. 185-256.
8. Wolf, J., et al., *Multifactorial comparison of photobioreactor geometries in parallel microalgae cultivations*. Algal Research, 2016. **15**: p. 187-201.
9. Bosma, R., et al., *Design and construction of the microalgal pilot facility AlgaePARC*. Algal Research, 2014. **6, Part B**: p. 160-169.
10. Kumar, K., et al., *Recent trends in the mass cultivation of algae in raceway ponds*. Renewable and Sustainable Energy Reviews, 2015. **51**: p. 875-885.
11. Sousa, C., et al., *Growth of the microalgae *Neochloris oleoabundans* at high partial oxygen pressures and sub-saturating light intensity*. Bioresource Technology, 2012. **104**: p. 565-570.
12. de Andrade, G.A., et al., *Optimization of biomass production in outdoor tubular photobioreactors*. Journal of Process Control, 2016. **37**: p. 58-69.
13. Barbosa, M.J., et al., *Microalgae cultivation in air-lift reactors: modeling biomass yield and growth rate as a function of mixing frequency*. Biotechnology and Bioengineering, 2003. **82**: p. 170-179.
14. Zou, N. and A. Richmond, *Effect of light-path length in outdoor flat plate reactors on output rate of cell mass and on EPA in *Nannochloropsis* sp.* Journal of Biotechnology, 1999. **70**: p. 351-356.
15. Quinn, J.C., et al., *Nannochloropsis production metrics in a scalable outdoor photobioreactor for commercial applications*. Bioresource Technology, 2012. **117**: p. 164-171.
16. Rodolfi, L., et al., *Microalgae for oil: strain selection, induction of lipid synthesis and outdoor mass cultivation in a low-cost photobioreactor*. Biotechnol Bioeng, 2009. **102**.
17. Acién, F.G., et al., *Production cost of a real microalgae production plant and strategies to reduce it*. Biotechnology Advances, 2012. **30**: p. 1344-1353.
18. Del Campo, J.A., M. García-González, and M.G. Guerrero, *Outdoor cultivation of microalgae for carotenoid production: current state and perspectives*. Applied Microbiology and Biotechnology, 2007. **74**: p. 1163-1174.
19. Bosma, R., et al., *Towards increased microalgal productivity in photobioreactors*. International Sugar Journal, 2010. **112**: p. 74-85.
20. Tredici, M.R. and G.C. Zittelli, *Efficiency of sunlight utilization: Tubular versus flat photobioreactors*. Biotechnology and Bioengineering, 1998. **57**: p. 187-197.
21. Fernandez, F.G.A., et al., *Airlift-driven external-loop tubular photobioreactors for outdoor production of microalgae: assesment of design and performance*. Chemical Engineering Science, 2001. **56**: p. 2721-2732.
22. Jimenez, C., et al., *The Feasibility of industrial production of *Spirulina* (*Arthrospira*) in Southern Spain*. Aquaculture, 2003. **217**: p. 179-190.
23. Cuaresma, M., et al., *Horizontal or vertical photobioreactors? How to improve microalgae photosynthetic efficiency*. Bioresource Technology, 2011. **102**: p. 5129-5137.
24. Slegers, P.M., et al., *Design scenarios for flat panel photobioreactors*. Journal of Applied Energy, 2011. **88**: p. 3342-3353.
25. Pulz, O. and W. Gross, *Valuable products from biotechnology of microalgae*. Applied Microbiology and Biotechnology, 2004. **65**: p. 635-648.
26. Jorquera, O., et al., *Comparative energy life-cycle analyses of microalgal biomass production in open ponds and photobioreactors*. Bioresource Technology, 2010. **101**: p. 1406-1413.
27. Richmond, A., *Handbook of microalgal culture : biotechnology and applied phycology* 2004: Oxford [etc.] : Blackwell science.
28. Marquez, F.J., et al., *Inhibitory effect of oxygen accumulation on the growth of *Spirulina platensis**. Biotechnology Letters, 1995. **17**: p. 225-228.
29. Slegers, P.M., et al., *Scenario analysis of large scale algae production in tubular photobioreactors*. Applied Energy, 2013. **105**: p. 395-406.

References

30. Grima, E.M., et al., *Photobioreactors: light regime, mass transfer, and scaleup*. Journal of Biotechnology, 1999. **70**: p. 231-247.
31. Posten, C., *Design principles of photo-bioreactors for cultivation of microalgae*. Engineering in Life Sciences, 2009. **9**: p. 165-177.
32. Vandanjon, L., et al., *Effects of shear on two microalgae species. Contribution of pumps and valves in tangential flow filtration systems*. Biotechnology and Bioengineering, 1999. **63**: p. 1-9.
33. Sompech, K., Y. Chisti, and T. Srinophakun, *Design of raceway ponds for producing microalgae*. Biofuels, 2012. **3**: p. 387-397.
34. Weissman, J.C., R.P. Goebel, and J.R. Benemann, *Photobioreactor design: Mixing, carbon utilization, and oxygen accumulation*. Biotechnology and Bioengineering, 1988. **31**: p. 336-344.
35. Richmond, A., *Open systems for the mass production of photoautotrophic microalgae outdoors: physiological principles*. Journal of Applied Phycology, 1992. **4**: p. 281-286.
36. Velds, C.A., *Zonnestraling in Nederland (Solar radiation in The Netherlands)*. Klimaat van Nederland. Vol. 3. 1992: KNMI. 166.
37. Foyer, C. and R. Leegood, *Energetics and transport in aquatic plants MBL lectures in biology, volume 4*. FEBS Letters, 1986. **194**: p. 194-194.
38. Miron, A.S., et al., *Bubble-column and airlift photobioreactors for algal culture*. AIChE Journal, 2000. **46**: p. 1872-1887.
39. Kliphuis, A., et al., *Metabolic modeling of Chlamydomonas reinhardtii: energy requirements for photoautotrophic growth and maintenance*. Journal of Applied Phycology, 2011. **24**: p. 253-266.
40. Chisti, Y., *Biodiesel from microalgae*. Biotechnology Advances, 2007. **25**: p. 294-306.
41. Zhu, C.J. and Y.K. Lee, *Determination of biomass dry weight of marine microalgae*. Journal of Applied Phycology, 1997. **9**: p. 189-194.
42. Benvenuti, G., et al., *Microalgal triacylglycerides production in outdoor batch-operated tubular PBRs*. Biotechnology for Biofuels, 2015. **8**: p. 1-9.
43. ASTM. *Reference Solar Spectral Irradiance: ASTM G-173*. 19 August 2015]; Available from: <http://rredc.nrel.gov/solar/spectra/am1.5/astmg173/astmg173.html>.
44. Bosma, R., et al., *Prediction of volumetric productivity of an outdoor photobioreactor*. Biotechnology and Bioengineering, 2007. **97**: p. 1108-1120.
45. Tredici, M.R., et al., *A vertical alveolar panel (VAP) for outdoor mass cultivation of microalgae and cyanobacteria*. Bioresource Technology, 1991. **38**: p. 153-159.
46. Grima, E., et al., *Productivity analysis of outdoor chemostat culture in tubular air-lift photobioreactors*. Journal of Applied Phycology, 1996. **8**: p. 369-380.
47. Qiang, H., Y. Zarmi, and A. Richmond, *Combined effects of light intensity, light-path and culture density on output rate of Spirulina platensis (Cyanobacteria)*. European Journal of Phycology, 1998. **33**: p. 165-171.
48. Janssen, M., et al., *Scale-up aspects of photobioreactors: effects of mixing-induced light/dark cycles*. Journal of Applied Phycology, 2000. **12**: p. 225-237.
49. Janssen, M., et al., *Efficiency of light utilization of Chlamydomonas reinhardtii under medium-duration light/dark cycles*. Journal of Biotechnology, 2000. **78**: p. 123-137.
50. Takache, H., J. Pruvost, and H. Marec, *Investigation of light/dark cycles effects on the photosynthetic growth of Chlamydomonas reinhardtii in conditions representative of photobioreactor cultivation*. Algal Research, 2015. **8**: p. 192-204.
51. Michels, M.H.A., et al., *Effect of biomass concentration on the productivity of Tetraselmis suecica in a pilot-scale tubular photobioreactor using natural sunlight*. Algal Research, 2014. **4**: p. 12-18.
52. Camacho-Rodríguez, J., et al., *A quantitative study of eicosapentaenoic acid (EPA) production by Nannochloropsis gaditana for aquaculture as a function of dilution rate, temperature and average irradiance*. Applied Microbiology and Biotechnology, 2013: p. 1-12.
53. Rodolfi, L., et al., *Microalgae for oil: Strain selection, induction of lipid synthesis and outdoor mass cultivation in a low-cost photobioreactor*. Biotechnology and Bioengineering, 2009. **102**: p. 100-112.
54. Zittelli, G.C., R. Pastorelli, and M.R. Tredici, *A modular flat panel photobioreactor (MFPP) for indoor mass cultivation of Nannochloropsis sp. under artificial illumination*. Journal of Applied Phycology, 2000. **12**: p. 521-526.
55. San Pedro, A., et al., *Outdoor pilot-scale production of Nannochloropsis gaditana: Influence of culture parameters and lipid production rates in tubular photobioreactors*. Bioresource Technology, 2014. **169**: p. 667-676.
56. Zittelli, G.C., et al., *Production of eicosapentaenoic acid by Nannochloropsis sp. cultures in outdoor tubular photobioreactors*. Journal of Biotechnology, 1999. **70**: p. 299-312.
57. Arbib, Z., et al., *Long term outdoor operation of a tubular airlift pilot photobioreactor and a high rate algal pond as tertiary treatment of urban wastewater*. Ecological Engineering, 2013. **52**: p. 143-153.

References

58. Blanco, A.M., et al., *Outdoor cultivation of lutein-rich cells of Muriellopsis sp. in open ponds*. Applied Microbiology and Biotechnology, 2007. **73**: p. 1259-1266.
59. Boussiba, S., et al., *Lipid and biomass production by the halotolerant microalga Nannochloropsis salina*. Biomass, 1987. **12**: p. 37-47.
60. San Pedro, A., et al., *Outdoor pilot production of Nannochloropsis gaditana: Influence of culture parameters and lipid production rates in raceway ponds*. Algal Research, 2015. **8**: p. 205-213.
61. Cheng-Wu, Z., et al., *An industrial-size flat plate glass reactor for mass production of Nannochloropsis sp. (Eustigmatophyceae)*. Aquaculture, 2001. **195**: p. 35S-49.
62. Tredici, M.R., *Photobiology of microalgae mass cultures: understanding the tools for the next green revolution*. Biofuels, 2009. **1**: p. 143-162.
63. Breuer, G., et al., *Opportunities to improve the areal oil productivity of microalgae*. Bioresource Technology, 2015. **186**: p. 294-302.
64. Richmond, A. and Z. Cheng-Wu, *Optimization of a flat plate glass reactor for mass production of Nannochloropsis sp. outdoors*. Journal of Biotechnology, 2001. **85**: p. 259-269.
65. Fernandez, F.G.A., et al., *Modeling of biomass productivity in tubular photobioreactors for microalgal cultures: Effects of dilution rate, tube diameter, and solar irradiance*. Biotechnology and Bioengineering, 1998. **58**: p. 605-616.
66. De Vree, J.H., et al., *Comparison of four outdoor pilot-scale photobioreactors*. Biotechnology for Biofuels, 2015. **8**.
67. Melis, A., *Photosystem-II damage and repair cycle in chloroplasts: what modulates the rate of photodamage in vivo ?* Trends in Plant Science, 1999. **4**: p. 130-135.
68. Takache, H., et al., *Experimental and theoretical assessment of maximum productivities for the microalgae Chlamydomonas reinhardtii in two different geometries of photobioreactors*. Biotechnology Progress, 2010. **26**: p. 431-440.
69. Cuaresma, M., et al., *Luminostat operation: A tool to maximize microalgae photosynthetic efficiency in photobioreactors during the daily light cycle?* Bioresource Technology, 2011. **102**(17): p. 7871-7878.
70. Slegers, P.M., et al., *Scenario evaluation of open pond microalgae production*. Algal Research, 2013.
71. Pruvost, J., et al., *Systematic investigation of biomass and lipid productivity by microalgae in photobioreactors for biodiesel application*. Bioresource Technology, 2011. **102**: p. 150-158.
72. Lee, E., et al., *Design tool and guidelines for outdoor photobioreactors*. Chemical Engineering Science, 2014. **106**: p. 18-29.
73. Grima, E.M., et al., *Outdoor turbidostat culture of the marine microalga Tetraselmis sp.* Aquaculture Research, 1994. **25**: p. 547-555.
74. Quinn, G.P. and M.J. Keough, *Experimental design and data analysis for biologists*. 2009, Cambridge [u.a.]: Cambridge Univ. Press.
75. Molina, E., F.G.A. Fernandez, and M.Y. Chisti, *Tubular photobioreactor design for algal cultures*. Journal of Biotechnology, 2001. **92**: p. 113-131.
76. Olivieri, G., et al., *Photobioreactors for microalgal cultures: A model for photosynthesis rate assessment*. Chemical Engineering Transactions, 2013. **32**: p. 1039-1044.
77. Qiang, H. and A. Richmond, *Productivity and photosynthetic efficiency of Spirulina platensis as affected by light intensity, algal density and rate of mixing in a flat plate photobioreactor*. Journal of Applied Phycology, 1996. **8**: p. 139-145.
78. Olivieri, G., et al., *Photobioreactors for microalgal cultures: A Lagrangian model coupling hydrodynamics and kinetics*. Biotechnology Progress, 2015. **31**: p. 1259-1272.
79. Gómez-Pérez, C.A., et al., *CFD simulation for reduced energy costs in tubular photobioreactors using wall turbulence promoters*. Algal Research, 2015. **12**: p. 1-9.
80. Moberg, A.K., et al., *Simulated cell trajectories in a stratified gas-liquid flow tubular photobioreactor*. Journal of Applied Phycology, 2011. **24**: p. 357-363.
81. Zou, N. and A. Richmond, *Light-path length and population density in photoacclimation of Nannochloropsis sp. (Eustigmatophyceae)*. Journal of Applied Phycology, 2000. **12**: p. 349-354.
82. Zijffers, J.W., et al., *Maximum photosynthetic yield of green microalgae in photobioreactors*. Marine biotechnology, 2010. **12**: p. 708-718.
83. Fisher, T., et al., *The kinetics of the photoacclimation response of Nannochloropsis Sp. (Eustigmatophyceae): a study of changes in ultrastructure and PSU density*. Journal of Phycology, 1998. **34**: p. 818-824.
84. de Mooij, T., et al., *Antenna size reduction as a strategy to increase biomass productivity: a great potential not yet realized*. Journal of Applied Phycology, 2015. **27**: p. 1063-1077.
85. van Bodegom, P., *Microbial Maintenance: A Critical Review on Its Quantification*. Microbial Ecology, 2007. **53**: p. 513-523.

References

86. Sforza, E., S. Urbani, and A. Bertucco, *Evaluation of maintenance energy requirements in the cultivation of Scenedesmus obliquus: effect of light intensity and regime*. Journal of Applied Phycology, 2015. **27**: p. 1453-1462.
87. J.Geider, R. and B.A. Osborne, *Respiration and microalgal growth: a review of the quantitative relationship between dark respiration and growth*. New Phytologist, 1989. **112**: p. 327-341.
88. Gnansounou, E. and J. Kenthorai Raman, *Life cycle assessment of algae biodiesel and its co-products*. Applied Energy, 2016. **161**: p. 300-308.
89. Quinn, J.C. and R. Davis, *The potentials and challenges of algae based biofuels: A review of the techno-economic, life cycle, and resource assessment modeling*. Bioresource Technology, 2015. **184**: p. 444-452.
90. Slade, R. and A. Bauen, *Micro-algae cultivation for biofuels: Cost, energy balance, environmental impacts and future prospects*. Biomass and Bioenergy, 2013. **53**: p. 29-38.
91. Trucano, T.G., et al., *Calibration, validation, and sensitivity analysis: What's what*. Reliability Engineering & System Safety, 2006. **91**: p. 1331-1357.
92. Béchet, Q., A. Shilton, and B. Guieysse, *Modeling the effects of light and temperature on algae growth: State of the art and critical assessment for productivity prediction during outdoor cultivation*. Biotechnology Advances, 2013. **31**: p. 1648-1663.
93. Coles, J.F. and R.C. Jones, *Effect of temperature on photosynthesis-light response and growth of four phytoplankton species isolated from a tidal freshwater river*. Journal of Phycology, 2000. **36**: p. 7-16.
94. Raven, J.A. and R.J. Geider, *Temperature and algal growth*. New Phytologist, 1988. **110**: p. 441-461.
95. Sukenik, A., *Ecophysiological considerations in the optimization of eicosapentaenoic acid production by Nannochloropsis sp. (Eustigmatophyceae)*. Bioresource Technology, 1991. **35**: p. 263-269.
96. Klok, A.J., et al., *Simultaneous growth and neutral lipid accumulation in microalgae*. Bioresource Technology, 2013.
97. Santos, A.M., et al., *Biomass and lipid productivity of Neochloris oleoabundans under alkaline-saline conditions*. Algal Research, 2013. **2**: p. 204-211.
98. Wang, B. and C.Q. Lan, *Biomass production and nitrogen and phosphorus removal by the green alga Neochloris oleoabundans in simulated wastewater and secondary municipal wastewater effluent*. Bioresource Technology, 2011. **102**: p. 5639-5644.
99. Webb, W.L., M. Newton, and D. Starr, *Carbon Dioxide Exchange of Alnus rubra. A Mathematical Model*. Oecologia, 1974. **17**: p. 281-291.
100. Dubinsky, Z., P.G. Falkowski, and K. Wyman, *Light harvesting and utilization by phytoplankton*. Plant and Cell Physiology, 1986. **27**: p. 1335-1349.
101. Geider, R.J., H.L. Macintyre, and T.M. Kana, *A dynamic model of photoadaptation in phytoplankton*. Limnology and Oceanography, 1996. **41**: p. 1-15.
102. Pirt, S.J., *Maintenance energy: a general model for energy-limited and energy-sufficient growth*. . Archives of microbiology, 1982. **133**: p. 300-302.
103. Sforza, E., et al., *Effect of specific light supply rate on photosynthetic efficiency of Nannochloropsis salina in a continuous flat plate photobioreactor*. Applied Microbiology and Biotechnology, 2015. **99**: p. 8309-8318.
104. Rosso, L., J.R. Lobry, and J.P. Flandrois, *An Unexpected Correlation between Cardinal Temperatures of Microbial Growth Highlighted by a New Model*. Journal of Theoretical Biology, 1993. **162**: p. 447-463.
105. J.H. de Vree, R.B., M. Janssen, M.J. Barbosa, R.H. Wijffels, *Turbidostat operation in outdoor photobioreactors*. 2016.
106. Breuer, G., et al., *Effect of light intensity, pH, and temperature on triacylglycerol (TAG) accumulation induced by nitrogen starvation in Scenedesmus obliquus*. Bioresource Technology, 2013. **143**: p. 1-9.
107. Vejrazka, C., et al., *Photosynthetic efficiency of Chlamydomonas reinhardtii in flashing light*. Biotechnology and Bioengineering, 2011. **108**(: p. 2905-2913.
108. von Stockar, U. and J.S. Liu, *Does microbial life always feed on negative entropy? Thermodynamic analysis of microbial growth*. Biochimica et Biophysica Acta (BBA) - Bioenergetics, 1999. **1412**: p. 191-211.
109. Daniel, R.M. and M.J. Danson, *Temperature and the catalytic activity of enzymes: A fresh understanding*. FEBS Letters, 2013. **587**: p. 2738-2743.
110. Dubinsky, Z. and N. Stambler, *Photoacclimation processes in phytoplankton: mechanisms, consequences, and applications*. Aquatic Microbial Ecology, 2009. **56**: p. 163-176.
111. Mooij, T., et al., *Antenna size reduction as a strategy to increase biomass productivity: a great potential not yet realized*. Journal of Applied Phycology, 2014. **27**: p. 1063-1077.

References

112. Mayers, J.J., K.J. Flynn, and R.J. Shields, *Influence of the N:P supply ratio on biomass productivity and time-resolved changes in elemental and bulk biochemical composition of Nannochloropsis sp.* Bioresource Technology, 2014. **169**: p. 588-595.
113. Wijffels, R.H., O. Kruse, and K.J. Hellingwerf, *Potential of industrial biotechnology with cyanobacteria and eukaryotic microalgae.* Current Opinion in Biotechnology, 2013. **24**: p. 405-413.
114. Zhu, L., *Biorefinery as a promising approach to promote microalgae industry: An innovative framework.* Renewable and Sustainable Energy Reviews, 2015. **41**: p. 1376-1384.
115. Schenk, P.M., et al., *Second Generation Biofuels: High-Efficiency Microalgae for Biodiesel Production.* BioEnergy Research, 2008. **1**: p. 20-43.
116. Vanthoor-Koopmans, M., et al., *Biorefinery of microalgae for food and fuel.* Bioresource Technology, 2013. **135**: p. 142-149.
117. Bureau of Labor statistics, Occup. Employ. Stat.
118. Molina Grima, E., et al., *Recovery of microalgal biomass and metabolites: process options and economics.* Biotechnology Advances, 2003. **20**: p. 491-515.
119. Commision, E., Eurostat.
120. Curacao, G.o.t.C.o., Notification: Rates for electricity and water.
121. Welfare, G.o.t.C.o.C.M.o.S.D.L.a., *European social charter. 4th National Report on the implementation of the European Social Charter, Article 16.*
122. Schreuders, C.d.F.B.a.K., Curacao Bus. Mag.: p. 18-21.
123. Peters, M.S., Timmerhaus, K., *Plant design and economics for chemical engineers.* 1991(4th edition).
124. Goldman, J.C., Water Research, 1979: p. 119-136.
125. Dillschneider, R., et al., *Biofuels from microalgae: Photoconversion efficiency during lipid accumulation.* Bioresource Technology, 2013. **142**: p. 647-654.
126. Shammas, N.K., and Wang, L.K., *Water Engineering: Hydraulics, Distribution and Treatment.* 2015(1st edition).
127. Acién Fernández, F.G., et al., *Airlift-driven external-loop tubular photobioreactors for outdoor production of microalgae: assessment of design and performance.* Chemical Engineering Science, 2001. **56**: p. 2721-2732.
128. Shilton, A., *Pond Treatment Technology.* Water Intelligence Online, 2006. **5**.
129. Sierra, E., et al., *Characterization of a flat plate photobioreactor for the production of microalgae.* Chemical Engineering Journal, 2008. **138**: p. 136-147.
130. Craggs, R., D. Sutherland, and H. Campbell, *Hectare-scale demonstration of high rate algal ponds for enhanced wastewater treatment and biofuel production.* Journal of Applied Phycology, 2012. **24**: p. 329-337.
131. de Godos, I., et al., *Evaluation of carbon dioxide mass transfer in raceway reactors for microalgae culture using flue gases.* Bioresource Technology, 2014. **153**: p. 307-314.
132. Beek, W.J., Muttzall, K.M.K., van Hevuen, J.W., *Transport phenomena.* 2000(2nd edition).
133. Bird, R.B., Stewart, W.E., Lightfoot, E.N., *Transport phenomena.* 2007(2nd edition).
134. Kern, D.Q., *Process Heat Transfer.* 1950(1st edition).
135. Couper, J.R.P., W.R., Fair, J.R., Walas, S.M., *Chemical Process Equipment.* 2012(3rd edition).
136. Towler, G.a.S., R., *Chemical Engineering Design.* 2013(2nd edition): p. 103-160.
137. Eftekharzadeh, S., Baasiri, M.M. and Lindahl Jr., P.A., *Cooling Technology Institute Annual Conference.* 2003: p. 1-21.
138. Borowitzka, M.A., *Algal Culturing Techniques.* 2005(1st edition): p. 205-218.
139. Elger, D., Williams, B.C., Crowe, C.T., Roberson, J.A., *Engineering Fluid Mechanics.* 2013(10th edition): p. 359-405.
140. Ketheesan, B. and N. Nirmalakhandan, *Development of a new airlift-driven raceway reactor for algal cultivation.* Applied Energy, 2011. **88**: p. 3370-3376.
141. Chiamonti, D., et al., *Review of energy balance in raceway ponds for microalgae cultivation: Re-thinking a traditional system is possible.* Applied Energy, 2013. **102**: p. 101-111.
142. Melis, A., *Solar energy conversion efficiencies in photosynthesis: Minimizing the chlorophyll antennae to maximize efficiency.* Plant Science, 2009. **177**: p. 272-280.
143. Luca, P.D., A. Musacchio, and R. Taddei, *Acidophilic algae from the fumaroles of Mount Lawu (Java, locus classicus of Cyanidium caldarium Geitler).* Giornale botanico italiano, 1981. **115**: p. 1-9.
144. Davis, R., A. Aden, and P.T. Pienkos, *Techno-economic analysis of autotrophic microalgae for fuel production.* Applied Energy, 2011. **88**: p. 3524-3531.
145. Slegers, P.M., et al., *Logistic analysis of algae cultivation.* Bioresource Technology, 2015. **179**: p. 314-322.

References

146. Zhang, K., S. Miyachi, and N. Kurano, *Photosynthetic performance of a cyanobacterium in a vertical flat-plate photobioreactor for outdoor microalgal production and fixation of CO₂*. *Biotechnology Letters*, 2001. **23**: p. 21-26.
147. Tredici, M.R., et al., *Energy balance of algal biomass production in a 1-ha "Green Wall Panel" plant: How to produce algal biomass in a closed reactor achieving a high Net Energy Ratio*. *Applied Energy*, 2015. **154**: p. 1103-1111.
148. Bilad, M.R., et al., *Harvesting microalgal biomass using a magnetically induced membrane vibration (MMV) system: Filtration performance and energy consumption*. *Bioresource Technology*, 2013. **138**: p. 329-338.
149. Chauton, M.S., et al., *A techno-economic analysis of industrial production of marine microalgae as a source of EPA and DHA-rich raw material for aquafeed: Research challenges and possibilities*. *Aquaculture*, 2015. **436**: p. 95-103.
150. Richmond, A., Hu, Q., *Handbook of Microalgal culture: Applied phycology and Biotechnology*. 2013.
151. Sharma, N.K., et al., *Sustainability and cyanobacteria (blue-green algae): facts and challenges*. *Journal of Applied Phycology*, 2011. **23**: p. 1059-1081.
152. Uduman, N., et al., *Dewatering of microalgal cultures: A major bottleneck to algae-based fuels*. *Journal of Renewable and Sustainable Energy*, 2010. **2**: p. 012701.
153. de Farias Silva, C.E. and A. Bertucco, *Bioethanol from microalgae and cyanobacteria: A review and technological outlook*. *Process Biochemistry*.
154. Pruvost, J., Le Borgne, F., Artu, A., Cornet, J.-F., *Photobioreaction Engineering*. 2016. **48**.
155. Leonard, A., et al., *Cyanobacteria immobilised in porous silica gels: exploring biocompatible synthesis routes for the development of photobioreactors*. *Energy & Environmental Science*, 2010. **3**: p. 370-377.
156. Melis, A., *Photosynthesis-to-fuels: from sunlight to hydrogen, isoprene, and botryococcene production*. *Energy & Environmental Science*, 2012. **5**: p. 5531-5539.
157. Yen, H.-W., et al., *CO₂, NO_x and SO_x removal from flue gas via microalgae cultivation: A critical review*. *Biotechnology Journal*, 2015. **10**: p. 829-839.
158. Mikkelsen, M., M. Jorgensen, and F.C. Krebs, *The teraton challenge. A review of fixation and transformation of carbon dioxide*. *Energy & Environmental Science*, 2010. **3**: p. 43-81.
159. Zhang, Y., A. Kendall, and J. Yuan, *A comparison of on-site nutrient and energy recycling technologies in algal oil production*. *Resources, Conservation and Recycling*, 2014. **88**: p. 13-20.
160. Garcia Alba, L., et al., *Microalgae growth on the aqueous phase from Hydrothermal Liquefaction of the same microalgae*. *Chemical Engineering Journal*, 2013. **228**: p. 214-223.
161. Biller, P., et al., *Nutrient recycling of aqueous phase for microalgae cultivation from the hydrothermal liquefaction process*. *Algal Research*, 2012. **1**: p. 70-76.
162. Fon Sing, S., et al., *Pilot-scale continuous recycling of growth medium for the mass culture of a halotolerant Tetraselmis sp. in raceway ponds under increasing salinity: A novel protocol for commercial microalgal biomass production*. *Bioresource Technology*, 2014. **161**: p. 47-54.
163. Kim, J., et al., *Continuous harvest of marine microalgae using electrolysis: effect of pulse waveform of polarity exchange*. *Bioprocess and Biosystems Engineering*, 2014. **37**: p. 1249-1259.
164. Farid, M.S., et al., *Using nano-chitosan for harvesting microalga Nannochloropsis sp.* *Bioresource Technology*, 2013. **131**: p. 555-559.
165. Trent, J.D., Embaye, T., Buckwalter, P., Richardson, T.-M., Kagawa, H., Reinsch, S., Martis, M., *Renewable Energy*, 2010.
166. Ras, M., J.P. Steyer, and O. Bernard, *Temperature effect on microalgae: A crucial factor for outdoor production*. *Reviews in Environmental Science and Biotechnology*, 2013. **12**: p. 153-164.
167. Lu, J., C. Sheahan, and P. Fu, *Metabolic engineering of algae for fourth generation biofuels production*. *Energy & Environmental Science*, 2011. **4**: p. 2451-2466.
168. Nieuwenhuijse, A., *Ministry of Economic affairs, Agriculture and Innovation: Dutch horticulture*. 2010.
169. Harris, L., et al., *Potential impact of biofouling on the photobioreactors of the Offshore Membrane Enclosures for Growing Algae (OMEGA) system*. *Bioresource Technology*, 2013. **144**: p. 420-428.

Summary

Microalgae have received much interest from industry as a promising sustainable feedstock for the production of food, feed, bulk chemicals, and biofuels. Currently, high production costs, as a result of the low areal productivities, limit the use of microalgae at an industrial scale. The reactor design most suitable for the commercial production of microalgae needs to be optimized. Productivity in the most suitable reactor system should be maximized by using the best operational strategy. In this thesis we focussed on maximizing the areal productivity for different reactor concepts by applying different operational strategies

In **chapter 2**, construction of the AlgaePARC (Algae Production And Research Centre) pilot facility was described. This facility was constructed to bridge the gap between fundamental research and commercial scale production. The pilot facility allows the comparison and improvement of pilot scale photobioreactors and operational strategies under identical outdoor conditions. Four reactor designs were installed at the pilot facility: open raceway pond, horizontal tubular reactor, vertically stacked horizontal tubular reactor and flat panel photobioreactor. The development of the facility, decisions made during the construction process are discussed. Further, for each reactor design, details including technical specifications, measurements and supporting facilities are discussed.

Operational strategies influence the performance of photobioreactors, therefore we compared the performance of four outdoor photobioreactors cultivated operated at different dilution rates in **Chapter 3**. In this chapter, the productivity and photosynthetic efficiency of *Nannochloropsis* sp. CCAP 211/78 were compared. The optimal dilution rate was determined for each photobioreactor by operation of the different photobioreactors at different dilution rates. Vertical photobioreactors resulted in higher areal productivities and photosynthetic efficiencies, 19-24 g m⁻² d⁻¹ and 2.4-4.2%. Lower areal productivity and photosynthetic efficiency were found for the horizontal systems; 12-15 g m⁻² d⁻¹ and 1.5-1.8%. The higher ground areal productivity in vertical systems could be explained by light dilution in combination with a higher ground areal light interception. In the raceway pond low productivities were obtained, due to the long optical path in this system and lower mixing rate. Areal productivities in all systems increased with increasing photon flux densities up to a photon flux density of 20 mol m⁻² d⁻¹. Photosynthetic efficiencies remained constant in all systems with increasing photon flux densities. The highest photosynthetic efficiencies obtained were; 4.2% for the vertical tubular photobioreactor, 3.8% for the flat panel reactor, 1.8% for the horizontal tubular reactor, and 1.5% for the open raceway pond. Photobioreactor light interception should be optimized to maximize ground areal productivity and photosynthetic efficiency.

In **chapter 4**, the effect of biomass concentration on the performance of *Nannochloropsis* sp. CCAP211/78 was studied in three outdoor pilot-scale photobioreactors. The following reactor designs were considered in this chapter: open raceway pond (OPR), horizontal tubular (HT) photobioreactor and a vertically stacked horizontal tubular (VT) photobioreactor. All reactors were operated continuously as turbidostat at different biomass concentrations. Highest areal productivities were obtained on days with a high light intensity for all systems, while days with a low light intensity resulted in the highest photosynthetic efficiencies. Ground areal biomass concentration exceeding 51 g m⁻² had a negative effect on the areal productivity and

photosynthetic efficiency. In the tubular systems only one biomass concentration exceeded the ground areal biomass loading of 51 g m^{-2} : the biomass concentration of 2.0 g L^{-1} (68 g m^{-2}) in the vertically stacked horizontal tubular photobioreactor. For this system and biomass concentration a decrease in areal productivity was observed compared to values obtained for other biomass concentrations. In the open raceway pond the highest biomass concentration, exceeded the value of 51 g m^{-2} as well. Consequently, a lower areal productivity was obtained for this biomass concentration. Overall highest areal productivities were obtained for OPR and VT, most likely due to more efficient ground areal light interception. The observation that night biomass loss was coupled to net growth was reported. At lower biomass concentrations and concomitant higher growth rates the specific night biomass losses were higher. Microalgal specific light absorption coefficient was correlated to biomass concentration; higher biomass concentrations resulted in higher specific absorption coefficients, resulting in a steeper light gradient.

In **chapter 5** model parameters that allow the prediction of microalgal growth with mathematical models were determined for two oleaginous strains; *Neochloris oleoabundans* and *Nannochloropsis* sp. With the determined model parameters algal growth can be predicted under process conditions that can be expected during large scale production, on the productivity of microalgae cultivation systems. Simulations showed that a less tight temperature control ($20 - 35 \text{ }^\circ\text{C}$) resulted in a 20-30% reduction in productivity compared to a more tight temperature control ($24-28 \text{ }^\circ\text{C}$). The specific growth rate and specific absorption coefficient showed to have a big impact on the prediction and it is hypothesized that the maximal specific growth rate of *Nannochloropsis* sp. differs considerably among strains.

In **Chapter 6** the feasibility the commercial production of microalgae is analysed via a techno-economic evaluation of for a 100 hectares facility for six locations. The projections made in this chapter result in a current biomass production cost of $3.4 \text{ €}\cdot\text{kg}^{-1}$ for microalgae cultivation in Spain, with an expected reduction to $0.5 \text{ €}\cdot\text{kg}^{-1}$ in ten years. A sensitivity analysis reveals the roadmap to achieve this.

In **Chapter 7**, the status of microalgae production technologies considering the insights obtained in this thesis is discussed. Limitations that currently hinder stable production taking place for long periods of time are presented and possible solutions are discussed. Projections are made on the effect of solving these limitations on the reduction in the biomass production

Overall, in this thesis the first comparison on the effect of different reactor designs and operational strategies is made. An outlook is made on the future of microalgae production, which pinpoints bottlenecks that need to be solved in the near future.

Acknowledgements

Acknowledgements

Rene bedankt voor de enorm grote kans die je mij hebt gegeven. Ik ben enorm vereerd dat ik aan het project AlgaePARC heb mogen werken onder jou begeleiding. Als begeleider veraste je me vaak met de richting van de vraag, maar ik kreeg altijd de tijd om tot een antwoord te komen.

Maria, bedankt voor je begeleiding! Ik heb enorm veel geleerd van je in de afgelopen jaren. Ik hoop dat we in de toekomst nog veel kunnen samenwerken in de algenwereld.

Rouke, jij bent een van de belangrijkste personen in mijn wetenschappelijke carrière. Onze samenwerking begonnen vele jaren geleden toen ik als boekie mijn HBO afstudeerstage bij je kwam doen. Ik ben enorm blij dat uitgerekend jij mij hebt begeleid tijdens mijn promotie onderzoek, en dat we enorm fijn hebben samengewerkt aan het AlgaePARC project.

Marcel, jij kwam er later bij als begeleider, ik heb enorm veel van je geleerd op het gebied van algen, fotobioreactoren en modelleren. Bedankt voor alles.

Ellen, met jouw heb ik tijdens mijn promotie onderzoek heel erg fijn samengewerkt. Ik hoop dat we deze samenwerking in de toekomst kunnen voortzetten.

Niels, from you have learned the trick of outdoor cultivation, well at least some basics. I have enjoyed working together with you and I have learned a lot from you. I hope we will meet many times in Southern Spain or somewhere else enjoying a glass of Cardenal Mendoza.

Giulia and **Iago**, my algae siblings. We have grown to each other as siblings and I have learned a lot from the two of you. We have supported each other in difficult times and enjoyed life in the many happy moments we shared. Without the two of you my PhD and myself would have been different. Thank you for everything!

Rafa, thanks for all your advices and all the other things that you helped me with! You are a very good friend!

Snezana of Mama! Wat ben ik enorm blij dat wij hebben samengewerkt. Je bent iemand met een enorme hoeveelheid positieve energie. Ik hoop dat we in de toekomst weer een keertje kunnen samenwerken.

Fred, je bent mijn held! Zonder jou ervaring, kennis en enorme toewijding zou AlgaePARC niet zijn geworden wat het is voor mij!

I would like to thank the people with whom I have worked closely during my years at the AlgaePARC: **Rick, Ruud, Mathijs, Jesus, Maria C, Christa**.

Jelke en **Peter**, mijn vakantie maatjes en gymratten. Ik hoop dat “The tripod” nog lang blijft staan en dat we nog vele reizen en avonturen zullen beleven onder het genot van een speciaal biertje!

Of course there are many friends from various groups that also deserve a big thank you for listening to my algae stuff: **Marcela, Mia, Amaya, Paolo, Valentina, Annelien, Maria** and **Angel, Klaske** en **Rick, Lenneke** en **Sina, Anne** en **Lenny, Francisco** and **Lena, Marjon**,

Acknowledgements

Levi, Derk and Christos. The housemates cannot be forgotten: **Daniela** “the Queen”, **Bart, Paolo, Luis, Stijn, Celia, Mirthe and Victor.** The colleagues: **Youri, Camilo, Pauline, Kiira, Carl and Lucille, Luci and Christina, Fabian, Aleks, Enrico, Michel, Michiel, Guido, Tim, Joao.**

I would also like to so my gratitude to the students who have helped me with my work: **Remco, Erik, Gerard, Pieter, Mark, Lisanne, Nick, Kim, Christos and Lukas**

Een special plekje verdienen de mensen waarmee mijn biotechnologie verhaald is begonnen in Leeuwarden en met wie ik nog steeds goed contact heb: **Jan Willem, Jaring en Linda-Lou, Roxanne, Jose, Jildou, Sjoerd, Jelte Jan en Emiel en Sandra!**

Roalah, Untagaja en Haimil! Bedankt voor jullie steun tijdens een heel groot deel van mijn promotie onderzoek! Ik heb enorm veel van jullie geleerd ook veel dingen die ik mij waarschijnlijk nog niet eens realiseer.

Ward, ook wij kennen elkaar nog vanuit Leeuwarden! Met veel plezier heb ik altijd met je samengewerkt en ik ben enorm blij dat ik met jou ALCUSO ben begonnen! Ik hoop dat we nog vele jaren als compagnon zullen hebben.

Nanda! Wat ben ik blij dat jij mijn zusje bent! Ik ben enorm trots op jou op wat je hebt bereikt en nog meer op wat je nog gaat bereiken! Er ligt een wereld aan je voeten zus! **Papa,** bedankt voor je steun en je toewijding! Je bent een enorm voorbeeld voor mij! Gelukkig voor mij lijkt ik in veel dingen op jou! Ik wil nog veel van je te leren. **Mama,** in andere dingen lijkt ik weer heel veel op jou. Ik ben blij dat ik ook bij jou altijd terecht kan en ik hoop dat we samen nog veel mooie reizen en wandelingen kunnen maken (Of gewoon vogels kijken om de hoek!).

Catalina, Mi vida preciosa, within a short time we have grown very close and we have been on very nice adventures! Many more will follow as we will travel around the globe or maybe even further! Where ever we are, we are together! Te amo mas cada dia!

About the author

Jeroen Hendrik de Vree was born on the 10th of May 1985 in Woerden, the Netherlands. After completing high school Jeroen started Biotechnology at the Applied University Van Hall Larenstein in 2004. Jeroen graduated from his BSc degree in 2008 on auto inhibitory compounds in of high density cultivations of Microalgae. The work for the BSc thesis was carried out at the Bioprocess Engineering department of Wageningen University and Researchcentre.

In 2008 Jeroen started with a MSc study in Biotechnology at the Wageningen University and Researchcentre. In 2010 an

MSc thesis resulted in the completion of the degree. During the MSc thesis the potential of microalgal carbon capture for power plants was studied at the Bioprocess Engineering department at the Wageningen University and Researchcentre. In February 2011, Jeroen started working on his PhD on maximizing and comparing microalgal productivity in different pilot-scale outdoor photobioreactors. The results of the PhD research are described in this thesis. Currently, Jeroen works as a consultant in ALCUSO, a company founded by him and Ward Blanken. Next to the consultancy work Jeroen is currently working as a post-doctoral researcher at the University of Bergen.



List of publications

List of publications

Breuer, G., Evers, W.A.C., **de Vree, J.H.**, Kleinegris, D.M.M., Martens, D.E., Wijffels, R.H., Lamers, P.P. *Analysis of Fatty Acid content and Composition in Microalgae*, Journal of Visualized Experiments, 2013 (80). DOI: 10.3791/50628

Bosma, R., **de Vree, J.H.**, Slegers, P.M., Janssen, M., Wijffels, R.H., Barbosa, M.J. *Design and construction of the microalgal pilot facility AlgaePARC*, Algal Research, 2014, 6B:160-169. DOI:10.1016/j.algal.2014.10.006

de Vree, J.H., Bosma, R., Janssen, M., Barbosa, M.J., Wijffels, R.H. *Comparison of four outdoor pilot-scale photobioreactors*, Biotechnology for Biofuels, 2015, 8:215. DOI: 10.1186/s13068-015-0400-2.

de Vree, J.H., Bosma, R., Janssen, M., Barbosa, M.J., Wijffels, R.H. *Turbidostat operation of outdoor pilot-scale photobioreactors*, Algal Research, 2016 18:198-208. DOI:10.1016/j.algal.2016.06.006

Ruiz, J., Olivieri, G., **de Vree, J.H.**, Bosma, R., Willems, P., Reith, J.H., Eppink, M.H.M., Kleinegris, D.M.M., Wijffels, R.H., Barbosa, M.J. *Towards industrial products from microalgae*. Energy & Environmental Science, 2016

de Vree, J.H., Slegers, P.M., Bosma, R., Janssen, M., Barbosa, M.J., Wijffels, R.H. *Parameter estimation for *Neochloris oleoabundans* and *Nannochloropsis* sp. for modelling microalgal growth*. (In preparation for submission)

Lian, J., Meijer, S., **de Vree, J.H.**, Heryanto, C., Bosma, R., Wijffels, R.H., Barbosa, M.J., Smidt, H., Sipkema, D. *Microbes growing along with the alga *Nannochloropsis* sp. CCAP211/78 in different outdoor pilot-scale photobioreactors*. (In preparation for submission)

Overview of completed training activities

Overview of completed training activities

Overview of completed training activities

Discipline specific courses and activities:

VLAG course microalgae photobioreactors (2013)
Batch Process Modelling using MVDA (2012)
National Biotechnology symposium (2011)
1st Young Algaeneers Symposium (2012)
2nd Young Algaeneers Symposium (2014)
3rd Young Algaeneers Symposium (2016)
Alg'n'chem (2014)
2nd EABA symposium (2015)
Spotfire essentials (2014)
Climate KIC presentation and discussion (2014)
AlgaePARC consortium meetings (2010-2015)

General courses and activities:

VLAG PhD Week (2011)
Project and Time management (2012)
Interpersonal communication for PhD students (2012)
Teaching and supervising thesis students (2011)
PhD competence assessment (2012)
Presentation skills (2013)
PhD course scientific writing (2013)

Optional courses and activities:

Preparation of the research proposal (2010)
PhD study trip Spain (2012)
Weekly group meetings (2010/2016)